Distribution Agreement:

In presenting this thesis or dissertation as a partial fulfillment of the requirements for an advanced degree from Emory University, I hereby grant to Emory University and its agents the non-exclusive license to archive, make accessible, and display my thesis or dissertation in whole or in part in all forms of media, now or hereafter known, including display on the world wide web. I understand that I may select some access restrictions as part of the online submissions of this thesis or dissertation. I retain all ownership rights to the copyright of the thesis or dissertation. I also retain the right to use in future works (such as articles or books) all or part of this thesis or dissertation.

Signature:

_____ _____

Jennifer L. Bon Date

Design and Development of Novel Methods for C–H Functionalization for Amination and C–C Bond Formation

By

Jennifer L. Bon

Doctor of Philosophy

Chemistry

_____

Simon B. Blakey, Ph.D.
Advisor

_____

Frederick Menger, Ph.D.
Committee Member

_____

Huw M. L. Davies, Ph.D.
Committee Member

Accepted:

_____

Lisa A. Tedesco, Ph.D.

Dean of the James T. Laney School of Graduate Studies

_____

Date

Design and Development of Novel Methods for C–H Functionalization for Amination and C–C Bond Formation

By

Jennifer L. Bon

B.S., James Madison University, 2009

Advisor: Simon B. Blakey, Ph.D.

An abstract of

A dissertation submitted to the Faculty of the

James T. Laney School of Graduate Studies of Emory University

in partial fulfillment of the requirements for the degree of

Doctor of Philosophy

in Chemistry

2014

Abstract

Design and Development of Novel Methods for C–H Functionalization for Amination and C–C Bond Formation

By

Jennifer L. Bon

Building complex molecules from simple starting materials is the heart of organic chemistry. Recently, the functionalization of generally unreactive C–H bonds has been a common target for such transformations due to their ubiquity and the atom economy associated with the transition. A family of ruthenium(II) 2,6-bis(imido)pyridyl complexes was developed for the intermolecular C–H amination of benzylic C–H bonds using sulfamate esters in a racemic fashion. A chiral derivative of the bisimidopyridyl ligand framework was proposed and progress was made toward its synthesis. Separately, molecular recognition was also explored as a means of inducing enantioselectivity in C–H amination reactions. A pyridinebisoxazoline-derived ligand was proposed and progress was made toward its synthesis. Carbon-carbon bond forming reactions for coupling aryl rings are of interest to the medicinal and materials communities. Methodology for the direct coupling of benzobisthiazoles and aryl halides using a copper/palladium co-catalytic system was developed and optimized, and the substrate scope was explored. This was expanded to the synthesis of cruciform structures and the functionalization of thiazolothiazole. Dehydrogenative carbon-carbon bond forming methodology for the synthesis of thiophene substituted benzothiazole derivatives was developed.

Design and Development of Novel Methods for C–H Functionalization for Amination and C–C Bond Formation

By

Jennifer L. Bon

B.S., James Madison University, 2009

Advisor: Simon B. Blakey, Ph.D.

A dissertation submitted to the Faculty of the

James T. Laney School of Graduate Studies of Emory University

in partial fulfillment of the requirements for the degree of

Doctor of Philosophy

in Chemistry

2014

Acknowledgments

This would not have been possible without the support and guidance of so many people. First and foremost Simon, thank you for inviting me to join your lab. You are an excellent advisor and teacher. I've learned so much from you these past five years. Dr. Davies and Dr. Menger, thank you for serving on my thesis committee. I've appreciated the guidance and suggestions you've had for me every step of the way. Dr. McDonald - thank you for agreeing to serve on my proposal committee, you were such a valuable resource. I would also like to thank Dr. Marder and his group at Georgia Tech for their collaboration, and the whole materials group of the Center of Selective C–H Functionalization for teaching me so much about materials chemistry.

I would like to thank Dr. Scott Lewis and Dr. Ben DeGraff for taking a chance on me as an undergrad and offering me places in their labs. Undergraduate research made me fall in love with science again and it may sound cliché but I truly would not be where I am today if it hadn't been for you.

To the many mentors I've had including Monya Ruffin, Tracy McGill, Meisa Salaita, and Jessica Barzilai among others, thank you for inspiring me and supporting me.

To my friends and family that have supported me throughout this whole process, thank you for your patience.

And last but certainly not least - to my labmates past and present - you guys are the best.

Table of Contents

1 Ruthenium Bis(imido)pyridyl Complexes as Catalysts for Achiral and Chiral Intramolecular Amination 1

1.1 Introduction.....1

1.2 Proposed Ligand Framework 5

1.3 Results and Discussion. 7

1.4 Optimization ligand design and reaction conditions for amination 11

1.5 Examination of substrate scope in C–H amination using catalyst **25**.....15

1.6 Bis(imido)pyridyl Complexes as Catalysts for Chiral Intramolecular Amination ...

.....19

1.7 Chiral Ligand Synthesis.....20

1.8 Synthesis of Mixed Ferrocenes in a Model System.....24

1.9 Conclusion 25

2 Intermolecular Amination via a Molecular Recognition Catalyst 27

2.1 Introduction.....27

2.2 Molecular recognition in enantioselective catalysis 29

2.3 Proposed Molecular Recognition Catalyst.....33

2.4 Ligand Synthesis.....34

2.5 Conclusion 41

3 Benzodipyrrolidone *via* C–H Functionalization.....42

3.1 Introduction 42

3.2 Proposed C–H Functionalization Synthesis.....49

3.3 Synthesis and Exploration of the Model System 52

3.4 Synthesis of BDP core *via* C–H Functionalization.....54

3.5 Conclusion 58

4 Synthesis of 2,6-Difunctionalized Benzobisthiazoles *via* C–H Functionalization 59

4.1 Introduction 59

4.2 C–H Functionalization of Benzothiazole 62

4.3 Initial Exploration of Difunctionalization of BBT 66

4.4 Optimization of coupling conditions 68

4.5 Probing the Scope of Aryl halides Amenable to the C–H Functionalization of **14** 80

4.6 Synthesis of Cruciform Structures *via* 2,6-Difunctionalization of Benzobisthiazole **14**.....86

4.7 C–H Functionalization of Thiazolothiazole 91

4.8 Conclusions 92

5 Dehydrogenative Cross Coupling of Benzothiazole.....94

5.1 Introduction 94

5.2 Results and Discussion 100

5.3 Optimization of dehydrogenative cross coupling of **1** with 2- methylthiophene 102

5.4 Conclusion.....117

6 Experimental Procedures and Characterization 119

6.1 General Information.....119

6.2 Chapter 1 Procedures and Characterization.....121

6.3 Chapter 2 Procedures and Characterization.....149

6.4 Chapter 3 Procedures and Characterization 158

6.5 Chapter 4 Procedures and Characterization 166

6.6 Chapter 5 Procedures and Characterization.....187

References.....192

List of Schemes

Scheme 1.1. Hofmann-Löffler-Freytag reaction for the formation of cyclic and fused amines 2

Scheme 1.2. Transition metal catalyzed nitrene insertion reaction by Breslow and Gellman 2

Scheme 1.3. Transfer hydrogenation from Dayan and Cetinkaya 6

Scheme 1.4. Epoxidation from Dayan and Cetinkaya 6

Scheme 1.5. Cyclopropanation from Bianchini and Lee 7

Scheme 1.6. Synthesis of **9** from aniline and 2,6-diacetyl pyridine 7

Scheme 1.7. Amination using a Ru bis(imido)pyridyl catalyst 8

Scheme 1.8. Synthesis of catalyst **26** 12

Scheme 1.9. Examination of catalyst **26** for C–H amination 12

Scheme 1.10. Synthesis of complex **28** 15

Scheme 1.11. 28 as a catalyst for C–H amination 15

Scheme 1.12. literature precedent for C–H amination with carbamates 17

Scheme 1.13. Carbamate substrate in Ru bisimido catalytic system 17

Scheme 1.14. Lebel's *N*-tosyloxycarbamate cyclization 18

Scheme 1.15. Synthesis and exploration of *N*-tosyloxycarbamate **38** in C–H amination with **25** 18

Scheme 1.16. Synthesis of **44** 21

Scheme 1.17. Cleavage of ethylbenzene chiral directing group to synthesize **45** from **44** ... .22

Scheme 1.18. Synthesis of $Rh_2((S)\text{-nttl})_4$ **(47)** 23

Scheme 1.19. Aziridinaiton of indene with **45** 23

Scheme 2.1. Initial attempts at intermolecular amination using intramolecular conditions and catalyst **1**.....28

Scheme 2.2. Crabtree and Brudvig's oxidation of ibuprofen.....30

Scheme 2.3. Molecular recognition catalyst for epoxidation.....30

Scheme 2.4. Regiocontrol in intermolecular epoxidation 32

Scheme 2.5. Formation of anhydride **10** from Kemp's triacid.....35

Scheme 2.6. Formation of **16** from diethyloxalate and acetone via **15**, and conversion of **16** into brominated pyridine **14**.....36

Scheme 2.7. Formation of boronic acid for potential Suzuki coupling.....36

Scheme 2.8. Formation of stannane **19** for Stille coupling 37

Scheme 2.9. Stille coupling for the formation of **20** 37

Scheme 2.10. Stille coupling for the formation of **21** 37

Scheme 2.11. Generation of the Cbz protected stannane **24** 37

Scheme 2.12. Stille coupling of **24** and **14**, and formation of acid chloride **27** from **26** 38

Scheme 3.1. Synthesis of benzodipyrrolidone by Wudl and coworkers 47

Scheme 3.2. Synthesis of thiophene-flanked benzodipyrrolidone **20** by Wudl and coworkers.....48

Scheme 3.3. Synthesis of thiophene-flanked benzodipyrrolidone **24** by Rumer and coworkers.....49

Scheme 3.4. Carbene insertion with phenyl as the donor group from Davies to generate **25**.....50

Scheme 3.5. Hu and coworkers use of 2-thiopheno derived donor/acceptor carbene for rhodium catalyzed insertion.....50

Scheme 3.6. Carbene insertion with thiophene as the donor group from Davies 50

Scheme 3.7. Amination of from M. Christina White 51

Scheme 3.8. Amination from Liu and coworkers.....51

Scheme 3.9. Synthesis of diazo **28** 53

Scheme 3.10. Carbene insertion and initial attempt at hydrolysis 53

Scheme 3.11. Hydrolysis of ester **29** to **30**.....53

Scheme 3.12. Synthesis of lactam **32** from **30** 54

Scheme 3.13. Synthesis of (*S*,*S*-*trans*)-**33** from cyclohexadiene and diazo **28** 57

Scheme 3.14. Hydrolysis, amination and attempted cyclization to form **9**.....58

Scheme 4.1. Synthesis of BBT-thiophene polymer **12** by Jenekhe.....61

Scheme 4.2. Synthesis of **13** from Evers and coworkers 61

Scheme 4.3. Synthesis of **14** and substituted benzobisthiazole **16** from Jefferies-EL 62

Scheme 4.4. Palladium free synthesis of **18** from Miura 62

Scheme 4.5. Synthesis of **17** from phenylboronic acid from Liu and coworkers 64

Scheme 4.6. Z.-Z. Huang's methodology for the synthesis of **17**.....65

Scheme 4.7. Thiazole ring closing C–H functionalization.....65

Scheme 4.8. Synthesis of benzobisthiazole (**14)** 66

Scheme 4.9. Direct application of Z.-Z. Huang's conditions for the synthesis of **20** 67

Scheme 4.10. Synthesis of compounds **23-26**.....86

Scheme 4.11. Synthesis of **27** by Jeffries-EL.....87

Scheme 4.12. Synthesis of benzobisoxazole cruciform **29** by Miljanić.....87

Scheme 4.13. Synthesis of **30** from **14** 88

Scheme 4.14. Attempted Sonagashira coupling of **30** with 1-hexyne to generate **31** 88

Scheme 4.15. Suzuki coupling of **30** with 4-nonylphenylboronic acid to generate 4,8-functionalized product **32** 89

Scheme 4.16. Synthesis of potassium trifluoroborate salt **33**.....89

Scheme 4.17. Synthesis of **34** from **30** *via* Suzuki cross coupling.....90

Scheme 4.18. Synthesis of **35** from **34** *via* C–H functionalization 91

Scheme 4.19. Synthesis of **36** by Rannou and coworkers.....92

Scheme 4.20. Synthesis of **37** by Yamashita and coworkers 92

Scheme 4.21. Synthesis of **37** via C–H functionalization 92

List of Figures

Figure 1.1. Intramolecular amination by Che and coworkers using ruthenium porphyrin catalyst (**5**).....3

Figure 1.2. Du Bois's intramolecular amination using catalyst $Rh_2(esp)_2$ (**6**).....3

Figure 1.3. Du Bois's intramolecular amination using catalyst $Rh_2(S\text{-nap})_4$ (**7**).....4

Figure 1.4. Blakey's intramolecular amination using ruthenium indenyl pybox catalyst, **8**.....5

Figure 1.5. Bis(imido)pyridyl framework.....6

Figure 1.6. Metalation of ligand **9** with ruthenium dimer **10** to generate **11**.....8

Figure 1.7. Synthesis of bisimido ligands **9**-**17**.....9

Figure 1.8. Catalysts synthesized to study the effects of sterics, electronics, and ancillary ligands on conversion of **12** to **13**.....10

Figure 1.9. Examination of complexes **18**-**25** as catalysts for C–H amination.....12

Figure 1.10. Solvent screen in C–H amination with sulfamate ester **12**.....13

Figure 1.11. Effect of additives on the C–H amination of sulfamate **12**.....14

Figure 1.12. Exploration of the scope of sulfamate esters in C–H amination with catalyst **25**.....16

Figure 1.13. Sites for modification of the bis(imido)pyridine ligand core.....19

Figure 1.14. Proposed ferrocene derived ruthenium complex.....19

Figure 1.15. Retrosynthesis of ligand **40**.....20

Figure 1.16. Crystal structure of sulfonimidamide **44**.....22

Figure 1.17. Attempted synthesis of mixed ferrocene **49**.....24

Figure 1.18. Delayed addition of cyclopentadieneide to improve the synthesis of mixed ferrocenes **49**, **52**, and **53** 25

Figure 2.1. Proposed radical mechanism of C–H amination 27

Figure 2.2. Energy barriers (in kcal/mol) for H abstraction from various positions on simple sulfamate esters 28

Figure 2.3. Molecular recognition catalyst developed in the Crabtree and Brudvig lab ..29

Figure 2.4. Hydrogen bonding in Crabtree and Brudvig's system of molecular recognition for oxidation.....30

Figure 2.5. Bach's molecular recognition catalyst.....31

Figure 2.6. Bach and coworker's intermolecular epoxidation 32

Figure 2.7. Achiral non-hydrogen bonding catalyst used for regiocontrol control experiments 32

Figure 2.8. Our proposed molecular recognition catalyst **8** for intermolecular amination... 33

Figure 2.9. Proposed scheme for intermolecular amination 34

Figure 2.10. Retrosynthetic plan for the molecular recognition pybox ligand **9** 35

Figure 2.11. (a) Test system for the formation of the indenyl pybox. (b) Actual system for the formation of the indenyl pybox 39

Figure 2.12. Conditions for the formation of indenyl amide **29** 39

Figure 2.13. Optimization of amide bond formation using CDI.....40

Figure 2.14. Optimization of amide bond formation using CDI to generate **27** 40

Figure 3.1 Common DPP polymers 42

Figure 3.2 Synthesis of common BDP polymers **1** and **2** 43

Figure 3.3 Structures of **3** and **4** showing dihedral angels of 38° and 12.7° respectively ....
.....44

Figure 3.4 Onset of 735 nm and max 639 nm **5**, onset of 796 nm and max 630 nm for **6**, onset of 860 nm and max 722 nm for **7**, onset of 1006 nm and max 1562 nm for **8**.....45

Figure 3.5. Aza-BDP dye used by Müllen.....45

Figure 3.6 Alkylated BDP polymer **9** with a LUMO of -3.53 eV, acylated BDP polymer **10** with a LUMO level of -3.84 eV.....46

Figure 3.7. Retrosynthesis of BDP using C–H functionalization.....49

Figure 3.8. Polymer containing a thiophene substituted at the 2-position is fully conjugated, while a polymer containing a 3-substituted thiophene is cross conjugated ...51

Figure 3.9. Model system for amination of an internal olefin.....52

Figure 3.10. Iron porphyrin catalyst **26** used for amination of on internal olefin to generate **27**.....52

Figure 3.11. Synthesis of double insertion product **33**.....55

Figure 3.12. Synthesis of (*S*)-**29** and (*R*)-**29** from diazo **28** using Rh_2(*R*-DOSP)$_4$ and Rh_2(*S*-DOSP)$_4$.....55

Figure 3.13. Analysis of matched/mismatched effect on synthesis of **33**.....56

Figure 3.14. Crystal structure of (*S,S-trans*)-**33**.....57

Figure 4.1 Benzobisthiazole-based small molecules and polymers.....59

Figure 4.2 Cross-linked benzobisthiazole polymers.....60

Figure 4.3. Drug targets that incorporate benzothiazole.....60

Figure 4.4. Amgen process methodology for the synthesis of **18** using PXPd and CuI(Xantphos).....63

Figure 4.5. Catalytic cycle proposed by J. Huang and coworkers 63

Figure 4.6. Ofial's methodology for the formation of **18** from phenyl silanes and stannanes 64

Figure 4.7. Initial exploration of aryl bromide scope of the C–H functionalization of **14** 67

Figure 4.8. Optimization of C–H difunctionalization of **14** starting from J. Huang's conditions 68

Figure 4.9. Effect of $Pd(OAc)_2$ and PXPd with $Cu(OAc)_2$ and CuI•Xantphos on the synthesis of **20**.....69

Figure 4.10. Comparison of precoordinated copper and precoordinated palladium with and without additional phosphine ligand in the synthesis of **20** 70

Figure 4.11. Efficacy of copper(I) versus copper(II) in the synthesis of **20** 71

Figure 4.12. Examination of DMF, xylenes, DMA, toluene and dioxane as solvents for the conversion of **14** to **20**.....72

Figure 4.13. Impact of temperature on conversion of **14** to **20**.....73

Figure 4.14. Impact of increasing loading of copper at 115 °C on the conversion to **20** .74

Figure 4.15. Palladium free control reaction.....75

Figure 4.16. Proposed mechanism for the formation of **21** 76

Figure 4.17. Exploration of decreased temperature and high copper loading on the conversion of **14** to **20**.....77

Figure 4.18. Examination of monodentate ligands in the synthesis of **20** 78

Figure 4.19. Examination of bidentate ligands in the synthesis of **20** 79

Figure 4.20. Attempted coupling of **14** with bromonapthtalenediimide **25** to give **26**.....83

Figure 4.21. Attempted Molander-type cross couplings of **30** with **33** 91

Figure 5.1. Dehydrogenative cross coupling of heterocycles giving heterocoupling, homocoupling and undesired regioisomers. 94

Figure 5.2. Coupling of benzothiazole (**1**) with 1-methylimidazole to give **2** and with 4,5-dimethylthiazole to give **3** by Ofial and coworkers.....95

Figure 5.3. Coupling of thiazoles with oxazoles using palladium and copper developed by You and coworkers 96

Figure 5.4. Coupling of thiazoles with oxazoles using only copper developed by You and coworkers.....96

Figure 5.5. Copper only coupling of azoles from Wang.....97

Figure 5.6. Zhang and coworkers coupling of activated arenes with benzothiazoles with copper.....98

Figure 5.7. Zhang and coworkers coupling of activated arenes.....99

Figure 5.8. Yang's functionalization of thiophenes. 99

Figure 5.9. Effect of ligands on dehydrogenative cross coupling of **1** and 2-methylthiophene 104

Figure 5.10. Effect of amine ligands on dehydrogenative cross coupling on **1** and 2-methylthiophene 105

Figure 5.11. Effect of changing palladium sources on dehydrogenative cross coupling of **1** with 2-methylthiophene 108

Figure 5.12. Effect of using the HBF_4 salt of tricyclohexyphosphine and triphenylphosphite ligands on dehydrogenative cross coupling of **1** with 2-methylthiophene 109

Figure 5.13. Effect of phosphine ligands with disparate steric demands on dehydrogenative cross coupling of **1** with 2-methylthiophene 110

Figure 5.14. Exploration of phosphine versus phosphine oxide ligands for dehydrogenative cross coupling of **1** with 2-methylthiophene 111

Figure 5.15. Effect of the ratio of copper to phosphine ligand on dehydrogenative cross coupling of **1** with 2-methylthiophene 112

Figure 5.16. Effect of various Cu(II) complexes as catalysts for the copper sources on dehydrogenative cross coupling of **1** with 2-methylthiophene 114

Figure 5.17. Effect of changing sterics and electronics on the pyridine base on dehydrogenative cross coupling of **1** with 2-methylthiophene 115

List of Tables

Table 4.1. Exploration of aryl halide substrate scope for the C–H functionalization reaction with **14**. All yields are isolated.....81

Table 4.2. Aryl halide substrates to probe the limitations of the C–H functionalization methodology. All yields are isolated 84

Table 5.1. Coupling of **1** with 3-hexylthiophene, difluorobenzothiadiazole, pentafluorobenzene and 2-methylthiophene 101

Table 5.2. Examination of oxidants for the oxidative coupling of **1** and 2-methylthiophene 102

Table 5.3. Effect of solvents on dehydrogenative cross coupling of **1** and 2-methylthiophene 106

Table 5.4. Effect of carbonate bases on dehydrogenative cross coupling of **1** with 2-methylthiophene 116

Table 5.5. Effect of changing equivalencies of pyridine on dehydrogenative cross coupling of **1** with 2-methylthiophene.....117

Table 5.6. Effect of changing equivalencies of 2-methylthiophene on the selectivity of the dehydrogenative cross coupling of **1** with 2-methylthiophene 117

Abbreviations

Ac	acetyl
AcOH	acetic acid
9-BBN	9-borabicyclo[3.3.1]nonene
BBT	benzobisthiazole
BDP	benzodipyrrolidone
Boc	*tert*-butoxycarbonyl
Bn	benzyl
Br	broad
BT	benzothiazole
n-BuLi	*n*-butyllithium
Cbz	benzyloxycarbonyl
d	doublet
dba	dibenzylideneacetone
DCE	1,2-dichloroethane
DCM	dichloromethane
DIBAL-H	diisobutylaluminum hydride
DMA	*N*,*N*-dimethylacetamide
DMAP	*N*,*N*-dimethylaminopyridine
DME	1,2-dimethoxyethane
DMF	*N*,*N*-dimethylformamide
DMPU	*N*,*N*'-dimethyl-*N*,*N*'-propylene urea

DMSO	dimethylsulfoxide
DPP	diketopyrrolopyrrole
DPPB	1,4-bis(diphenylphosphino)butane
DPPF	1,1’-bis(diphenylphosphino)ferrocene
DPPP	1,4-bis(diphenylphosphino)propane
EDCI	1-ethyl-3-(3-dimethylaminopropylcarbodiimide)
equiv.	equivalent
ESI	electrospray ionization
EtOAc	ethyl acetate
HOBt	1-hydroxybenzotriazole
HRMS	high resolution mass spectroscopy
KHMDS	potassium *bis*(trimethylsilyl)amide
LA	Lewis acid
LAH	lithium aluminum hydride
LDA	lithium diisopropylamide
LiHMDS	lithium *bis*(trimethylsilyl)amide
m	multiplet
mmol	millimole
Naph	naphtyl
NBS	*N*-bromosuccinimide
NIS	*N*-iodosuccinimide
NMO	*N*-methylmorpholine *N*-oxide
NMR	nuclear magnetic resonance

OFET	organic field effect transistor
OPV	organic photovoltaic
OTFT	organic thin film transistor
Ph	phenyl
pybox	bis(oxazolinyl)pyridine
ppm	parts per million
PTSA	*para*-toluenesulfonic acid
q	quartet
quint	quintet
rt	room temperature
s	singlet
sep	septet
t	triplet
TBDMS	*tert*-butyldimethylsilyl
TBDPS	*tert*-butyldiphenylsilyl
Tf	trifluoromethanesulfonyl
TFA	trifluoroacetic acid
TFAA	trifluoroacetic anhydride
THF	tetrahydrofuran
TMS	trimethylsilyl
Ts	*para*-toluenesulfonyl

1. Ruthenium Bis(imido)pyridyl Complexes as Catalysts for Achiral and Chiral Intramolecular Amination

1.1 Introduction

Due to the prevalence and importance of nitrogen-containing molecules in nature, there is great interest in developing efficient means of stereoselectively and chemoselectively introducing nitrogen functionality into minimally functionalized organic molecules.[1] Until recently the synthetic community has relied heavily on techniques such as nucleophilic displacement and imine alkylation to build nitrogen functionality.[2] C–H amination provides an attractive alternative route to the installation of nitrogen functionality in place of relatively unreactive C–H bonds.

Traditional methods of C–H amination, or the conversion C–H bonds into C–N bonds, have been around for decades. One of the earliest examples is the Hofmann-Löffler-Freytag reaction for the formation of cyclic amines (Scheme 1.1).[3] Treatment of *N*-halo amines with strong acid and heat or light generates the δ- or γ-ammonium salt. The ammonium salt can then be cyclized by treatment with base to generate a heterocycle. Primary *N*-halogenated amines can be converted into the corresponding piperidines and pyrrolidines (Scheme 1.1a), while secondary halogenated amines form bridged and fused ring systems (Scheme 1.1b). Although this methodology has been used for decades, it requires the use of strong acid, strong base and the generation of a free radical, limiting its utility to simple substrates.

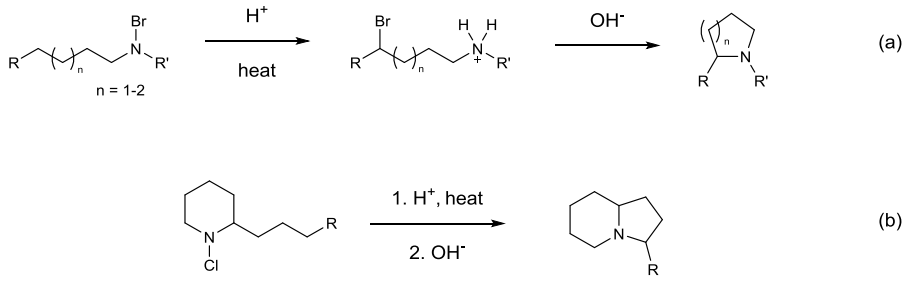

Scheme 1.1. Hofmann-Löffler-Freytag reaction for the formation of cyclic and fused amines.

The first example of transition metal-catalyzed amination of a C–H bond was reported by Breslow and Gellman in the early 1980's.[4] Treatment of 2,5-diisopropylbenzylsulfonimide (**1**) with diacetoxy iodobenzene gave them iminoiodiane (**2**) (Scheme 1.2). Breslow and Gellman explored both porphyrin and nonporphyrin catalysts in combination with three different transition metals: iron, manganese and rhodium. They found that a nonporphyrin rhodium catalyst, $Rh_2(OAc)_4$, afforded the best ratio of desired insertion product **3** (86%) to the undesired elimination product **4** (0.2%), with only 5 % of starting iminoiodiane **2** recovered.

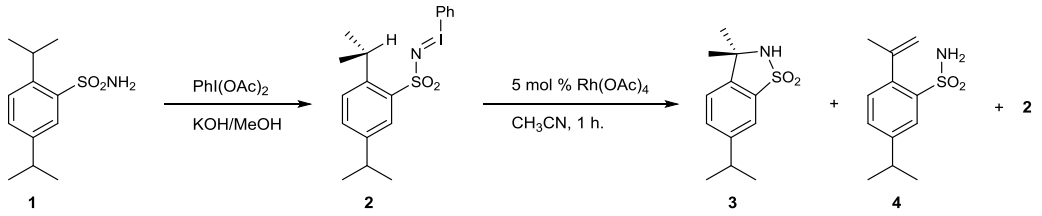

Scheme 1.2. Transition metal catalyzed nitrene insertion reaction by Breslow and Gellman.

Some years later, Che and coworkers developed a new method for intramolecular C–H amination using ruthenium porphyrin based catalyst **5** to carry out similar reactions (Figure 1.1).[5] They used sulfamate esters instead of sulfonamides and oxidized the amine *in situ* using $PhI(OAc)_2$.

entry	substrate	product	% yield[b]	% ee[b]
1[b]	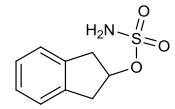	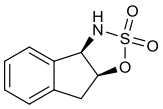	57	71
2			53	81
3[c]			39	82
4[d]			39	77
5[b]	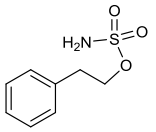	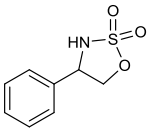	53	69
6			43	82
7[c]			35	87
8	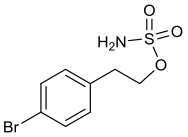	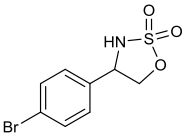	46	78
9[c]			31	86

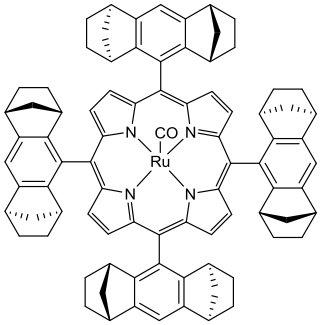

5

Figure 1.1. Intramolecular amination by Che and coworkers using ruthenium porphyrin catalyst (**6**). (a) General conditions: 80 °C in C_6H_6, 2 h; **5**:substrate:$PhI(OAc)_2$:Al_2O_3 0.1:1:1.4:2.5. (b) In CH_2Cl_2 at 40 °C. (c) Reaction temperature 5 °C. (d) In toluene at 0 °C.

The Du Bois group also developed a successful means of intramolecular C–H amination that provides good enantiomeric induction.[6] They developed both dirhodium carboxylate (**6**) and carboxamidate (**7**) catalysts that allow for amination of various benzylic, allylic, and a few examples of alkyl C–H bonds in good yields and with high selectivity (Figures 1.2 and 1.3).[7]

entry	substrate	product	% yield[a]
1	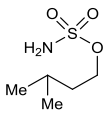	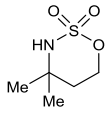	92
2[b]	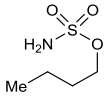	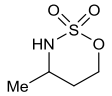	90

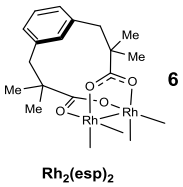

6

$Rh_2(esp)_2$

Figure 1.2. Du Bois's intramolecular amination using catalyst $Rh_2(esp)_2$ (**6**). (a) Reactions were carried out using 0.15 mol% catalyst **6**, $PhI(OAc)_2$, and MgO in CH_2Cl_2. (b) With 1 mol% of catalyst.

entry	substrate	product	% yield[a]	% ee[b]
1	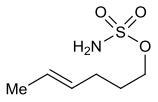	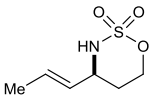	51	54
2	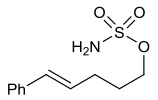	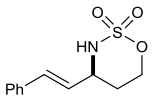	48	12
3	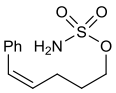	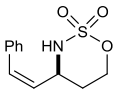	55	84
4 R=H	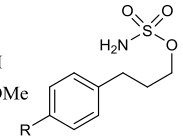	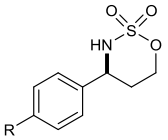	85	92
5 R=OMe			89	83
6	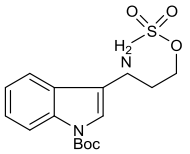	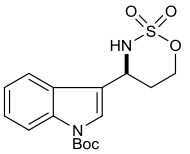	98	92

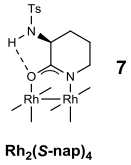

7

Rh_2(*S*-nap)$_4$

Figure 1.3. Du Bois's intramolecular amination using catalyst Rh_2(*S*-nap)$_4$ (**7**) shown at right. (a) Reactions were carried out using 2 mol% catalyst **7**, PhI=O and 3Å MS in CH_2Cl_2. (b) Determined by chiral HPLC.

These results were consistent with the results of Che, which showed that protons at electron rich benzylic positions were most amenable towards amination.

Concurrently, Blakey and coworkers developed a method for intramolecular enantioselective C–H amination using ruthenium (II)-pybox catalyst **8** (Figure 1.4).[8] With their conditions, Blakey and coworkers observed slightly lower yields than Du Bois found with catalysts **6** and **7**, but better enantioselectivity than DuBois observed with **7** for many of the same substrates (Figure 1.4).

entry	substrate	product	% yield[a]	% ee[b]
1[c]	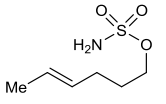	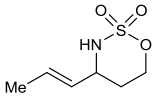	60	89
2 R=H	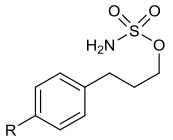	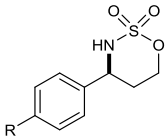	93	80
3[c] R=H			84	84
4[c] R=OMe			68	90
5[d] R=Br			60	88[d]
6	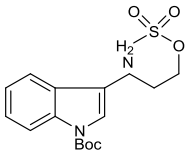	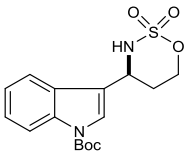	58	92

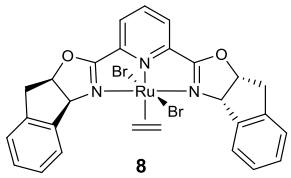

8

Figure 1.4. Blakey's intramolecular amination using ruthenium indenyl pybox catalyst, **8**. (a) Reactions were carried out using 5 mol% catalyst **8**, $PhI(O_2C^tBu)_2$ (1.1 equiv), AgOTf (5 mol %), MgO (2.3 equiv), C_6H_6, 22 °C, 24 h. (b) Determined by HPLC on a chiral stationary phase. (c) Reaction carried out at 4 °C. (d) Absolute stereochemistry determined by X-ray crystallography, all other configurations assigned by analogy.

Although these techniques offer powerful methods of benzylic and allylic functionalization, there remain few options for alkyl functionalization and enantioselctivities above 90% are rarely seen.

1.2 Proposed Ligand Framework

In order to address limited substrate scope, challenges with enantioselective amination, and difficulties in ligand synthesis we hypothesized using the 2,6-bis(imido)pyridyl framework as an alternative (Figure 1.5). 2,6-Bis(imido)pyridyl ligands are isoelectronic with pybox, being neutral six electron donors but unlike pyboxes they are redox active.[9] This activity might help stabilize a reactive metallonitrene intermediate and open up new substrate classes. The bis(imido)pyridyl framework is also highly tunable and easily synthesized in one step from commercially available precursors

which makes them strong candidates as ligand systems.[9,10]

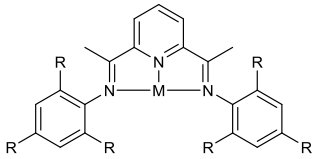

Figure 1.5. Bis(imido)pyridyl framework.

A number of bis(imido)pyridyl metal complexes have been synthesized with a wide variety of first and second row transition metals. Although their reactivity in C–H amination reactions has not been reported, they have been used in a number of other applications.

Ruthenium bis(imido)pyridyl complexes have been used by Dayan and Cetinkaya for the transfer hydrogenation of acetophenone from 2-propanol (Scheme 1.3)[10] and for the epoxidation of cyclohexene with PhIO as the oxidant (Scheme 1.4).[11]

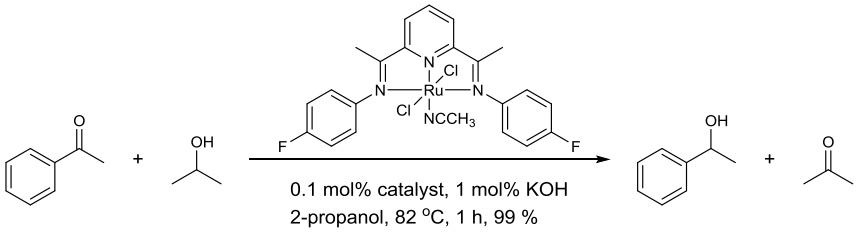

Scheme 1.3. Transfer hydrogenation from Dayan and Cetinkaya.

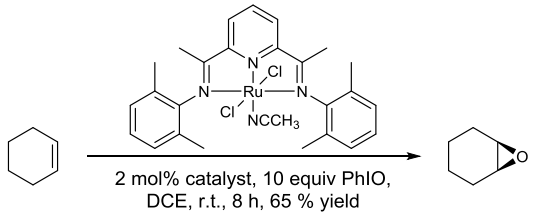

Scheme 1.4. Epoxidation from Dayan and Cetinkaya.

Bianchini and Lee demonstrated the use of Ru(II) bis(imido)pyridyl complexes for cyclopropanation of styrene using ethyldiazoacetate (Scheme 1.5).[12]

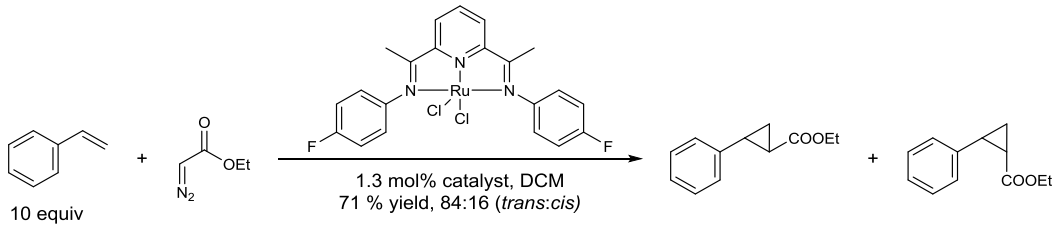

Scheme 1.5. Cyclopropanation from Bianchini and Lee.

1.3 Results and Discussion

In our studies we chose to start from the simplest ruthenium bis(imido)pyridyl complex and explore both electronic and steric substitutions on the aniline rings. The phenyl derivative of the ligand **9** was synthesized from 2,6-diacetyl pyridine and aniline according to the literature procedure in 81 % yield (Scheme 1.6).[6]

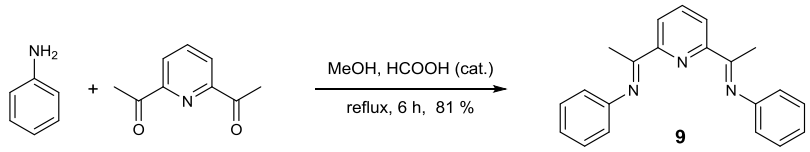

Scheme 1.6. Synthesis of **9** from aniline and 2,6-diacetyl pyridine.

The metal complex was generated from ruthenium dimer **10**. Initial attempts to synthesize compound **11** using literature procedure from Dayan and Cetinkaya by combining ligand **9** and ruthenium dimer complex **10** in refluxing ethanol under an atmosphere of ethylene were unsuccessful.[10] However switching the solvent to DCM gave the desired compound in 7 % yield (Figure 1.6).

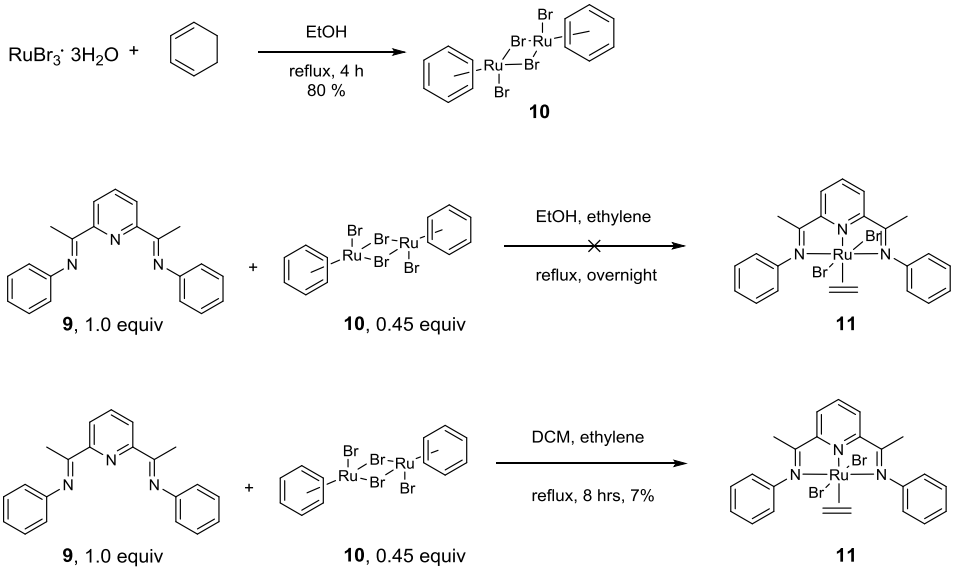

Figure 1.6. Metalation of ligand **9** with ruthenium dimer **10** to generate **11**.

Initial reactivity tests with sulfamate ester **12** were conducted using conditions established from exploration with ruthenium pybox catalysts.[8] Using 5 mol% catalyst loading, $PhI(OAc)_2$ as an external oxidant and DCM as solvent 34 % conversion to **13** was obtained based on crude NMR analysis (Scheme 1.7).

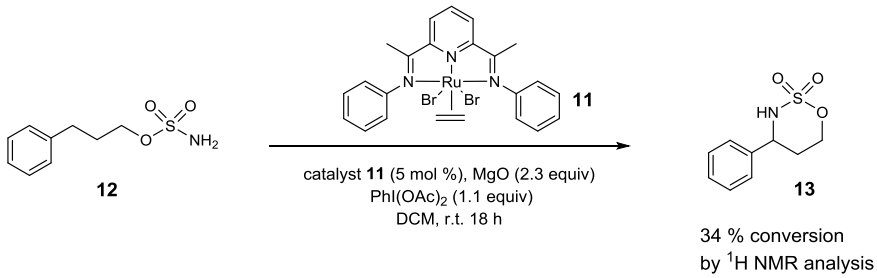

Scheme 1.7. Amination using a Ru bis(imido)pyridyl catalyst.

This led us to synthesize a series of ligands with varying electronic and steric properties to explore the effect on the conversion (Figure 1.7).[13]

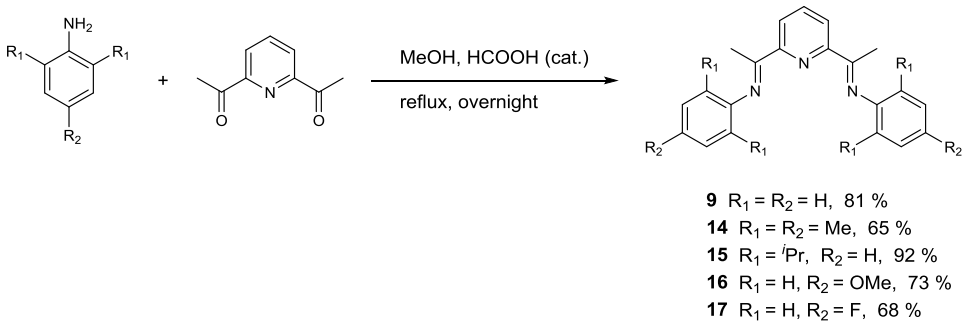

Figure 1.7. Synthesis of bisimido ligands **9**-**17**.

To give three distinct levels of steric inhibition, a ligand with methyl groups at the ortho positions (**14**) and a ligand with isopropyl groups at the ortho positions (**15**) were made to compare to ligand **9**. To examine the impact of the electronics of the ligand on the conversion of **12** to **13** the *p*-methoxy substituted ligand (**16**) and the *p*-fluoro substituted ligand (**17**) were also synthesized.

In addition to substituents on the bis(imido)pyridyl ligand, the impact of the halogen ligand was examined by synthesizing both the bromide and chloride complexes, and the ancillary ligand was changed from ethylene to acetonitrile and to carbon monoxide giving the series of complexes shown in Figure 1.8. Because the yield of **18** with the chloride ligands was significantly greater than the yield of **19** with the bromide ligands, chloride was chosen as the standard halogen ligand for all other ligand systems. Chloride complexes were synthesized from dichloro(*p*-cymene)ruthenium(II) dimer in the same manner that the bromide complexes were synthesized from the di-μ-bromobis[(benzene)bromoruthenium(II)]. Because carbon monoxide complex **18** could be synthesized more efficiently than ethylene complex **20** or acetonitrile complex **21**, carbon monoxide was chosen as the basis of comparison for ancillary ligands.

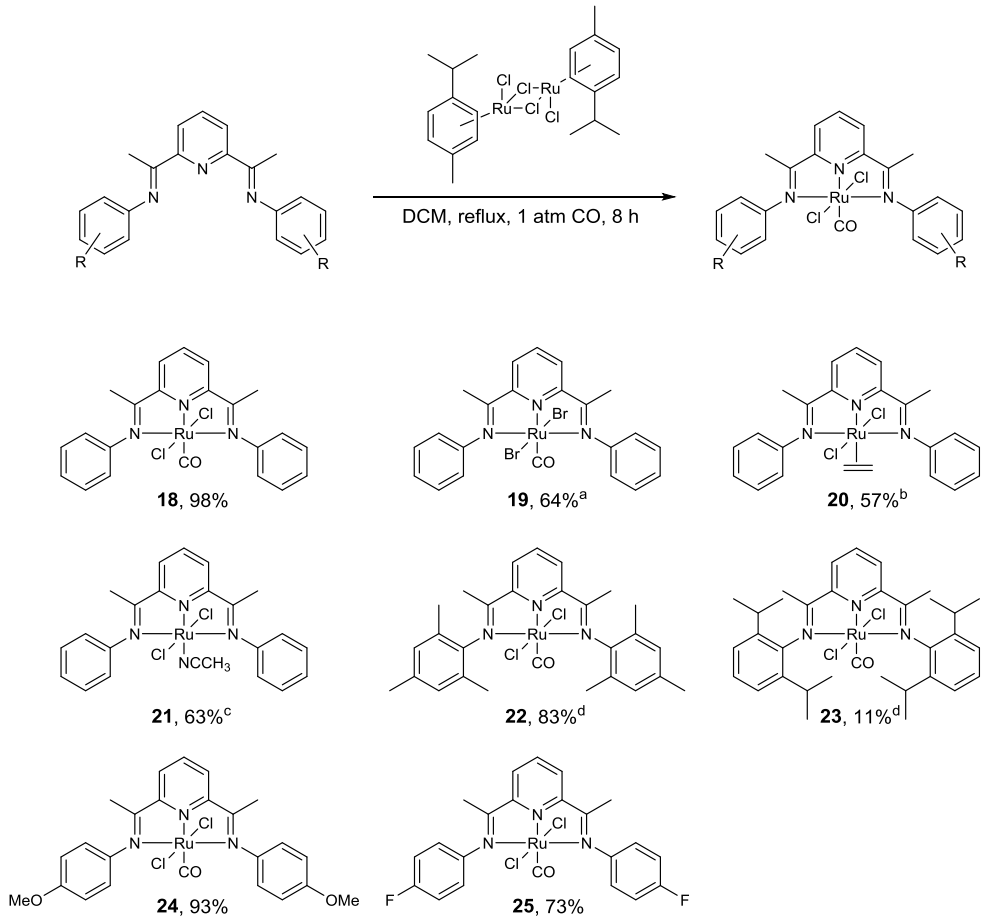

Figure 1.8. Catalysts synthesized to study the effects of sterics, electronics, and ancillary ligands on conversion of **12** to **13**. (a) metalation performed with di-μ-bromobis[(benzene)bromoruthenium(II)] (**10**) instead of dichloro(*p*-cymene)ruthenium(II) dimer (b) metalation conducted under 1 atm ethylene instead of CO (c) worked up in 1:1 CH_3CN/DCM d) reaction run for 5 days in THF at 150 ^oC in a sealed tube.

To synthesize the complexes with acetonitrile as the ancillary ligand the metallation reaction was carried out under an atmosphere of nitrogen. After the solvent was removed the residue was dissolved into a 1:1 mixture of DCM:MeCN. Synthesis of the triphenylphosphine derivative was also attempted but with little success. None of the desired product could be isolated from the reaction mixture.

Ligands **22** and **23** required forcing conditions to drive the reaction to completion due to increased steric demands. After 5 days at 150 °C in THF in a sealed tube **22** was synthesized in 83 % yield while similar conditions for **23** only gave 11 % yield with a large amount of starting ligand recovered.

1.4 Optimization of ligand design and reaction conditions for amination

The entire catalyst series was examined in the C–H amination reaction with sulfamate ester **12** to give cyclized product **13** (Figure 1.9). Comparing entries 1 and 2, changing the halogen makes little difference in conversion. Changes in the ancillary ligand did have a small impact conversion for the reaction. Moving from CO to ethylene to MeCN increased the conversion from 26 %, to 27 % to 32 % respectively (entries 1, 4 and 3). Sterically blocking the *ortho*-positions on the aromatic ring was detrimental to conversion. Even methyl groups were enough to bring conversion down from 26 % to 18 %. The biggest impact on reaction efficiency was from the introduction of an electronically withdrawing group *para* to the imine. Having fluorine at that position increased the conversion to 48 % while a donating *p*-methoxy group decreased the conversion to 16 % relative to the unsubsituted ligand.

12 **13**

entry	catalyst	% conversion[a]
1	**18**	26 %
2	**19**	24 %
3	**20**	27 %
4	**21**	32 %
5	**22**	18 %
6	**23**	19 %
7	**24**	16 %
8	**25**	48 %

Figure 1.9. Examination of complexes **18**-**25** as catalysts for C–H amination. (a) Conversion determined as a ratio of starting material to product by GC.

With these data in mind an "ideal" catalyst was hypothesized to include both the MeCN ancillary ligand and the electron withdrawing *p*-fluoro group. Catalyst **25** was synthesized from ligand **17** in 85 % yield (Scheme 1.8).

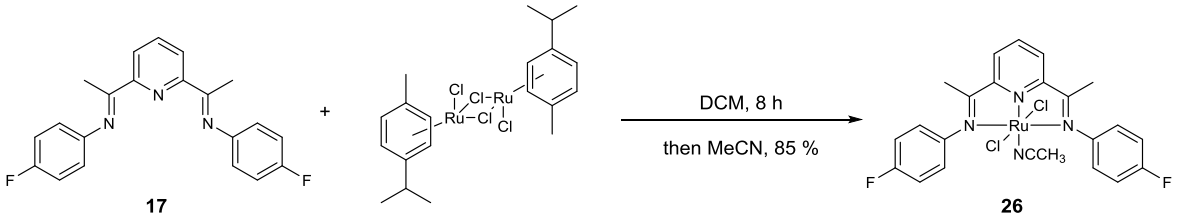

17 **26**

Scheme 1.8. Synthesis of catalyst **26**.

Unfortunately catalyst **26** did not significantly differ from **25**, giving 44 % conversion by GC (Scheme 1.9) where **25** gave 48 %.

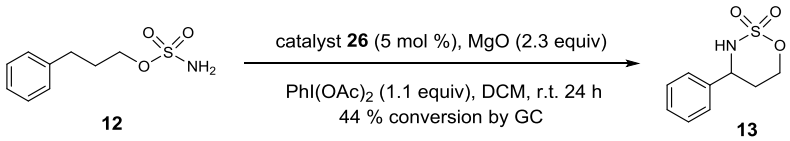

12 **13**

Scheme 1.9. Examination of catalyst **26** for C–H amination.

A brief solvent screen was carried out using catalyst **26** (Figure 1.10). Ethereal solvents diethyl ether and THF both gave poor conversions, 13 % and <5 % respectively (entries 2 and 3). Hexanes also performed poorly providing <5 % conversion. Benzene was not as good as the initial choice of DCM (25 % versus 44 %) but trifluorotoluene did improve conversion to 51 %. Trifluorotoluene was then examined in conjunction with catalyst **25** and afforded the best conversion at 73 % (entry 8). Therefore, all further optimization was carried out with trifluorotoluene and catalyst **25**.

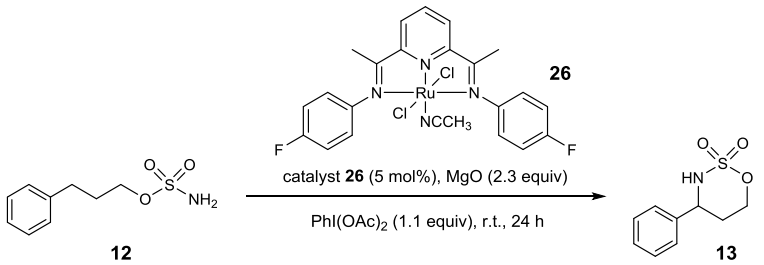

entry	solvent	% conversion[a]
1	DCM	44 %
2	diethylether	13 %
3	THF	>5 %
4	hexanes	>5 %
5	benzene	25 %
6	toluene	40 %
7	trifluorotoluene	51 %
8[b]	trifluorotoluene	73 %

Figure 1.10. Solvent screen in C–H amination with sulfamate ester **12**. (a) based on the ratio of product to starting material as determined by GC. (b) reaction was carried out using 5 mol% **25** (with L=CO).

In further optimization of this reaction the role of the additives was examined (Figure 1.11). It was found that MgO was beneficial but not necessary for the reaction to proceed; 73 % conversion was observed with it and 56 % without (entries 1 and 2). The choice of oxidant appears to play a more significant role. Moving from $PhI(OAc)_2$ to $PhI(OPiv)_2$ to $PhI(TPA)_2$ decreased conversions from 73 % to 46 % 34 % (entries 1, 3,

and 4). Increasing equivalents of the oxidant from 1.1 to 2.0 equiv also suppressed conversion (entry 5). Running the reaction at elevated temperature (40 °C) hindered the reaction, causing it to stop at 28 % conversion. Adding catalyst and oxidant in two equal batches 12 hours apart was also explored but the conversion was not improved.

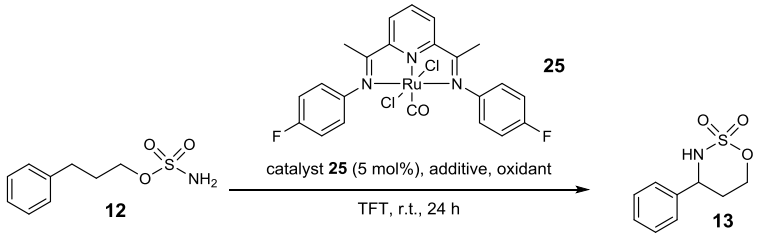

entry	additive	oxidant	% conversion[a]
1	MgO (2.3 equiv)	$PhI(OAc)_2$ (1.1 equiv)	73
2	none	$PhI(OAc)_2$ (1.1 equiv)	56
3	MgO (2.3 equiv)	$PhI(OPiv)_2$ (1.1 equiv)	46
4	MgO (2.3 equiv)	$PhI(TPA)_2$ (1.1 equiv)	34
5	MgO (2.3 equiv)	$PhI(OAc)_2$ (2.0 equiv)	38
6[b]	MgO (2.3 equiv)	$PhI(OAc)_2$ (1.1 equiv)	28
7[c]	MgO (2.3 equiv)	$PhI(OAc)_2$ (1.1 equiv)	41

Figure 1.11. Effect of additives on the C–H amination of sulfamate **12**. A) Based on the ratio of product to starting material as determined by GC. B) Reaction carried out at 40 °C. C) Catalyst and oxidant added in two equal batches 10 h apart.

Because addition of an electron withdrawing group to the *para*-position of the ligand was one of the most impactful changes, it was hypothesized that a stronger electron withdrawing group on the ring would be beneficial. To this end, the *p*-nitro derivative **28** was synthesized from *p*-nitroaniline and diacetylpyridine to give ligand **27** in 10 % yield, **27** was then metallated under standard conditions to give **28** in 34 % yield (Scheme 1.10).

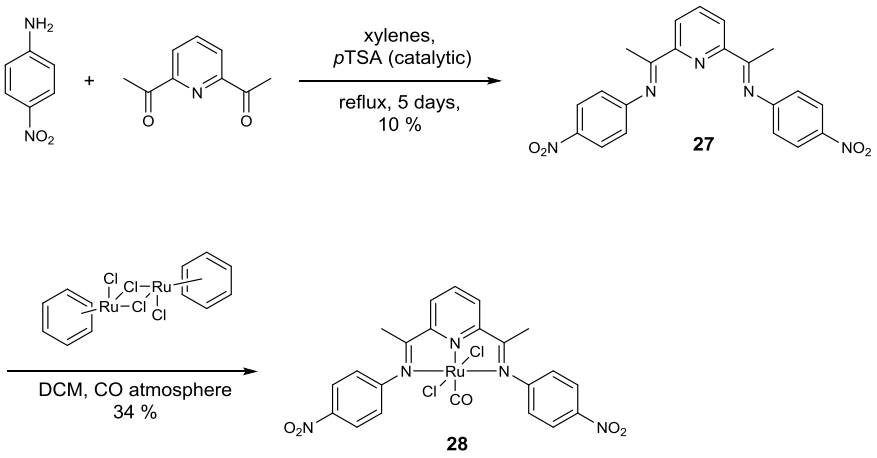

Scheme 1.10. Synthesis of complex **28**.

Unfortunately when **28** was tested in the model reaction only 35 % conversion of **12** to **13** was observed (Scheme 1.11).

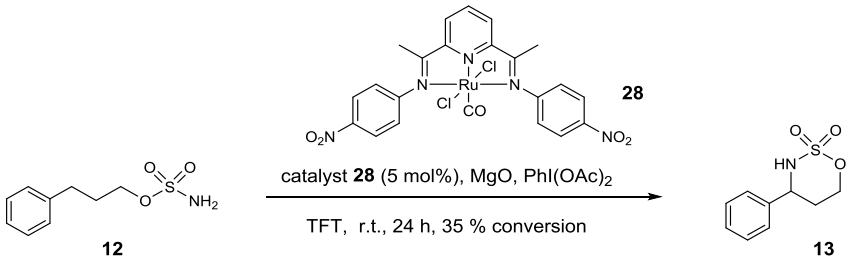

Scheme 1.11. **28** as a catalyst for C–H amination.

1.5 Examination of substrate scope in C–H amination using catalyst 25

To explore the generality of this catalyst system, other sulfamate esters were explored (Figure 1.12). *o*-Methoxyphenyl sulfamate ester gave only 15 % isolated yield of cyclized product **29** while the same substrate with Ru(indenylpybox) gave 68 % yield.[8] The Boc-protected indole produced a similar result with an 11 % isolated yield **30**. Indenyl sulfamate was tested in this system to see if 5-membered ring formation would

be tolerated or even preferred in this system, unfortunately only a trace of desired product **31** was observed. Both the *cis* and *trans* alkenes were explored to see if allylic positions were tolerated as well as the benzylic positions. The *cis*-alkene afforded only trace quantities of 6-membered ring product **32** but interestingly gave 6 % of 9-membered ring product **33** that results from insertion into the methyl position. The *trans* alkene gave only trace quantities of 6-membered ring product **34** and none of the 9-membered ring product was observed.

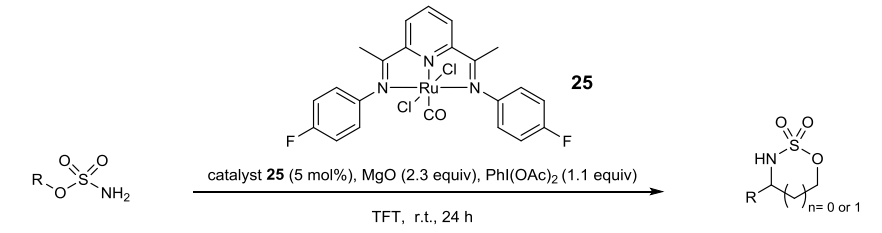

Sulfamate ester	Product	Isolated Yield
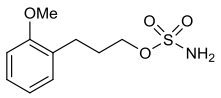	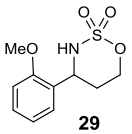 **29**	15 %
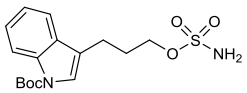	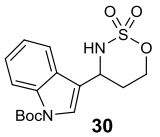 **30**	11 %
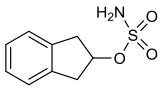	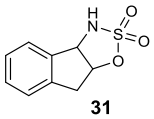 **31**	trace
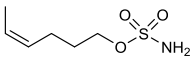	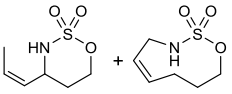 **32** **33**	**32** trace **33** 6%
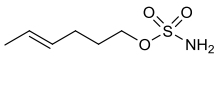	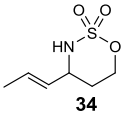 **34**	trace

Figure 1.12. Exploration of the scope of sulfamate esters in C–H amination with catalyst **25**.

Seeing that little progress was to be made from changing sulfamates, a larger step was taken to other substrate classes. The first to be explored was a carbamate which has previously been used by the Hayes group with dirhodium catalysts to give allylic C–H amination in moderate yield (Scheme 1.12).[14]

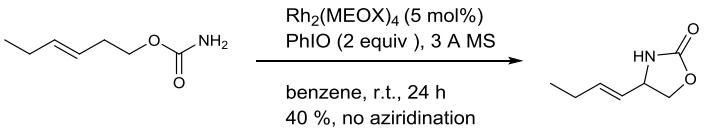

Scheme 1.12. Literature precedent for C–H amination with carbamates.

As our success with allylic positions had been limited, we chose to test phenethyl carbamate instead. Phenethyl carbamate **35** was synthesized based on the literature procedure from 2-phenylethanol and sodium isocyanate in 54 % yield (Scheme 1.13).[15] When **35** was tested in our catalytic system none of the cyclized product **36** was observed, in fact there was almost complete recovery of starting material after 24 hours.

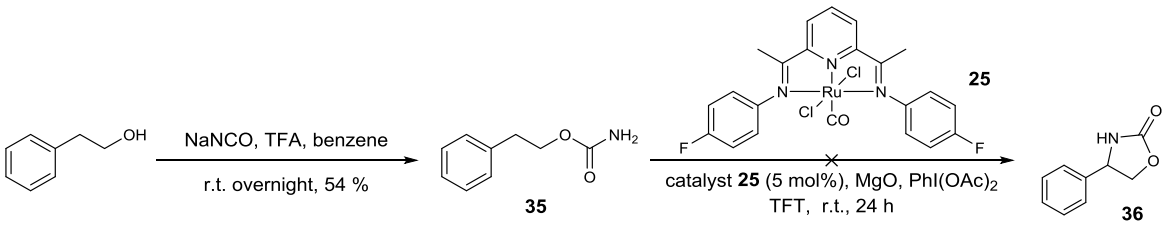

Scheme 1.13. Carbamate substrate in Ru bis(imido)pyridyl catalytic system.

Lebel and coworkers used *N*-tosyloxycarbamates to generate 5-membered rings from amination at benzylic positions in good yield (Scheme 1.14)[16] so we hypothesized they might be compatible with our ruthenium bis(imido)pyridyl system.

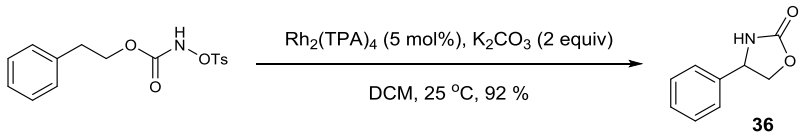

Scheme 1.14. Lebel's *N*-tosyloxycarbamate cyclization.

The substrate was synthesized based on the literature procedure starting from 2-phenylethanol.[17] Formation of the hydroxycarbamate **37** was followed by tosylation to give *N*-tosyloxycarbamate **38** in 8 % over two steps (Scheme 1.15). When **38** was reacted with catalyst **25** under standard conditions no reaction was observed and starting material was recovered almost quantitatively.

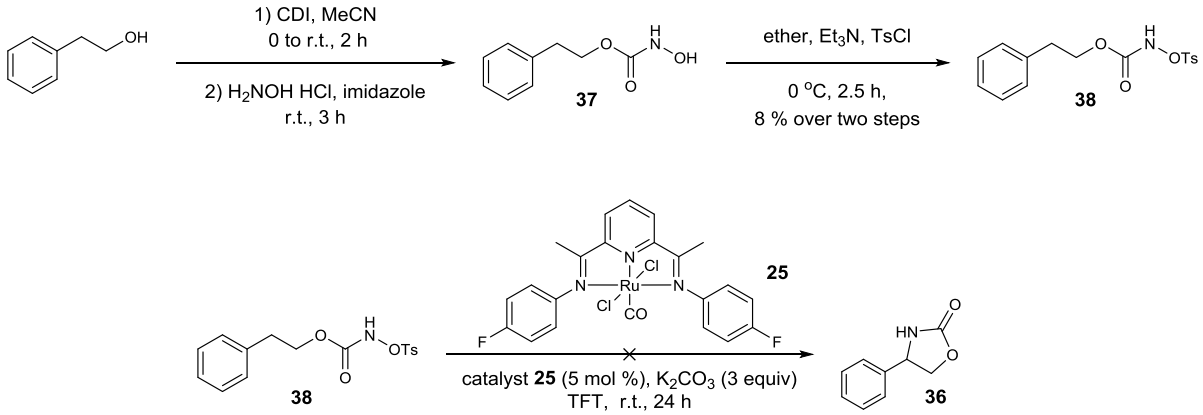

Scheme 1.15. Synthesis and exploration of *N*-tosyloxycarbamate **38** in C–H amination with **25**.

This system provides a robust, tunable and easy to access (the catalyst is synthesized in just two steps from commercial materials) method for C–H amination of benzylic C–H bonds with sulfamate esters. Due to its limited substrate scope and very modest yields it is unlikely to have a major impact in the field of achiral amination but if the ligand system could be made chiral there is still potential for it to move the field of enantioselective amination forward.

1.6 Bis(imido)pyridyl complexes as Catalysts for Chiral Intramolecular Amination

There are four positions one could conceivably modify on the bis(imido)pyridyl ligand in order to install chirality (Figure 1.13). First, it would be possible to append a chiral group to the back of the pyridine core such that it would hang above or below the ring creating a chiral pocket (Figure 1.13, R). Second, one could install a chiral center alpha to the imine instead of a methyl group (R'). Both of these modes have two major concerns in that they dramatically complicate ligand synthesis and the chiral group would be far removed from the active site. A third option is to put chiral groups at the *ortho* or *meta* positions on the ring (R''), but based on the results with methyl or isopropyl groups at the *ortho* positions those ligands would probably be very difficult to metallate and give low yields in the amination reaction. This leaves the fourth possibility, building chirality above and below the ring (R''') leaving ferrocene derivatives as the most promising option (Figure 1.14).

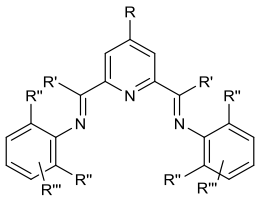

Figure 1.13. Sites for modification of the bis(imido)pyridine ligand core.

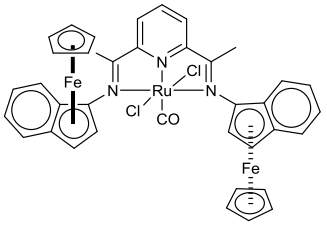

39

Figure 1.14. Proposed ferrocene derived ruthenium complex.

In order to make enantiopure catalyst we first desired enantiopure amino ferrocene (Figure 1.15). Retrosynthetically, enantiopure amino ferrocene **41** would come from the separation of two diastereomers of mixed amino ferrocene **42**. Diastereromers **42** in turn would come from the metallation of cyclopentadiene and the aminoindene **43**. Aminoindene **43** would come from the C–H amination of indene with chiral sulfonimidamide **44**. If azirdination is favored over amination, or if gives a mixture of aziridation and amination, this would be easily addressed since treatment of the aziridine with base should open the aziridine ring giving the desired amination product.

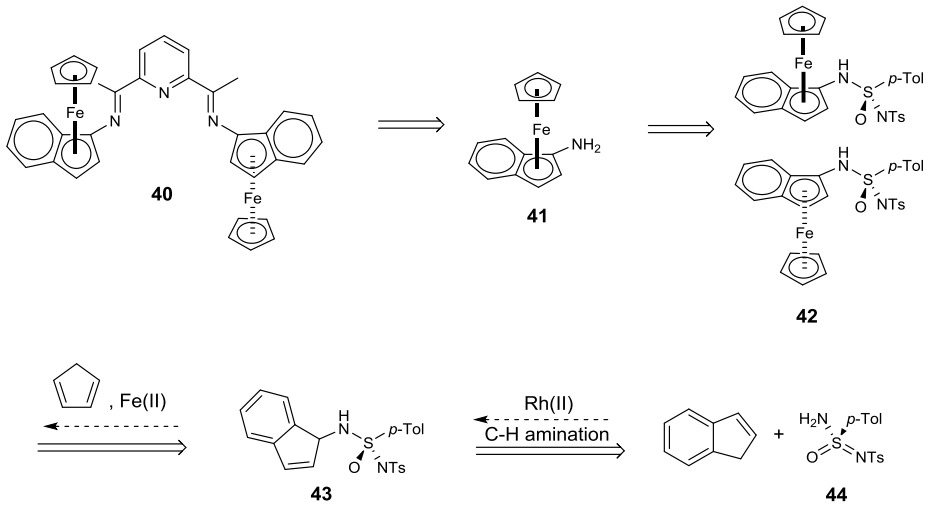

Figure 1.15. Retrosynthesis of ligand **40**.

1.7 Chiral Ligand Synthesis

Chiral sulfonimidamide **44** was synthesized based on the literature precedent from Dauban and Dodd.[18] Is it unclear which enantiomer of methylbenzylamine was used by Dauban and Dodd. They state "(*R*)-(-)-α-methybenzylamine" but the *R* enantiomer is the

(+) enantiomer. The (*S*)-(-)-α-methylbenzylamine was used in this work. **44** was synthesized from sodium *p*-toluenesulfinate, chloramine T trihydrate and (*S*)-(-)-α-methylbenzylamine in 48 % yield (Scheme 1.16).

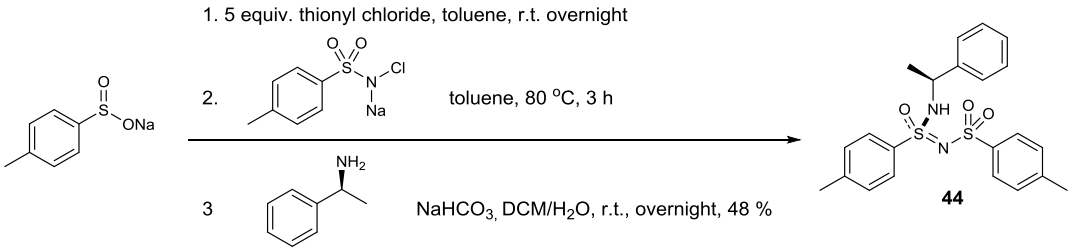

Scheme 1.16 Synthesis of **44**.

The material was recrystallized to purity from EtOH and a crystal structure was obtained to confirm the stereochemistry (Figure 1.16). This established different stereochemistry around sulfur than was reported by Dauban and Dodd indicating that they must have started with the (*R*)-(+) enantiomer of methylbenzylamine.

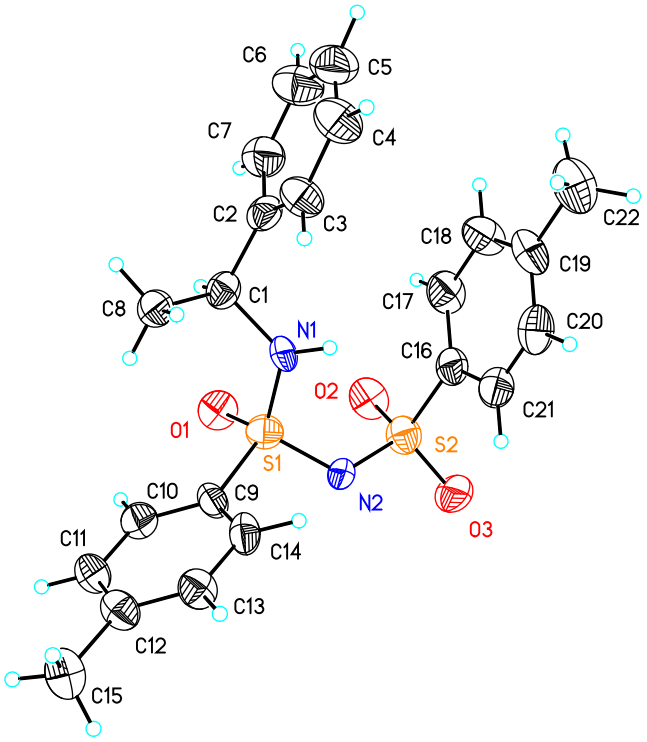

Figure 1.16. Crystal structure of sulfonimidamide **44**.

The ethylbenzene side chain was cleaved from the chiral auxiliary using TFA in 86 % yield to give sulfonimidamide **45** (Scheme 1.17).

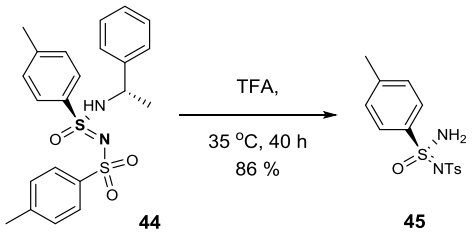

Scheme 1.17. Cleavage of ethylbenzene chiral directing group to synthesize **45** from **44**.

The Dauban and Dodd amination reactions using **45** are almost exclusively carried out with their $Rh_2((S)\text{-nttl})_4$ catalyst (**47**) so the catalyst was synthesized was according to their procedure.[18] Ligand **46** was made from the dehydration of L-^{t}leucine with 1,8-naphthalic anhydride which proceeded in 80 % yield. This was followed by ligand exchange with $Rh_2(OAc)_4$ in refluxing chlorobenzene to give **47** in 35 % yield (Scheme 1.18).

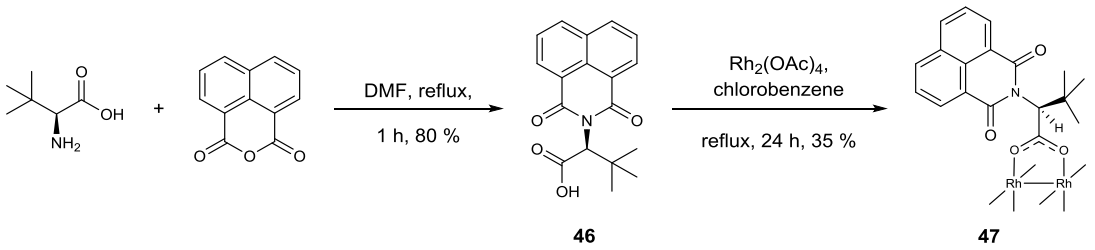

Scheme 1.18. Synthesis of $Rh_2((S)\text{-nttl})_4$ (**47**).

With both catalyst **47** and sulfonimidamide **45** in hand, the amination of indene was attempted using standard conditions (Scheme 1.19).[18] In this case the aziridine was the major product isolated and none of the amination product was observed. Dauban and Dodd report a strong match/mismatch effect between their catalyst and the sulfonamide, so if the other enantiomer of **45** is synthesized, the reaction efficiency may be greatly improved.[18]

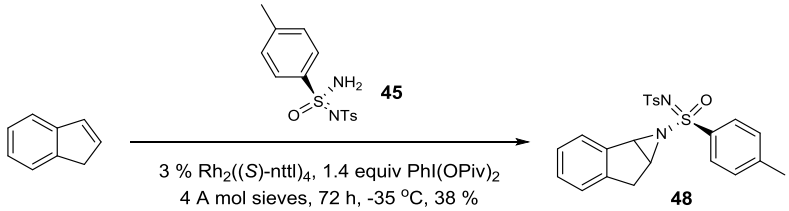

Scheme 1.19. Aziridinaiton of indene with **45**.

1.8 Synthesis of Mixed Ferrocenes in a Model System

During the synthesis of the sulfonimidamide we sought to establish a method for the synthesis of mixed ferrocenes. Working with a model system based on the synthesis from King and coworkers,[19] sodium hydride was added to a mixture of indene and cyclopentadiene at -78 °C (Figure 1.17). After removing the ice bath and warming the reaction to 45 °C, $FeCl_2$ was added. Even though indene and cyclopentadiene were used in a 1.2:1 ratio, ferrocene was the only product isolated, none of the mixed ferrocene **49** was observed. In case formation of the indenide **51** was the problem, indenide and cyclopentadienide **50** were synthesized separately and then added to $FeCl_2$ based on the procedure from Fu and coworkers,[20] but again, none of the desired product was formed, only 60 % of pure ferrocene was observed.

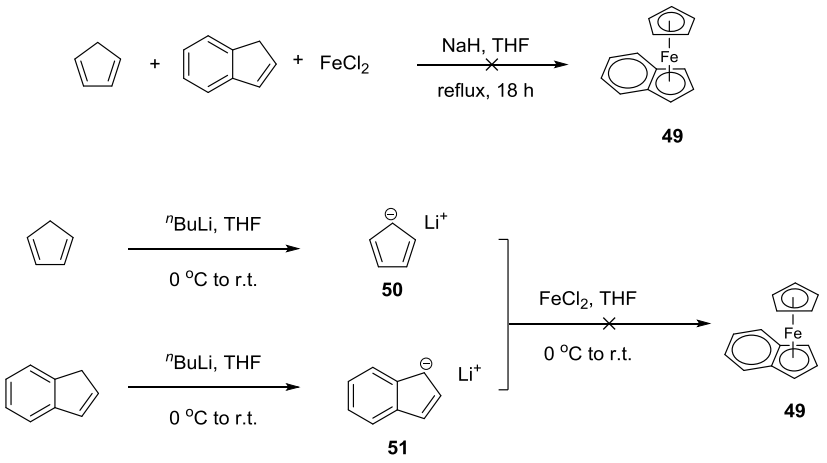

Figure 1.17. Attempted synthesis of mixed ferrocene **49**.

Because ferrocene was still being formed, indenide was combined with $FeCl_2$ and left to react for 16 hours before the addition of cyclopentadienide in order to give the indenide time to coordinate before ferrocene could be formed (Figure 1.18). Although

there was indication by crude NMR that some of the desired mixed ferrocene **49** had been formed by this method, the product decomposed upon purification and while standing in air.

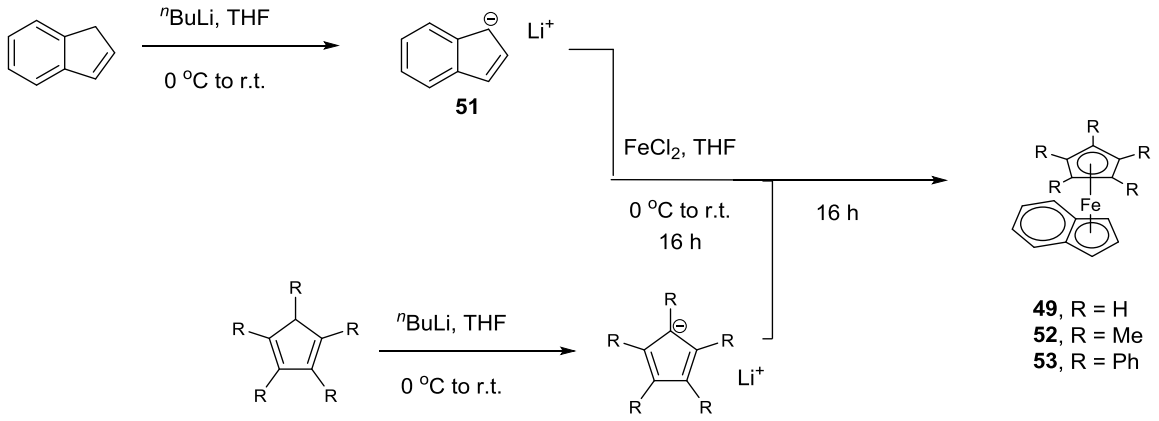

Figure 1.18. Delayed addition of cyclopentadieneide to improve the synthesis of mixed ferrocenes **49**, **52**, and **53**.

In order to form a more stable mixed ferrocene the pentamethylcyclopentadiene and the pentaphenylcyclopentadiene derivatives were both made (**52** and **53**).[21] In both of these cases some product was observed by crude NMR analysis but the material decomposed upon standing in air preventing purification or full characterization.

1.9 Conclusions

Considering the problems with stability of the mixed ferrocene and the problems with bulky groups on the bisiminopyridyl ligands both with metallation and reactivity the challenges of this problem started to outweigh the benefits. If the ferrocene was poorly stable it's unlikely that it would survive the dehydrative imine formation to make the

ligand. In the previous work bulky ligands needed forcing conditions for metallation on to ruthenium and with the pentaphenyl derivative being the most stable of the ferrocene it would be a struggle to metallate if went at all. The increasing difficulty of catalyst synthesis leads to an impractical catalysts.

There are also potential problems with reactivity. Under oxidative reaction conditions whatever ferrocene was incorporated into the ligand would likely be oxidized from Fe(II) to Fe(III). The bulkier ligands gave lower conversions suggesting this ligand may also perform poorly. With limited substrate scope and never observing conversions above 73 % even under the best of conditions, a new paradigm for intramolecular enantioselective C–H amination was needed.

2. Intermolecular Amination via a Molecular Recognition Catalyst

2.1 Introduction

Based on our work on intramolecular amination, the Blakey lab sought to expand that methodology to intermolecular amination. We had proposed a radical mechanism (Figure 2.1), but had little direct evidence of it so we consulted with computational collaborator, Jamal Musaev, on potential paths forward into intermolecular amination. His preliminary studies suggest that to help force hydrogen abstraction from an external source it would be beneficial to not have hydrogens in the β or γ positions on the sulfamate as their abstractions would be lower in energy than abstract from an external source (in the case of these calculations, methane) (Figure 2.2). His data also indicated the importance of the bisimido in stabilizing the transition state.

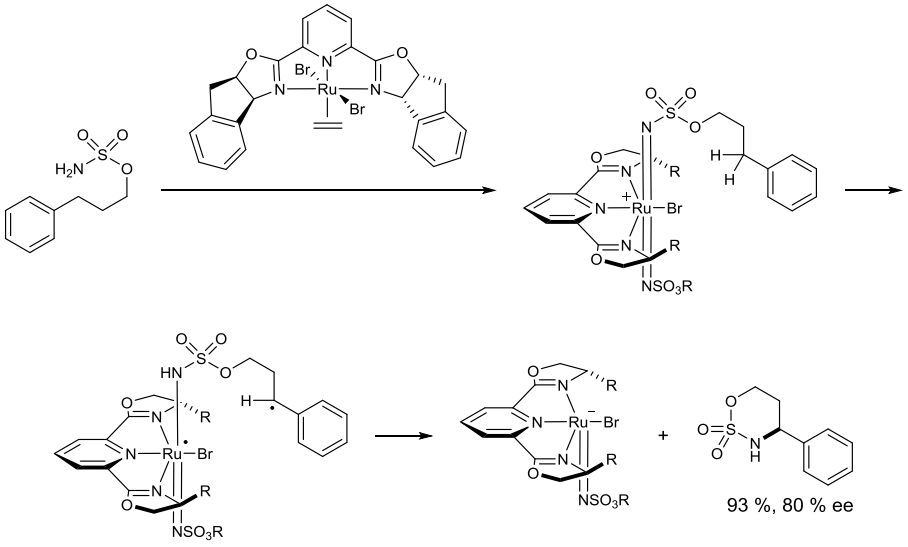

Figure 2.1. Proposed radical mechanism of C–H amination.

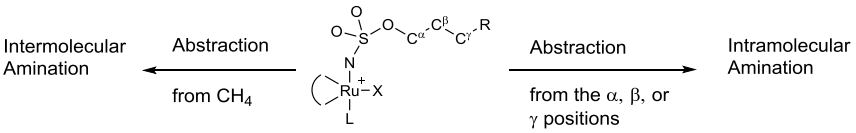

		C^{α}-H	C^{β}-H	C^{γ}-H	external (CH_4)
R = H	L = $NSO_2OCH_2CH_2H$	21.8	21.7	-----	21.8
R = CH_3	L = $NSO_2OCH_2CH_2CH_3$	21.4	15.9	14.4	17.7
R = CH_2Ph	L = $NSO_2OCH_2CH_2CH_2Ph$	21.4	14.7	5.8	20.8
R = CH_2Ph	L = CO	20.4	15.1	12.3	

Figure 2.2. Energy barriers (in kcal/mol) for H abstraction from various positions on simple sulfamate esters.

With this information in hand, preliminary attempts at intermolecular amination were carried out using the ideal conditions developed for intramolecular amination and sulfamate esters with no hydrogens that could be easily abstracted. Results were poor even with a large excess of substrate; very low yields, no enantioselectivity, and over oxidation products were found (Scheme 2.1).

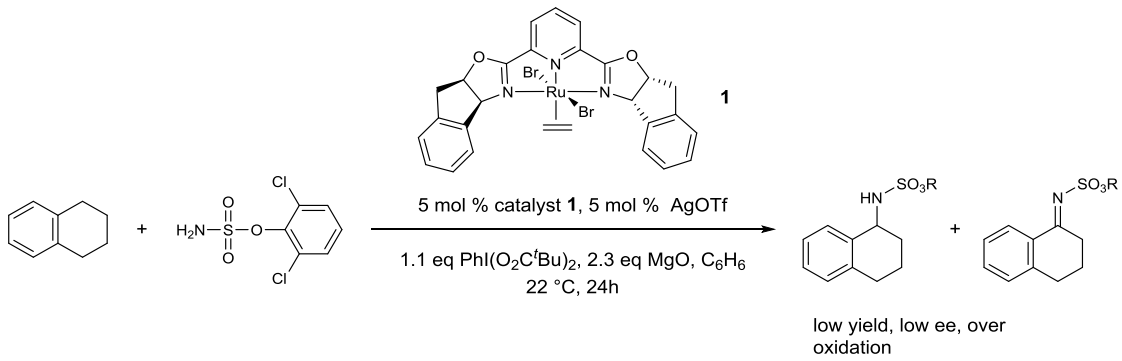

Scheme 2.1. Initial attempts at intermolecular amination using intramolecular conditions and catalyst **1**.

One possible explanation for this data is that the second step of the proposed mechanism (the hydrogen abstraction) is occurring, but the newly formed radical was diffusing away before the third step (the rebound), in which the new C–N bond is formed, could take place. This means if there was a way to hold the substrate in place for both the

abstraction and the rebound, this methodology could be very effective. This lead to the idea of designing a catalyst with molecular recognition capabilities.

2.2 Molecular recognition in enantioselective catalysis

Relatively few labs are using molecular recognition in the context of C–H functionalization. Most use steric control or some form of pi stacking, but molecular recognition has great precedent in enzyme catalyzed reactions.[22,23] One of the best examples of molecular recognition for C–H functionalization comes from Crabtree and Brudvig who have designed a catalyst that uses molecular recognition to oxygenate saturated C–H bonds in a regioselective manner.[24] They use a nonporphyrin Mn(μ-O)$_2$ catalyst (**2**) and a carboxylic acid molecular recognition unit (Figure 2.3). The catalyst is made up of a terpyridine moiety, a phenyl linker and a U-turn group derived from Kemp's triacid which has the key carboxylic acid functionality.

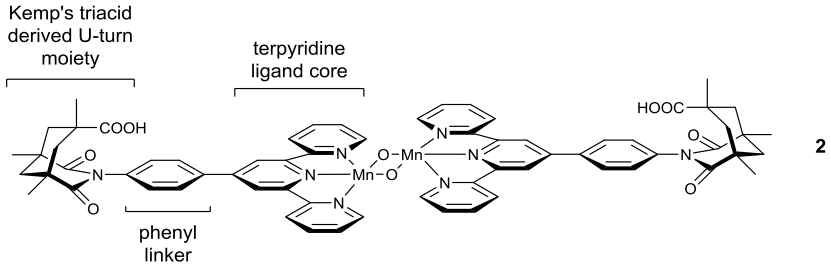

Figure 2.3. Molecular recognition catalyst developed in the Crabtree and Brudvig lab.

The molecular recognition arises via reversible hydrogen bonding between the carboxylic acid moiety on the catalyst and the corresponding carboxylic acid group on the substrate (Figure 2.4). This interaction positions a benzylic C–H directly above the active site of the Mn catalyst.

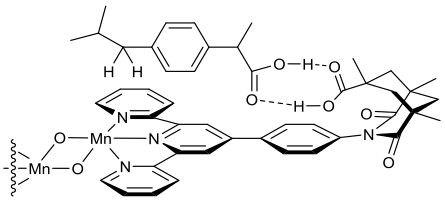

Figure 2.4. Hydrogen bonding in Crabtree and Brudvig's system of molecular recognition for oxidation. Molecular modeling studies suggest only 4.5 Å between the benzylic carbon and the metal center.

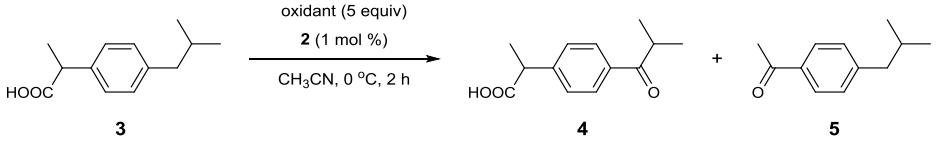

Scheme 2.2. Crabtree and Brudvig's oxidation of ibuprofen.

With the carboxylic acid functionality in place they observed 98.5 % selectivity for desired product **4** and only 1.5 % of undesired product **5** (Scheme 2.2). On the other hand, when the U-turn and molecular recognition moiety on the catalyst is replaced with just a phenyl group, removing all of the molecular recognition ability, they only generated 76 % of **4** and 24 % of **5**.[25] The same is true when the molecular recognition unit is in place but the system is flooded with excess acetic acid, thus tying up the recognition site. With 1 mol % catalyst loading they consistently observed low catalyst turnover (50-60) due to catalyst self-oxidation. By decreasing the equivalence of catalyst to 0.1 mol % they increased the turnover number to as much as 710, and the percent conversion also increased from 53 % to 58 % (from 50 % to 71 % at room temperature).

They found that the same catalyst can be used for controlling epoxidation of double bonds (Scheme 2.3).[22]

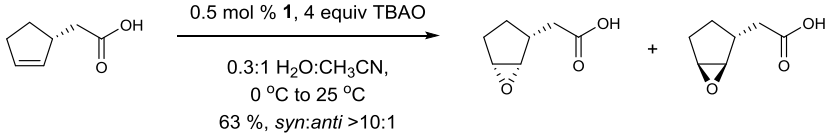

Scheme 2.3. Molecular recognition catalyst for epoxidation.

Although Crabtree and Brudvig get excellent results with the carboxylic acid molecular recognition moiety, they did not explore other hydrogen bond donor/acceptor pairs which could open up whole new classes of substrates with only minor structural changes to their catalyst.

The Bach group has also used molecular recognition for the enantio- and regioselective epoxidation of double bonds.[26] They use ruthenium porphyrin based catalyst **6** with a lactam based molecular recognition unit to bind lactam containing substrates, most commonly 3-vinylquinolone. Working under the same principles as Crabtree and Brudvig's catalyst, the hydrogen bond donor/acceptor group holds the substrate in place and positions it directly over the reactive metal center (Figure 2.5).

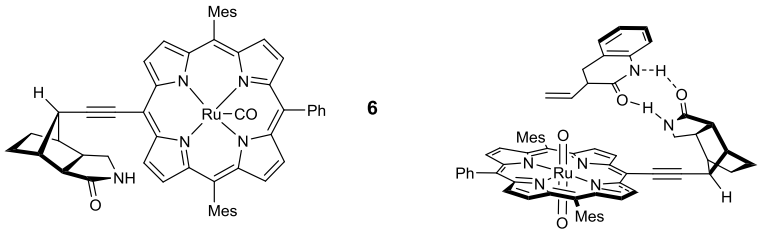

Figure 2.5. Bach's molecular recognition catalyst. (Shown with substrate bound at right.)

Optimal yields were found using benzene as solvent (Figure 2.6). Entries 5 and 6, which use the *N*-methylated substrate and *N*-methylated catalyst, respectively, show that the importance of the hydrogen bonding between the amide functionalities is not just for the yield, but also for the enantioselectivity.

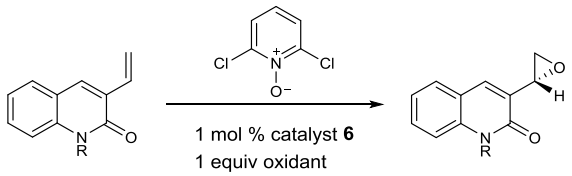

entry	substrate	solvent	% yield	% ee[a]
1	a	DCM	54	85
2	a	toluene	60	91
3	a	$PhCF_3$	53	94
4	a	benzene	71	95
5	b	benzene	55	< 5
6[b]	a	benzene	68	14
7[c]	a	benzene	71	95
8[d]	a	benzene	86	89

Figure 2.6. Bach and coworker's intermolecular epoxidation. (a) % ee was determined using chiral HPLC. (b) The *N*-methylated derivitave of the catalyst was used. (c) The enantiomer of the catalyst was used and the major product was the enantiomer of what is shown. (d) Reaction carried out at 50 °C

To investigate the regiocontrol afforded by their catalyst, Bach and coworkers also examined the epoxidation of a diolefinic substrate (Scheme 2.4).

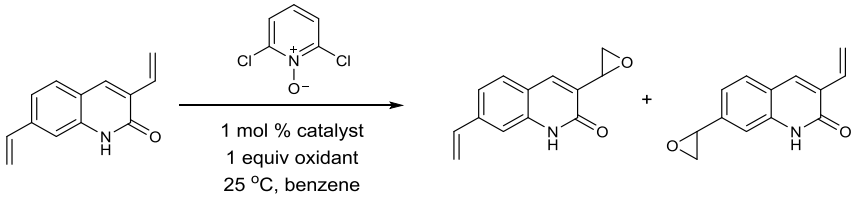

Scheme 2.4. Regiocontrol in intermolecular epoxidation.

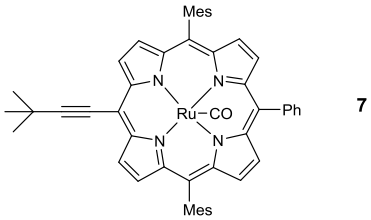

7

Figure 2.7. Achiral non-hydrogen bonding catalyst used for regiocontrol control experiments.

They found significant differences in product ratios when they used catalyst **6** versus when they used **7**, the same core catalyst but without the molecular recognition

unit (Figure 2.7). This again shows how important molecular recognition can be for regio- and enantioselectivity.

2.3 Proposed Molecular Recognition Catalyst

Based on the results by Bach, Crabtree and Brudvig, we believe adapting molecular recognition to C–H amination is a logical step. Both of these groups have demonstrated the utility and viability of molecular recognition for regio- and enantiomeric control for intermolecular oxidation reactions, and since those are issues still facing amination, molecular recognition could be the perfect solution. We envisage catalyst **8** (Figure 2.8)**,** which possesses the same phenyl linker, and U-turn/carboxylic acid moieties as Crabtree's catalyst **2**, but with a pybox ligand core typical of our catalysts, will provide a strong starting point for this research.

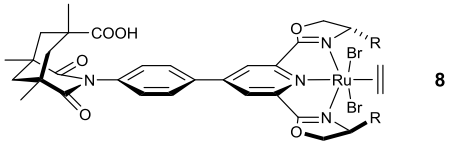

8

Figure 2.8. Our proposed molecular recognition catalyst **8** for intermolecular amination.

When this catalyst design is combined with the model transition states proposed earlier by Bach, Crabtree and Brudvig, and the bis(imido)pyridyl complex proposed for intramolecular amination (*vide supra*), one can envision a substrate like ibuprofen hydrogen bonding to the acid derivative and being held in place such that the benzylic hydrogens are directly over the reactive metallonitrene center (Figure 2.9). The hydrogen bonds should hold the substrate in place long enough for the new C–N bond to form but remain reversible enough for good catalyst turnover.

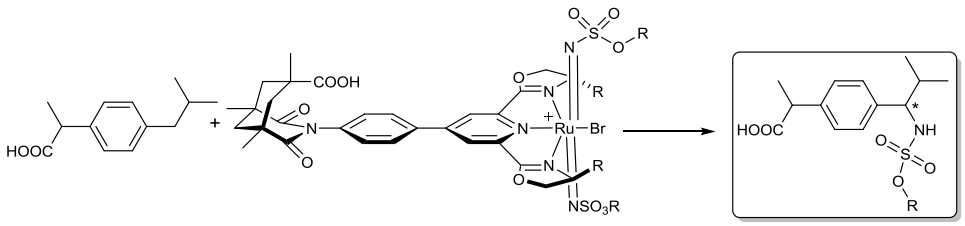

Figure 2.9. Proposed scheme for intermolecular amination.

2.4 Ligand Synthesis

Retrosynthetically, molecular recognition ligand **9** could come from the condensation of Kemp's triacid derived U-turn moiety **10** on to the indenyl pybox with the linker (**11**). The pybox portion could come from the amidation and cyclization of the appropriate amino alcohol onto diacid **12**. Acid **12** in turn would arise from the coupling of protected aniline **13** and bromopyridine **14**. The bromopyridine would come from chelidonic acid (**15**) via chelidamic acid (**16**).

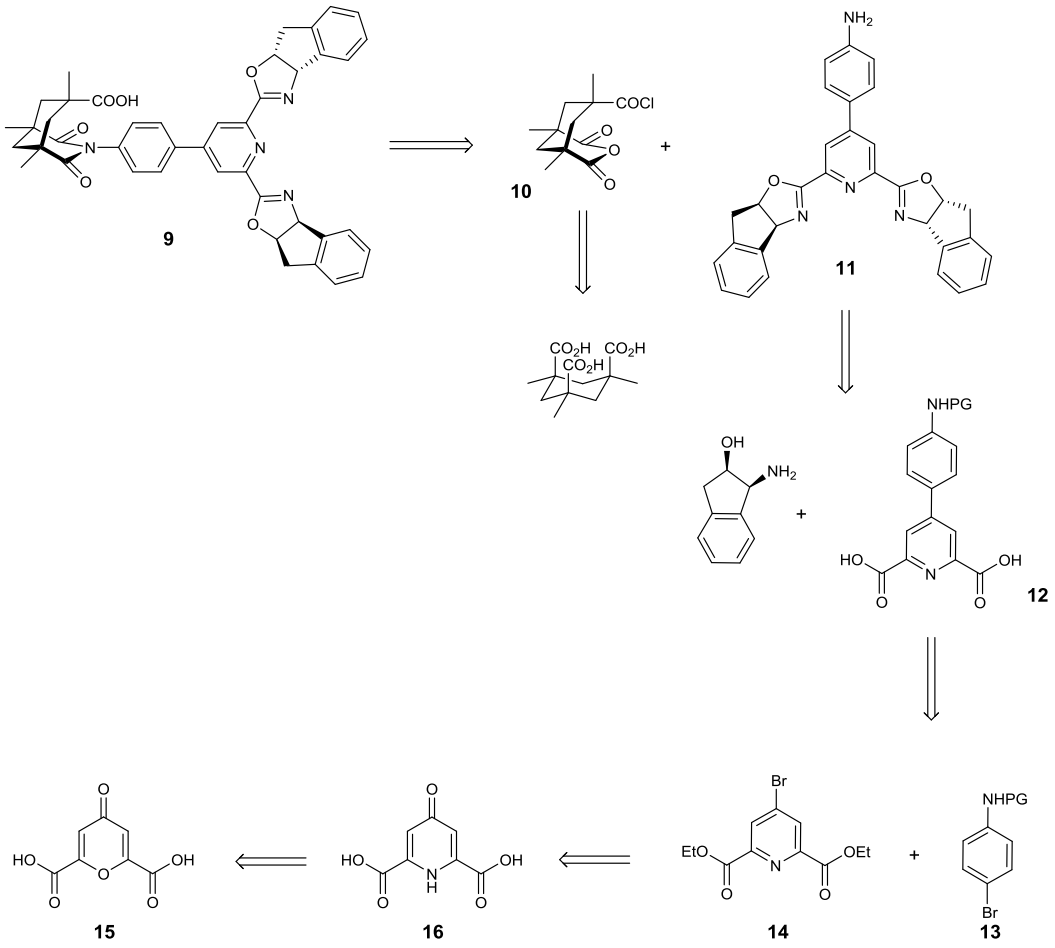

Figure 2.10. Retrosynthetic plan for the molecular recognition pybox ligand **9**.

The Kemp's triacid was successfully converted to anhydride **9** in 86 % yield following the known procedure (Scheme 2.5).[27]

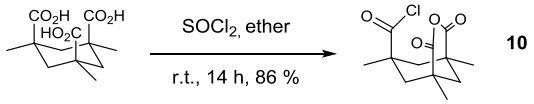

Scheme 2.5. Formation of anhydride **10** from Kemp's triacid.

The synthesis of pybox core **11** started with the known reaction of diethyl oxalate and acetone in strong base then strong acid to form chelidonic acid (**15**), albeit in low yield (Scheme 2.6). **15** was then converted to chelidamic acid (**16**) in aqueous NH_3 in

87 % yield over several days.[28] Bromination and esterification of **16** to give **14** was accomplished using PBr_5 followed by ethanol in 55 % yield.[29]

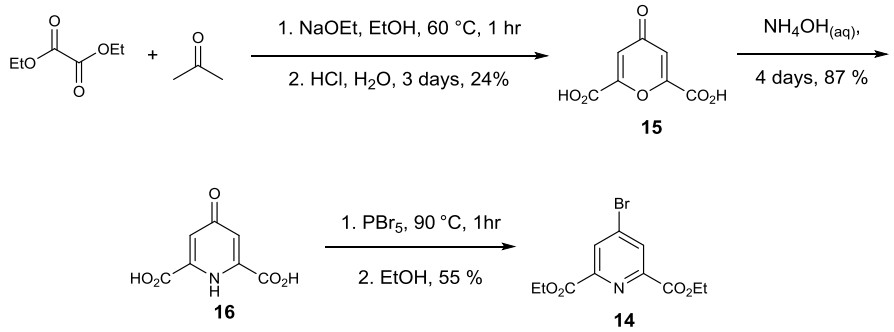

Scheme 2.6. Formation of **16** from diethyloxalate and acetone via **15**, and conversion of **16** to brominated pyridine **14**.

To generate the other coupling partner, commercially available 4-bromoaniline was Boc protected using Boc anhydride in water to give **17** in excellent yield (Scheme 2.7). Initial attempts to couple these groups together were through a Suzuki coupling. The aniline derivative was converted to the boronic acid using a lithium-halogen exchange reaction (Scheme 2.7). Although the desired product **18** was observed, yields were exceedingly and consistently low (5-12 %), so this path was deemed unfeasible and other coupling reactions were explored.

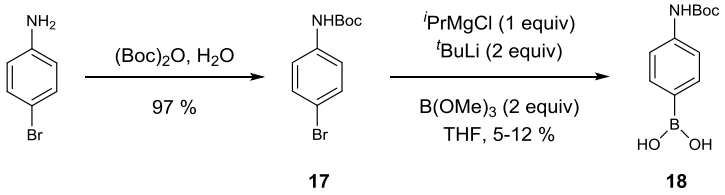

Scheme 2.7. Formation of boronic acid for potential Suzuki coupling.

Aniline **17** was converted to stannane **19** in reasonable yield (Scheme 2.8) and was then coupled to the halide **14** using Stille coupling conditions (Scheme 2.9). The best yields were achieved by the addition of one equivalent of CuTC.[30]

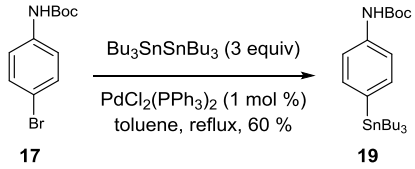

Scheme 2.8. Formation of stannane **19** for Stille coupling.

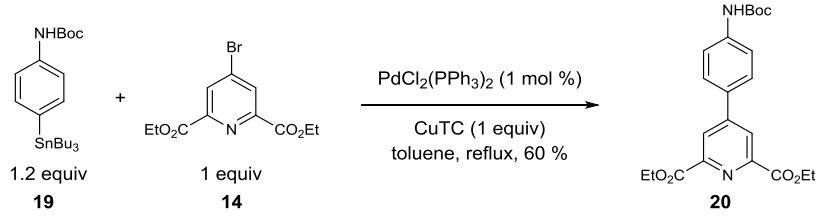

Scheme 2.9. Stille coupling for the formation of **20**.

Ester **20** was then hydrolized to acid **21** using LiOH followed by HCl (Scheme 2.10). Yields in this reaction were unreliable because of unintentional deprotection of the Boc group to give **22**. To get around this problem, Boc protection was replaced by Cbz protection. The Cbz protection was carried out using standard conditions to give **23** in 94 % yield (Scheme 2.11). Bromo arene **23** was converted to stannane **24** and the Stille coupling afforded **25** in good yield (Scheme 2.12). Hydrolysis of **25** to the corresponding diacid (**26**) was accomplished in 94 % yield followed by conversion to acid chloride **27** using $SOCl_2$ in 78 % yield.

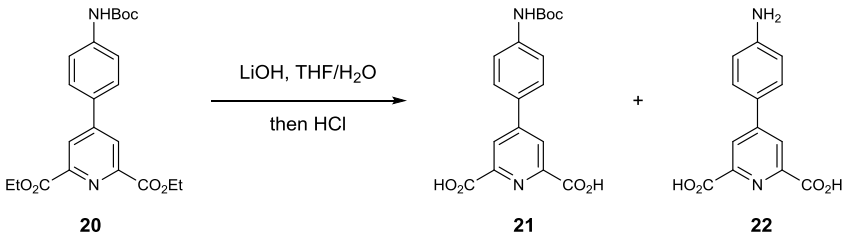

Scheme 2.10. Stille coupling for the formation of **21.**

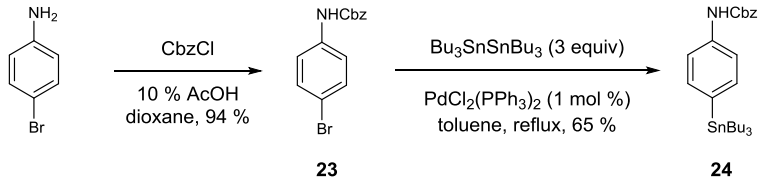

Scheme 2.11. Generation of the Cbz protected stannane **24**.

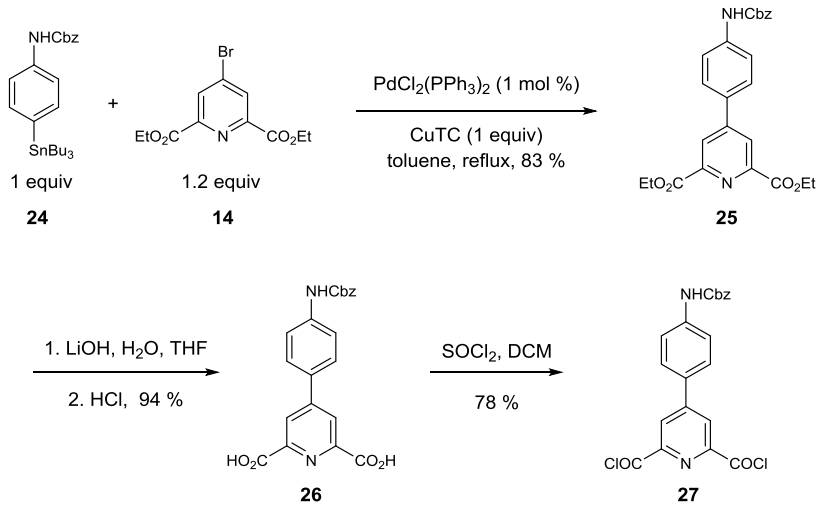

Scheme 2.12. Stille coupling of **24** and **14**, and formation of acid chloride **27** from **26**.

After formation of acid chloride **27**, the intention was to form the pybox structure using the method developed by Nishiyma.[31] Nishiyama's method has been previously used for the formation of pybox ligands with great success but was still tested on a model system before being applied to the advanced intermediate **27** (Figure 2.11a). Yields were lower than expected, but high enough to continue on to the full system. However, when these conditions were applied to the actual system, yields dropped dramatically (Figure 2.11b). After breaking up the two steps, (the amide bond formation and cyclization), the problem was found to be in the amide formation step. Various methods of amide bond formation were attempted and are shown in Figure 2.12.

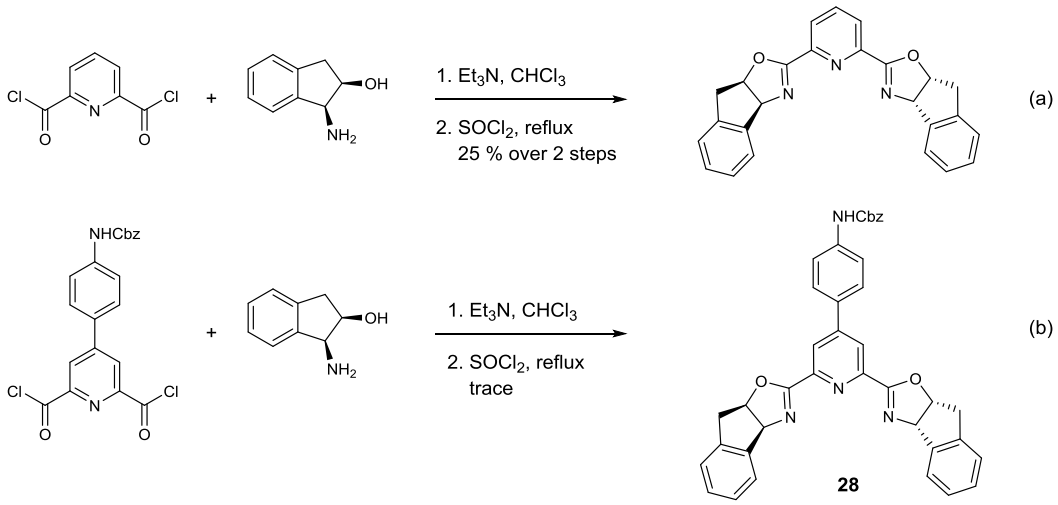

Figure 2.11. (a) Test system for the formation of the indenyl pybox. (b) Actual system for the formation of the indenyl pybox.

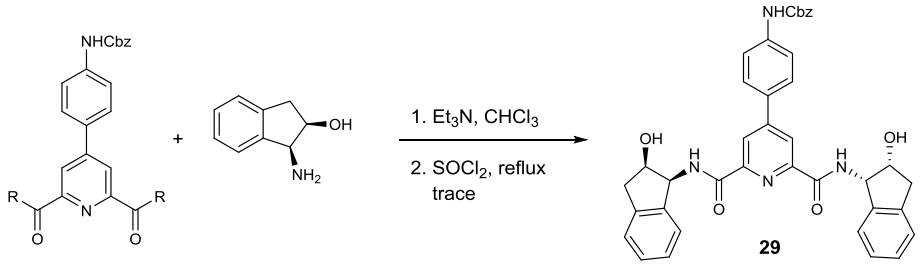

entry	conditions	R	% yield (model system)	% yield (actual system)
1	Et_3N, $CHCl_3$	Cl		8
2	NaH	OEt	35	< 5
3	IPAC, $KHCO_3$	Cl	21	< 5
4	PyBOP	OH	74	15
5	Carbonyldiimidazole	OH	75	31
6	EDCI	OH	trace	nd

Figure 2.12 Conditions for the formation of indenyl amide **29**.

Both PyBOP and CDI were very successful in model system tests and they also gave the best results in the actual system (entries 4 and 5). The yield with carbonyldiimidazole was best so a brief optimization study was undertaken (Figure 2.13).

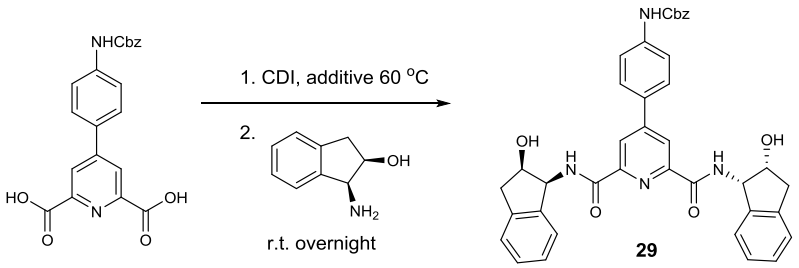

entry	solvent	time (h)	additive	% yield[a]
1	THF	1	none	31
2	DMF	1	none	27
3	THF	12	none	39
4	THF	1	DMAP	36
5	THF	1	4Å M.S.	24

Figure 2.13. Optimization of amide bond formation using CDI. (a) In all cases the acid, CDI, and additives were combined and heated to 60 °C for the length of time shown, at which point the heat was removed, the amino alcohol was added, and it was left to stir overnight.

Although yields were low, amide **29** was moved forward into the cyclization to generate the pybox core of the ligand (**28)**. Traditional ways of carrying out this cyclization were attempted this included $SOCl_2$/DCM,[31] mesylation and DAST[32] (Figure 2.14). Unfortunately none of these methods gave any evidence of product, all resulted in either messy decomposition or no reaction at all.

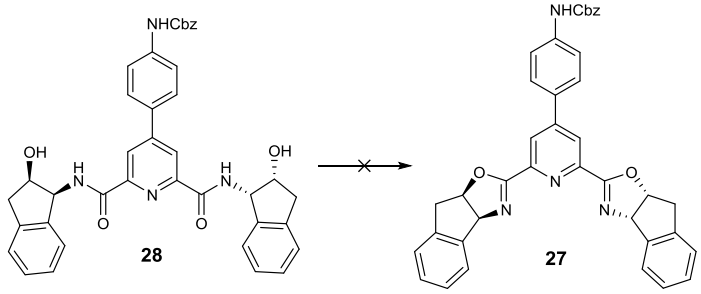

entry	conditions	% yield
1	$SOCl_2$ (5 equiv), DCM, r.t., overnight	no product isolated
2	MsCl, DCM, reflux, overnight	no product isolated
3	DAST, DCM, -78 °C, 10 h	no reaction

Figure 2.14. Optimization of amide bond formation using CDI to generate **27**.

2.5 Conclusion

With major difficulties apparent in the cyclization step, plus a number of low yielding steps, plus a relatively long ligand synthesis (in terms of number of steps), and limited potential substrate scope, it became clear to us at this point that this was not a route worth pursuing further. If this system was to be revisited, an oxazoline that is easier to close should be pursued instead of the indenyloxazoline which is routinely the most challenging to form by any means. This should allow the core of the ligand to be accessed more efficiently, making the true question of how this ligand framework performs in amination reactions easier to answer.

3. Benzodipyrrolidone Synthesis *via* C–H Functionalization

3.1 Introduction

Conjugated polymers have long been of interest to the materials and organic electronic communities due to their low cost, flexibility and ability to be processed in solution. Alternating or block copolymers with electron rich donor groups and electron poor acceptor groups allow for the synthesis of integrated circuits with blanket coating instead of patterned processing like one would need with separate electron rich and electron poor polymers. Having alternating donor-acceptor units also increases π-π stacking which governs intermolecular order. This makes these polymers and methods for their preparation very powerful tools.

Diketopyrrolopyrrole (DPP) is an electron poor acceptor molecule commonly used in donor/acceptor polymers. It is planar, highly conjugated core results in strong π-π interactions and electron withdrawing effects, and it is known for its exceptional stability.[33,34] These structures have become increasingly popular in organic thin film transistors (OTFTs) and organic photovoltaics (OPVs) due to hole mobilities up to 1.95 $cm^2V^{-1}s^{-1}$ for DPP-thienothiophene copolymer[35] and power conversion efficiency up to 5.5 % with DPP- phenylene copolymer (Figure 3.1).[36]

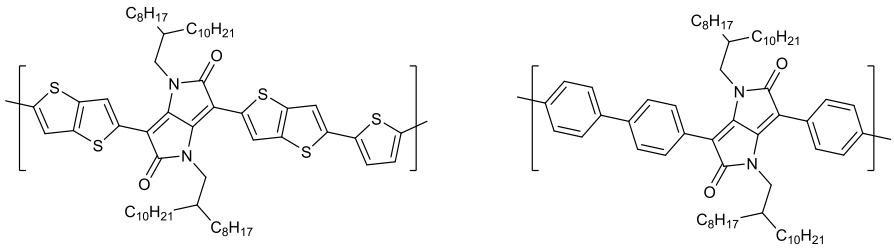

Figure 3.1 Common DPP polymers.

Benzodipyrrolidone (BDP) is considered a "stretched" diketopyrrolopyrrole. BDP incorporates the quinoid structure into the ground state reducing the bond length alteration which in turn results in small band gap polymers and reduces reorganization energy upon excitation (Figure 3.2).[37]

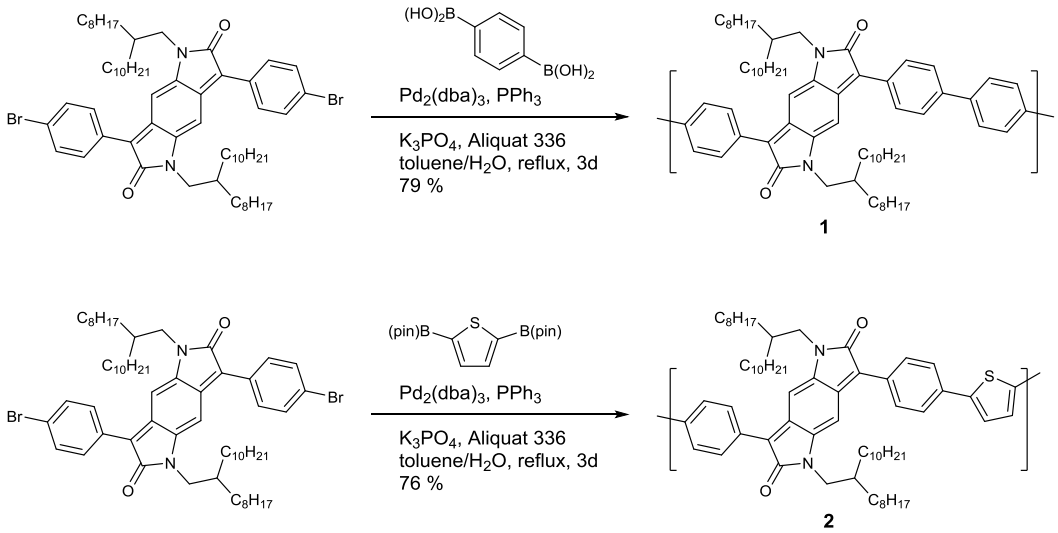

Figure 3.2 Synthesis of common BDP polymers **1** and **2**.

Although phenyl rings adjacent to the BDP core are common, their presence twists the molecule out of planarity giving a 38° dihedral angle between the ring and the core (Figure 3.3).[33] Replacing the phenyl ring with a smaller thiophene, furan or even selenophene ring is one way to overcome this problem; the dihedral angle for the thiophene derivative is just 12.7°.[38] This increased conjugation causes and the charge carrier mobilities to increase as well, in some cases by as much as an order of magnitude.[39–41]

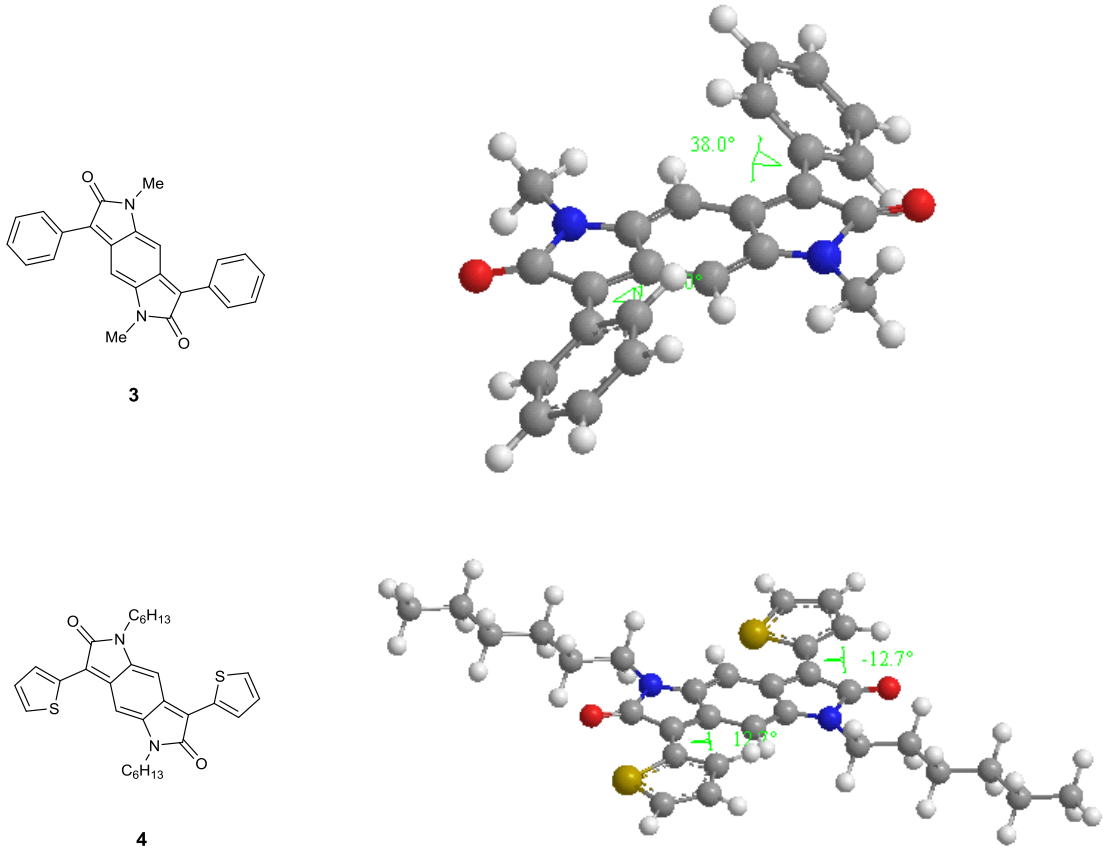

Figure 3.3 Structures of **3** and **4** showing dihedral angels of 38° and 12.7° respectively.

Despite the large dihedral angle, absorption onsets between 700 nm and 800 nm are common for BDP polymers, which falls within the range of a small band gap polymer (Figure 3.4). Thiophene-flanked BDPs can be pushed to significantly higher wave numbers through judicious choice of an alternating donor groups.[38]

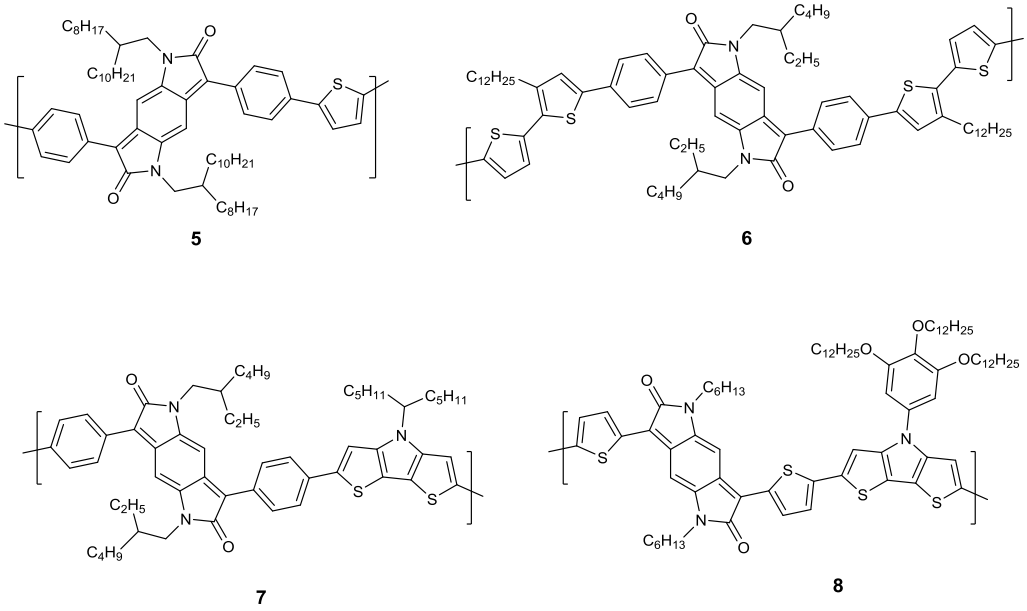

Figure 3.4 Onset of 735 nm and max of 639 nm for **5**, onset of 796 nm and max of 630 nm for **6**,[37] onset of 860 nm and max 722 nm for **7**,[42] onset of 1006 nm and max 1562 nm for **8**.[38]

A similar structure used by the Müllen group is the difluoroboradiazabenzodipyrrolidone (aza-BDP). Replacing the oxygen of the lactam with nitrogen and using a difluorobora-bridge to tether a pendant pyridine generates compounds of considerable value due to their interesting properties. The material retains the good thermal and photochemical stability, high absorption and quantum yields of traditional BDPs, but there is a significant bathochromic, or red shift, in the absorption and LUMO levels as low as -4.13 eV are observed. These structures are typically used as small molecules, not as polymers (Figure 3.5).

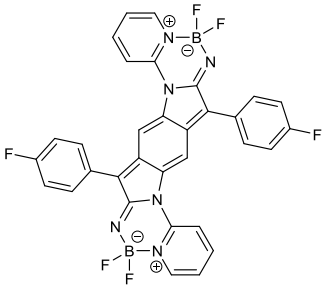

Figure 3.5. Aza-BDP dye used by Müllen.

Controlling HOMO and LUMO levels is crucial for stability and for matching donor and acceptor units. Polymers based on DPP, BDP or other bislactams have lower LUMO levels than naphthalene tetracarboxylic diimide or perylenetetracarboxylic diimide based polymers, which negatively affects the effectiveness of electron injection and air stability of the polymer.[40] Zhang and coworkers found that acylating the nitrogen of the lactam reduced the electron density in the ring, lowering the LUMO level for the monomer and associated polymer (Figure 3.6). This improved the reversibility of reductive doping over alkylated BDP, making these molecules better for applications in n-type OFETs.

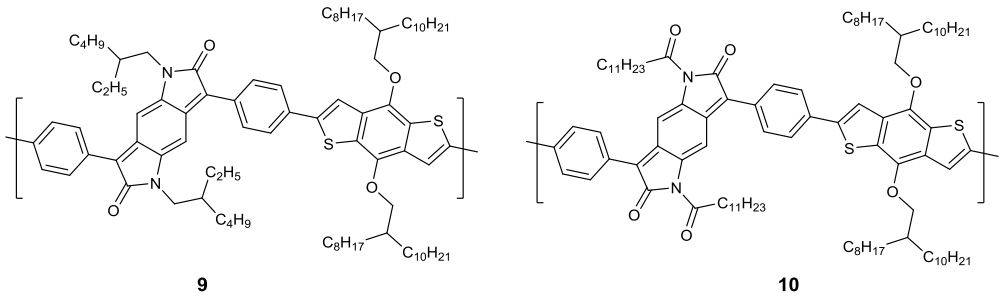

9 10

Figure 3.6 Alkylated BDP polymer **9** with a LUMO of -3.53 eV, acylated BDP polymer **10** with a LUMO level of -3.84 eV.

Benzodipyrrolidones are typically made via the condensation of *p*-phenylenediamine with mandalic acid to give amide **11** (Scheme 3.1). Cyclization on concentrated sulfuric acid gives tricycliclactam **12** from **11** in 95 % yield. Lactam **12** is then oxidized to **13** with potassium persulfate in refluxing ethanol in 75 % yield. Alkylation of **13** is completed using the corresponding alkyl halide to give **14** in 60 % yield in 4 steps and 48 % overall yield.

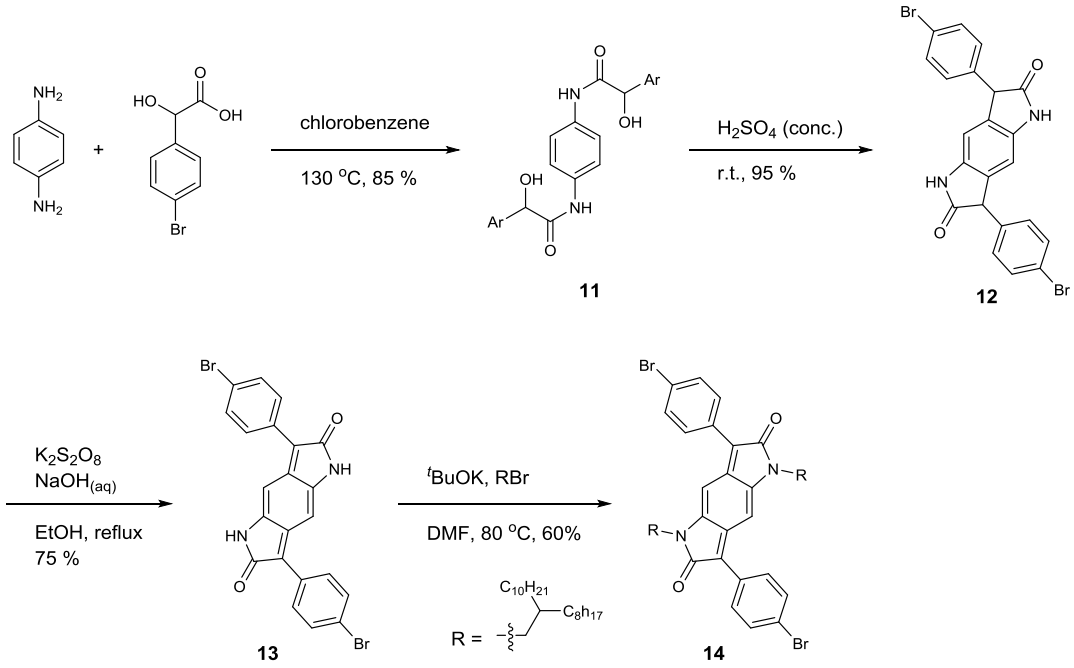

Scheme 3.1. Synthesis of benzodipyrrolidone by Wudl and coworkers.

Although the yields of benzodipyrrolidone **14** are moderate, conditions are quite harsh and do not allow for much diversity of functional groups. One notable example is thiophene; the initial condensation will not proceed with α-hydroxy-thiopheneacetic acid which would be used to make the thiophene analogues. To overcome this problem other syntheses have been developed by the Wudl[38] and Rumer labs for the formation of thiophene analogues (Scheme 3.2 and Scheme 3.3). Wudl's route begins with the condensation of 1,4-cyclohexanedione with hexylamine under O_2 to give dianiline **15**. Treatment of **15** with chloroacetyl chloride gave **16** in 73 % yield, which was then treated with molten $AlCl_3$ to give dioxindole **17**. Radical halogenation with NBS in CCl_4 gave **18** in 57 % yield. Reductive debrominaiton using sodium iodide gave **19**. Finally, Stille coupling was used to install the thiophene rings to give **20** in 6 steps and 11 % over all

yield. Again, this route employs some very harsh conditions in a very linear fashion to get to **20** in relatively low yield.

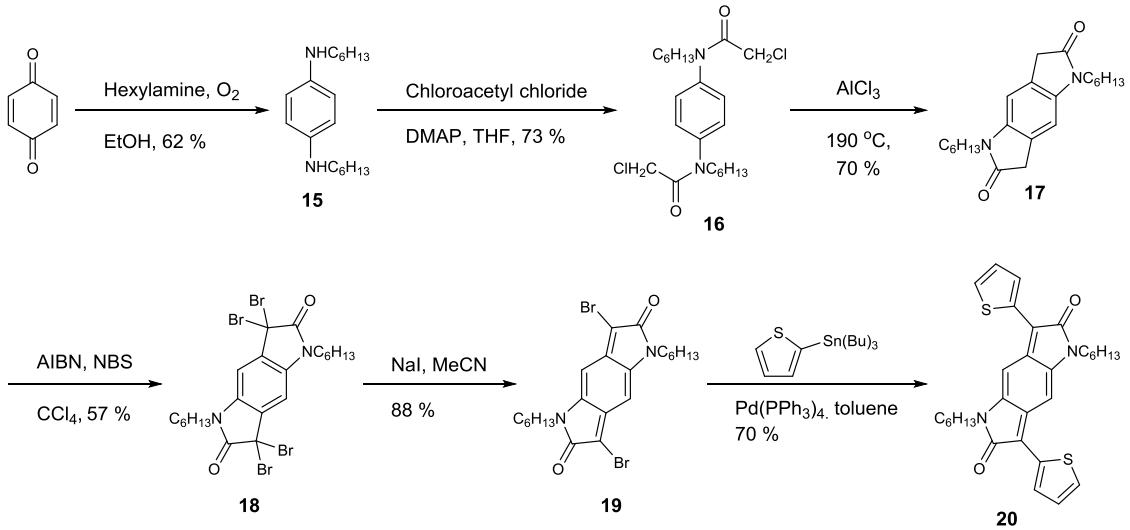

Scheme 3.2 Synthesis of thiophene-flanked benzodipyrrolidone **20** by Wudl and coworkers.

Rumer's synthesis began with the Swern oxidation of hydroxy amide **21** followed by Pummerer reactions to close the lactam rings and give **22** (Scheme 3.3). CAN oxidation then gives **23** in 69 % yield over three steps. Grignard reactions immediately followed by reductions using NaH_2PO_2, NaI, and AcOH, immediately followed by selective DDQ oxidation afforded **24** in three additional steps or six total steps and 24 % overall yield. Although this synthesis does not use the harsh conditions of the previous methods, it is still six steps long and half of those are oxidation state changes, not bond forming reactions.

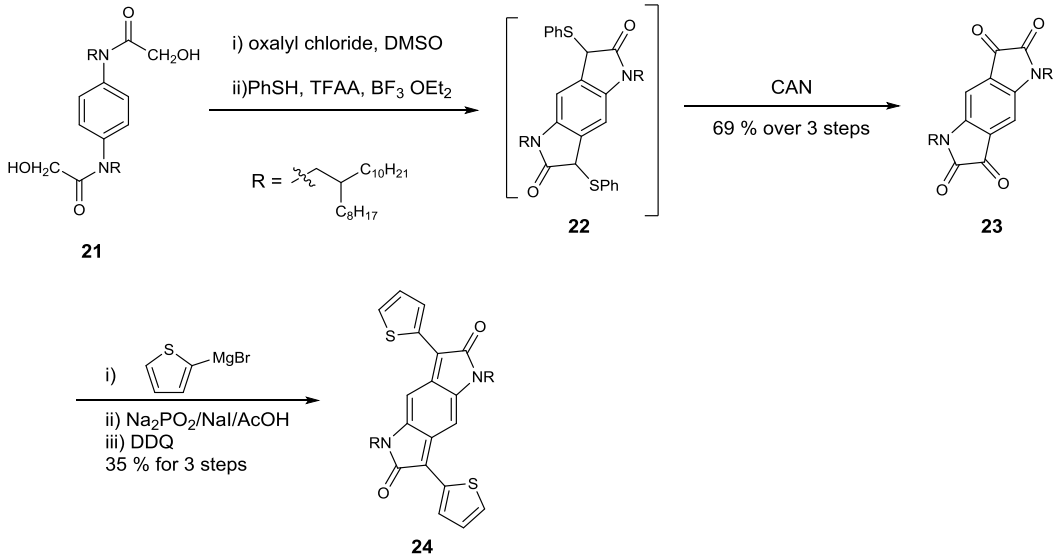

Scheme 3.3. Synthesis of thiophene-flanked benzodipyrrolidone **24** by Rumer and coworkers.

3.2 Proposed C–H Functionalization Synthesis

This work seeks to use the power of C–H functionalization to streamline the synthesis of BDP derivatives and through the use of much milder and more efficient conditions, broadening the scope of the synthesis (Figure 3.7). The proposed synthesis would start from a double carbene insertion into cyclohexadiene with an aryl diazoacetate. Subsequent C–H amination would close both the lactam rings. Finally oxidation to the quinoid would finish the synthesis in just three steps.

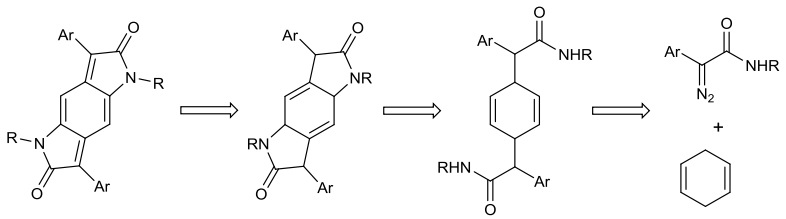

Figure 3.7. Retrosynthesis of BDP using C–H functionalization.

Most of the steps in the series are well precedented, starting with the carbene insertion. Insertion into cyclohexadiene with phenyl diazoacetate using a dirhodium catalyst is known (Scheme 3.4).[43–48] To simplify the synthesis, using an amide as the acceptor group would be preferable; however that insertion has not been demonstrated in the literature to date. The double insertion required for this work is unprecedented.

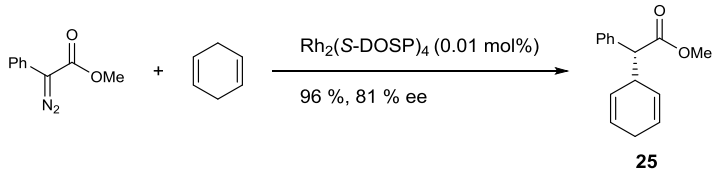

25

Scheme 3.4. Carbene insertion with phenyl as the donor group from Davies to generate **25**.[48]

There are recent examples of donor/acceptor carbene chemistry with 2-thiophene as the donor group in addition to enoates (Scheme 3.5)[49] but insertion into cyclohexadiene is only precedented with the 3-thiophene (Scheme 3.6).[50] This system requires the 2-thiophene for conjugation leaving that as a challenge for this work. Only a thiophene substituted at the 2-position will be fully in conjugation with the surrounding aromatic functionality, thiophenes substituted at the 3-position are cross-conjugated (Figure 3.8).

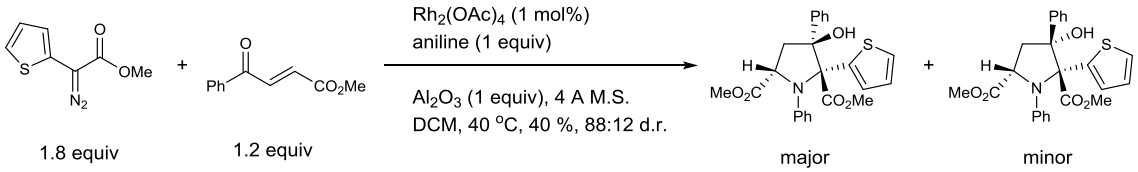

1.8 equiv 1.2 equiv major minor

Scheme 3.5. Hu and coworkers use of 2-thiopheno derived donor/acceptor carbene for rhodium catalyzed insertion.

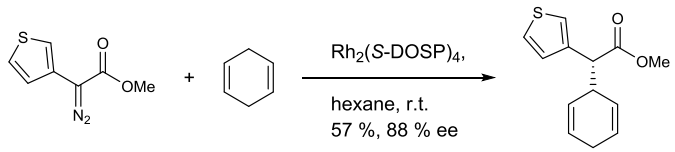

Scheme 3.6. Carbene insertion with thiophene as the donor group from Davies.

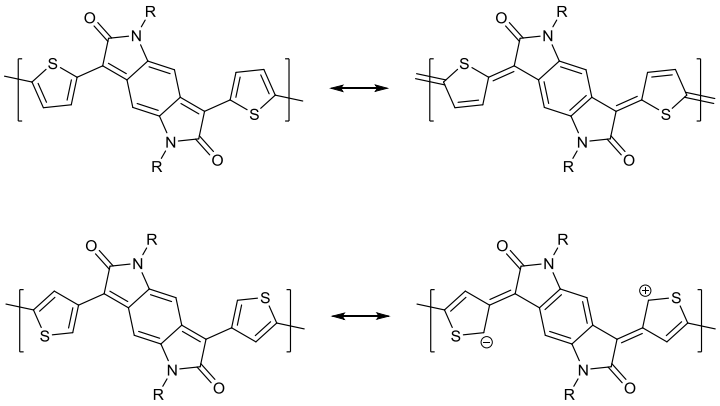

Figure 3.8. Polymer containing a thiophene substituted at the 2-position is fully conjugated, while a polymer containing a 3-substituted thiophene is cross conjugated.

Amination at secondary allylic positions is established as well. The White lab developed a method for amination with carbamates using a palladium sulfoxide catalyst (Scheme 3.7).[51] Liu and coworkers found they could perform a similar amination with amides using palladium acetate and a chromium salen complex as a cocatalyst (Scheme 3.8).[52] Both groups found they needed and electron withdrawing group on the nitrogen such as tosyl to increase the acidity of the proton on nitrogen for the reaction to proceed. Because both of these reactions go through allyl palladium transition states they should be applicable to the proposed methodology even though the location of the desired C–N bond is an sp^2 center in the starting material.

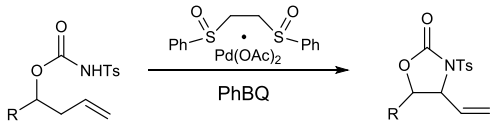

Scheme 3.7. Amination of from M. Christina White.

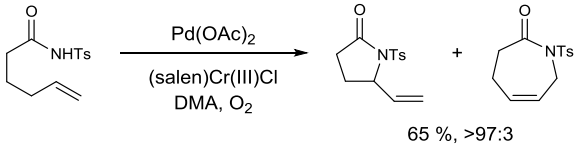

Scheme 3.8. Amination from Liu and coworkers.

At the time there were no examples of allylic C–H amination into internal olefins, only terminal olefins, so to prove that the allyl palladium species could be formed from an internal olefin we proposed the model system shown in Figure 3.9.

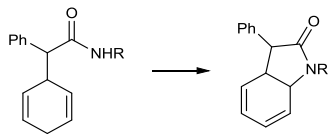

Figure 3.9. Model system for amination of an internal olefin.

Since then aminations of internal olefins have been published in the literature like the example from M. Christina White shown in Figure 3.10 using iron porphyrin catalyst **26** to give **27** in 72 % yield.[53]

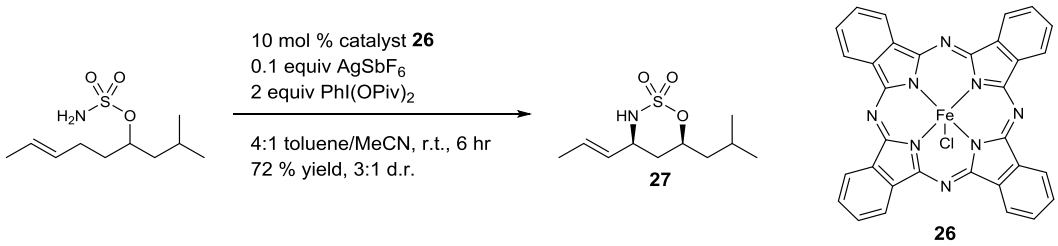

Figure 3.10. Iron porphyrin catalyst **26** used for amination of on internal olefin to generate **27**.

3.3 Synthesis and Exploration of the Model System

The synthesis of the model system required the generation of a cyclic olefin with a pendant amide. Since amides have not been used at the acceptor group in donor/acceptor carbene chemistry, we decided to do the insertion with an ester, which is well precedented, and convert the ester to the amide after insertion. To that end, methyl phenyldiazoacetate (**28**) was synthesized from the corresponding methyl ester using *p*ABSA and DBU in 58 % yield based on the literature procedure (Scheme 3.9).[54]

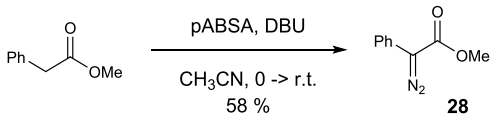

Scheme 3.9. Synthesis of diazo **28**.

From there, the carbene insertion was carried out using $Rh_2(OAc)_4$ in DCM to give **29** in 92 % yield. However an initial attempt at hydrolysis of the ester proved unsuccessful (Scheme 3.10). Hydrolysis to acid **30** was accomplished by moving from LiOH at room temperature in THF/H_2O to NaOH in refluxing MeOH/H_2O (Scheme 3.11).

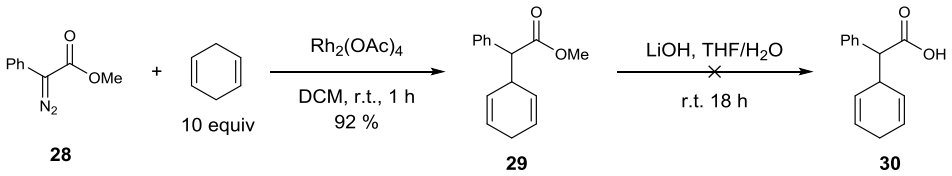

Scheme 3.10. Carbene insertion and initial attempt at hydrolysis.

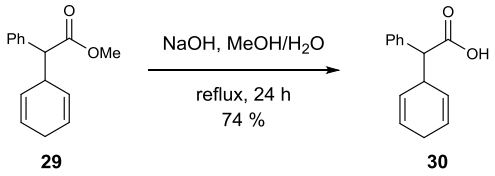

Scheme 3.11. Hydrolysis of ester **29** to **30**.

Acid **30** was then converted to *N*-tosylamide **31** using tosyl isocyanate in 74 %, and using conditions developed by the White lab the amination of *N*-tosylamide **31** to give lactam **32** was accomplished in 21 % yield (Scheme 3.12). A majority of starting material was recovered, but there were some unidentified decomposition products observed as well. The ^{1}H NMR of the isolated lactam **32** clearly showed the conjugated diene with four peaks between 5 and 6 ppm and the amide proton that was present in the NMR spectrum of **31** had disappeared.

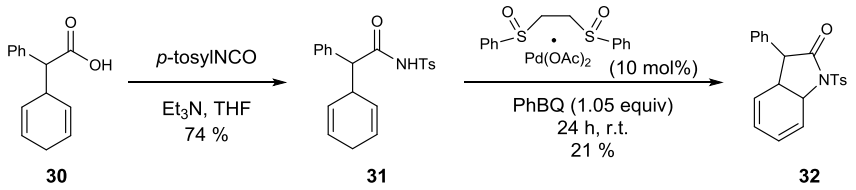

Scheme 3.12. Synthesis of lactam **32** from **30**.

3.4 Synthesis of BDP core *via* C–H Functionalization

This gave us sufficient confirmation that we were ready to move to the double insertion system. Since the cyclohexadiene is traditionally used in excess to prevent dimer formation, our initial plan was to do the two carbene insertions sequentially in two separate pots so we could have an excess of substrate each time. With this in mind we added diazo **28** to ester **29** over 30 minutes but we only observed the formation of carbene dimer **34** (Figure 3.11, entry 1). Slowing down the addition of diazo **28** from 30 minutes to 3 hours to 6 hours increased yield of **33** from 0 to 8 % (entries 1-3). Slowing down addition any more would increase dimer formation in the syringe as the diazo will decompose on standing at room temperature. Doubling the equivalents of substrate **29** made no difference in preventing formation of dimer **34** and did not change the isolated yield of **33**.

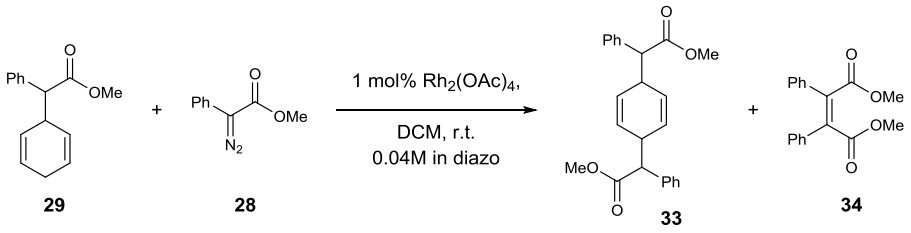

29 **28** **33** **34**

entry	equiv of **29**	addition time (h)	yield of **33**
1	5	.5	0 (only dimer)
2	5	3	trace
3	5	6	8 %
4	10	6	7 %

Figure 3.11. Synthesis of double insertion product **33**.

It was unclear to us what impact the stereochemistry of the first insertion was having on the second insertion. The first insertion could be locking the ring into a conformation such that the C–H bonds for the second insertion are in unfavorable orientations. To better control for and understand match/mismatched case we moved to chiral rhodium catalysts that are well precedented for doing this insertion enantioselectively, Rh_2(*R*-DOSP)$_4$ and Rh_2(*S*-DOSP)$_4$. Both enantiomers of **29** were synthesized from the corresponding enantiomers of Rh_2(DOSP) in good yield (Figure 3.12). Stereochemistry was assigned by analogy to literature precedent and not independently verified.[47]

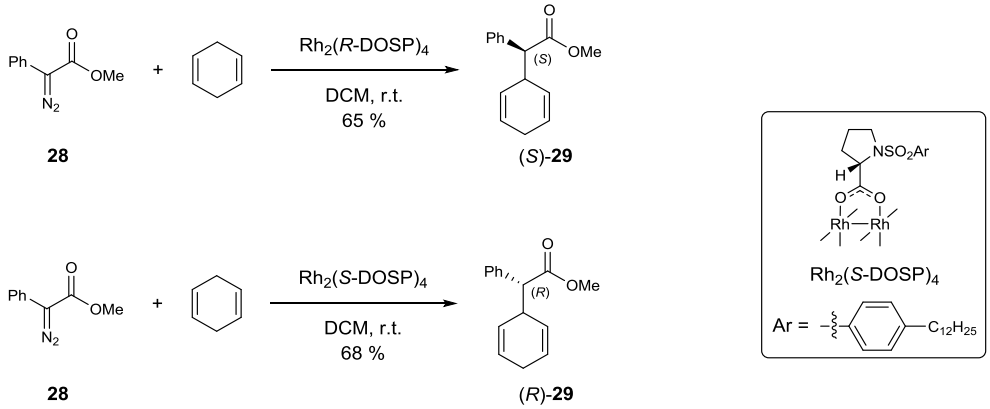

28 (*S*)-**29** **28** (*R*)-**29**

Figure 3.12. Synthesis of (*S*)-**29** and (*R*)-**29** from diazo **28** using Rh_2(*R*-DOSP)$_4$ and Rh_2(*S*-DOSP)$_4$.

With both enantiomers in hand, they were separately subjected to second insertions conditions using a variety of chiral rhodium catalysts (Figure 3.13). When (*S*)-**29** was used in conjunction with Rh_2(*R*-DOSP)$_4$, which gives (*S*,*S*)-**33**, the yield was 23 % (entry 1). Conversely, when (*S*)-**29** was used with Rh_2(*S*-DOSP)$_4$, which gives (*S*,*R*)-**33**, the yield was only 6 % (entry 2) suggesting that the match/miss-match effect is significant. This was supported by starting with (*R*)-**29**. Rh_2(*S*-DOSP)$_4$ gave 28 % yield of (*R*,*R*)-**33** while Rh_2(*R*-DOSP)$_4$ gave 10 % of (*R*,*S*)-**33** (entries 5 and 6). Other rhodium catalysts confirmed the importance of matching the chiral centers. Starting from (*S*)-**29**, neither Rh_2(*S*-biTISP)$_4$ nor Rh_2(*S*-PTAD)$_4$ gave any of the miss-matched *S*,*R* product, but starting with (*R*)-**29** Rh_2(*S*-biTISP)$_4$ and Rh_2(*S*-PTAD)$_4$ gave 31 % and 19 % of (*R*,*R*)-**33**.

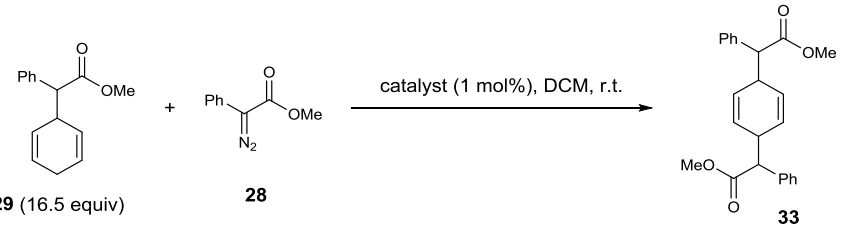

entry	*SM*	catalyst	result	
1	(*S*)-**29**	Rh_2(*R*-DOSP)$_4$	23 %	(*S*,*S*)-**33**
2	(*S*)-**29**	Rh_2(*S*-DOSP)$_4$	6 %	(*S*,*R*)-**33**
3	(*S*)-**29**	Rh_2(*S*-biTISP)$_4$	no product	(*S*,*R*)-**33**
4	(*S*)-**29**	Rh_2(*S*-PTAD)$_4$	no product	(*S*,*R*)-**33**
5	(*R*)-**29**	Rh_2(*S*-DOSP)$_4$	28 %	(*R*,*R*)-**33**
6	(*R*)-**29**	Rh_2(*R*-DOSP)$_4$	10 %	(*R*,*S*)-**33**
7	(*R*)-**29**	Rh_2(*S*-biTISP)$_4$	31 %	(*R*,*R*)-**33**
8	(*R*)-**29**	Rh_2(*S*-PTAD)$_4$	19 %	(*R*,*R*)-**33**
9[a]	(*R*)-**29**	(^{t}BuPheBox^{i}Pr)IrCl$_2$(OH$_2$)	trace	(*R*,*R*)-**33**
10[b]	(*R*)-**29**	Rh_2(*S*-DOSP)$_4$	46 %	(*R*,*R*)-**33**

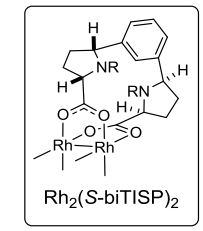

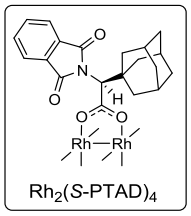

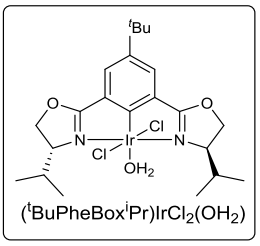

Figure 3.13. Analysis of matched/mismatched effect on synthesis of **33**. (a) solvent was trifluorotoluene. (b) 3:1 ratio of **28**:**29**.

The same reaction was also attempted with an iridium catalyst developed by our lab for insertion enantioselective insertion of donor/acceptor carbenoids into

cyclohexadiene[55] but there was only trace of the desired product with the majority of the starting material recovered (entry 9).

It was hypothesized that the diazo could be used in excess instead of the substrate. This would increase the amount of dimer side product but it may help drive the reaction to completion. Running the reaction with 3:1 diazo to substrate increased the yield of (*R*,*R*)-**33** from 28 % (entry 5) to 46 % (entry 10).

With the knowledge that the stereocenters in the product needed to match and an excess of diazo is beneficial, it follows that both insertions could be done in one pot.

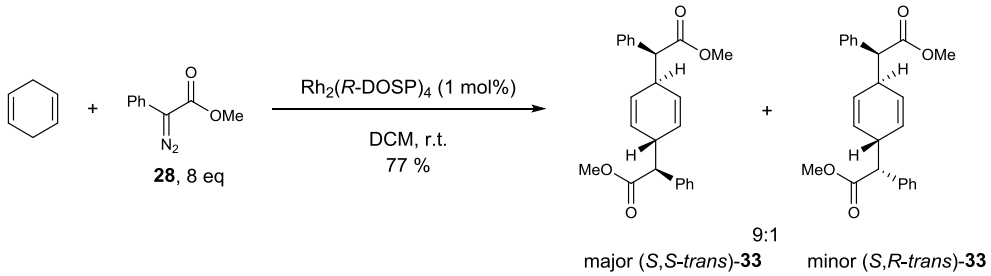

Scheme 3.13. Synthesis of (*S*,*S*-*trans*)-**33** from cyclohexadiene and diazo **28**.

To our delight using 8 equivalents of **28** and Rh_2(*R*-DOSP)$_4$ gave (*S*,*S*-*trans*)-**33** as the major product in a 9:1 ratio with (*S*,*R*-*trans*)-**33** in 77 % overall yield (Scheme 3.13). The stereochemistry of the major isomer was confirmed by x-ray crystallography (Figure 3.14).

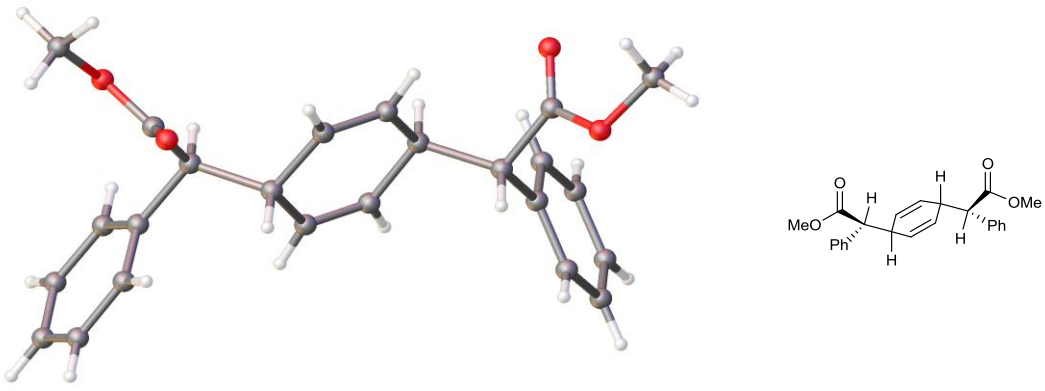

Figure 3.14. Crystal structure of (*S*,*S*-*trans*)-**33**.

Ester (*S,S-trans*)-**33** was hydrolyzed to diacid **35** without epimerization using the same NaOH, MeOH/H_2O conditions as were used with the model system (Scheme 3.14). Formation of di(tosylamide) **36** from tosyl isocyanate followed in 25 % yield.

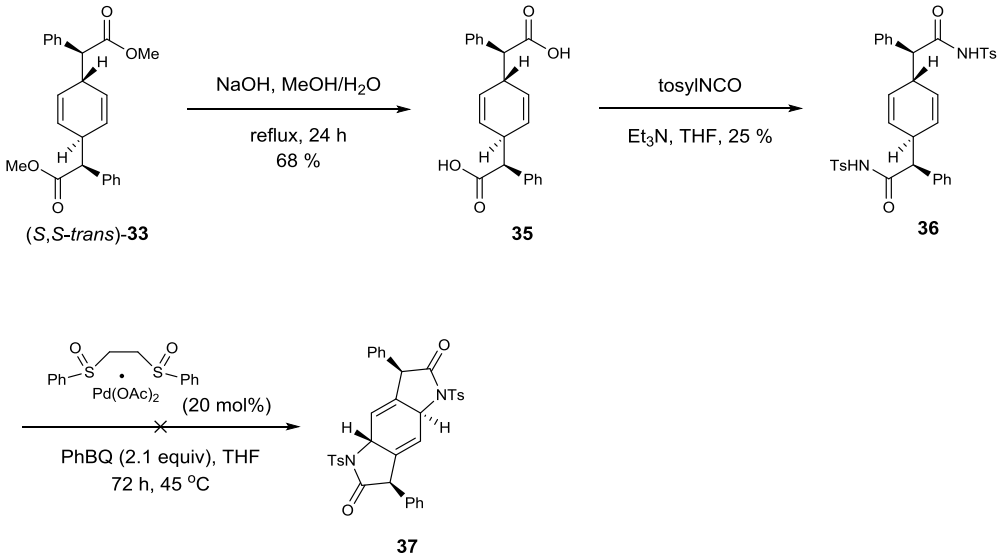

Scheme 3.14. Hydrolysis, amination and attempted cyclization to form **9**.

Unfortunately, when amination was attempted using White's conditions none of amination product **37** was observed.

3.5 Conclusion

Now that optimization of the key carbene insertion step is complete it should be possible to move forward and explore the amination step in greater detail to finish the synthesis of the benzodipyrrolidone. Recent advances in carbene insertion including the use of 2-substituted thiophenes as donor groups mean this synthetic pathway may be even more powerful. The current synthesis stands at 5 steps from the synthesis of diazo **28** and 8 % over all yield to reach diamide **36**. Ring closing amination and oxidation are all that remain.

4. Synthesis of 2,6-Difunctionalized Benzobisthiazoles *via* C–H Functionalization

4.1 Introduction

Small molecule organic semiconductors are increasingly becoming a powerful alternative to metallic semiconductors having mobilities from 10^{-2} up to 15 $cm^2V^{-1}s^{-1}$ compared with amorphous silicon and crystalline silicon which have mobilities around 0.5 $cm^2V^{-1}s^{-1}$ and 10^3 $cm^2V^{-1}s^{-1}$, respectively.[56,57] Benzobisthiazoles (BBT) are a popular monomer in these structures. Acting as an electron-poor acceptor unit in n-type materials or in alternating donor/acceptor materials, the fused rings of BBT make for excellent structural rigidity enhancing both 2-D and 3-D order in the system.[56] The strong π-π interactions between molecules lead to high temperature resistance with thermal decomposition temperatures above 500 °C in some cases (Figure 4.1, **1**). Incorporating electron poor heterocycles also increases the ionization potential of a material leading to increased stability to oxygen compared to poly(3-hexylthiophene).[58]

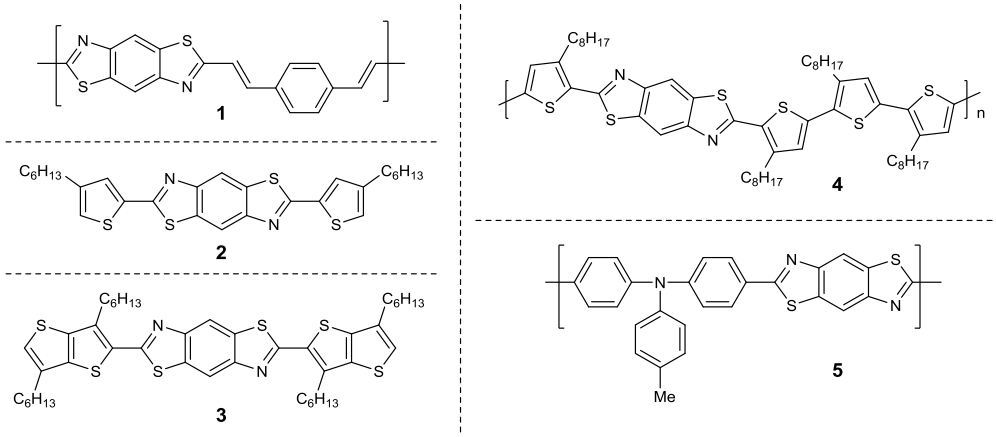

Figure 4.1 Benzobisthiazole-based small molecules and polymers. Polymer **1** with thermal decomposition temperature of 560 °C based on TGA analysis.[59] Small molecule **2** used in organic semiconductors that shows 3-dimensional self-assembly. **3** was explored in OFET devices and shown to have mobilities up to $3x10^{-3}$ cm^2/Vs.[60] Semiconducting co-polymer **4** has shown mobility of ~0.01 cm^2/Vs in OFET devices.[60] Polymer **5** with conductivity of $4.1x10^{-4}$ S/cm.[61]

While BBT rigid polymers have extremely high tensile strengths, they have relatively low axial compressive strengths. One way to compensate for this is to cross-link the polymer, generally through high temperature annealing (Figure 4.2).[62]

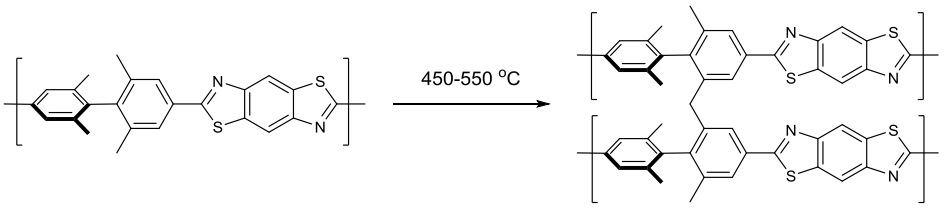

Figure 4.2 Cross-linked benzobisthiazole polymers.

Beyond materials chemistry, benzothiazoles can also be found in the medicinal chemistry literature. 2-Substituted benzothiazoles have been explored as antitumor agents (Figure 4.3, **6**),[63] HIV-1 specific reverse transcriptase inhibitors (**7**),[64] and orexin receptor antagonists (**8**).[65] Although no benzobisthiazoles appear in drug targets at this time, that may change as more robust and gentle methodologies emerge for their synthesis and functionalization.

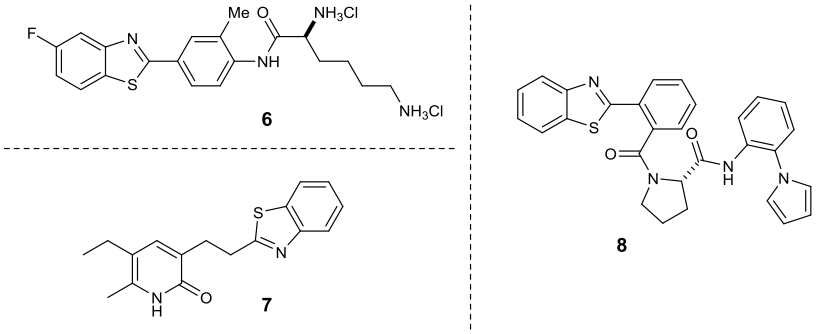

Figure 4.3. Drug targets that incorporate benzothiazole.

Current syntheses of substituted benzobisthiazoles typically involve the condensation of an aldehyde or acid with 2,5-diamino-1,4-benzenedithiol dihydrochloride (**9**). Jenekhe's synthesis of thiophene benzobisthiazole block copolymers starts with the condensation of the thiophene aldehyde with **9** to give substituted benzobisthiazole **10** in

only 12 % yield (Scheme 4.1).[60] To polymerize **10**, bromination of the 5-position of the thiophenes was carried out with NBS to generate **11**, which was followed by Stille coupling to generate BBT-thiophene polymer **12** in three steps and 6 % overall yield.

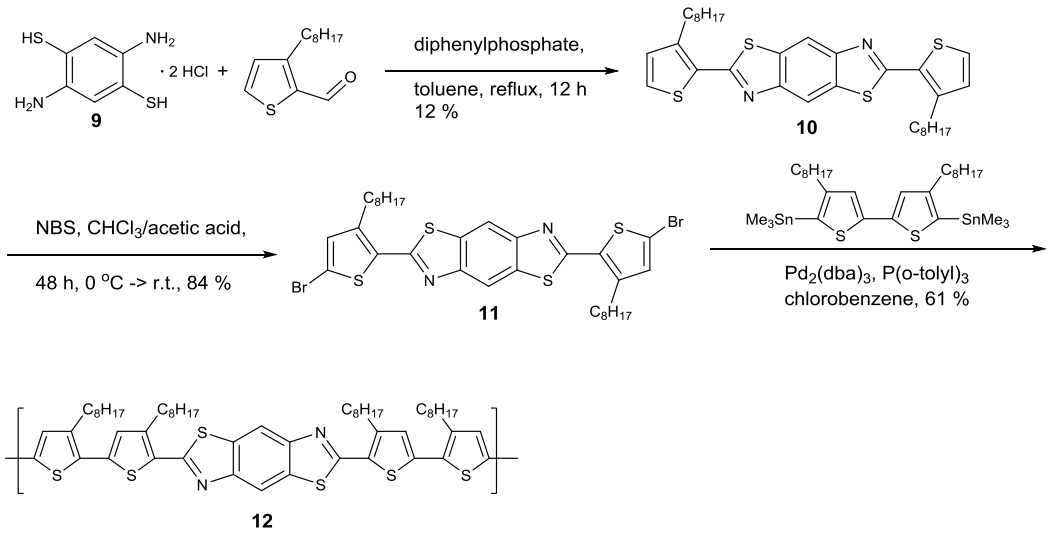

Scheme 4.1. Synthesis of BBT-thiophene polymer **12** by Jenekhe.

The Evers group took a similar approach to the formation of **13**, although in much better yield.[66] Starting from the acid instead of the aldehyde, they were able to generate 2,6-di(thiophen-2-yl)benzobisthiazole (**13**) in 80 % yield (Scheme 4.2).

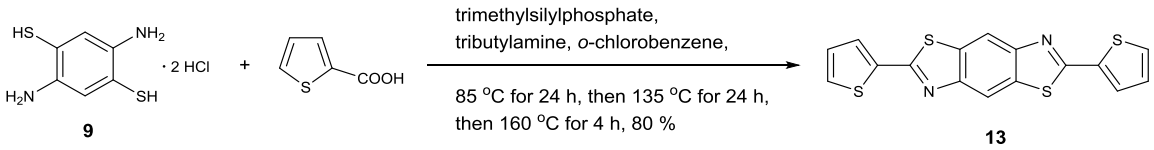

Scheme 4.2. Synthesis of **13** from Evers and coworkers.

In 2009 Jeffries-EL developed a method of forming the thiazole ring that did not require the harsh conditions found in other methods.[67] Using rare earth metal triflates as Lewis acid catalysts they were able to generate both unsubstituted benzobisthiazole **14** and various substituted benzobisthiazoles from **9** and the corresponding triethylorthoester (Scheme 4.3).

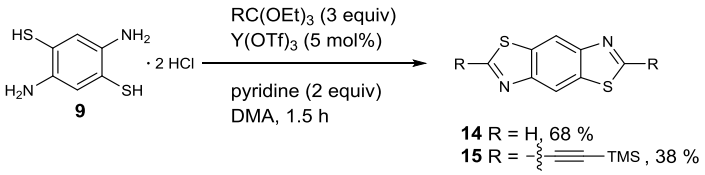

Scheme 4.3. Synthesis of **14** and substituted benzobisthiazole **15** from Jefferies-EL.

4.2 C–H Functionalization of Benzothiazole

Recently there has been a lot of progress in the synthesis of benzothiazole derivatives *via* C–H functionalization. Due to of the acidity of the thioimidate proton (pKa = 27.0), it is a relatively easy C–H bond to break making it a nice target for such methodology.

In 2008 Miura found that aryl iodides could be coupled with benzothiazole **16** using stoichiometric copper.[68] Phenylbenzothiazole (**17**) was synthesized from iodobenzene and benzothiazole in 74 % yield using CuI with PPh_3 as a ligand (Scheme 4.4). The reaction required a temperature of 160 °C in order to proceed palladium-free, and yields ranged from 71-83 %.

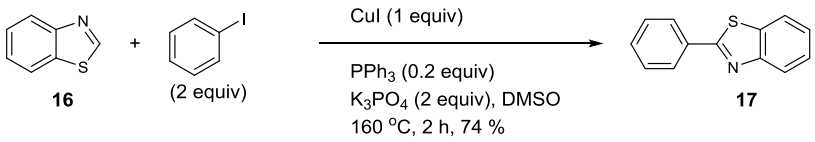

Scheme 4.4. Palladium-free synthesis of **17** from Miura.

An Amgen process group led by J. Huang found the yield could be improved and the conditions made milder by using Cu(Xantphos)I and PXPd as cocatalysts for the reaction (Figure 4.4).[69] They found it was possible to couple benzothiazole **17** with *p*-bromotoluene to generate **18** in 97 % yield.

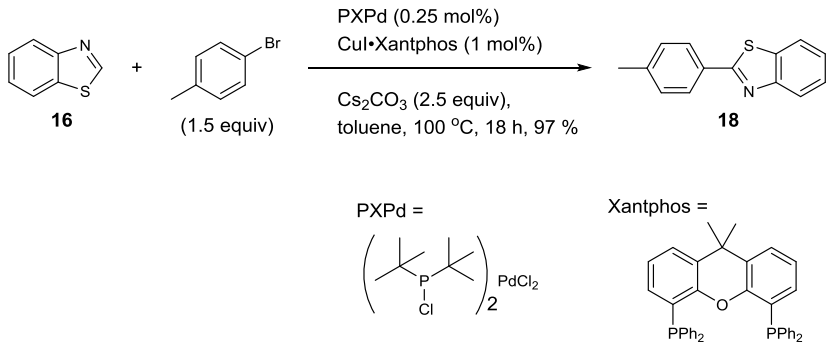

Figure 4.4. Amgen process methodology for the synthesis of **18** using PXPd and CuI(Xantphos).

A catalytic cycle is proposed in which copper coordinates to the nitrogen of the thiazole, then in a base assisted fashion breaks the thioimidate C–H bond (Figure 4.5). Palladium is responsible for the oxidative insertion into the aryl-halide bond. This is followed by transmetallation from copper to palladium, then reductive elimination from palladium generates the new C–C bond. X-ray crystallography confirmed that the copper coordinates to the lone pair of the thiazole nitrogen to form a tetrahedral complex. It is postulated that this binding serves to decrease the pKa of the thioimidate position even further, facilitating the base-assisted deprotonation and subsequent anion binding to copper.

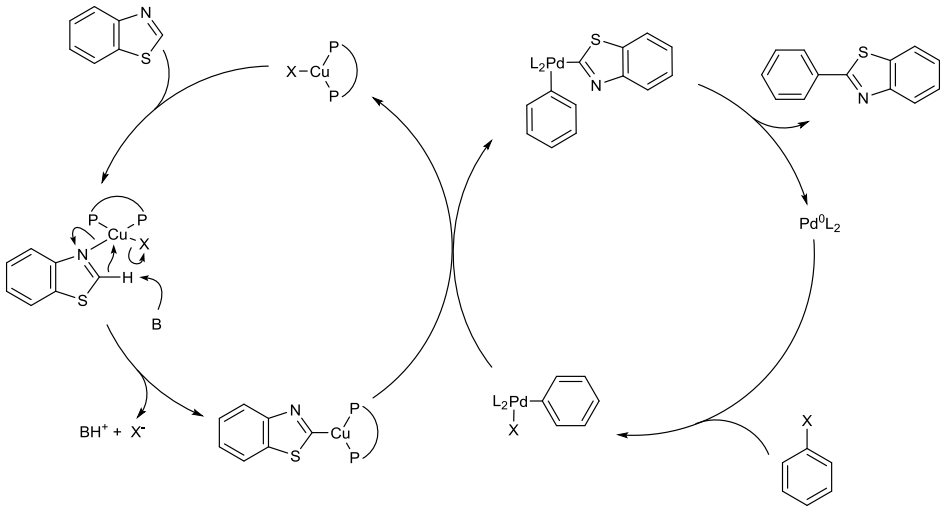

Figure 4.5. Catalytic cycle proposed by J. Huang and coworkers.

In 2011 it was found that the coupling of phenyl silanes gave 2-phenylbenzothiazole **17** in 93 % yield with catalytic palladium acetate and stoichiometric copper acetate (Figure 4.6).[70] Ofial also showed that phenyl stannanes could be coupled under the same conditions to give **17** in 58 % yield. The reaction required AgF in both cases to oxidize the Pd^0 to Pd^{II}. At lower copper loadings product was still formed (66 % with 1 equiv $Cu(OAc)_2$), but silane dimerization to biphenyl became competitive.

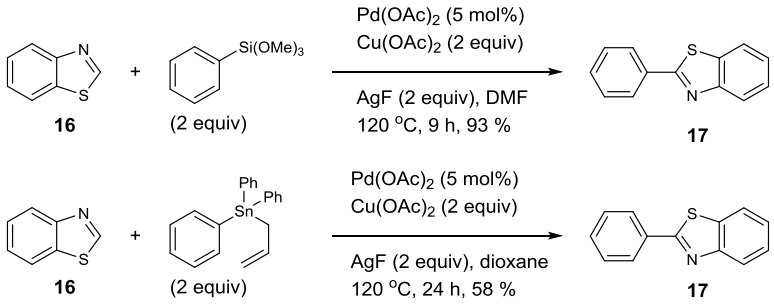

Figure 4.6. Ofial's methodology for the formation of **17** from phenyl silanes and stannanes.

Concurrently, the boronic acid coupling was shown to be effective by Liu and coworkers (Scheme 4.5).[71] They found that aerobic conditions gave the best yields, however running the reaction under an O_2 atmosphere the oxidative hydroxylation of the phenylboronic acid was the major product.

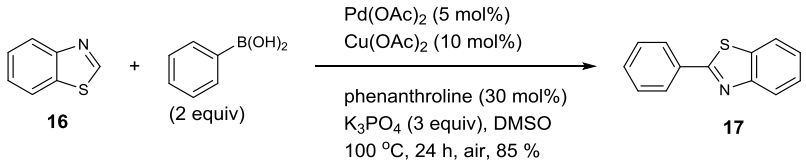

Scheme 4.5. Synthesis of **17** from phenylboronic acid from Liu and coworkers.

The same year that Liu and Ofial demonstrated couplings from aryl boronic acids, silanes and stannanes, Z.-Z. Huang's laboratory showed the same coupling could be performed with aryl bromides (Scheme 4.6).[72] Again, $Pd(OAc)_2$ and $Cu(OAc)_2$ are used with great success. In this case, as in the Amgen work, a phosphine ligand was required.

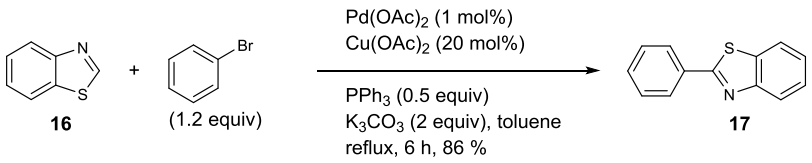

Scheme 4.6. Z.-Z. Huang's methodology for the synthesis of **17**.

It has also been shown that C–H functionalization could be used to make substituted benzothiazoles *via* thiazole ring-closing instead of C-2 functionalization. Recently, Punniyamurthy and coworkers developed a method for the formation of benzoxazoles and benzothiazoles from the arylamide or arylthioamide, using 1-iodo-4-nitrobenzene as the catalyst and oxone as the terminal oxidant (Scheme 4.7).[73] They were able to generalize this methodology to almost 60 examples with various substitution patterns around both rings covering both electron rich and poor substituents. This transformation from thioamide **19** to benzothiazole **18** is very well known and can be carried out using a number of reagents including $K_3Fe(CN)_6$,[74] $FeCl_3$,[75] chloranil/hν,[76] $PdCl_2$,[77] $Mn(OAc)_3$,[78] I_2,[79] DMP,[80] and DDQ,[81] among others.

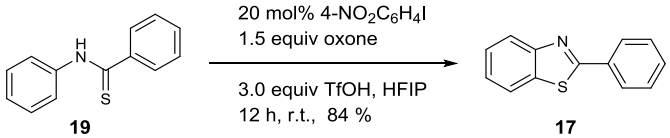

Scheme 4.7. Thiazole ring closing C–H functionalization.

Although there are numerous methods for the C-2 functionalization of benzothiazole, none of these methods have been applied to benzobisthiazole. C–H functionalization is anticipated to be an efficient way to access difunctionalized benzobisthiazoles for materials chemistry applications, providing an elegant alternative to aryl carboxylic acid condensations or routes through the orthoester.

4.3 Initial Exploration of Difunctionalization of BBT

After synthesizing benzobisthiazole (**14**) according to literature procedure (Scheme 4.8),[67] initial studies began with the low cost, readily available $Pd(OAc)_2/Cu(OAc)_2$ cocatalytic system that multiple labs previously found to be successful. Using conditions from Z.-Z. Huang with 2.5 equivalents of phenylbromide did not give the difunctionalized benzobisthiazole **20** as the major product (Scheme 4.9); instead the monofunctionalized **21** predominated. To our surprise **22**, the product of functionalization at the 4 position, was also observed. The formation of **22** suggested that this methodology could be adapted or optimized for the functionalization of the aryl positions, but that avenue has not been pursued.

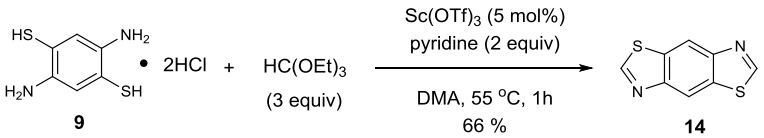

Scheme 4.8. Synthesis of benzobisthiazole (**14**).

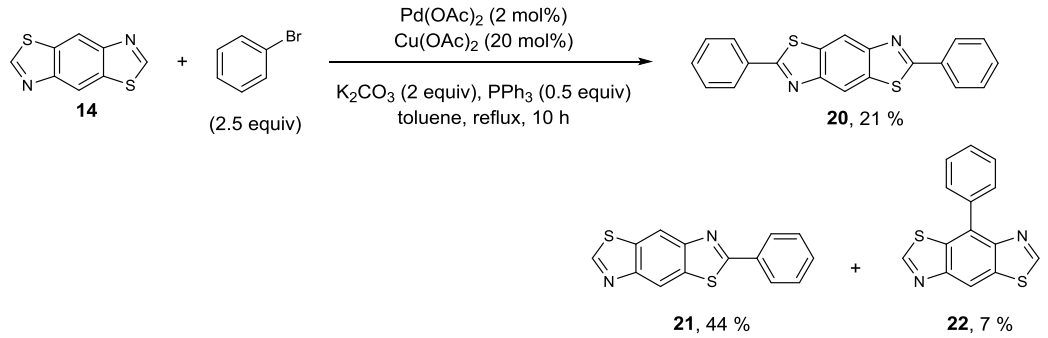

Scheme 4.9. Direct application of Z.-Z. Huang's conditions for the synthesis of **20**.

This methodology was quickly explored using 2.5 equivalents of three other aryl halides: 4-bromoanisole, 2-bromothiophene and 1-bromo-2,3,4,5,6-pentafluorobenzene (Figure 4.7). In all cases the monofunctionalized product was major, and in the cases of 4-bromoanisole and the 1-bromo-2,3,4,5,6-pentafluorobenzene only trace amounts of the difunctionalized products were isolated.

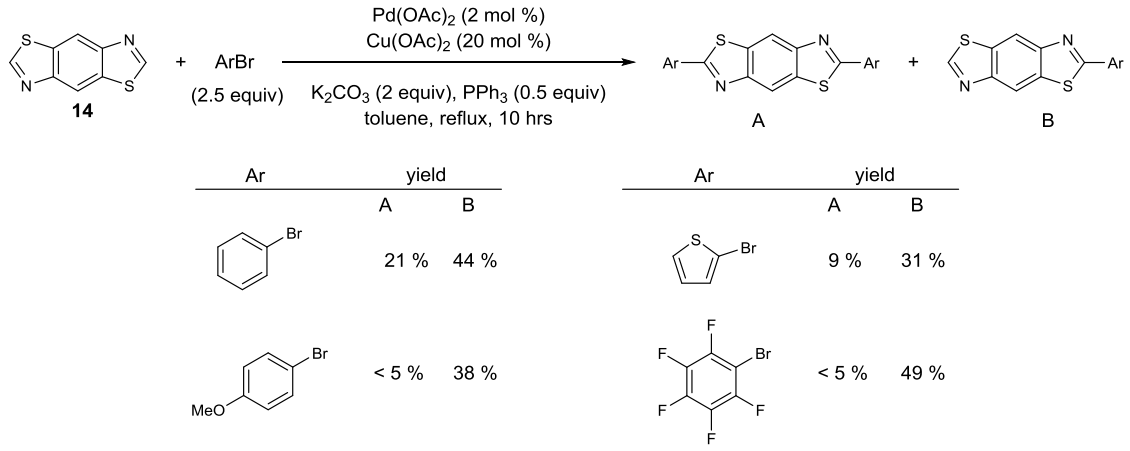

Figure 4.7. Initial exploration of aryl bromide scope of the C–H functionalization of **14**.

While these studies were underway, our collaborators Daijun Feng and Seth Marder at the Georgia Institute of Technology began their optimization from J. Huang's conditions with 4 equivalents of aryl bromide. They struggled to get good conversion to difunctionalized product **24** in toluene (Figure 4.8).[69] However, they found changing solvents to DMF and increasing the temperature to 135 °C allowed for 83 % conversion

to the desired product after 18 hours. The same reaction conditions at 90 °C for 18 hours resulted in no conversion to either the mono or difunctionalized products, indicating a very strong temperature dependence.

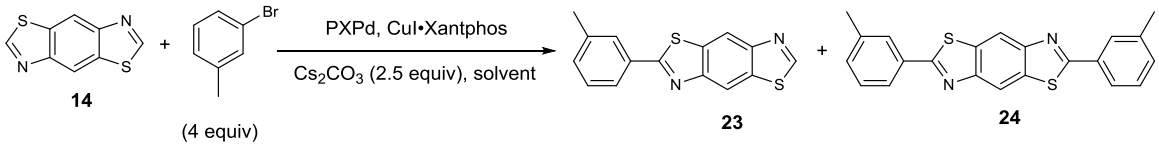

entry	solvent	temperature	time	yield **23**	yield **24**
1	toluene	r.t. -> reflux	18 hrs	NR	NR
2	DMF	r.t. -> 90 °C	18 hrs	NR	NR
3	DMF	135 °C	18 hrs	0 %	83 %

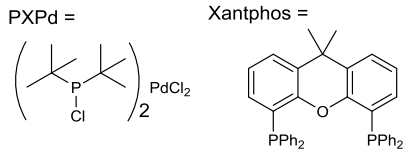

Figure 4.8. Optimization of C–H difunctionalization of **14** starting from J. Huang's conditions.

4.4 Optimization of coupling conditions

In light of this result, a formal optimization was undertaken using $Pd(OAc)_2$ (1 mol%), $Cu(OAc)_2$ (20 mol%), PPh_3 (0.5 equiv), and K_2CO_3 (2 equiv) in DMF at 135 °C as initial conditions (Figure 4.9A).[82] A GC assay was developed to monitor the appearance of **21** and subsequently **20** versus an internal standard of anthracene. Initial experiments explored $Pd(OAc)_2$ (Figure 4.9A and B) versus PXPd (Figure 4.9C and D) in the reaction with either $Cu(OAc)_2$ (Figure 4.9A and C) or CuI•Xantphos (Figure 4.9B and D). It was found that all combinations of $Pd(OAc)_2$ or PXPd with $Cu(OAc)_2$ or CuI•Xantphos gave **20** as the major product and reached completion around 5 hours. In reactions with PXPd (Figure 4.9C and D) there appeared to be some decomposition of the product over time. For example, with PXPd and $Cu(OAc)_2$ there was 75 % of product after 4.5 hours but less than 50 % at the 8.5 hour mark (Figure 4.9C). Because all

conditions produced **20** in good conversion, the most accessible conditions (acetates instead of specialized phosphine ligands) were used for further optimization.

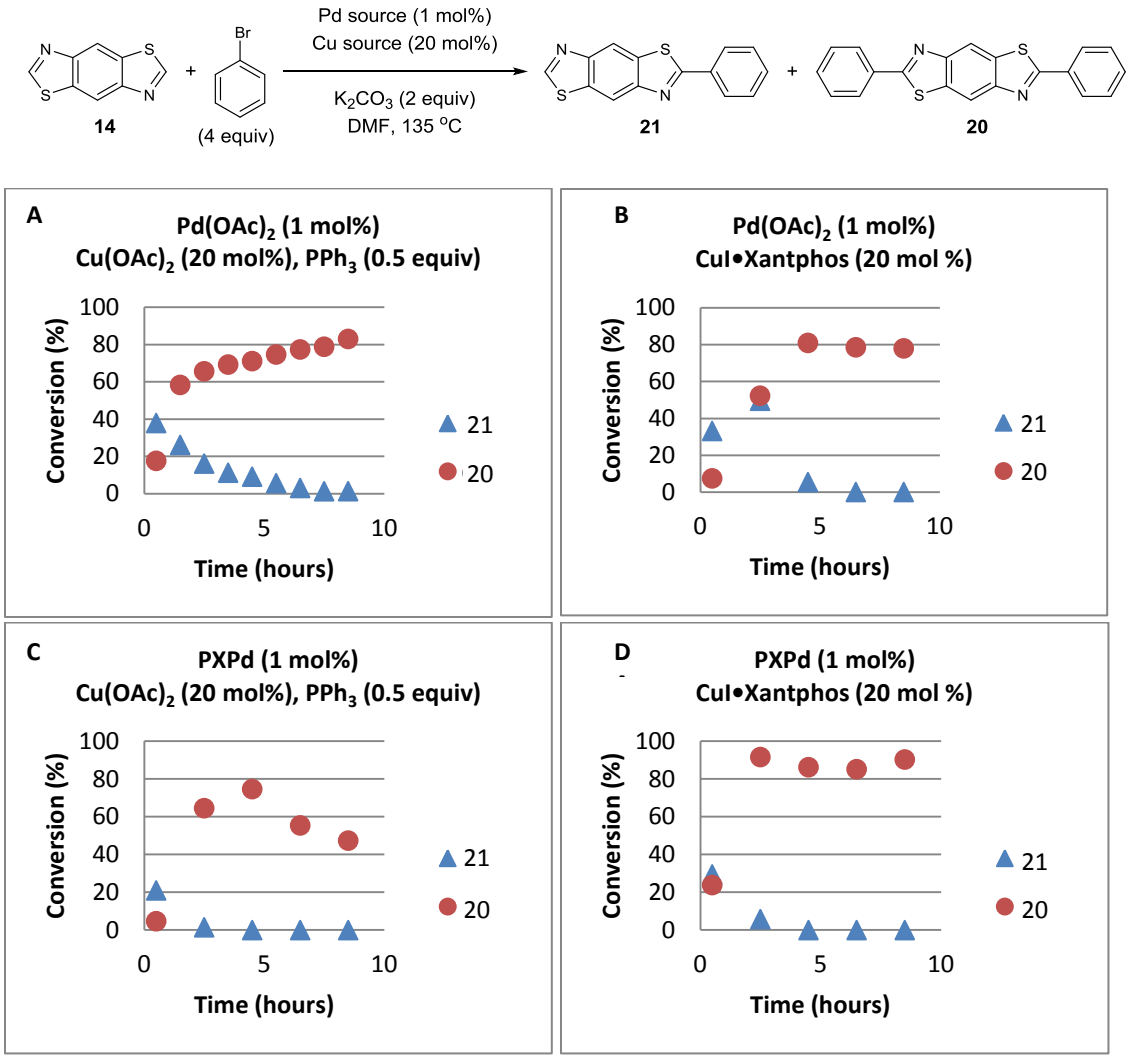

Figure 4.9. Effect of $Pd(OAc)_2$ and PXPd with $Cu(OAc)_2$ and CuI•Xantphos on the synthesis of **20**.

In the reaction using $Pd(OAc)_2$ with CuI•Xantphos (Figure 4.9B), no additional phosphine was added based on the hypothesis that only copper required the phosphine ligand, so by using a precoordinated copper phosphine complex additional copper was not necessary. To confirm this hypothesis, the reaction was run again with 0.5 equivalents of PPh_3 added to the reaction (Figure 4.10A), and the results were

comparable to that of the reaction with no additional phosphine (Figure 4.9B/4.10B). This result suggests either the palladium does not require a ligand or just enough of the Xantphos ligand was dissociating from the copper and coordinating to the palladium for palladium turnover.

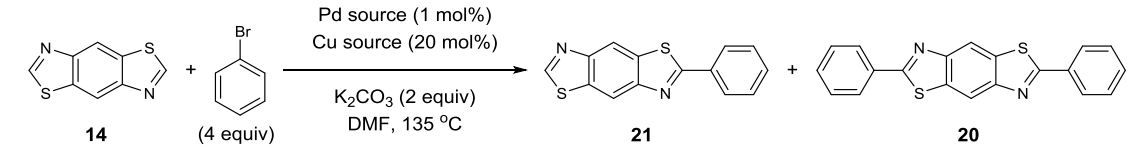

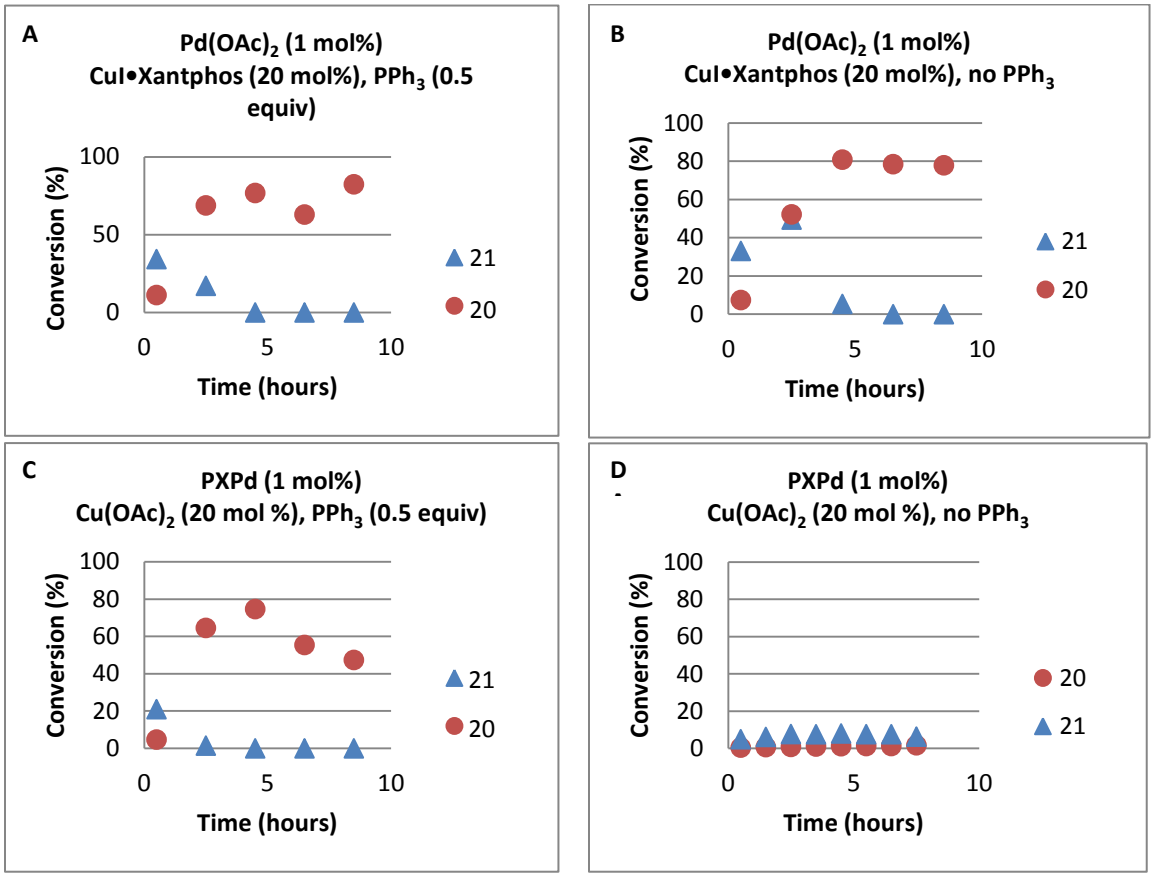

Figure 4.10. Comparison of precoordinated copper and precoordinated palladium with and without additional phosphine ligand in the synthesis of **20**.

When a precoordinated palladium (PXPd), $Cu(OAc)_2$, and additional PPh_3 were used the reaction proceeded well (Figure 4.10C); again, some product decomposition of the product was observed in the presence of PXPd. When the external phosphine was

removed from these conditions, leaving only the palladium ligated, the reaction did not generate either **20** or **21** suggesting the copper requires a phosphine ligand for the reaction to proceed (Figure 4.10D).

It was also established that the reaction proceeds well with both Cu(I) and Cu(II). Switching from $Cu(OAc)_2$ to CuI with PPh_3 and $Pd(OAc)_2$ resulted in a slight increase in the rate of conversion to **20** (Figure 4.11A and B).

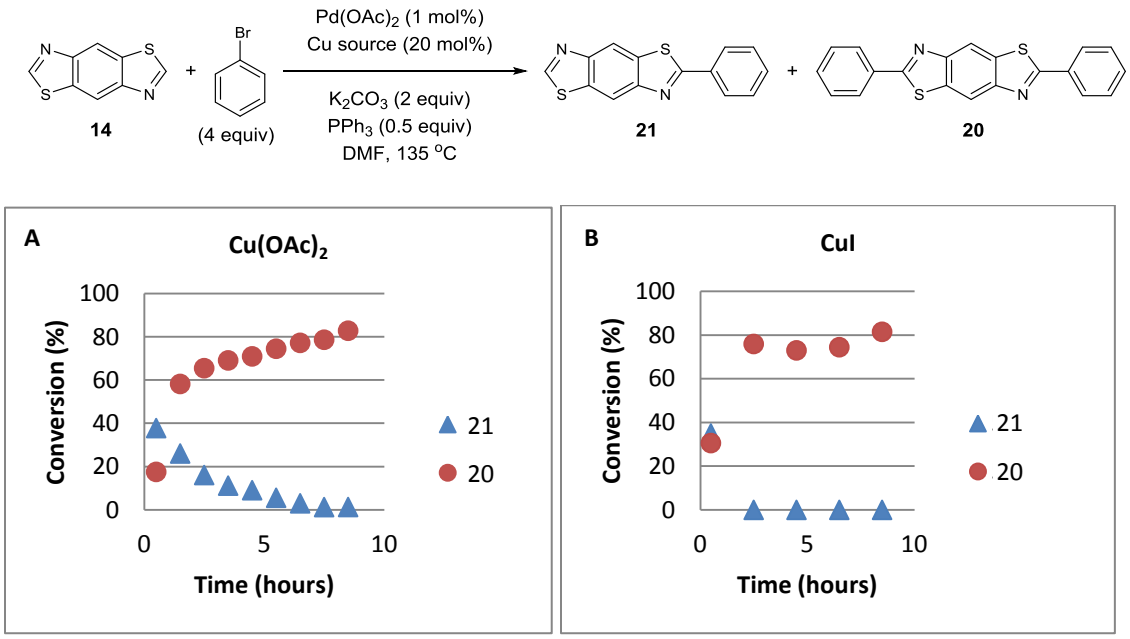

Figure 4.11. Efficacy of copper(I) versus copper(II) in the synthesis of **20**.

Based on initial results from Daijun Feng showing significant changes with solvent and temperature, a solvent screen was undertaken (Figure 4.12). Using dioxane, toluene, DMF, DMA and xylenes, dioxane and toluene gave the lowest conversion to **20** (Figure 4.12D and E), while DMA (Figure 4.12C) and xylenes (Figure 4.12B) both leveled off around 70 % conversion to **20**. DMF gave the highest conversion at 83 % after 8.5 hours (Figure 4.12A).

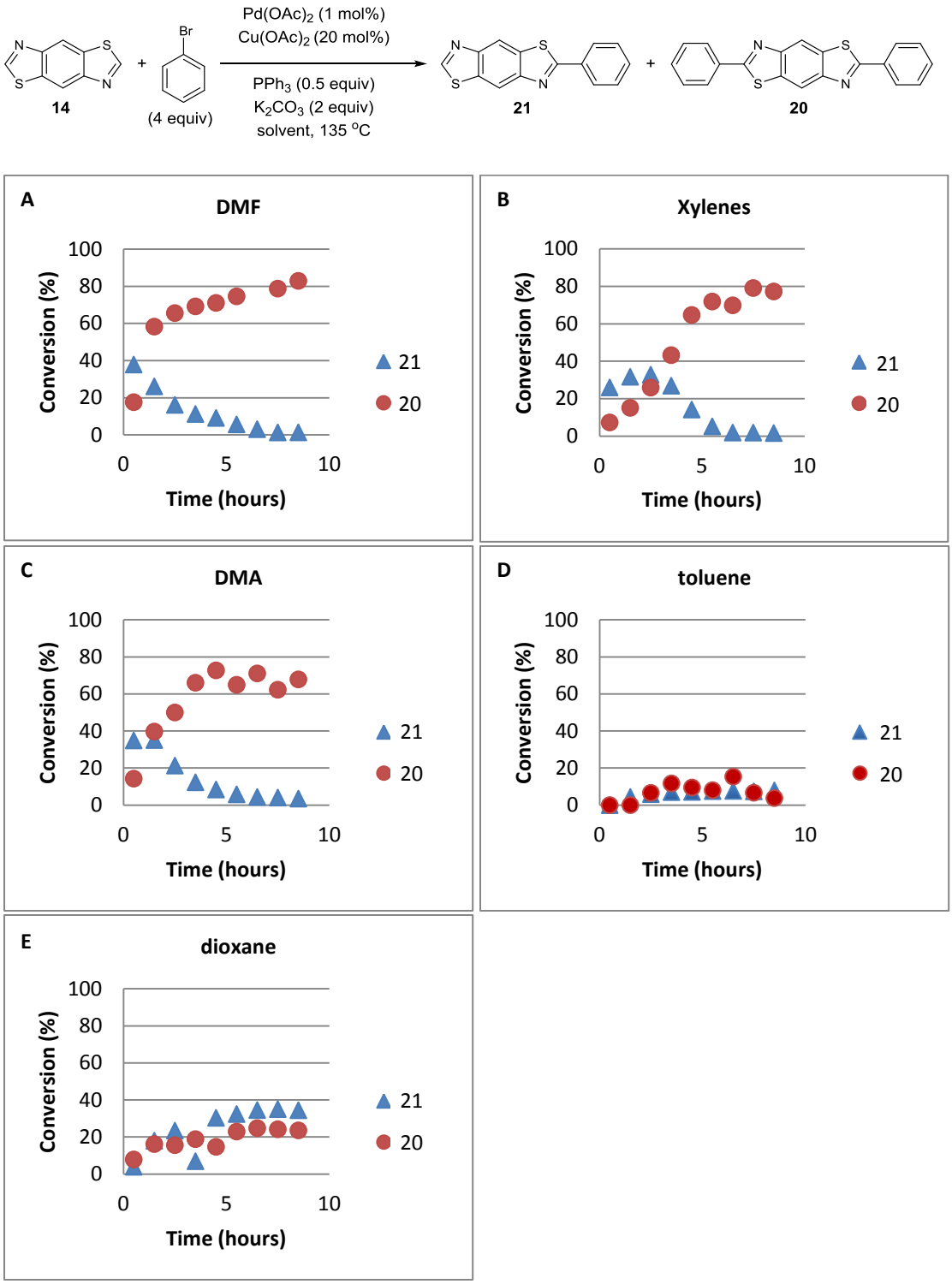

Figure 4.12. Examination of DMF, xylenes, DMA, toluene, and dioxane as solvents for the conversion of **14** to **20**. Reactions in toluene and dioxane were heated to reflux.

To determine if this was due to the properties of the solvent itself or due to the higher temperatures available with those solvents, the reaction with DMF was run at lower temperature (Figure 4.13). By decreasing the temperature to 115 °C, conversion to **21** falls to about 20 % and only trace amounts of **20** is observed (Figure 4.13B). Decreasing further to 85 °C gives only trace of **20** (Figure 4.13C). This is consistent with the extreme temperature dependence that was observed previously in this work.

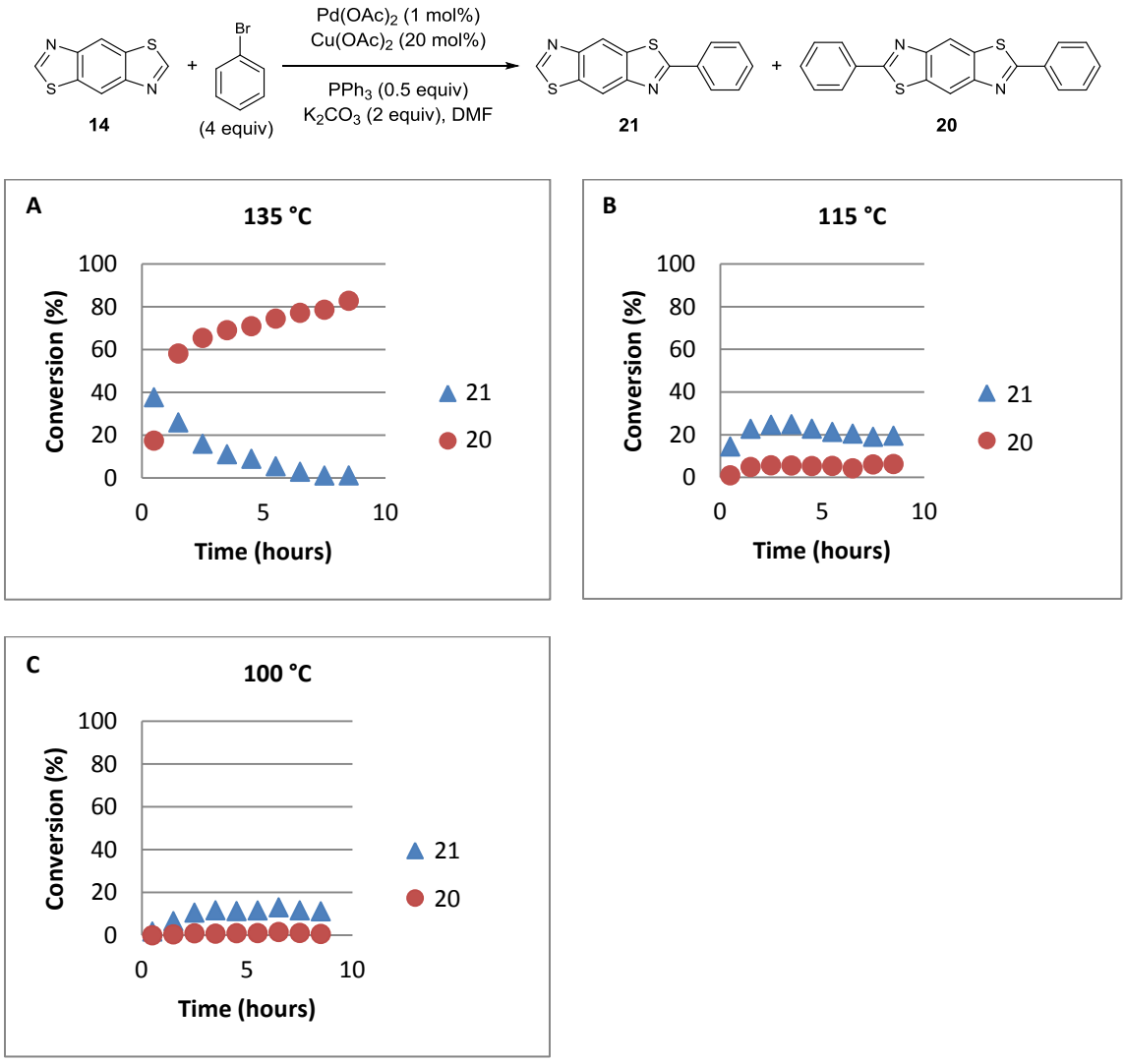

Figure 4.13. Impact of temperature on conversion of **14** to **20**.

Noticing that at 115 °C conversion to **20** was limited to 20 % with 20 % copper in the solution (Figure 4.13B/4.14A) suggested that the issue may be copper turnover. At lower temperature the copper cycle may become too slow for the reaction to proceed catalytically. This suggests a way to increase conversion at lower temperature would be to increase the copper loading in the reaction. Increasing the copper loading to 0.5 equivalents brought the reaction to completion in about 8 hours (Figure 4.14B). With 0.75 equiv $Cu(OAc)_2$ the reaction reached 93 % conversion to **20** in 3.5 hours (Figure 4.14C), and with 1 equiv $Cu(OAc)_2$ the reaction was done in less than 30 minutes (Figure 4.14D).

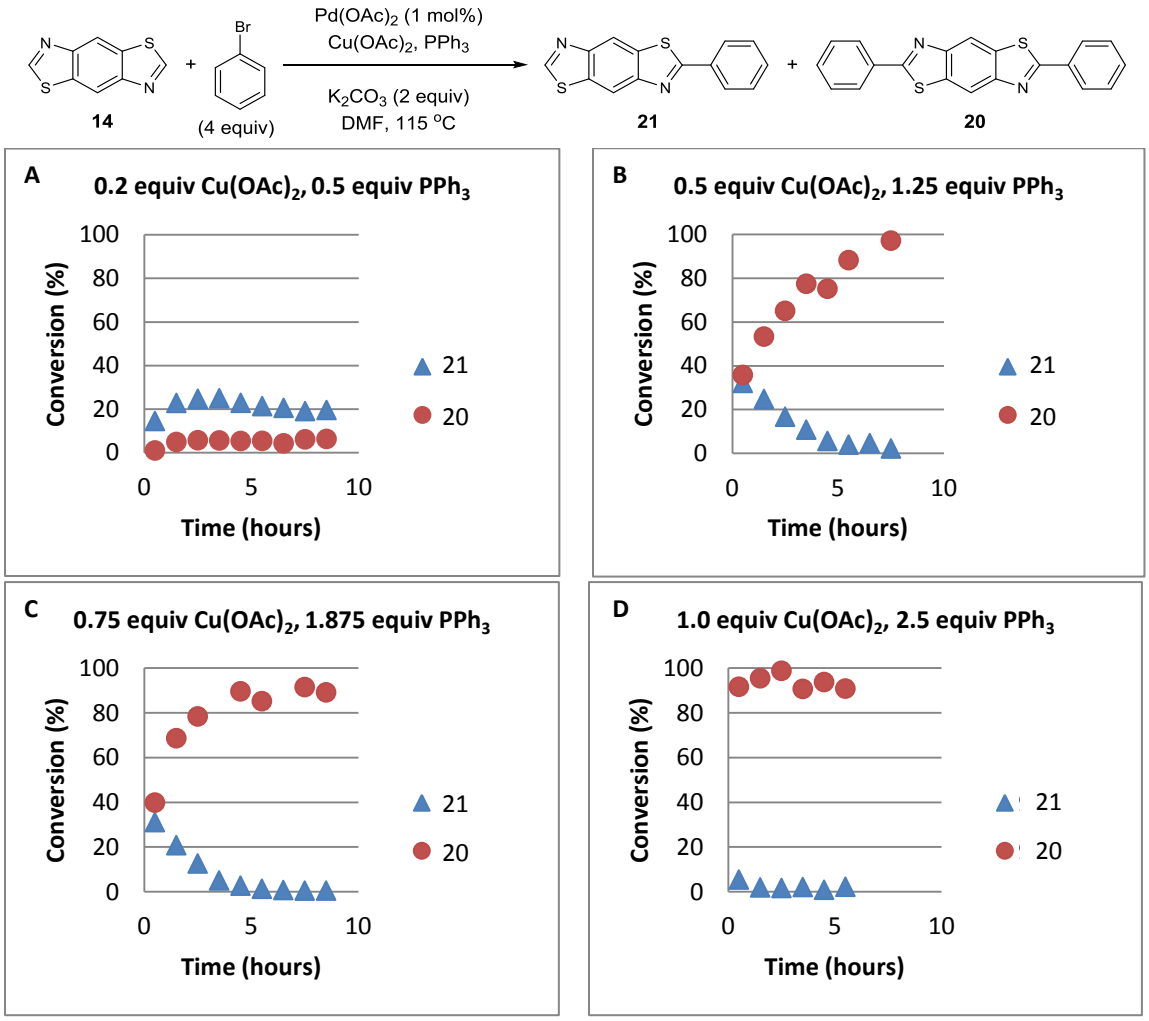

Figure 4.14. Impact of increasing loading of copper at 115 °C on the conversion to **20**.

Because similar reactions have been carried out with only copper, without a second metal, we were curious if our system could proceed with no palladium but high copper loading (Figure 4.15). Unfortunately we found only trace of the desired product without palladium, indicating the palladium is indeed necessary.

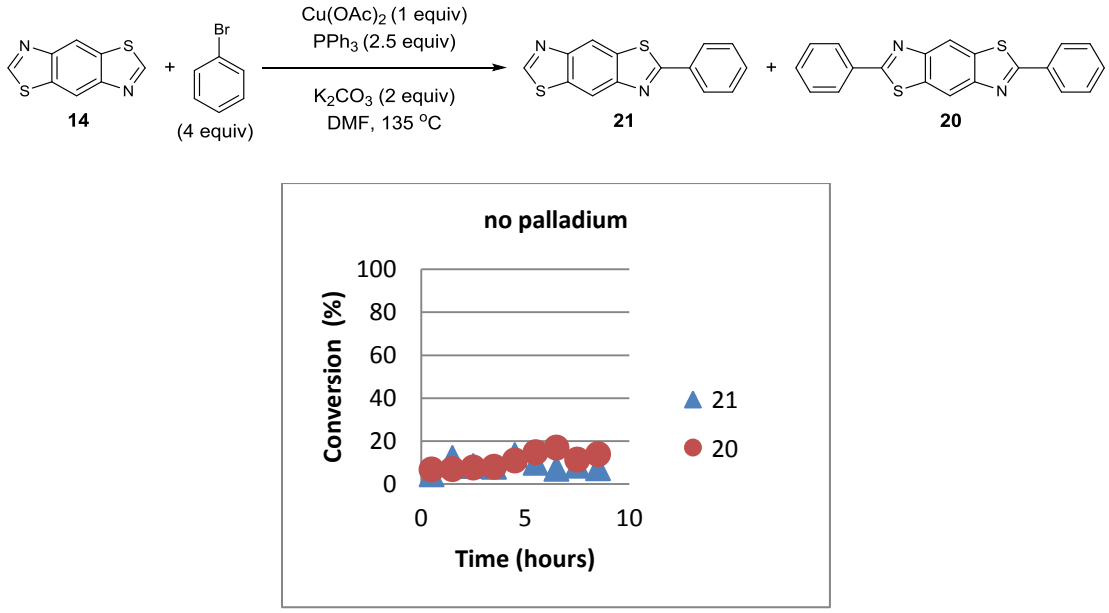

Figure 4.15. Palladium-free control reaction.

This data supports the mechanism proposed by J. Huang for the functionalization of benzothiazole (Figures 4.5 and 4.16). In this mechanism the copper coordinates to the thiazole nitrogen and then inserts into the thioimidate positions, likely in a base-assisted fashion. Palladium oxidatively inserts into the aryl-halogen bond. From there a transmetallation occurs and both the thiazole and the aryl portion end up on the same metal. We do not have the evidence to know if the system transmetallates from copper to palladium or from palladium to copper, but it seems likely to transmetallate to palladium. Once the transmetallation occurs, reductive elimination forms the new carbon-carbon bond to generate **21**. The halide can then dissociate from copper as X^-.

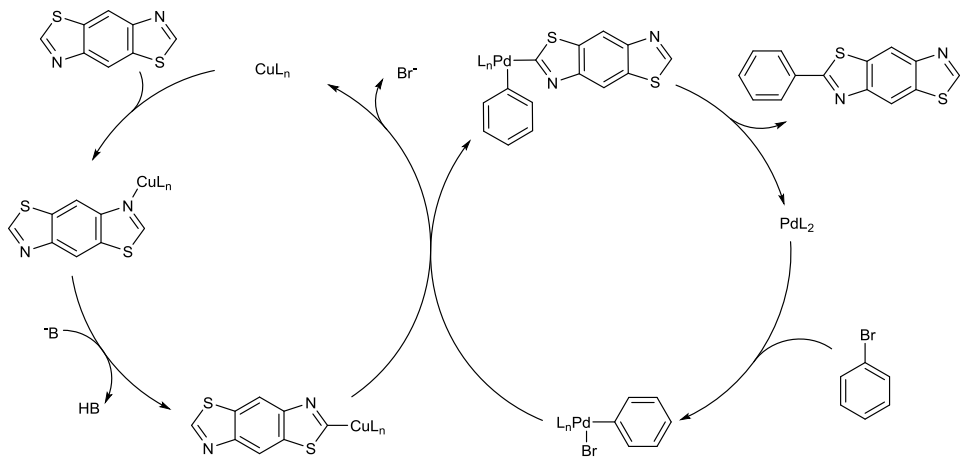

Figure 4.16. Proposed mechanism for the formation of **21**.

Establishing that at lower temperatures copper turnover was rate limiting suggested that by using more copper the reaction could be carried out at lower temperature. Running the reaction at 100 °C and 85 °C with 1 equiv of copper showed this was not the case (Figure 4.17A and B). This indicates that maybe the copper insertion into the thioimidate position or transmetallation may be the slow step so even with additional copper the reaction is getting held up at this step.

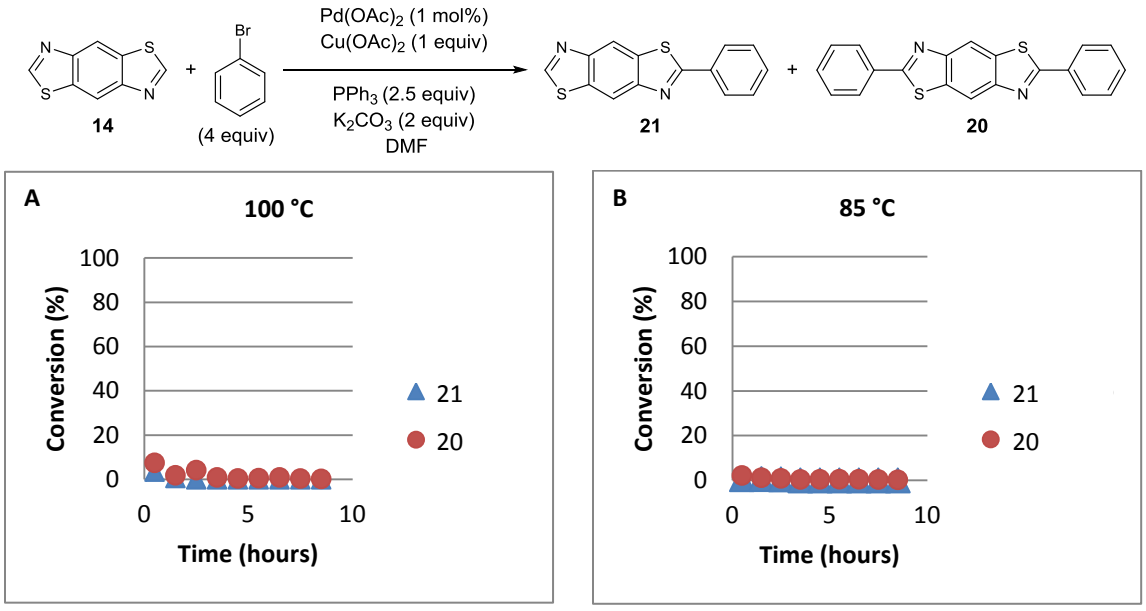

Figure 4.17. Exploration of decreased temperature and high copper loading on the conversion of **14** to **20**.

Altering the phosphine ligand was hypothesized to facilitate the copper cycle, leading us to explore a variety of monodentate and bidentate phosphine ligands at low temperature (Figure 4.18). In this study we found a number of ligands that would allow the reaction to proceed at lower temperature; however, it was difficult to identify trends in this data. Using tricyclohexylphosphine gave no significant improvement and still gave only trace **20** (Figure 4.18B). Using electron rich aromatics like tris(*p*-methoxyphenyl)phosphine or trifurylphosphine allowed the reaction to progress well at the reduced temperature (Figure 4.18D and E). Using an electron poor phosphine like tris(*p*-trifluoromethylphenyl)phosphine also increases conversion versus triphenylphosphine making overall trends difficult to tease out (Figure 4.18C).

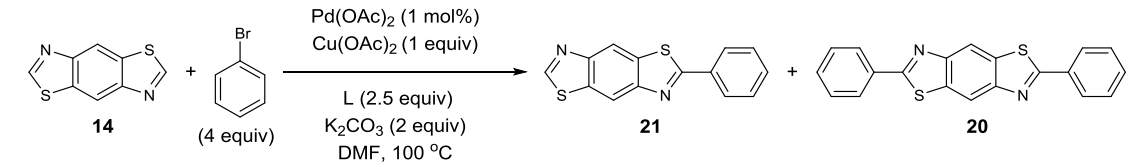

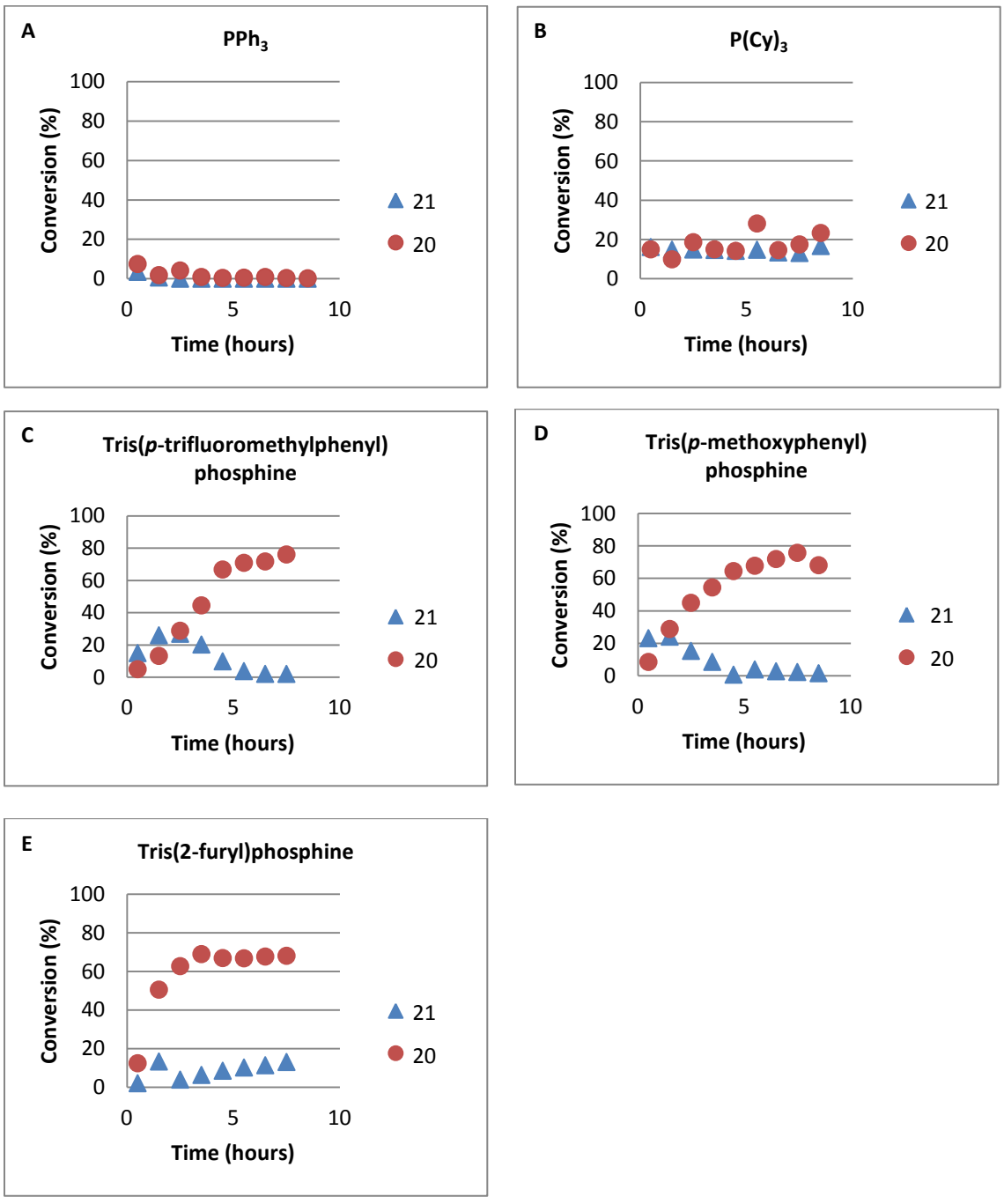

Figure 4.18. Examination of monodentate ligands in the synthesis of **20**.

Bidentate ligands were also explored with mixed success (Figure 4.19). DPPB and DPPP gave dramatically different results, with DPPP giving very little of **20** (Figure 4.19B) and DPPB going to 78 % conversion to **20** in 5.5 hours (Figure 4.19A). This suggests a large dependence on both sterics and the bite angle of the ligand. DPPF also performed poorly, only reaching 11 % conversion after 8.5 hours (Figure 4.19C). Xantphos, on the other hand, reached 73 % conversion after 8.5 hours and had not yet reached a plateau in product formation (Figure 4.19D).

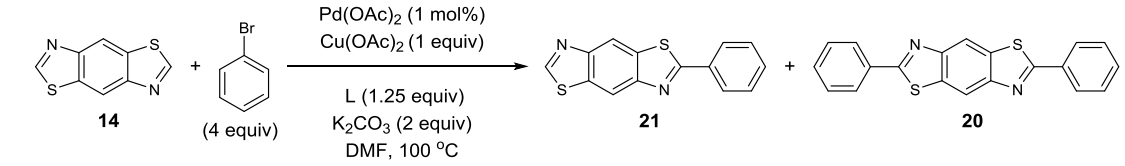

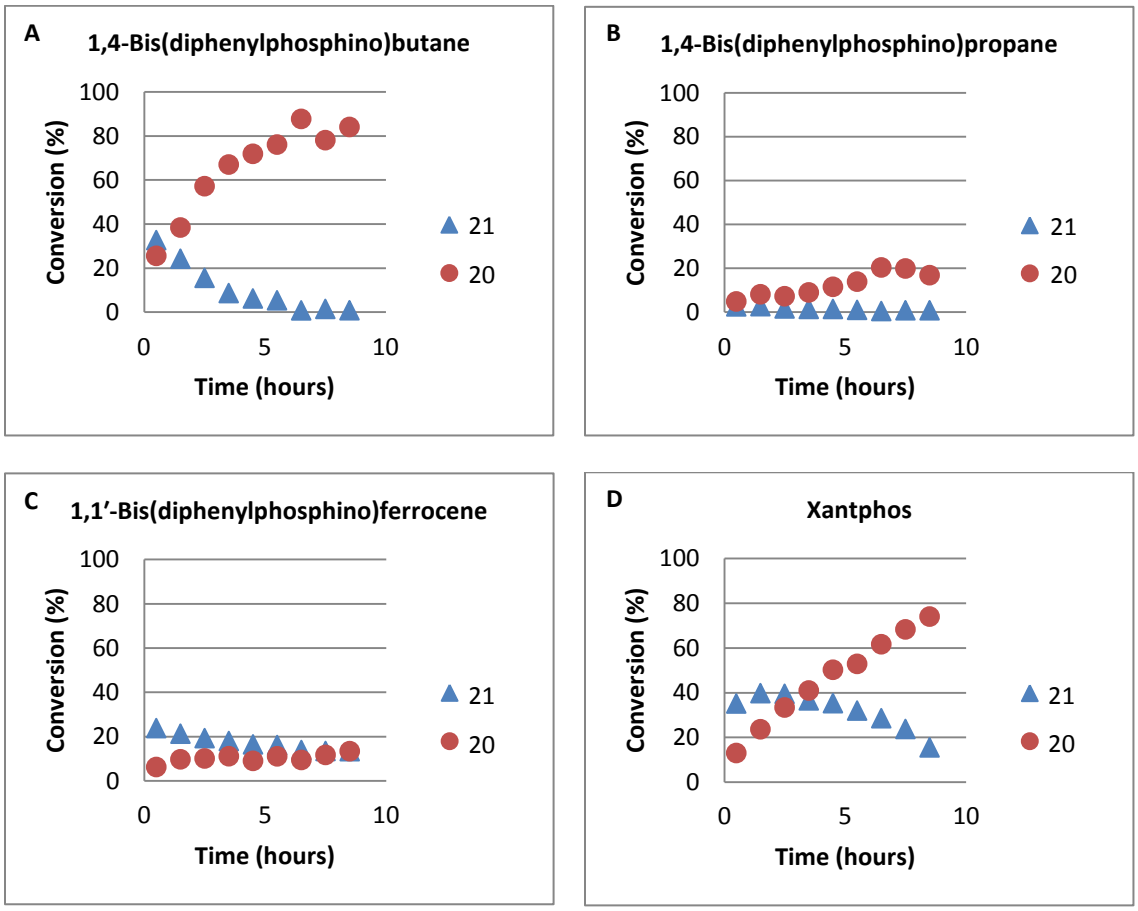

Figure 4.19. Examination of bidentate ligands in the synthesis of **20**.

Based on these findings we found a number of sets of optimal conditions. Using 20 mol% $Cu(OAc)_2$ with PPh_3 and $Pd(OAc)_2$ in DMF at 135 °C gives 82 % conversion to **20** in 8.5 hours. If lower temperatures are desired due to substrate or product sensitivity, then 1 equiv of copper with 2.5 equiv of PPh_3 can be used at 115 °C to give 92 % conversion to **20** in 0.5 hours. Tris(*p*-methoxyphenyl)phosphine can be used as the phosphine ligand in place of PPh_3 at 100 °C with 1 equiv of copper to reach 76 % conversion in 7.5 hours.

4.5 Probing the Scope of Aryl halides Amenable to the C–H Functionalization of 14

Using the conditions developed in our optimization studies which employed DMF at 135 °C with 20 mol % copper acetate and triphenylphosphine as the ligand, we examined the scope of aryl bromides that were tolerated in this reaction. We found simple aryl bromides were generally well-tolerated. The isolated yield of **20** held up well compared to the conversion determined by GC (71 %, Table 4.1 entry 1). 3-Bromotoluene as a coupling partner gave a higher yield at 81 % isolated (Table 4.1, entry 2). Both 2-bromothiophene and 2-bromo-3-hexylthiophene were explored and gave similar yields at 49 and 43 % respectively (Table 4.1, entries 3 and 4).

The reaction with 4-bromoanisole gave only 38 % of the desired product but also gave a small amount of **21** (Table 4.1, entry 5). This is likely due to P-C functionalization of the triphenylphosphine and arylation of benzobisthiazole with phenyl instead of *p*-methoxyphenyl. In this case after the copper has inserted into the thioimidate C–H bond, one of the C–P bonds of a PPh_3 coordinated to the copper breaks,

and the phenyl ring is transferred to the BBT. This has been observed previously in other cross couplings of electron rich aryl halides.[83]

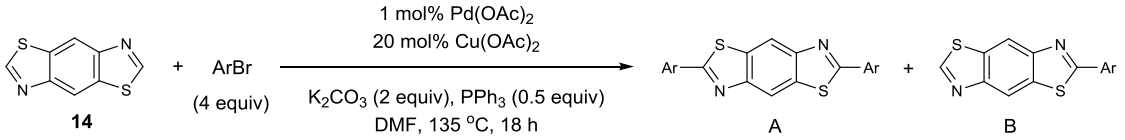

entry	ArBr	Yield A	Yield B	entry	ArBr	Yield A	Yield B
1		71	--	9	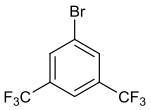	72	--
2	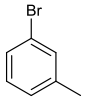	81	--	10	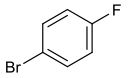	--	--
3	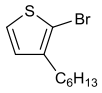	43	--	11	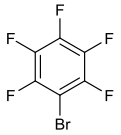	--	--
4		49	--	12	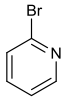	66	7
5	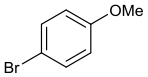	38[a]	--	13	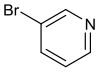	58	23
6	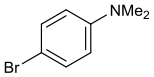	--	--	14		--	--
7	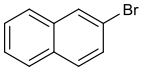	--	--	15	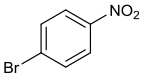	--	51
8	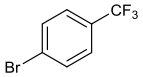	77	--				

Table 4.1. Exploration of aryl halide substrate scope for the C–H functionalization reaction with **14**. All yields are isolated. A) 8 % of **21** was also isolated.

4-Bromo-*N*,*N*-dimethylaniline was explored as a coupling partner, and none of the desired product was observed by crude NMR or mass spectrometry (Table 4.1, entry 6).

2-Bromonaphthalene was also examined in the reaction, and no product was observed (Table 4.1, entry 7).

Electron poor substrates like *p*-bromotrifluoromethylbenzene and 3,5-bistrifluoromethyl-1-bromobenzene gave good yields, 77 % and 72 %, respectively (Table 4.1, entries 8 and 9). Other electron poor substrates like 1-bromo-4-fluorobenzene and bromopentafluorobenzene gave none of the desired product (Table 4.1, entries 10 and 11). Both 2-bromo- and 3-bromopyridine gave the desired product in 66 and 58 % yield respectively. However, the monofunctionalized product was isolated in both of these cases (Table 4.1, entries 12 and 13). This is most likely due to the poor solubility of the monofunctionalized intermediates. In both of these cases, the monofunctionalized product is very insoluble even at elevated temperatures and likely precipitated out of the reaction solution before it could be converted to the difunctionalized product. 2-Bromopyrimidine was explored based on the success of the 2-bromopyridine, but unfortunately no product was observed by crude NMR or by mass spectrometry (Table 4.1, entry 14). The insolubility hypothesis for the poor yields of the pyridine derivatives was supported by the reaction with 4-bromo-nitrobenzene. Only the monofunctionalized product was isolated, and it was very insoluble. This result which is consistent with the reaction stopping at the monofunctionalized product because it precipitated out before it could progress to the difunctionalized product.

In an effort to generate building blocks for electron transport applications, bromonaphthalenediimide **25** was explored. Previously there have been no C–H functionalization methodologies that involve this compound. Only Stille and Suzuki

couplings have been used to successfully incorporate this group into small molecules and polymers.

Unfortunately, none of our optimized sets of conditions were successful in converting the bromonaphthalenediimide **25** to the desired product **26** (Figure 4.20). The reduction product **27** was isolated as well as hydroxylated product **28**. **28** is likely the result of the S_NAr reaction with trace water in the solution.

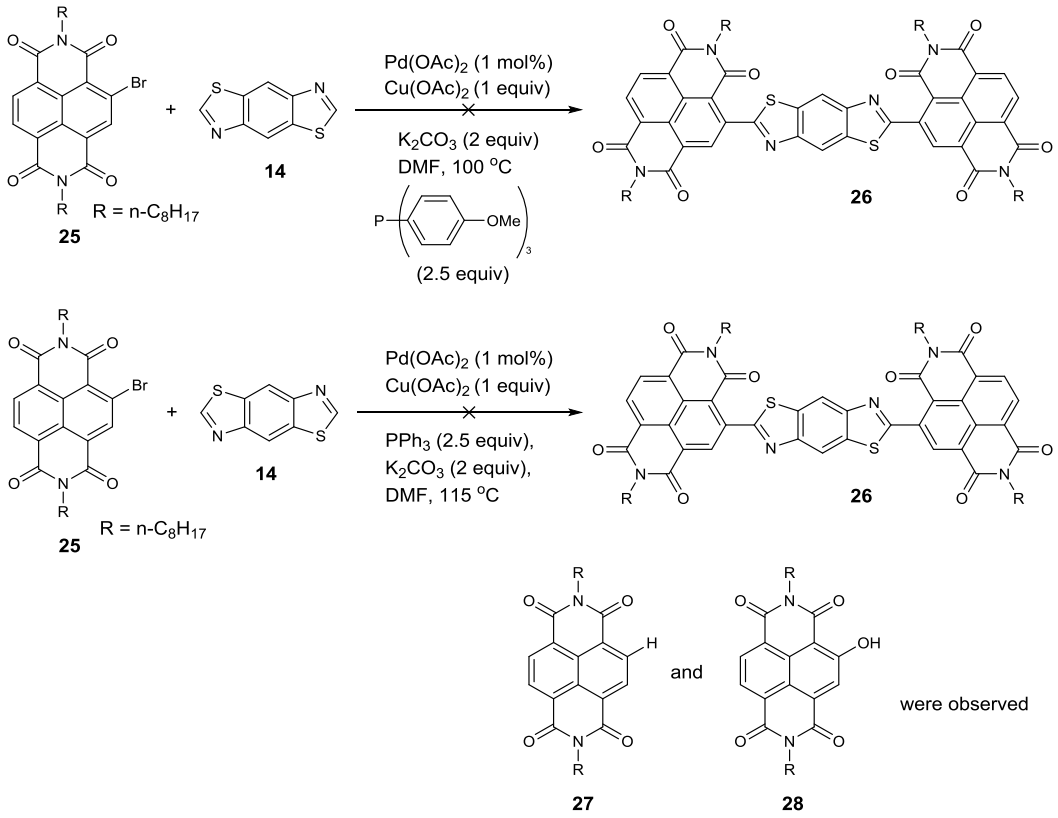

Figure 4.20. Attempted coupling of **14** with bromonapthtalenediimide **25** to give **26**.

The naphthalenediimide substrate was significantly more complex than the simpler aromatics that had been explored, so there were a number of complications that could have arisen. At this point aryl groups with ortho substituents had not been explored, so a simple steric issue could be preventing the reaction. There was also no

evidence that coordinating groups, like a diimide, ester or amide, would be tolerated in this reaction.

To explore these potential complications, an aryl bromide with a non-coordinating ortho substituent was examined. 1-Bromo-2-isopropylbenzene gave a yield of 54 % (Table 4.2, entry 2), which is significantly lower than the yields with bromobenzene or 3-bromotoluene, suggesting sterics does play a role in the naphthalenediimide's lack of reactivity (Table 4.1, entries 1 and 2). There was however still more than 50 % of the desired product isolated with the ortho-isopropyl substrate indicating there are likely other factors involved beyond sterics.

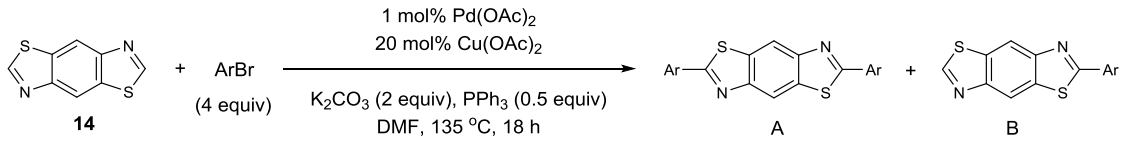

entry	ArBr	Yield A	Yield B	entry	ArBr	Yield A	Yield B
1	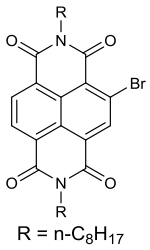 R = n-C_8H_{17}	--	--	5	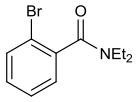	15	--
2	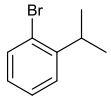	54	--	6	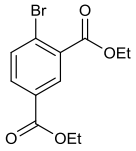	--	--
3	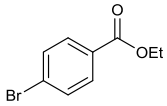	52	--	7	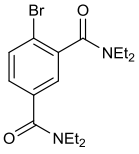	--	--
4	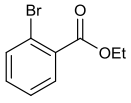	37	--	8	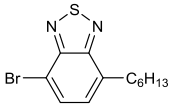	--	--
				9	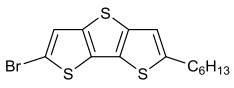	--	--

Table 4.2. Aryl halide substrates to probe the limitations of the C–H functionalization methodology. All yields are isolated.

The next hypothesis to test was that after the palladium had inserted into the carbon-bromine bond, it was coordinating to the carbonyl and the formation of the palladacycle prevented palladium turnover and ultimately product formation. First, we looked at a substrate with an ethylester in the para position to establish compatibility of an ester with the palladium catalytic cycle when the ester is not in the position to form a palladacycle. Giving 52 % yield (Table 4.2, entry 3), the ester was tolerated to a certain extent but was detrimental to the reaction. To explore coordination to an ortho substituent, the ortho-diethylamide (**29**) and the ortho-ethylester (**30**) were synthesized from the corresponding acid chloride (Scheme 4.9). Moving the ester to the ortho position dropped the yield to 37 %. This is due to the combination of steric blocking and the position of the ester for palladicycle formation following insertion into the carbon-halogen bond.

Switching to diethylamide **29**, the yield was even lower at 15 % (Table 4.2, entry 5) which is consistent with coordination of the palladium causing difficulties since the amide is the better coordinating group and the reaction had about half the yield.

Pushing this further, diamide **31** and diester **32** were synthesized from the corresponding diacids *via* the acid chlorides and then explored in the coupling reaction. In both cases none of the desired product was isolated (Table 4.2, entries 6 and 7).

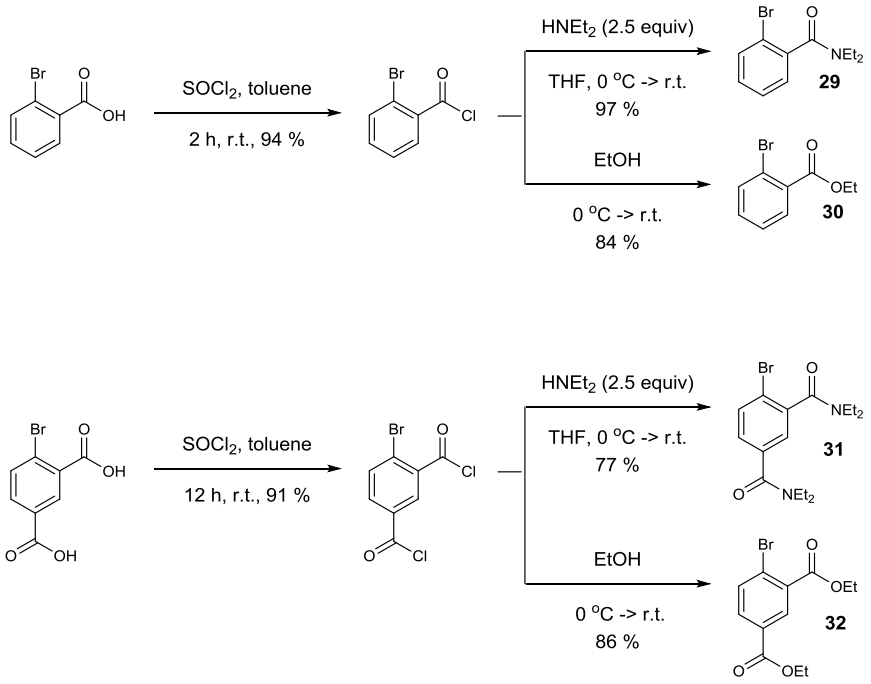

Scheme 4.10. Synthesis of compounds **29**-**32**.

We also explored the benzothiadiazole and dithienothiophene as substrates for this coupling due to their prevalence in common organic electronic molecules. Unfortunately neither substrate gave the desired product (Table 4.2., entries 8 and 9).

4.6 Synthesis of Cruciform Structures *via* 2,6-Difunctionalization of Benzobisthiazole 14

One complication in tuning the HOMO and LUMO levels of a conjugated framework is that the frontier molecular orbitals are generally quite spread out, and their overlap makes them difficult to modulate independently. Some researchers have moved to X-shaped cruciform structures in order to control HOMO and LUMO levels more independently. These structures have two perpendicular π-systems that intersect at a conjugated core. Benzobisoxazole has been used by Miljanić as a core for such

molecules. To prepare an array of these molecules for testing they must start from the tetrabromoquinone and go through 2,5-diamio-3.6-dibromo-1,4-benzenediol (**33**) (Scheme 4.11),[84] which can then be condensed with benzoic acid to access the 2,6-functionalizatized product **34**. Then traditional cross coupling chemistry can be used for functionalization of the 4- and 8- positions to generate **35** in 83 % yield (Scheme 4.12).[85] The thiol derivative of **33** is not a known compound.

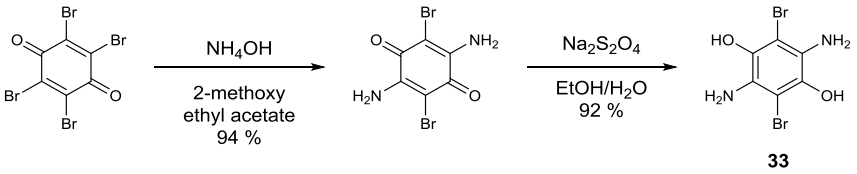

Scheme 4.11. Synthesis of **33** by Jeffries-EL.

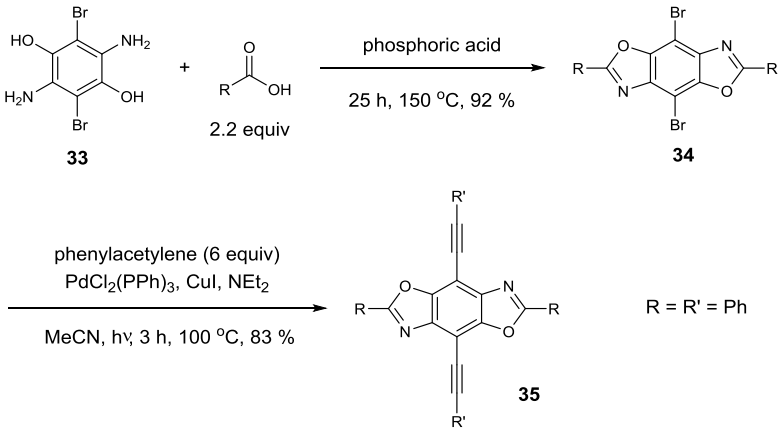

Scheme 4.12. Synthesis of benzobisoxazole cruciform **35** by Miljanić.

We hypothesized that our C–H functionalization methodology should allow for easy access to the benzobisthiazole derivative of these compounds in many fewer steps than the benzobisoxazoles. Daijun Feng, our collaborator in Seth Marder's laboratory at Georgia Institute of Technology, developed a method for the bromination of the 4 and 8

positions of **14** (Scheme 4.13). With **36** in hand, the aryl axis could be functionalized using traditional cross coupling methodology. Because the 2 and 6 positions of **14** require copper for activation, there is no concern regarding the undesired 2,6-functionalization in a traditional palladium catalyzed cross coupling, allowing for a divergent synthesis of benzobisthiazole cruciforms.

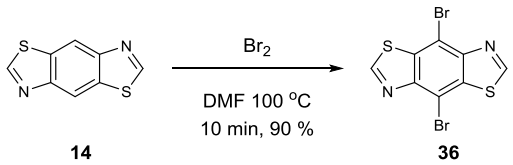

Scheme 4.13. Synthesis of **36** from **14**.

Initial attempts at functionalization were carried out with Sonagoshira coupling with 1-hexyne (Scheme 4.14). Unfortunately there was no reaction in this case.

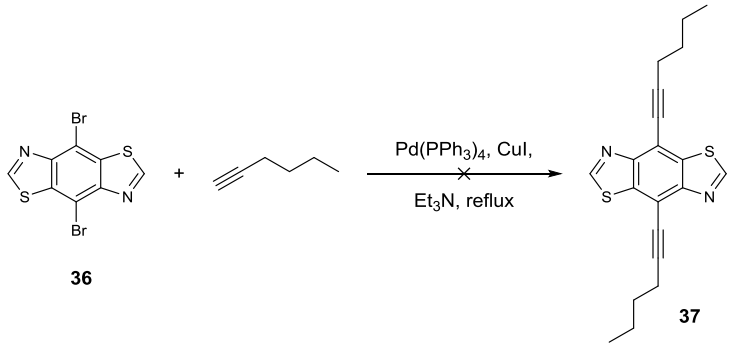

Scheme 4.14. Attempted Sonagashira coupling of **36** with 1-hexyne to generate **37**.

Moving to Suzuki coupling with (4-nonylphenyl)boronic acid (Scheme 4.15), there was product observed by crude ^{1}H NMR but it was difficult to purify the product away from the starting material. This is likely due to the surfactant nature of the product, causing it to streak on silica and alumina gel columns.

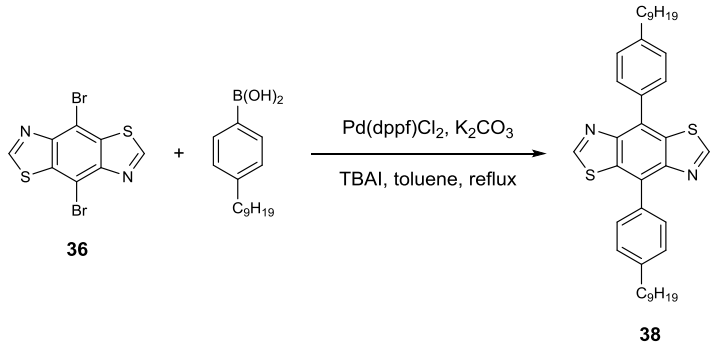

Scheme 4.15. Suzuki coupling of **36** with 4-nonylphenylboronic acid to generate 4,8-functionalized product **38**.

It was hypothesized that moving to Molander-type Suzuki coupling could improve the reaction. In this case the starting material would now be a salt and should be easier to isolate away from the product even if the reaction does not reach completion. The trifluoroborate potassium salt was synthesized according to literature procedure from the boronic acid in good yield (Scheme 4.16).[86] This was carried through into the coupling reactions in a number of literature conditions including $Pd(OAc)_2$ in refluxing MeOH and $Pd(dppf)Cl_2$ in refluxing EtOH, but there was no reactivity under any conditions (Figure 4.21).

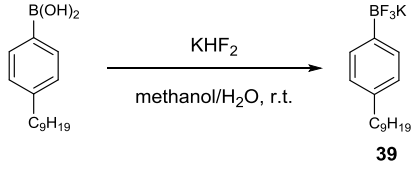

Scheme 4.16. Synthesis of potassium trifluoroborate salt **39**.

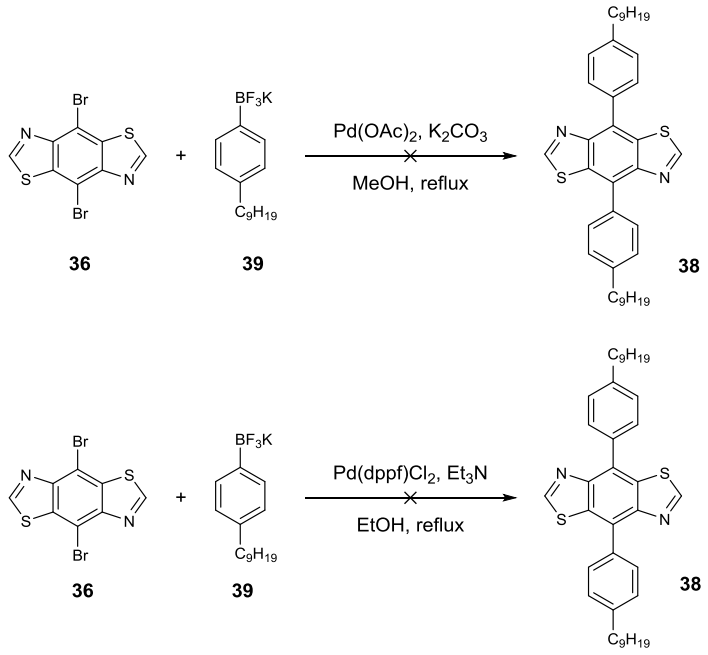

Figure 4.21. Attempted Molander-type cross couplings of **36** with **39**.

From here we returned to traditional Suzuki conditions with phenyl boronic acids, but to changed the R group on the phenyl ring to reduce the surfactant-like qualities and simplify purification. Moving to the *tert*-butylphenylboronic acid, we were able to drive the reaction to completion and purify the product **40** away from the remaining boronic acid (Scheme 4.17).

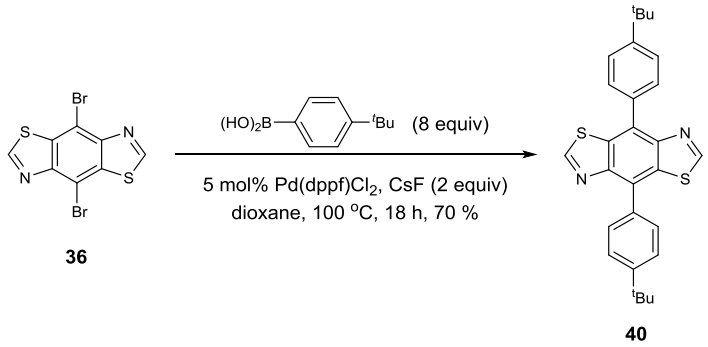

Scheme 4.17. Synthesis of **40** from **36** *via* Suzuki cross coupling.

With 4,8-functionalized product **40** in hand, the C–H coupling proceeded under standard conditions to give cruciform structure **41** in good yield (Scheme 4.18).

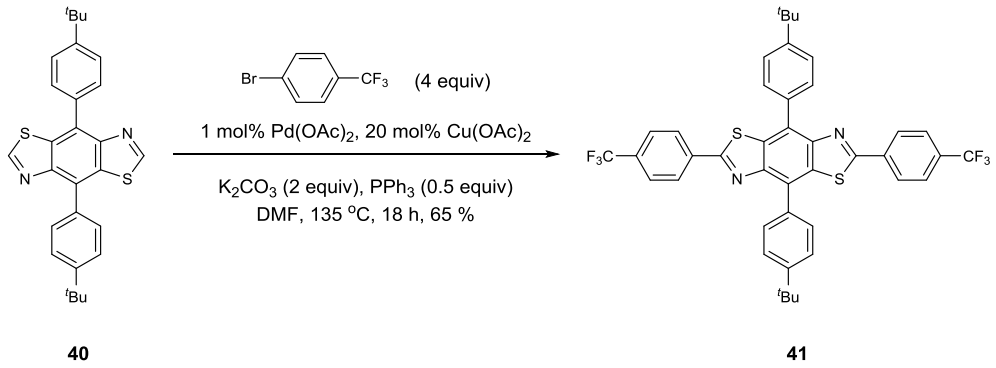

40 **41**

Scheme 4.18. Synthesis of **41** from **40** *via* C–H functionalization.

Although this molecule was not examined in a device, it gives proof of principle that C–H functionalization could provide a modular synthesis of a series of complex molecules in a truly orthogonal way.

4.7 C–H Functionalization of Thiazolothiazole

Thiazolothiazoles are another class of compounds commonly used in n-type materials due to highly efficient intermolecular interactions, high electron affinities and enhanced stability to oxygen.[87–89] Their synthesis is typically from ethanedithioamide and the corresponding aldehyde, refluxing in high boiling solvents for a day or more (Schemes 4.19 and 4.20).[87,90] Although this procedure is general and robust, it requires the synthesis of aryl aldehydes for each substitution pattern, and the harsh conditions can be intolerant of delicate products. Direct functionalization of the premade thiazolothiazole core is typically quite challenging and leads to decomposition.

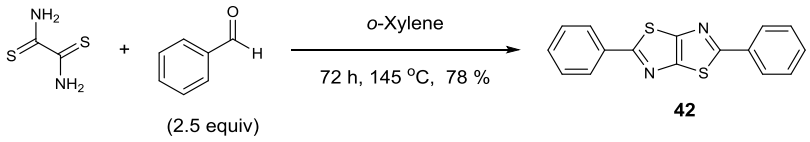

Scheme 4.19. Synthesis of **42** by Rannou and coworkers.[90]

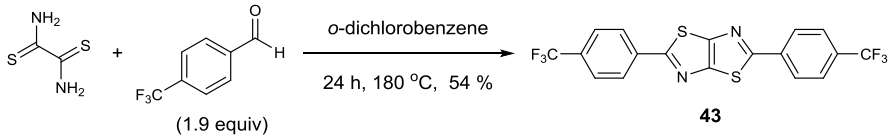

Scheme 4.20. Synthesis of **43** by Yamashita and coworkers.[87]

We found that our conditions for the 2,6-functionalization of BBT were gentle enough to allowed for the 2,5-functionalization of thiazolothiazole in good yield without decomposition. **43** was synthesized from thiazolothiazole **44** in 65 % yield using the C–H functionalization conditions developed on benzobisthiazole **14**.

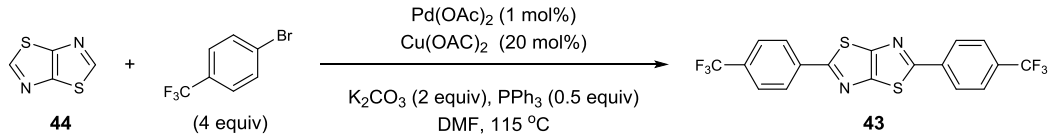

Scheme 4.21. Synthesis of **43** via C–H functionalization

4.8 Conclusions

A general method for the difunctionalization of benzobisthiazole and its derivatives was developed. It works well with electron poor aryl halides until solubility prevents the reaction from reaching completion. The methodology struggles with bromothiophene and derivatives, but is tolerant of alkyl substituted aryl bromides. The methodology fails to couple bromonaphthalenediimide, likely due to a combination of steric inhibition and palladium coordination to the carbonyl. Because this reaction mechanistically requires copper, it is possible to orthogonally synthesize cruciform

derivatives from 4,8-dibromobenzobisthiazole. The methodology has been expanded to the functionalization of thiazolothiazole as well.

5. Dehydrogenative Cross Coupling of Benzothiazole

5.1 Introduction

Moving from C–H/C–Br coupling to dehydrogenative coupling offers a number of advantages, most importantly removing the requirement for prefunctionalized starting materials. However, there are more challenges associated with oxidative coupling than with C–H/C–X coupling. Selectivity is a major concern both in heterodimer versus homodimer formation and in regioselectivity if one of the coupling partners has more than one available hydrogen (Figure 5.1). To combat the problem of dimer formation, one of the coupling partners it typically used in large excess, which is impractical if both parts are valuable or late stage materials. Regioselectivity issues are normally avoided by judicious selection of substrates that only contain one sp^2 C–H bond or have one proton that is significantly more acidic than the others. Since 2011 the number of publications involving dehydrogenative couplings has increased dramatically and great advancements have been made, specifically in the cross coupling of 1,3-azoles with arenes. This has largely come in the form of Cu, Cu/Pd, and Pd catalyzed couplings.

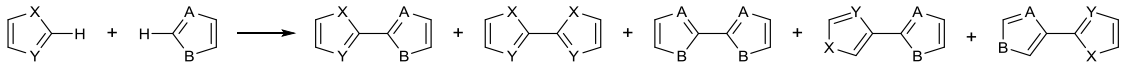

Figure 5.1. Dehydrogenative cross coupling of heterocycles giving heterocoupling, homocoupling and undesired regioisomers.

In 2011 Ofial published a method for the oxidative cross coupling of two thiazoles using $Pd(OAc)_2$ as the catalyst with $Cu(OAc)_2$ and AgF or $AgNO_3$ as additives under air (Figure 5.2).[91] Based on the characterization of precipitates isolated after the reaction, it is clear the Ag^+ is being reduced to Ag^0, indicating it is the terminal oxidant in

the reaction. However the control reaction coupling benzothiazole (**1**) with *N*-methylimidazole under an atmosphere of N_2 gives 63 % yield of heterocoupled product **2** instead of the 91 % yield when run under air, showing that O_2 is also necessary. They propose the copper catalyzes the oxidation of Pd(0) by O_2 in the presence of substiochiometric of Ag^+ in analogy to the Wacker process.[91] These conditions worked well for coupling benzothiazoles or benzimidazole with a variety of azoles. For example benzothiazole (**1**) reacted with 4,5-dimethylthiazole to give desired heterocoupled product **3** in 92 % yield.

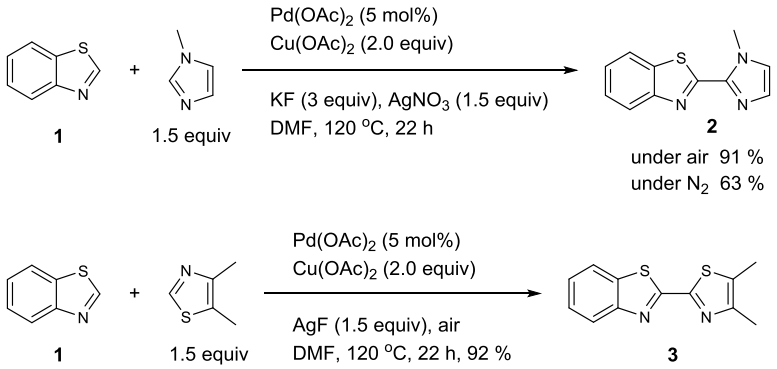

Figure 5.2. Coupling of benzothiazole (**1**) with 1-methylimidazole to give **2** and with 4,5-dimethylthiazole to give **3** by Ofial and coworkers.

The following year Jinsong You published a number of papers involving oxidative cross coupling of azoles.[92–96] He initially used $PdCl_2$ and CuCl as cocatalysts and $Cu(OAc)_2$ as the oxidant to couple substituted thiazoles and oxazoles in good yields (58-90 %), but there was homodimer present in all cases (Figure 5.3).[94] Yield of the thiazole dimer was consistently higher than that of the oxazole. Notably, this reaction only takes an hour where most examples of this type of reaction take a day or more, and these reactions were run with a 1:1 ratio of the azoles.

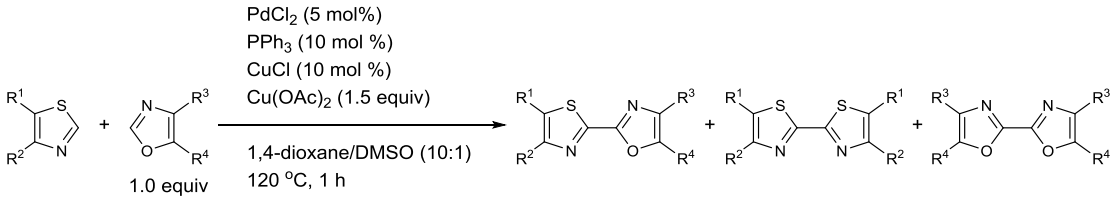

R^1 = Me, R^2 = Me, R^3 = H, R^4 = Ph	68 %	15 %	4 %
R^1 = CO_2Et, R^2 = H, R^3 = H, R^4 = Ph	66 %	15 %	7 %
R^1 = Me, R^2 = Me, R^3 = Me, R^4 = CO_2Et	90 %	5 %	trace
R^1 = CO_2Et, R^2 = H, R^3 = Me, R^4 = CO_2Et	71 %	15 %	<5 %

Figure 5.3. Coupling of thiazoles with oxazoles using palladium and copper developed by You and coworkers

Later the same year, the You group published a palladium-free version of the same reaction, this time using $Cu(OAc)_2$ as the only catalyst and Ag_2CO_3 as the oxidant under an O_2 atmosphere (Figure 5.4).[92] Yields are generally the same or slightly lower than their previous reactions with palladium catalysts, and there is a general increase in homodimer formation particularly with the oxazole. Reaction time was 24 hours, and the temperature was 140 °C versus the palladium conditions which proceeded at 120 °C. This is an important development in that it is palladium free and only requires one copper reagent. However using the same metal to insert into both C–H bonds may provide less mechanistic differentiation between the two coupling partners which likely contributes to the higher levels of dimer formation compared to the reaction with palladium.

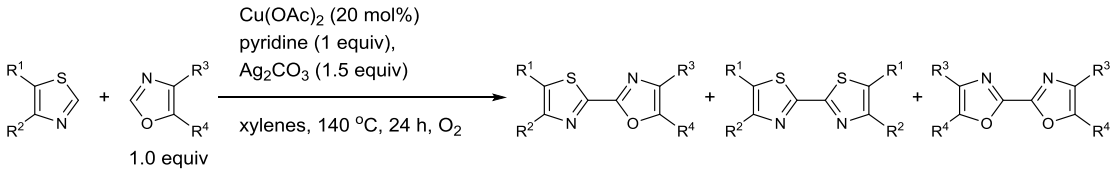

R^1 = Me, R^2 = Me, R^3 = H, R^4 = Ph	65 %	13 %	19 %
R^1 = CO_2Et, R^2 = H, R^3 = H, R^4 = Ph	65 %	13 %	11 %
R^1 = Me, R^2 = Me, R^3 = Me, R^4 = CO_2Et	73 %	18 %	8 %
R^1 = CO_2Et, R^2 = H, R^3 = Me, R^4 = CO_2Et	63 %	21 %	<5 %

Figure 5.4 Coupling of thiazoles with oxazoles using only copper developed by You and coworkers.

Also in 2012, Wang and coworkers found that azoles could be coupled using only copper acetate as both the catalyst and the oxidant with no ligand or base added (Figure 5.5).[97] The reaction was run in DMSO at 130 °C under an inert atmosphere. They found that increasing or decreasing the temperature, or adding additional oxidants, including O_2, were all detrimental to the reaction. Benzothiazoles were coupled with a variety of 5-substituted oxazoles and thiazole. Using an oxazole with a hydrogen at the 5-position lead to a decrease in yield versus substrates with that position blocked, 50 % versus 84 %, but the reaction did still progress. Yields of thiazole coupling were consistently 75-90 % and did not change significantly with varying electronic substitution of the coupling partner. They did not indicate how much, if any, of the homodimerization products were isolated.

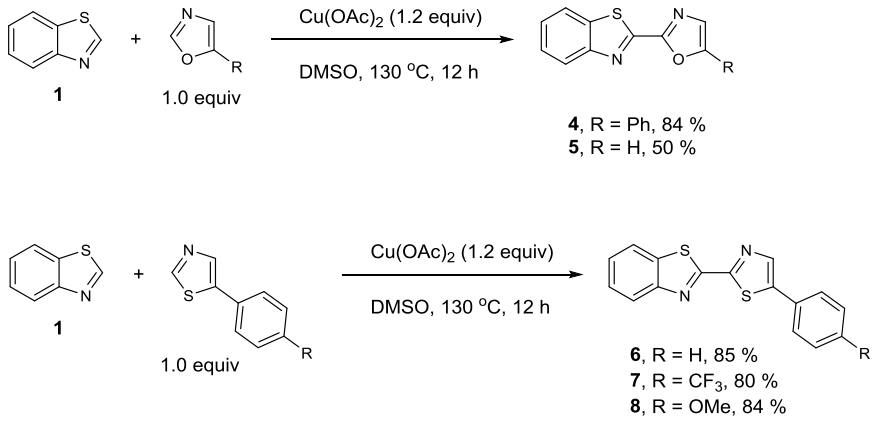

Figure 5.5. Copper only coupling of azoles from Wang.

In 2012 Zhang and coworkers found that not only could benzothiazoles and thiazole be coupled with copper, benzothiazoles could also be coupled with electron poor aromatic rings (Figure 5.6).[98] Pentafluorobenzene (**9**) was coupled with **1** using CuCl as the catalyst with 4,4'-dimethoxy-2,2'-bipyridine and di-*tert*-butyl peroxide as the oxidant

to give **10** in 71 % yield. 18 % of the homocoupled pentafluorobenzene was also isolated. Substitution around the benzothiazole was also explored with both electron donating and electron withdrawing groups at the 5-position giving reduced yields; the reaction with **11** gave 50 % of **12**, and the reaction with **13** gave 55 % of **14**.

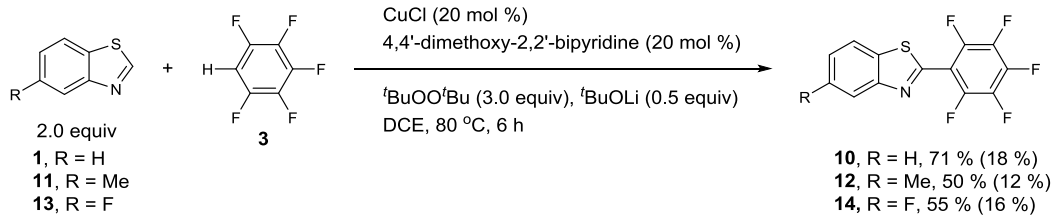

Figure 5.6 Zhang and coworkers coupling of activated arenes with benzothiazoles with copper. Yields in parentheses are of the benzothiazole homodimer.

Concurrently, Su put forth a method for coupling unactivated arenes with benzoxazoles using palladium acetate as the catalyst and copper bromide and O_2 as oxidants (Figure 5.7).[99] Benzene was used as a cosolvent with DMA in a ratio of 2:1. There is one example of benzothiazole (**1**) coupling with benzene to give **15**, but the yield is significantly lower, only 52 % versus 79 % for benzoxazole. They propose that copper is not inserting into the C–H bond of the oxazole, but instead acts as a Lewis acid binding to the nitrogen of the azole and increasing the acidity of the hydrogen. Methyl and halogen substitution on benzene was also explored. Both were well tolerated (yields between 74-80 %), but regioselectivity was poor (not shown).

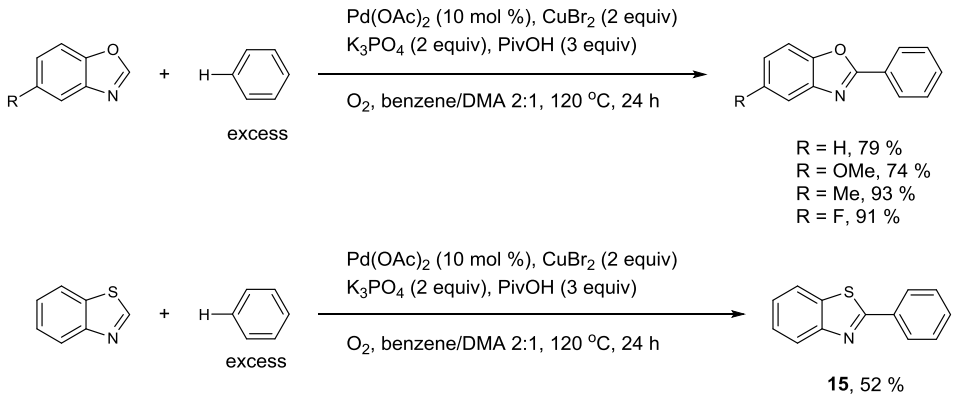

Figure 5.7. Zhang and coworkers coupling of activated arenes.

In 2014 Yang found that thiophenes could be dehydrogenatively cross coupled in a similar manner (Figure 5.8).[100] Unlike the benzene couplings from Zhang, thiophene is not used as cosolvent in these reactions. Yields were high for thiophenes with small alkyl chains at the 2-position with 63 % for methyl (**16**) and 92 % for ethyl (**17**), but fell for cyano (**18**, 48 %), bromo (**19**, 34 %), phenyl (**20**, 53 %), or acyl (**21**, 41 %) substitutions. Furans were not compatible with these coupling conditions due to oxidative degradation. Thiazoles with the 2-position blocked were coupled at the 5-position in moderate to excellent yield, (53 % for methyl **22** and 97 % for ^{i}butyl **23**). They do not report how much, if any, of the homocoupled products were isolated.

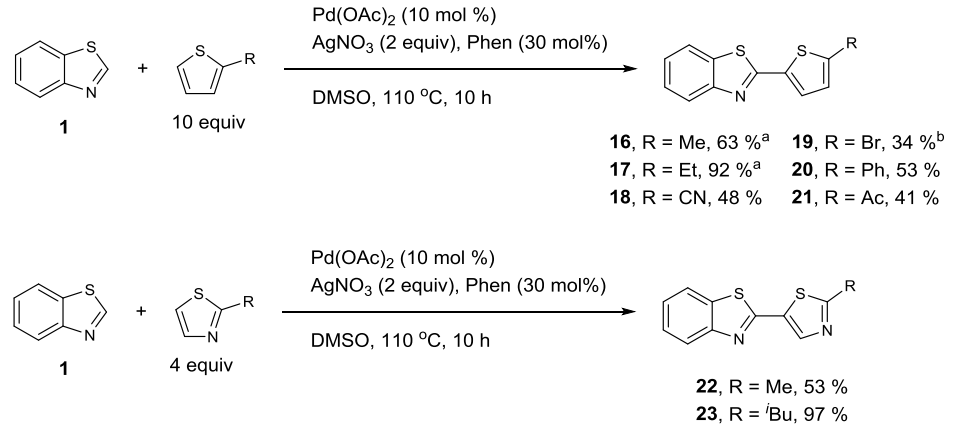

Figure 5.8 Yang's functionalization of thiophenes. a) 4 equiv of the thiophene used. b) Reaction run over 40 h.

Although the work of Yang is significant, significant challenges remain in this field. Thiazole/thiazole couplings can typically be carried out with a 1:1 ratio of the coupling partners, but thiophene and aryl ring couplings require large excess of one partner. Dimerization of one of the coupling partners remains a problem. Yields are generally high enough for medicinal chemistry applications, but the conversions are still much too low polymerization applications. For step-growth polymerization, molecular weight increases exponentially with increases in conversion. To achieve high molecular weights necessary for polymer applications conversions must be greater than 99 %. Selectivity must also be a priority; if homocoupling competes with heterocoupling the alternating nature if the polymer can be compromised and the electronic properties will not be uniform throughout the material.

Because our proposed mechanism for the C–H functionalization cross coupling of benzobisthiazole with bromoarenes involved two separate catalytic cycles for the activation of the thiazole and the C–Br bond, the same mechanism in dehydrogenative coupling should allow us to suppress homodimer formation through independently tuning each catalytic cycle. By tuning the cycles separately, we should be able to reach 1:1 ratio of coupling partners even with thiophenes and other challenging substrates.

5.2 Results and Discussion

As a starting point we examined the coupling of three diverse substrates: 3-hexylthiophene, pentafluorobenzene and difluorobenzothiadiazole (Table 5.1). In the reaction of benzothiazole **1** with 3-hexylthiophene, benzothiazole dimer (**24**) was the major product, but an inseparable 2:1 mixture of regioisomers of the heterodimeric

products **25** and **26** was also generated. Unfortunately none of the desired products were observed in the reactions with pentafluorobenzene or difluorobenzothiadiazole by either crude ^{1}H NMR or mass spectrometry. In both cases only benzothiazole homodimer **24** was observed.

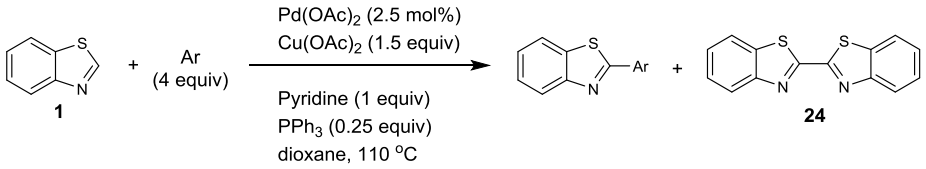

entry	Ar	heterocoupled product (yield)	yield of **24**
1	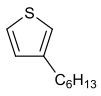	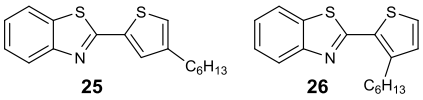 **25** **26** 7 % combined 2:1 mixture (**25**:**26**)	8 %
2	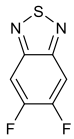	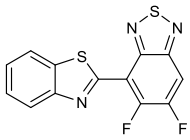 **27,** 0 %	10 %
3	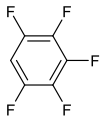	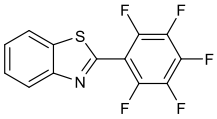 **10**, 0 %	12 %
4		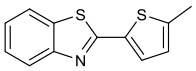 **16**, 15 %	9 %

Table 5.1. Coupling of **1** with 3-hexylthiophene, difluorobenzothiadiazole, pentafluorobenzene and 2-methylthiophene.

In light of this, we returned to thiophene but chose to use 2-methylthiophene. Having one of the 2-positions blocked eliminated formation of regioisomers as a complicating factor. 2-Methylthiophene gave 15 % of the desired product **16** in the initial test.

5.3 Optimization of dehydrogenative cross coupling of 1 with 2-methylthiophene

Because we proposed to suppress the formation of homodimer **24** by tuning the copper and palladium catalytic cycles separately, we first needed to find an oxidant other than copper so oxidant and catalyst could be manipulated individually. This also allowed us the option of using ligands to tune the reactivity of copper without requiring the use of stoichoimetric ligands.

After establishing an HPLC assay for 2-methylthiophene, **1**, **16, 24**, and anthracene to be used as an internal standard, we tested a number of oxidants in the coupling reaction (Table 5.2). With copper acetate, which was the oxidant used in much of the literature precedent and in the initial tests, there was a small amount of heterodimer **16** formed but the major product was homodimer **24**. TEMPO showed the most reactivity overall, giving 20 % of **16** and 40 % of **24**, which accounts for all of the benzothiazole in solution. Oxone showed no reactivity at all, producing neither homodimer **24** nor the desired product **16**. Silver oxide and silver carbonate both showed some reactivity but significantly less than TEMPO. TEMPO was therefore chosen as the oxidant moving forward with the optimization studies.

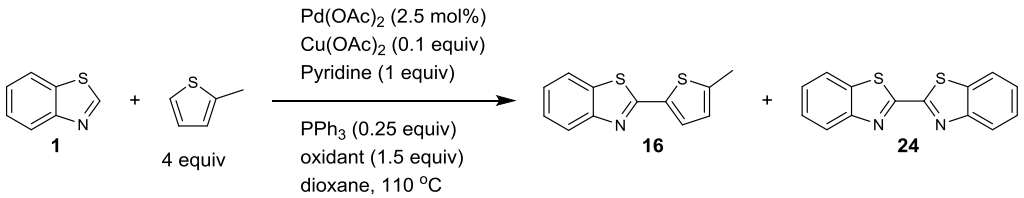

entry	oxidant	conversion **16**	conversion **25**
1	$Cu(OAc)_2$	8 %	30 %
2	TEMPO	20 %	28 %
3	Oxone	0 %	0 %
4	Ag_2O	12 %	25 %
5	Ag_2CO_3	19 %	26 %

Table 5.2. Examination of oxidants for the oxidative coupling of **1** and 2-methylthiophene. Conversions based on HPLC analysis versus anthracene as an internal standard.

Next a series of ligands were examined with the hypothesis that modifying the ligand on copper could speed up the copper catalytic cycle, increasing selectivity (Figure 5.9). Looking at PPh_3, Xantphos, trifurylphosphine, tricyclohexylphosphine, tris(*p*-trifuloromethylphenyl)phosphine, and tri(*p*-methoxyphenyl)phosphine, we found that although they all allowed the reaction to progress, homocoupled benzothiazole **24** was the major product in most cases. The exception was tris(*p*-methoxyphenyl)phosphine, which gave the desired heterocoupled product **16** as the major product in a ratio of about 2:1 with **24** (Figure 5.9F). This was the first set of conditions to give the desired product **16** as the major component. We also explored ethylene diamine and bipyridyl as potential ligands for copper in this reaction, but neither gave results comparable to that of the phosphine ligands (Figure 5.10).

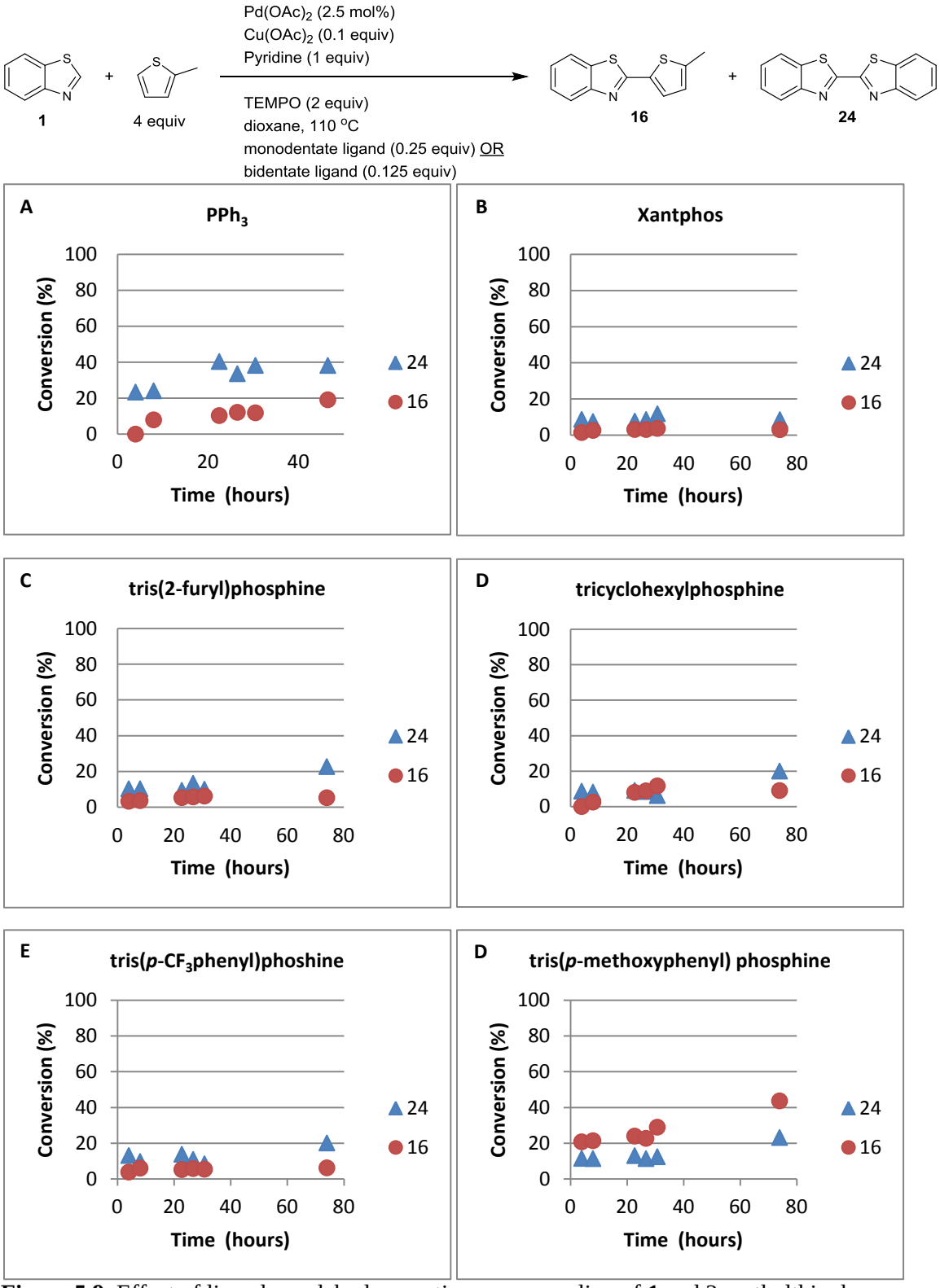

Figure 5.9. Effect of ligands on dehydrogenative cross coupling of **1** and 2-methylthiophene.

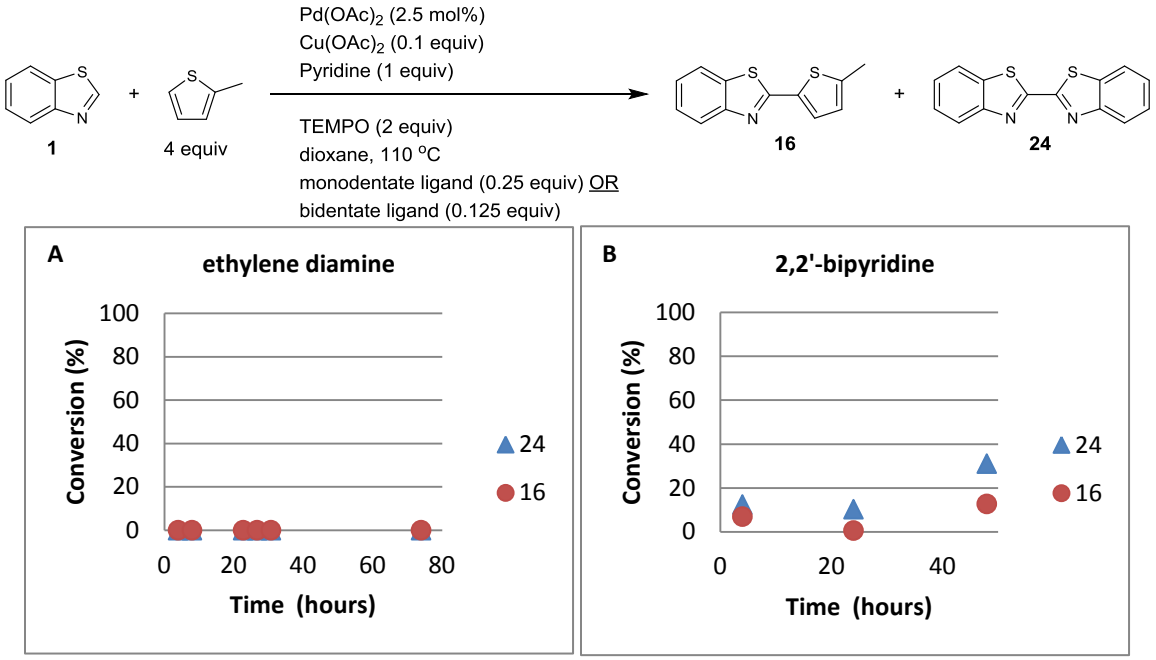

Figure 5.10. Effect of amine ligands on dehydrogenative cross coupling on **1** and 2-methylthiophene.

Based on the optimization of benzobisthiazole cross coupling, it was predicted that temperature could have a large impact on yield in dehydrogenative coupling. Initial test were conducted with dioxane at its boiling point, so other similar boiling and higher boiling solvents were explored. Looking at solvents DMF, DMAc, DMSO, toluene, trifluorotoluene, and xylenes (Table 5.3, entries 1-7), we found that none gave improved conversions to desired product **16** at 110 °C when compared to dioxane. Higher boiling solvents DMF, DMA and xylenes were then tested at 135 °C (Table 5.3, entries 8-10). Significant improvement was observed with DMA which gave 55 % of heterodimer **16** and only 21 % of homodimer **24**. This leaves the problem as one of selectivity because all of benzothiazole **1** is being consumed.

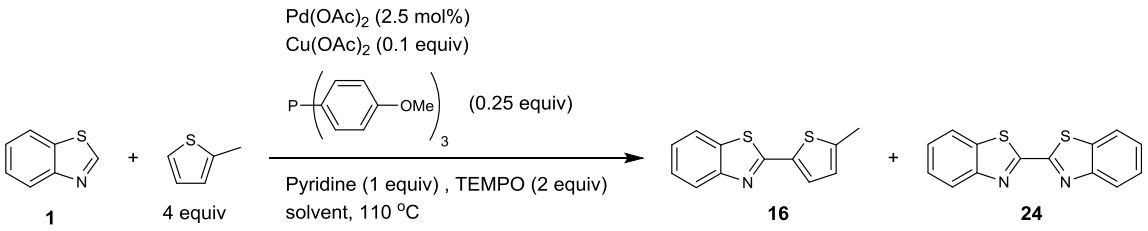

entry	solvent	conversion to **16**	conversion to **24**
1	1,4-dioxane	33 %	23 %
2	DMF	2 %	6%
3	DMA	0 %	5%
4	DMSO	0 %	0 %
5	toluene	5 %	11 %
6	trifluorotoluene	5 %	19 %
7	xylenes	7 %	8 %
8[a]	DMF	27 %	13 %
9[a]	DMA	55 %	20 %
10[a]	xylenes	34 %	11 %

Table 5.3. Effect of solvents on dehydrogenative cross coupling of **1** and 2-methylthiophene. Conversions based on HPLC analysis versus anthracene as an internal standard. A) Reactions carried out at 135 °C.

Alternative palladium sources were examined as another means of improving reaction selectivity (Figure 5.11). The palladium (0) sources $Pd(PPh)_3$ and $Pd_2(dba)_2$ showed generally poor selectivity, but conversions were relatively high at 37 % and 32 %, and 42 % and 26 % for **16** and **24** respectively (Figure 5.11, B and C). The palladium (II) sources generally gave better selectivity. Conversions were low with $PdCl_2$ at 15 % and 5 % but that represents a 3:1 ratio of **16** to **24** (Figure 5.11D). $Pd(OAc)_2$ and $Pd(TFA)_2$ had the best conversions by far with $Pd(TFA)_2$ giving 65 % conversion to heterodimer **16** (Figure 5.11, A and E). In both cases all of the benzothiazole has been consumed leaving the problem, again, as one of selectivity. The control reaction with no palladium was consistent with what was predicted from the mechanism, only **24** was observed (not shown). The success of the electron-deficient palladium catalyst suggests that the C–H activation is occurring through an electrophilic mechanism which has previously been observed with electron poor palladium species and

electron rich arenes.[101,102]

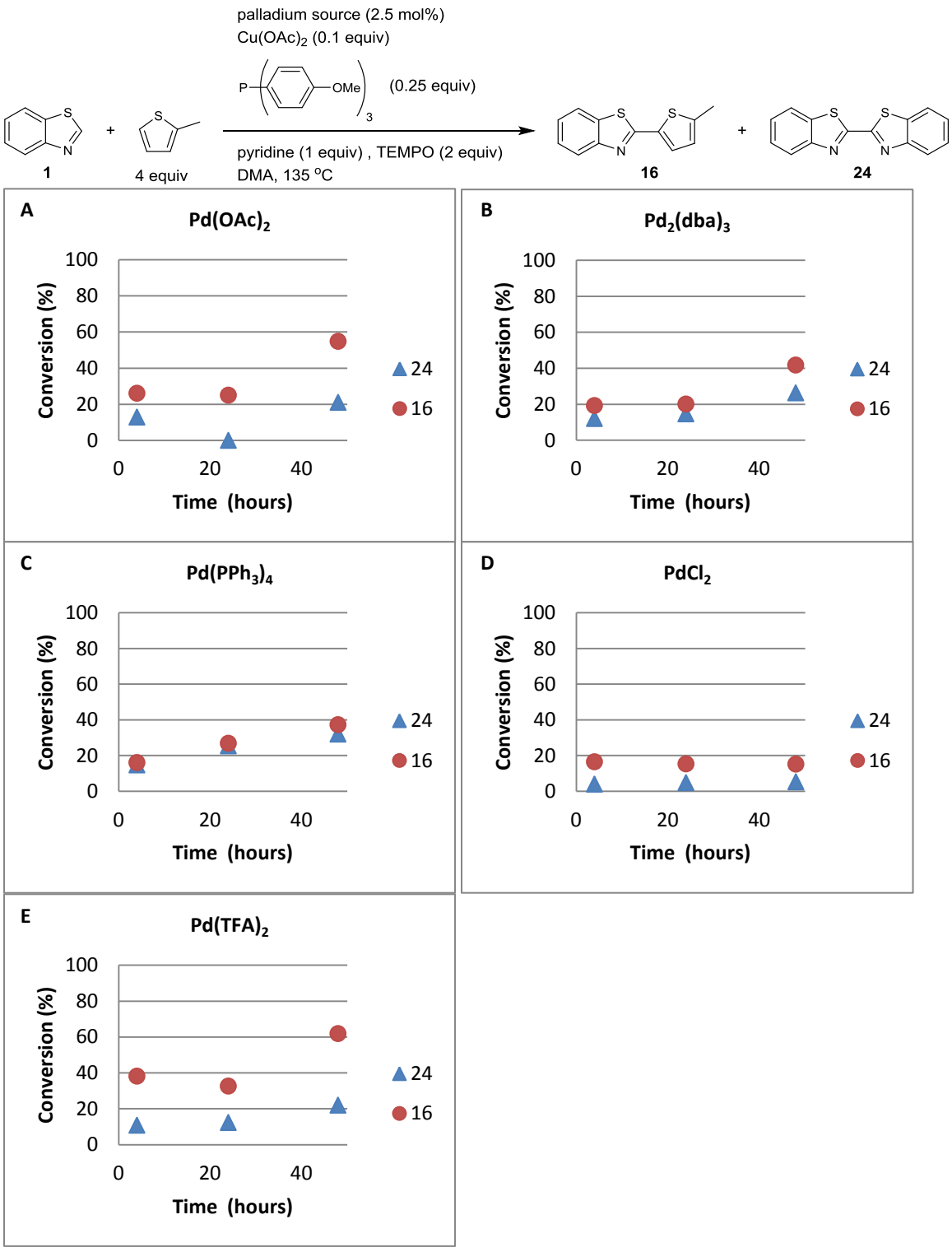

Figure 5.11. Effect of changing palladium sources on dehydrogenative cross coupling of **1** with 2-methylthiophene.

Because ligand modifications had had the largest impact of any changes to this point, we chose to screen additional types of ligands in hopes of seeing additional substantive improvements (Figures 5.12 and 5.13). The reaction almost shut down using PCy_3HBF_4, producing around 6 % of heterodimer **16** and 6 % of homodimer **24** (Figure 5.12A). Triphenylphosphite was also tested and only **24** was observed (Figure 5.12B). These results were similar to that of the control reaction in which the absence of any phosphine ligand afforded 18 % of **16** and 5 % of **24** (Figure 5.12C), indicating the phosphine is not necessary but is beneficial to the reaction. Interestingly, RuPhos and SPhos were almost entirely selective for the homodimer **24**, giving only trace of the desired product **16** (Figure 5.13, A and C). ^{t}BuXPhos shut down the reaction completely (Figure 5.13B), showing the reaction has a very narrow window of steric tolerance.

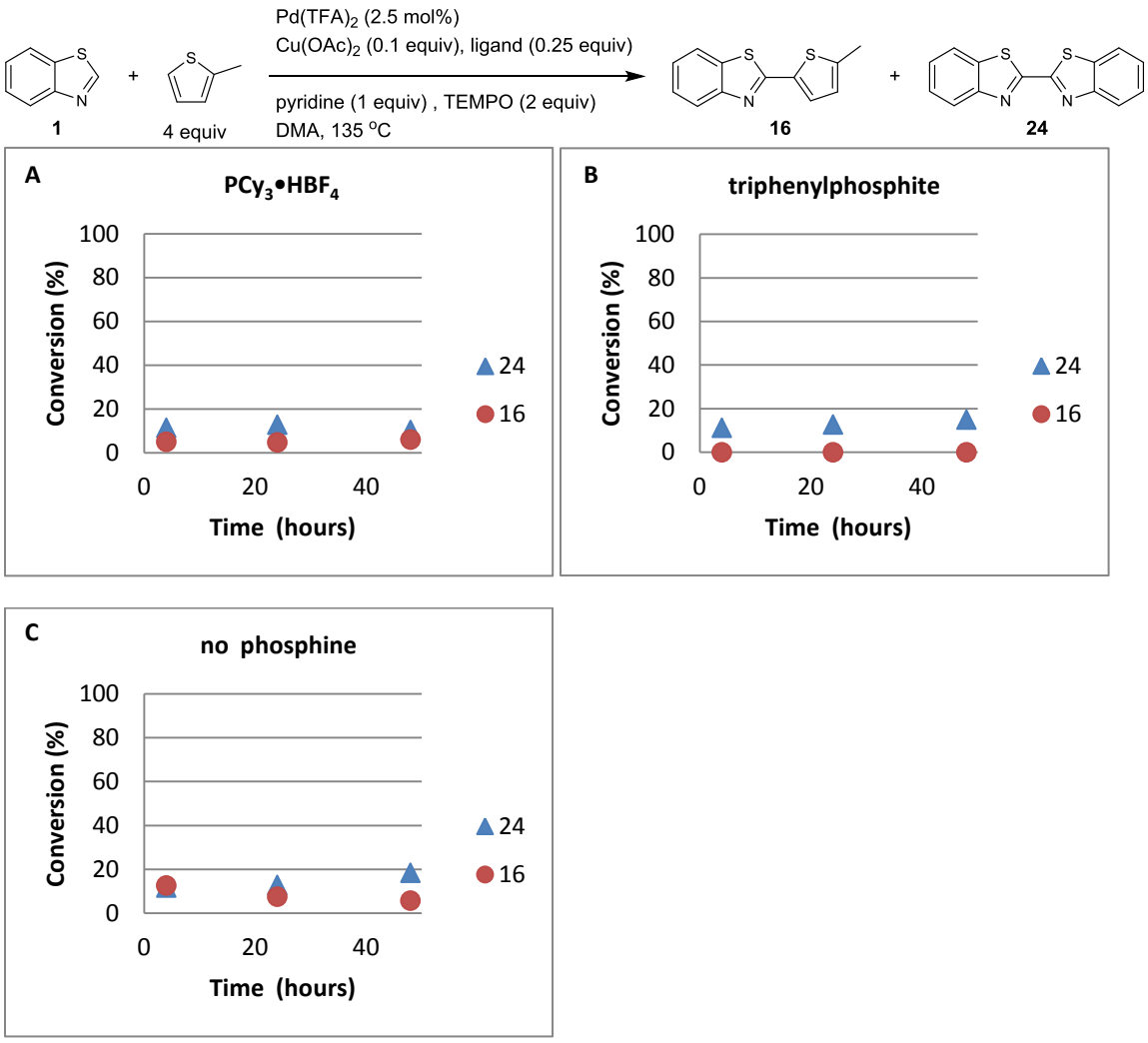

Figure 5.12. Effect of using the HBF_4 salt of tricyclohexyphosphine and triphenylphosphite ligands on dehydrogenative cross coupling of **1** with 2-methylthiophene.

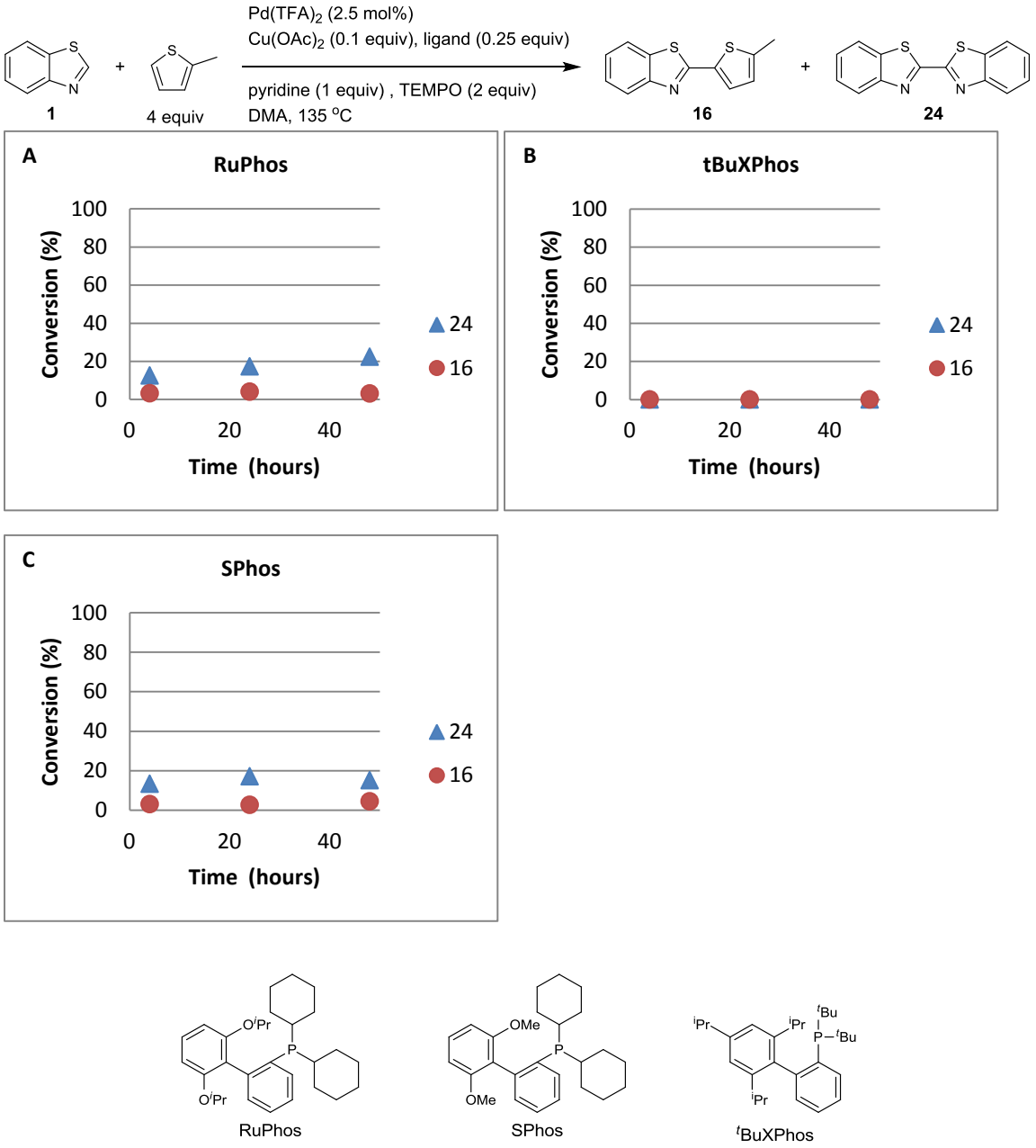

Figure 5.13. Effect of phosphine ligands with disparate steric demands on dehydrogenative cross coupling of **1** with 2-methylthiophene.

We also looked into phosphine oxides as ligands for this reaction (Figure 5.14). Because these reactions are run under oxidative conditions we hypothesized that the TEMPO is oxidizing the phosphine to the phosphine oxide, and the phosphine oxide is

the species actually present and acting as a ligand in the reaction mixture. However, when tris(*p*-methoxyphenyl)phosphine oxide was added to the reaction instead of tris(*p*-methoxyphenyl)phosphine the reaction was quite different; specifically there was a reversal in selectivity (Figure 5.14). With tris(*p*-methoxyphenyl)phosphine as the ligand after 48 hours there was 62 % of heterodimer **16** and 22 % of homodimer **24**. With tris(*p*-methoxyphenyl)phosphine oxide there was 51 % of homodimer **24** and 23 % of heterodimer **16**. This suggests that the phosphine binds to the copper before it can be oxidized, so the phosphine truly is the active ligand species.

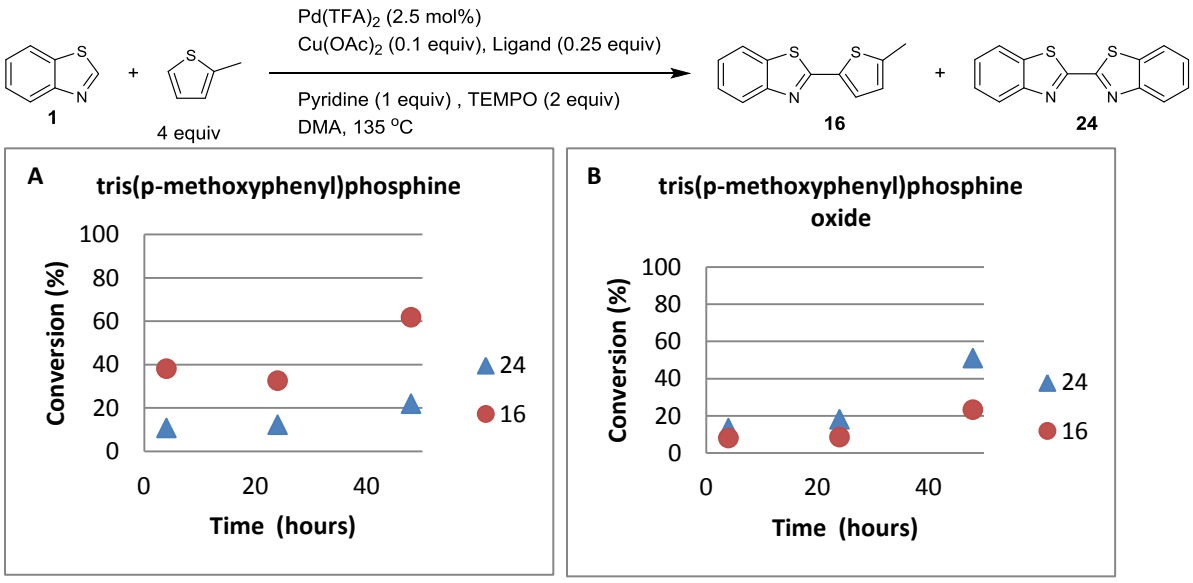

Figure 5.14. Exploration of phosphine versus phosphine oxide ligands for dehydrogenative cross coupling of **1** with 2-methylthiophene.

The equivalents of phosphine ligand with respect to copper was changed to see how it affected selectivity and conversion (Figure 5.15). When copper and phosphine were in a 1:1 ratio, yields of both **16** and **24** were high, but there was poor selectivity (Figure 5.15A). Increasing the ratio to 4:1 phosphine to copper, the yields were much

lower and the selectivity was still poor (Figure 5.15C), suggesting that the 2.5:1 ratio that has been used throughout these tests is in a sweet spot for this reaction.

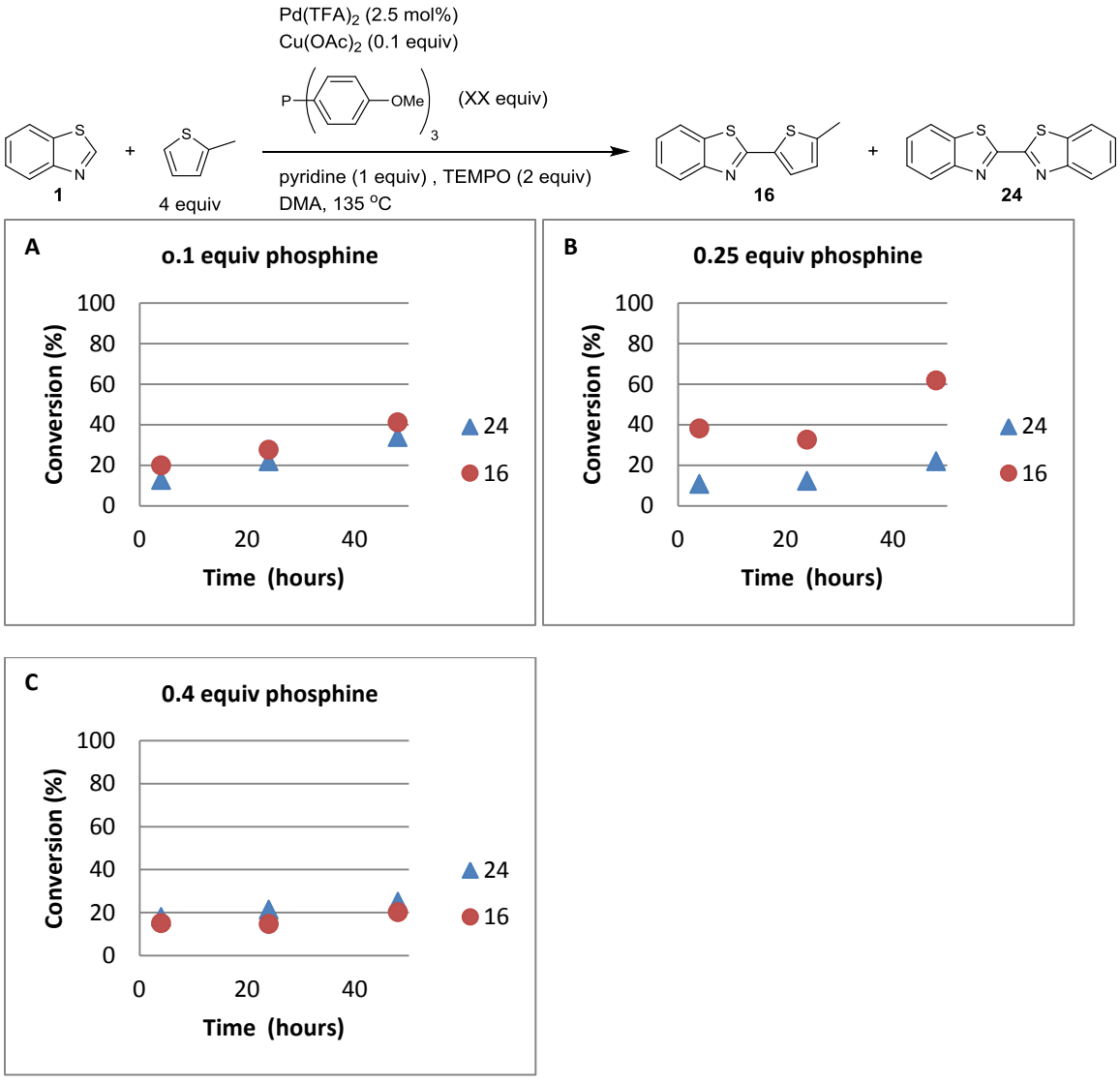

Figure 5.15. Effect of the ratio of copper to phosphine ligand on dehydrogenative cross coupling of **1** with 2-methylthiophene.

A series of Cu(II) salts were examined as alternative catalysts (Figures 5.16). $Cu(acac)_2$ and $Cu(OTf)_2$ were explored, but both gave very poor conversions to **16**, 7 % and 3 % respectively (Figure 5.16, B and C). Cu(2-ethylhexanoate)$_2$ showed poor

selectivity with **16** and **24** being generated in a 1:1 ratio, but the conversion of each was 32 % (Figure 5.16D). Copper acetate still gave the highest conversions at 62 % of heterodimer **16** and 22 % of homodimer **24** (Figure 5.16A). The copper salts $CuBr_2$, $CuCl_2$, CuBr, CuCl, CuI and CuI•Xantphos were also explored (not shown), but all performed poorly with homodimer **24** as the major product and conversions to **16** never above 10 %. The control reaction (not shown) with no copper was consistent with our proposed mechanism in which the copper inserts into the thiomidate C–H bond, so in the absence of copper there was no reaction.

Copper is known to bind to amine bases, so to elucidate whether the pyridine was acting as a base or as a ligand for copper, several substituted pyridines were explored (Figure 5.17). Using 2,6-ditertbutylpyridine gave much lower conversion (Figure 5.17A), while 2,4,6-trimethylpyridine (Figure 5.17B) gave conversions between that of the ^{t}butyl- and unsubstituted pyridine, showing that steric bulk on the pyridine is detrimental to the reaction. There is some computational evidence in similar systems that pyridines stabilize the Pd(0) species preventing the formation of palladium black.[101,103]

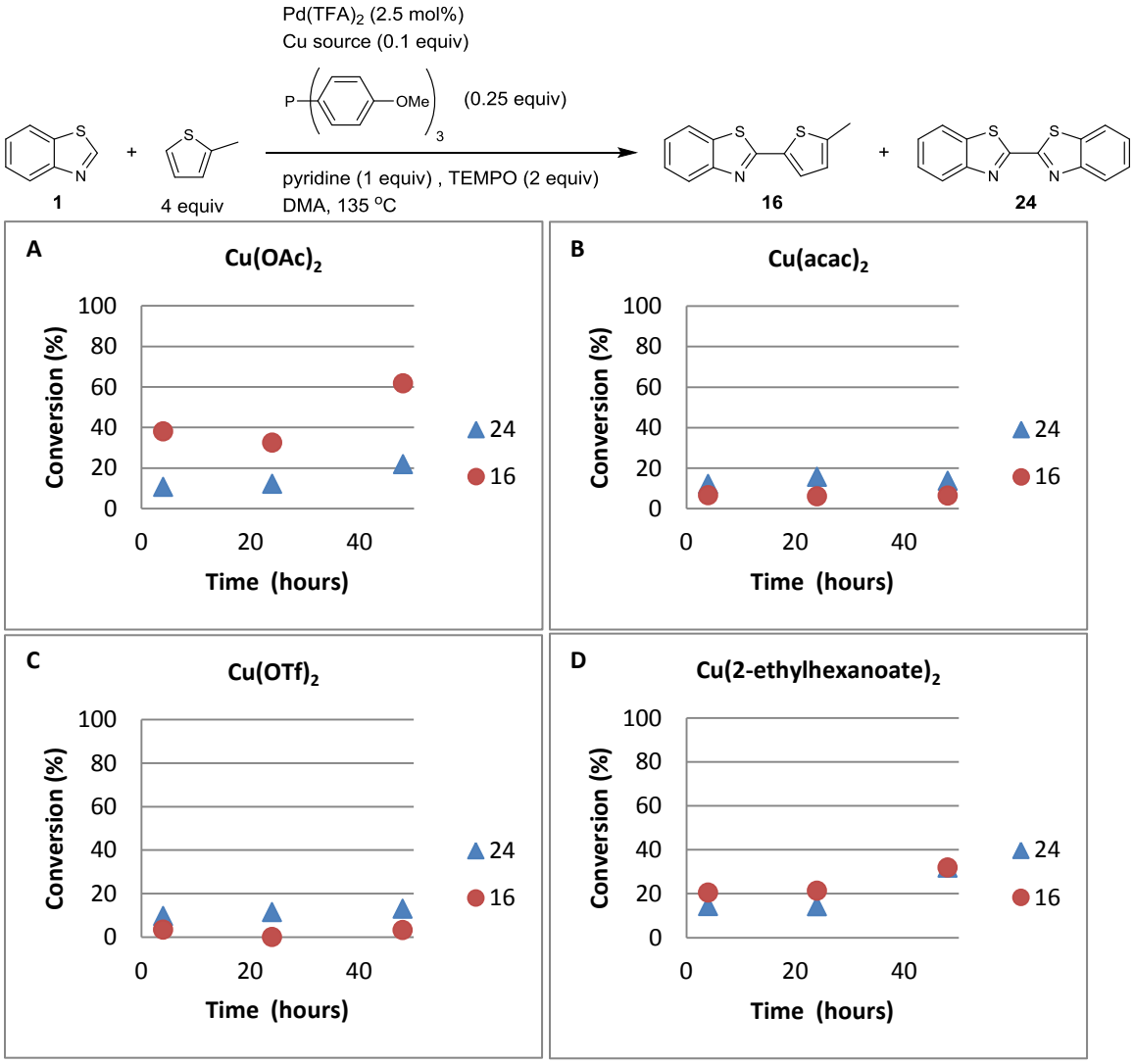

Figure 5.16. Effect of various Cu(II) complexes as the copper sources on dehydrogenative cross coupling of **1** with 2-methylthiophene.

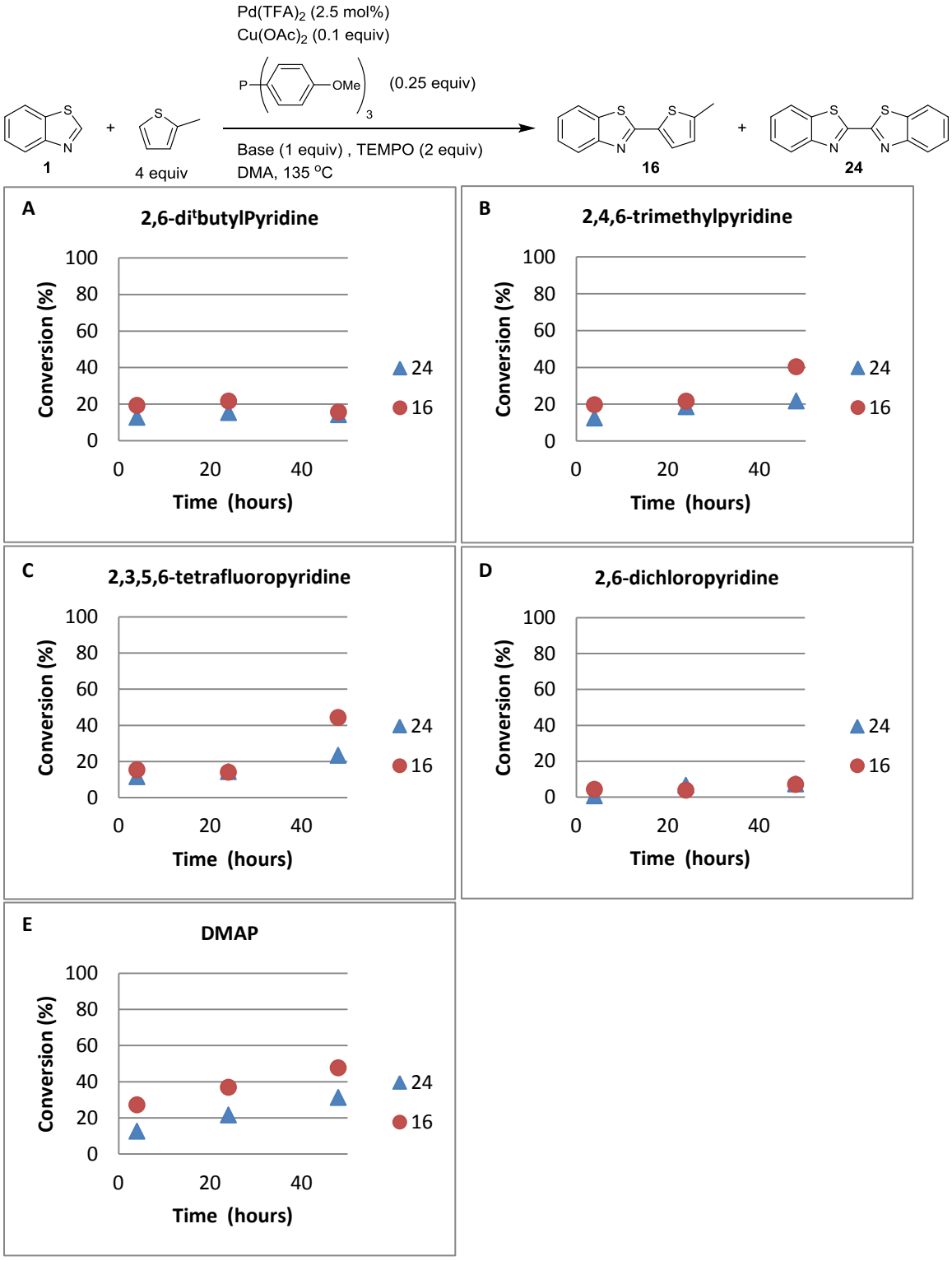

Figure 5.17. Effect of changing sterics and electronics on the pyridine base on dehydrogenative cross coupling of **1** with 2-methylthiophene.

We also hoped to use other bases to better elucidate the role of pyridine as a base separately from its role as a ligand. To that end, we tested carbonate bases as an alternative (Table 5.4). Unfortunantly neither cesium carbonate nor potassium carbonate allowed the reaction to procede to a significant degree.

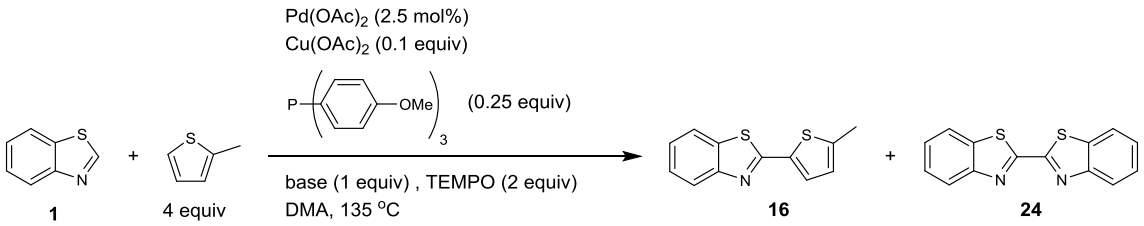

entry	base	conversion to **16**	conversion to **24**
1	K_2CO_3	<5 %	9 %
2	Cs_2CO_3	0 %	6%

Table 5.4. Effect of carbonate bases on dehydrogenative cross coupling of **1** with 2-methylthiophene. Conversions based on HPLC analysis versus anthracene as an internal standard.

Changing the equivalents of pyridine gave interesting results (Table 5.5). Using no pyridine or only 0.5 equiv of pyridine gave lower overall conversion (40 % and 38 % of **16** respectively) and selectivity of 1.4:1 and 1.5:1. Using much more pyridine (14 equiv) gave better conversion (49 %) and selectivity of 1.7:1. However, using 1 equivalent of pyridine gave 62 % of **16** with a selectivity ratio of 2.8:1, again suggesting a sweet spot for these conditions. Using 2 equivalents of pyridine gave 61 % of **16** but with a selectivity of just 1.7:1.

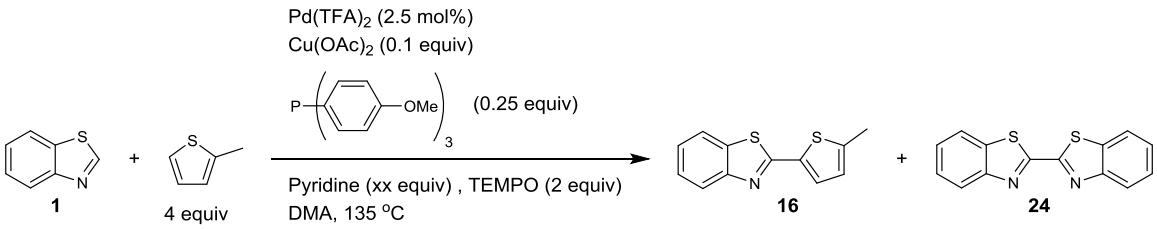

entry	equiv of pyridine	conversion to **16**	conversion to **24**
1	0	40 %	29 %
2	0.5	28 %	18 %
3	1.0	62 %	22 %
4	2.0	61 %	35 %
5	14.0	49 %	28 %

Table 5.5. Effect of changing equivalencies of pyridine on dehydrogenative cross coupling of **1** with 2-methylthiophene. Conversions based on HPLC analysis versus anthracene as an internal standard.

As a last resort to improve selectivity for the heterodimer over the homodimer, we explored the effect of increasing the ratio of thiophene to benzothiazole (Table 5.6). Using 8 equiv of thiophene did increase conversion to **16** to 71 % and selectivity to 4:1.

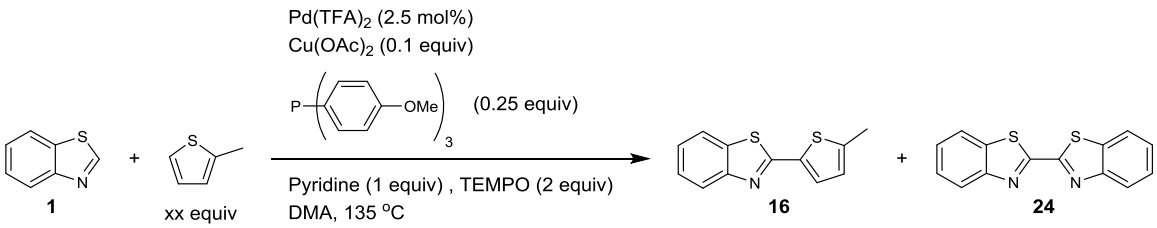

entry	equiv of thiophene	conversion to **16**	conversion to **24**
1	2	35 %	35 %
2	4	62 %	22 %
3	8	71 %	19 %

Table 5.6. Effect of changing equivalencies of 2-methylthiophene on the selectivity of the dehydrogenative cross coupling of **1** with 2-methylthiophene.

5.4 Conclusion

A method for the dehydrogenative cross coupling of benzothiazole and 2-methylthiophene has been developed. It appears these conditions are not going to

allow for the excellent selectivity and conversions we had predicted which be required to translate this work to a polymerization context. Changing palladium sources, copper sources, ligands, etc., allowed for some improvements in conversion. However the best conditions gave 62 % of **18**, but in a 2.8:1 ratio with **13** with 4 equivalents of thiophene, or 71% of **18** and 4:1 selectivity with 8 equiv of thiophene which is still far away from the 99 % conversions and high selectivity needed for polymerization applications. The success of the electron defficient $Pd(TFA)_2$ indicates the C–H activation of the thiophene is occuring in an elecrophilic manner meaning if the substrate scope was to be explored, the same conditions would likely only work with other electron rich aryl halides. A second optimization would be necessary for the functionalization of electron poor substrates. There are still remaing mechanistic questions in terms of the role of pyridine as a ligand or as a base. It is also unclear if the phosphine is remaining in the phosphine (III) oxidation state or if it is being oxidized to the phosphine (V) oxide. Reactions run with the phosphine oxide suggest the active ligand is the phosphine, but further ^{31}P NMR studies would be nesessary to verify this hypothesis. Once the mechanistic details are better understood, it is possible that these conditions could be tuned to give polymerization quality conversions.

6 Experimental Procedures and Characterization

6.1 General Information

All reactions were carried out under an atmosphere of nitrogen unless otherwise stated. All chemicals were purchased from Aldrich Chemical Company, TCI, or Strem and used without further purification unless otherwise stated. Anhydrous solvents were purified by passage through activated alumina using a *Glass Contours* solvent purification system unless otherwise stated. Trifluorotoluene and DMF were dried over activated molecular sieves. Dioxane was stored over activated molecular sieves and subjected to three freeze-pump-thaw cycles immediately prior to use. Solvents used in workup, extraction and column chromatography were used as received from commercial suppliers without prior purification. Analytical thin layer chromatography (TLC) was performed on precoated glass backed EMD 0.25 mm silica gel 60 plates. Visualization was accomplished with UV light or $KMnO_4$. Flash column chromatography was carried out using Silicycle Silia Flash® F60 silica gel (40-63 μm). High resolution mass spectra were obtained using a Thermo Electron Corporation Finigan LTQFTMS (at the Mass Spectrometry Facility, Emory University). ^{1}H and ^{13}C NMR spectra were obtained on a Varian Inova 600 spectrometer (600 MHz ^{1}H, 150 MHz ^{13}C), a Varian Inova 400 spectrometer (400 MHz ^{1}H, 100 MHz ^{13}C), or a Unity 400 spectrometer (400 MHz ^{1}H, 100 MHz ^{13}C) at room temperature in $CDCl_3$ with internal $CHCl_3$ as the reference (7.26 ppm for ^{1}H and 77.23 ppm for ^{13}C), unless otherwise stated. Chemical shifts (δ values) were reported in parts per million (ppm) and coupling constants (*J* values) in Hz. Solid

state NMR spectra were collected at room temperature with a Bruker 4mm HCN biosolids magic-angle spinning (MAS) probe and a Bruker Avance III 300 spectrometer. ^{13}C (75.48 MHz) spectra were collected with a MAS speed of 10kHz and 2ms ^{1}H - ^{13}C cross-polarization with ^{13}C RF field at 50kHz and ^{1}H ramped from 50kHz to 70kHz followed by a 6μs Hahn-echo π-pulse centered at 2 rotor cycles after the cross-polarization pulse, 100kHz SPINAL64[104] ^{1}H (300.13 MHz) decoupling. Recycle delays were set to 5*^{1}H T_1. ^{13}C chemical shifts in solid state experiments were referenced externally to TMS by setting the methylene of adamantane to 38.48ppm as a secondary reference. Infrared (IR) spectra were recorded using Thermo Electron Corporation Nicolet 380 FT-IR spectrometer.

6.2 Chapter 1 Procedures and Characterization

General procedure A for the synthesis of bisimino ligands:

Based on the literature procedure[105] a round bottomed flask was charged with the aniline (3 equiv), 2,6-diacetylpyridine (1 equiv), formic acid (5 mol %), and MeOH (0.8 M). The reaction mixture was refluxed overnight (14 h). The yellow solid was isolated by filtration and purified by recrystallization from hot MeOH to afford the corresponding bisimino ligand.

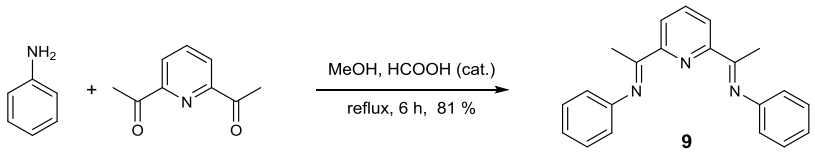

2,6-Bis(1-phenyliminoethyl)pyridine, 9

Prepared according to general procedure A from aniline (3.4 g, 36 mmol) and 2,6-diacetylpyridine (2.0 g, 12 mmol) in MeOH, giving the title compound as a yellow solid (1.11 g, 81 %). The ^{1}H NMR data are identical to literature.[105] ^{1}H NMR (400 MHz, $CDCl_3$) δ = 8.33 (d, 2H, *J* = 7.9 Hz), 7.87 (t, 1H, *J* = 7.9 Hz) 7.37 (t, 4H, *J* = 8.2 Hz), 7.11 (t, 2H, *J* = 7.3 Hz), 6.84 (d, 4H, *J* = 7.3 Hz), 2.39 (s, 6H).

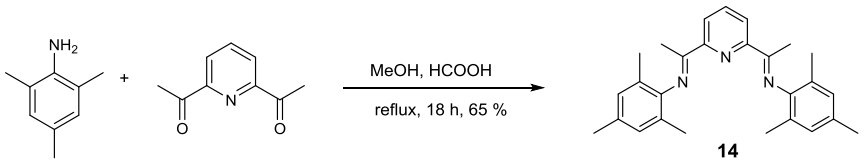

2,6-Bis[1-(2,4,6-trimethylphenylimino)ethyl]pyridine, 14

Prepared according to general procedure A from 2,4,6-trimethylaniline (2.052 g, 15.2 mmol) and 2,6-diacetylpyridine (850 mg, 5.2 mmol) in MeOH giving the title compound as a yellow solid, (1.32 g, 65 %). The ^{1}H NMR data are identical to literature.[106] ^{1}H NMR (400 MHz, $CDCl_3$) δ = 8.47 (d, 2H, *J* = 7.6 Hz), 7.91 (t, 1H, *J* = 7.8 Hz), 6.91 (s, 4H), 2.30 (s, 6H), 2.24 (s, 6H), 2.02 (s, 12H).

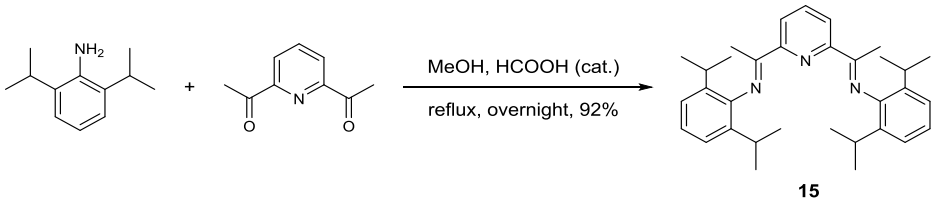

2,6-Bis[1-(2,6-diisopropylphenylimino)ethyl]pyridine, 15

Prepared according to general procedure A from 2,6-diisopropylaniline (815 mg, 4.60 mmol) and 2,6-diacetylpyridine (250 mg, 1.53 mmol) in MeOH, giving the title compound as a yellow solid, (608 mg, 92 %). The ^{1}H NMR data are identical to literature.[105] ^{1}H NMR (400 MHz, $CDCl_3$) δ 8.49 (d, 2H, *J* = 7.9 Hz), 7.93 (t, 1H, *J* = 7.9 Hz), 7.17 (d, 4H, *J* = 7.0 Hz), 7.11 (t, 2H, *J* = 6.8 Hz), 2.77 (sep, 2H, *J* = 6.8 Hz), 2.27 (s, 6H), 1.16 (d, 12H, *J* = 6.7 Hz), 1.16 (d, 12H, *J* = 7.0 Hz).

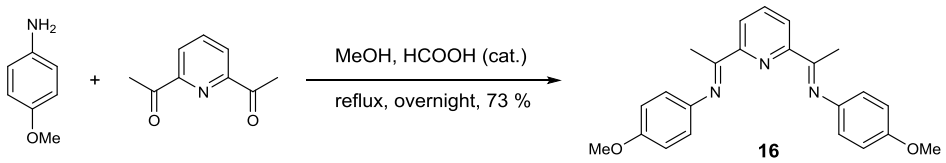

2,6-Bis[1-(4-methoxyphenylimino)ethyl]pyridine, 16

Prepared according to general procedure A from 4-methoxyaniline (453 mg, 3.86 mmol) and 2,6-diacetylpyridine (200 mg, 1.23 mmol) in MeOH, giving the title compound as a yellow solid (334 mg, 73 %). The ^{1}H NMR data are identical to literature.[107] ^{1}H NMR (400 MHz, $CDCl_3$) δ = 8.32 (d, 2H, *J* = 6.3 Hz), 7.78 (t, 1H, *J* = 7.8 Hz), 6.93 (d, 4H, *J* = 8.5 Hz), 6.82 (d, 4H, *J* = 8.8 Hz), 3.82 (s, 6H), 2.43 (s, 6H).

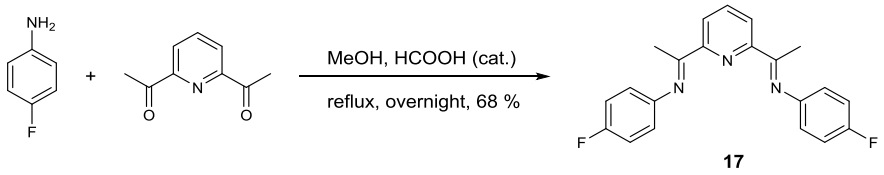

2,6-Bis[1-(4-fluorophenylimino)ethyl]pyridine, 17

Prepared according to general procedure A from 4-fluoroaniline (409 mg, 3.69 mmol) and 2,6-diacetylpyridine (200 mg, 1.23 mmol) in MeOH, giving the title compound as a yellow solid (265 mg, 68 %). The ^{1}H NMR data are identical to literature.[10] ^{1}H NMR (400 MHz, $CDCl_3$) δ = 8.31 (d, 2H, *J* = 7.8 Hz), 7.87 (t, 1H, *J* = 7.8 Hz), 7.14-6.69 (m, 4H), 6.88-6.75 (m, 4H), 2.40 (s, 6H).

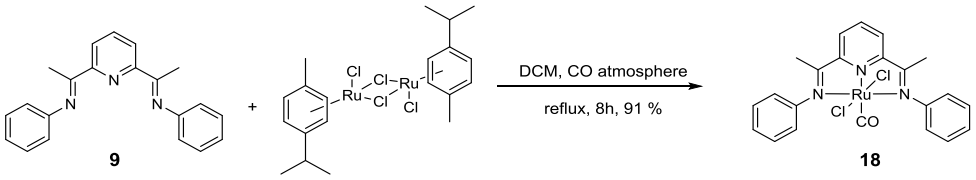

9 18

(2,6-Bis(1-phenyliminoethyl)pyridine)(carbonyl)dichlororuthenium(II), 18

Adapted from the literature procedure,[8] a 50 mL round-bottom flask was charged with 2,6-bis(1-phenyliminoethyl)pyridine (**9**, 300 mg, 0.958 mmol) and dichloro(*p*-cymene)ruthenium(II) dimer (351 mg, 0.575 mmol). The flask was purged with CO, and 20 mL of DCM (saturated with CO) was added. The reaction mixture was allowed to reflux under a balloon of CO for 8 h after which the solvent was removed under reduced pressure. The residue was dissolved in 4 mL DCM and recrystallized from Et_2O/DCM to give the title compound as a brown solid (480 mg, 98 %). ^{1}H NMR (400 MHz, $CDCl_3$) δ = 8.06 (t, 1H, *J* = 8.1 Hz), 7.88 (d, 2H, *J* = 8.1 Hz) 7.40 (t, 4H, *J* = 7.2 Hz), 7.28 (t, 2H, *J* = 5.1 Hz), 7.21 (d, 4H, *J* = 8.6 Hz), 2.56 (s, 6H); ^{13}C NMR (100 MHz, $CDCl_3$) δ = 172.0, 157.5, 151.5, 129.6, 127.4, 124.05, 120.5, 18.4; IR (thin film, cm^{-1}) ν = 1980, 1591, 1484, 1272; HRMS [- ESI] calculated for $C_{22}H_{18}N_3Cl_2ORu$ 511.98693, found 511.98759 [M-H^+].

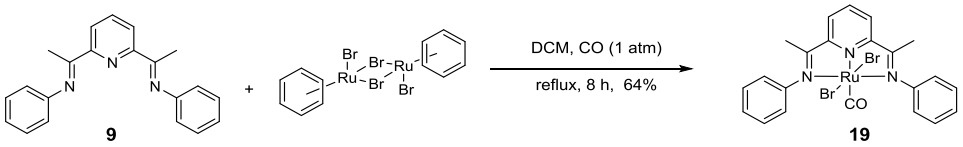

9 19

(2,6-Bis(1-phenyliminoethyl)pyridine)(carbonyl)dibromoruthenium(II), 19

Adapted from the literature procedure,[8] a 25 mL round-bottom flask was charged with 2,6-bis(1-phenyliminoethyl)pyridine (**9**, 130 mg, 0.42 mmol) and di-μ-bromobis[(benzene)bromoruthenium(II)] (169 mg, 0.25 mmol, 0.6 equiv). The flask

was purged with CO and 10 mL of DCM (saturated with CO) was added. The reaction mixture was allowed to reflux under a balloon of CO for 7 h after which the solvent was removed under reduced pressure. The residue was dissolved in 4 mL of DCM and recrystallized from benzene/DCM to give the title compound (162 mg, 64%). ^{1}H NMR (400 MHz, $CDCl_3$) δ = 8.05 (t, 2H, *J* = 8.6 Hz), 7.91 (d, 1H, *J* = 8.2 Hz), 7.37 (t, 4H, *J* = 7.4 Hz), 7.22-7.27 (m, 6H), 2.54 (s, 6H); ^{13}C NMR (100 MHz, $CDCl_3$) δ = 157.3, 151.6, 129.5, 128.6, 127.4, 124.0, 120.7, 94.9, 18.4 (C≡O signal not observed); IR (thin film, cm^{-1}) ν = 2025, 1982, 1955, 1431; HRMS [- ESI] calculated for $C_{22}H_{18}N_3Br_2ORu$ 601.88385, found 601.88420 [M-H^+].

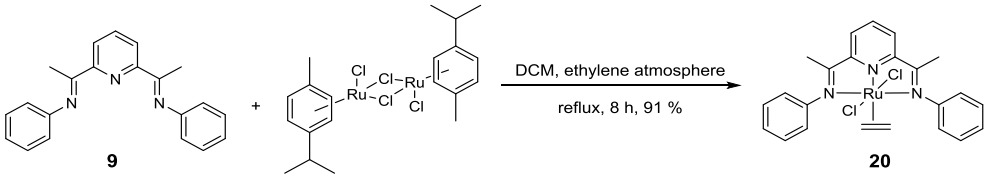

9 20

(2,6-Bis(1-phenyliminoethyl)pyridine)(dichloro)ethyleneruthenium(II), 20

Adapted from the literature procedure,[8] a 50 mL round-bottom flask was charged with 2,6-bis(1-phenyliminoethyl)pyridine (**9**, 300 mg, 0.958 mmol) and dichloro(*p*-cymene)ruthenium(II) dimer (351 mg, 0.575 mmol). The flask was purged with ethylene and 24 mL of DCM (saturated with ethylene) was added. The reaction mixture was allowed to reflux under a balloon of ethylene for 8 h after which the solvent was removed under reduced pressure. The residue was dissolved in 4 mL of DCM and recrystallized from Et_2O/DCM to give the title compound as a deep red solid (301 mg, 57 %). ^{1}H NMR (400 MHz, $CDCl_3$) δ = 8.01 (d, 2H, *J* = 7.8 Hz), 7.89 (t, 1H, *J* = 7.8 Hz), 7.41 (t, 4H, *J* = 7.4 Hz), 7.30 (t, 2H, *J* = 7.0 Hz), 7.03 (d, 4H, *J* = 7.4 Hz), 4.23 (s, 4H), 2.67 (s, 6H); ^{13}C NMR (100 MHz, $CDCl_3$) δ = 173.2, 157.4, 150.9, 132.0, 129.1, 126.6,

124.1, 121.2, 86.5, 19.2; IR (thin film, cm^{-1}) ν = 1590, 1481, 1448, 1313; HRMS [- ESI] calculated for $C_{21}H_{18}N_3Cl_3Ru$ 519.96881, found 519.96953 [M - ethylene + Cl^-].

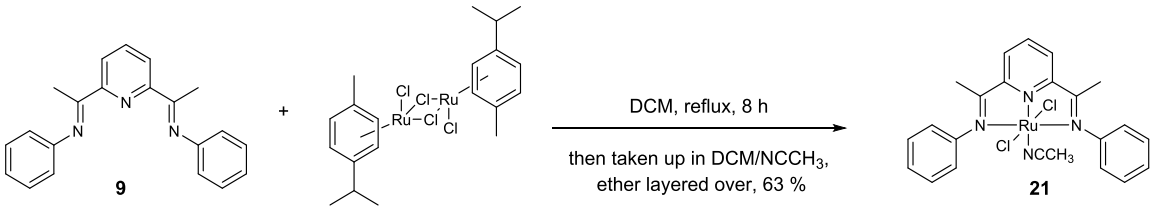

Acetonitrile(2,6-bis(1-phenyliminoethyl)pyridine)dichlororuthenium(II), 21

Adapted from the literature procedure,[8] a 25 mL round-bottom flask was charged with 2,6-bis(1-phenyliminoethyl)pyridine (**9**, 135 mg, 0.432 mmol) and dichloro(*p*-cymene)ruthenium(II) dimer (158 mg, 0.259 mmol). Degassed DCM (20 mL) was added. The reaction mixture was allowed to reflux under an atmosphere of N_2 for 8 h after which the solvent was removed under reduced pressure. The residue was dissolved in 4 mL of 1:1 CH_3CN/DCM solution and recrystallized from Et_2O/DCM to give the title compound as a deep purple solid (143 mg, 63 %). The ^1H NMR data are identical to literature.[10] ^1H NMR (400 MHz, $CDCl_3$) δ = 7.79 (d, 2H, *J* = 7.8 Hz), 7.57 (t, 1H, *J* = 7.8 Hz) 7.43-7.28 (m, 6H), 7.28-7.20 (m, 4H), 2.72 (s, 6H), 1.99 (s, 3H).

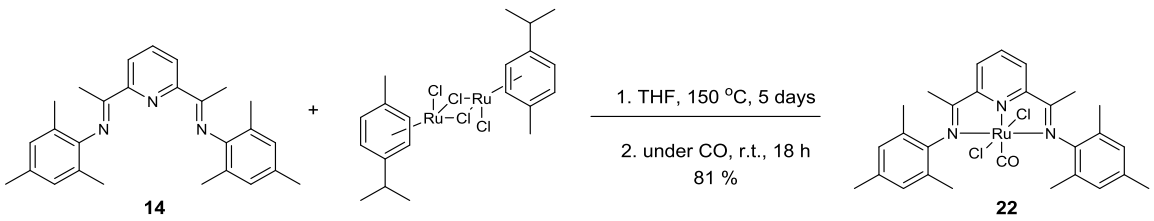

14 22

(2,6-Bis[1-(2,4,6-trimethylphenylimino)ethyl]pyridine)(carbonyl)dichlororuthenium(II), 22

A 50 mL Schlenk tube was charged with 2,6-bis[1-(2,4,6-trimethylphenylimino)ethyl]pyridine (**14**, 150 mg, 0.42 mmol) and di-μ-bromobis[(benzene)chlororuthenium(II)] (169 mg, 0.25 mmol, 0.6 equiv). THF (8 mL) was added and the flask was sealed under an atmosphere of N_2. The reaction mixture was allowed to reflux for 5 days at 150 °C in a sealed tube after which the reaction mixture was transferred to a round-bottom flask and stirred under a balloon of CO for 4 h at room temperature. The solvent was then removed under reduced pressure and the residue dissolved in 4 mL of DCM and recrystallized from Et_2O/DCM to give the title compound (286 mg, 81 %). The ^{1}H NMR data are identical to literature.[108] ^{1}H NMR (400 MHz, $CDCl_3$) δ = 8.09 (t, 1H, *J* = 8.1 Hz), 7.93 (d, 1H, *J* = 8.1 Hz), 6.86 (s, 4H), 2.47 (s, 6H), 2.26 (s, 12H), 2.25 (s, 6H).

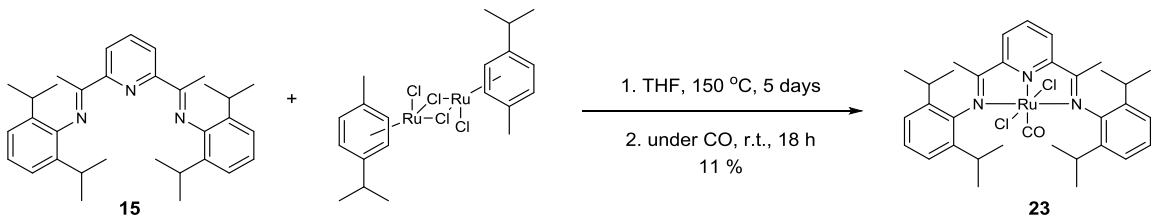

15 23

(2,6-Bis[1-(2,6-diisopropylphenylimino)ethyl]pyridine)(carbonyl)dichlororuthenium(II), 23

A 50 mL Schlenk tube was charged with 2,6-bis[1-(2,6-diisopropylphenylimino)ethyl]pyridine (**15**) (60 mg, 0.13 mmol) and dichloro(*p*-cymene)ruthenium(II) dimer (46 mg, 0.075 mmol, 0.6 equiv). THF (6 mL) was added, and the flask was sealed under a stream of N_2. The reaction mixture was allowed to reflux for 4 days at 150 °C in a sealed tube, after which the reaction mixture was transferred to a round-bottom flask and stirred under a balloon of CO for 6 h at room temperature. The solvent was then removed under reduced pressure and the residue dissolved in 4 mL of DCM and recrystallized from Et_2O/DCM to give the title compound (18 mg, 11%) The ^{1}H NMR data are identical to literature.[108] ^{1}H NMR (400 MHz, $CDCl_3$) δ = 8.12 (t, 1H, *J* = 8.0 Hz), 7.94 (d, 2H, *J* = 6.8 Hz), 7.37-7.10 (m, 6H), 3.35 (m, 4H), 2.50 (s, 6H), 1.25 (d, 12H, *J* = 6.7 Hz), 0.96 (d, 12H, *J* = 6.7).

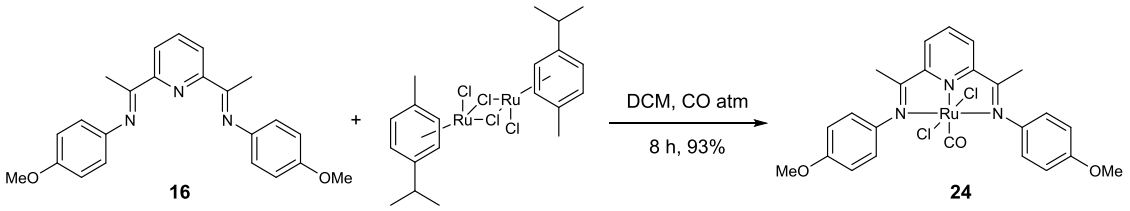

(2,6-Bis[1-(4-methoxyphenylimino)ethyl]pyridine)(carbonyl)dichlororuthenium(II), **24**

Adapted from the literature procedure,[8] a 25 mL round-bottom flask was charged with 2,6-bis[1-(4-methoxyphenylimino)ethyl]pyridine (**16**) (100 mg, 0.268 mmol) and dichloro(*p*-cymene)ruthenium(II) dimer (98 mg, 0.161 mmol, 0.6 equiv). The flask was purged with CO and 10 mL of DCM (saturated with CO) was added. The reaction mixture was allowed to reflux under a balloon of CO for 8 h, after which the solvent was removed under reduced pressure. The residue was dissolved in 4 mL of DCM and recrystallized from benzene/DCM to give the title compound (142 mg, 93 %). ^{1}H NMR (400 MHz, $CDCl_3$) δ = 8.03 (t, 1H, *J* = 8.1 Hz), 7.84 (d, 2H, *J* = 8.1 Hz), 7.17 (d, 4H, *J* = 9.1 Hz), 6.90 (d, 4H, *J* = 9.1 Hz), 3.83 (s, 6H), 2.57 (s, 6H); ^{13}C NMR (100 MHz, $CDCl_3$) δ = 171.6, 158.7, 157.6, 145.0, 138.1, 123.8, 122.2, 114.5, 55.7, 18.4, (C≡O shift not observed); IR (thin film, cm^{-1}) ν = 1956, 1603, 1502, 1249; HRMS [- ESI] calculated for $C_{24}H_{22}N_3O_3Cl_2Ru$ 572.00817, found 572.00852 [M-H^+].

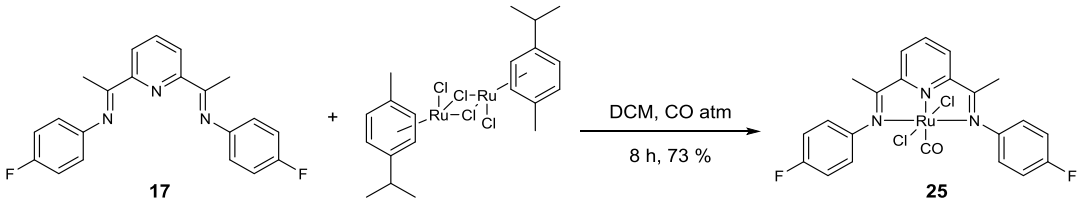

17 25

(2,6-Bis[1-(4-fluorophenylimino)ethyl]pyridine)(carbonyl)dichlororuthenium(II), 25

Adapted from the literature procedure,[8] a 25 mL round-bottom flask was charged with 2,6-bis[1-(4-fluorophenylimino)ethyl]pyridine (**17**) (100 mg, 0.287 mmol) and dichloro(*p*-cymene)ruthenium(II) dimer (105 mg, 0.172 mmol, 0.6 equiv). The flask was purged with CO and 10 mL of DCM (saturated with CO) was added. The reaction mixture was allowed to reflux under an atmosphere of CO for 7 h after which the solvent was removed under reduced pressure. The residue was dissolved in 4 mL of DCM and recrystallized from benzene/DCM to give the title compound (157 mg, 73%). ^{1}H NMR (400 MHz, $CDCl_3$) δ= 8.07 (t, 1H, *J* = 8.5 Hz), 7.89 (d, 2H, *J* = 7.93 Hz) 7.18 (dd, 4H, *J* = 8.9, 4.8 Hz), 7.08 (t, 4H, *J* = 8.70 Hz), 2.55 (s, 6H); ^{13}C NMR (100 MHz, $CDCl_3$) δ= 199.8, 172.4, 162.6, 157.2, 147.3, 138.1, 124.0, 122.1, 116.2, 18.1; IR (thin film, cm^{-1}) ν = 1954, 1499, 1215; HRMS [- ESI] calculated for $C_{22}H_{16}N_3OF_2Cl_2Ru$ 547.96820, found 547.96840 [M-H^+].

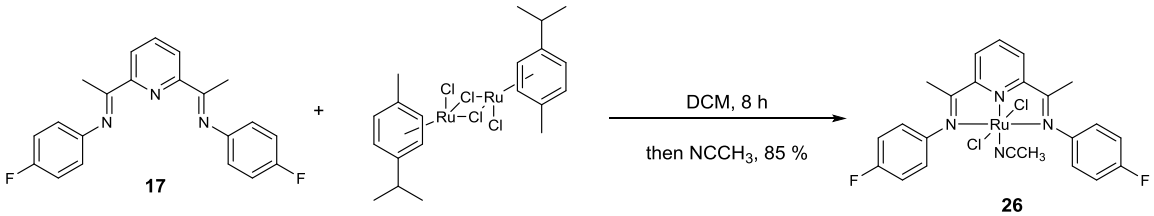

17 26

Acetonitrile(2,6-Bis[1-(4-fluorophenylimino)ethyl]pyridine)dichlororuthenium(II), 26

Procedure adapted from the literature.[10] A 25 mL round-bottom flask was charged with 2,6-bis[1-(4-fluorophenylimino)ethyl]pyridine (**17**) (160 mg, 0.472 mmol) and dichloro(*p*-cymene)ruthenium(II) dimer (173 mg, 0.283 mmol, 0.6 equiv). Degassed DCM (20 mL) was added. The reaction mixture was allowed to reflux under an atmosphere of N_2 for 7 h after which the solvent was removed under reduced pressure. The residue was dissolved in 4 mL of 1:1 CH_3CN/DCM solution and recrystallized from Et_2O to give the title compound (226 mg, 85%). ^{1}H NMR (400 MHz, $CDCl_3$) δ = 7.81 (d, 2H, *J* = 7.9 Hz), 7.59 (t, 1H, *J* = 7.9 Hz), 7.31 (dd, 4H, *J* = 8.8, 4.9 Hz), 7.06 (t, 4H, *J* = 8.7 Hz), 2.72 (s, 6H), 2.10 (s, 3H); ^{13}C NMR (100 MHz, $CDCl_3$) δ = 170.8, 163.0, 159.7, 146.0, 127.9, 125.6, 123.8, 122.7, 115.3, 17.4, 3.6; IR (thin film, cm^{-1}) ν = 1496, 1391, 1211, 1092; HRMS [- ESI] calculated for $C_{23}H_{19}N_4F_2Cl_2Ru$ 555.94996, found 555.95039 [M-H^+].

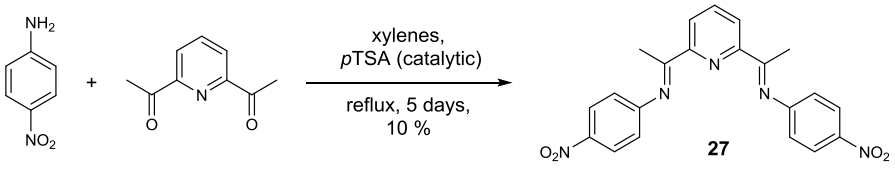

27

2,6-Bis[1-(4-nitrophenylimino)ethyl]pyridine, 27

2,6-Diacetylpyridine (1.18 g, 7.2 mmol) was added to 4-nitroaniline (3.00 g, 21.7 mmol, 3 equiv) in 50 mL of xylenes and 50 mg of *p*-toluenesulfonic acid was added. The flask

was fitted with a Dean-Stark trap and refluxed for 5 days (140 °C). The reaction mixture was concentrated to half its original volume and solid was collected *via* filtration to give the title compound as a yellow solid (284 mg, 10 %). The ^{1}H NMR data are identical to literature.[109] ^{1}H NMR (400 MHz, $CDCl_3$) δ = 8.35 (d, 2H, *J* = 7.8 Hz), 8.27 (d, 4H, *J* = 8.6 Hz), 7.93 (t, 1H, *J* = 7.2 Hz), 6.93 (d, 4H, *J* = 9.0 Hz), 2.40 (s, 6H).

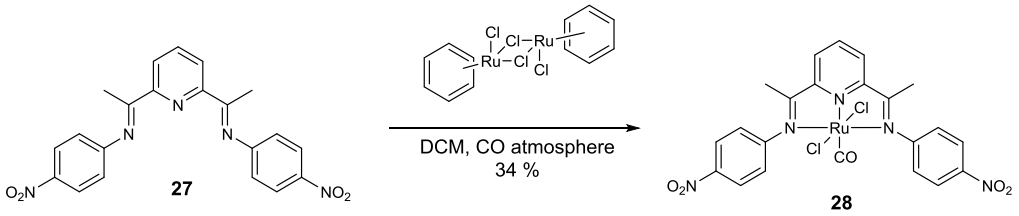

27 28

(2,6-Bis[1-(4-nitrophenylimino)ethyl]pyridine)(carbonyl)dichlororuthenium(II), 28

Adapted from the literature procedure,[8] a 50 mL round-bottom flask was charged with 2,6-bis(1[4-nitrophenylimino]ethyl)pyridine (**27**) (200 mg, 0.496 mmol) and dichloro(*p*-cymene)ruthenium(II) dimer (182 mg, 0.298 mmol, 0.6 equiv). The flask was purged with CO and 20 mL of DCM (saturated with CO) was added. The reaction mixture was allowed to reflux under a balloon of CO for 16 h after which the solvent was removed under reduced pressure. The residue was dissolved in 4 mL of DCM and recrystallized from benzene/DCM to give the title compound (61 mg, 34%). ^{1}H NMR (400 MHz, $CDCl_3$) δ = 8.32 (d, 4H, *J* = 8.6 Hz), 8.17 (t, 1H, *J* = 8.1 Hz), 8.01 (d, 2H, *J* = 8.1 Hz), 7.36 (d, 4H, *J* = 9.1 Hz), 2.61 (s, 6H); IR (thin film, cm^{-1}) ν = 1974, 1588, 1522, 1311; HRMS [- ESI] calculated for $C_{22}H_{16}N_5O_4Cl_2Ru$ 601.95720, found 601.95742 [M-H^+].

General procedure B for the cyclization of phenyl sulfamate ester 12 for GC analysis:

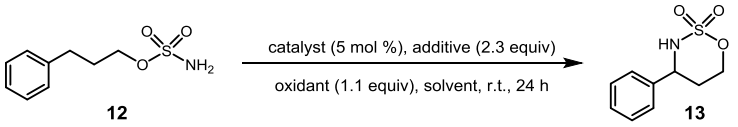

4-phenyl-1,2,3-oxathiazinane 2,2-dioxide, 13

A 7mL vial was charged with phenyl sulfamate ester **12** (17.5 mg, 0.08 mmol), catalyst (0.004 mmol, 0.05 equiv), additive (0.18 mmol, 2.3 equiv), and oxidant (0.088 mmol, 1.1 equiv). The vial was purged with nitrogen, and 1 mL (0.08 M) of dry solvent was added. The suspension was stirred at room temperature for 24 h and then quenched with 1 mL of MeOH. The reaction mixture was filtered through a celite plug, and the plug was washed with DCM (3 x 5 ml) and EtOAc (3 x 5 mL). The conversion was then determined by GC. The ^{1}H NMR data are identical to literature.[8] ^{1}H NMR (400 MHz, $CDCl_3$) δ = 7.30-7.43 (m, 4H), 4.78-4.92 (m, 2H), 4.65 (d, 2H, *J* = 11.6, 4.9, 1.5 Hz), 4.21 (d, 1H, *J* = 8.9 Hz), 2.24 (dtd, 1H, *J* = 14.5, 12.6, 4.9 Hz), 2.03 (dq, 1H, *J* = 14.7, 2.2 Hz); GC (CHIRASIL-DEX CB column) t_r = 16.6 min.

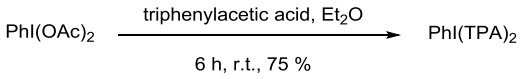

Phenyliodine bis(triphenylacetate)

Phenyliodine bis(triphenylacetate) was made according to the literature procedure.[110] Phenyliodine diacetate (322 mg, 1 mmol) was added to a mixture of triphenylacetic acid (576 mg, 2.0 mmol) in 15 mL Et_2O. The reaction mixture was stirred at room temperature for 6 h. The mixture was then filtered and the white solid recrystallized from chloroform and Et_2O to give the title compound (538mg, 75%). Its spectroscopic data

were a match to the literature.[110] IR (thin film, cm^{-1}) ν = 1645, 1223, 1192; HRMS [+ ESI] calculated 801.14777, found 801.14614 [$M+Na^+$].

General procedure C for cyclization of sulfamate esters for isolation:

A 7mL vial was charged with sulfamate ester (0.08 mmol), (2,6-bis[1-(4-fluorophenylimino) ethyl]pyridine)(carbonyl)dichlororuthenium(II) (**25**, 2.2mg, 0.004 mmol, 0.05 equiv), MgO (7.4 mg, 0.18 mmol, 2.3 equiv), and $PhI(OAc)_2$ (28.3 mg, 0.088 mmol, 1.1 equiv). The vial was purged with N_2 and dry trifluorotoluene (1 mL, 0.08 M) was added. The suspension was stirred at room temperature for 24 h and then quenched with 1 mL of MeOH. The reaction mixture was filtered through a celite plug,and the plug was washed with DCM (3 x 5 ml) and EtOAc (3 x 5 mL).

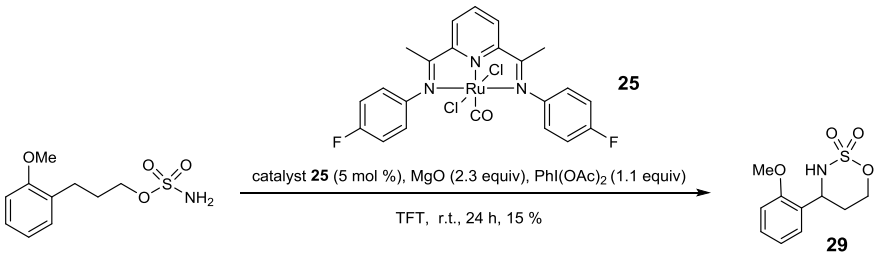

4-(2-methoxyphenyl)-1,2,3-oxathiazinane 2,2-dioxide, 29

Prepared according to general procedure C using 3-(2-methoxyphenyl)propyl sulfamate (19.6 mg, 0.08 mmol). Purification by flash chromatography on silica gel using 2:1 hexanes/EtOAc gave the title compound in 15 % (3.0 mg). The ^1H NMR data are identical to literature.[8] ^1H NMR (400 MHz, $CDCl_3$) δ = 7.30-7.36 (m, 1H), 7.19 (dd, 1H, *J* = 7.4, 1.6 Hz), 7.01-6.94 (m, 2H), 5.47 (d, 2H, *J* = 10.4 Hz), 4.90-4.82 (m, 2H), 4.61-4.55 (m, 1H), 3.89 (s, 3H), 2.52-2.44 (m, 1H), 1.70-1.60 (m, 1H).

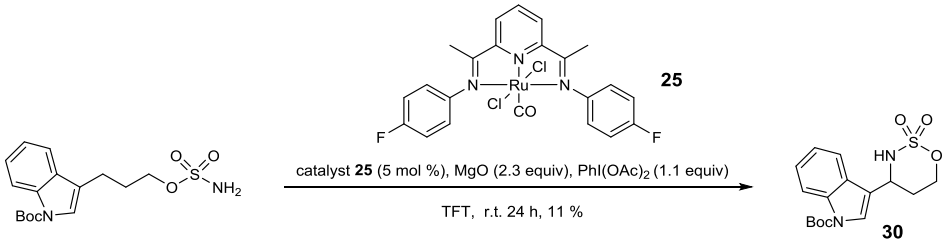

^{t}butyl-3-(2,2-dioxido-1,2,3-oxathiazinan-4-yl)-1*H*-indole-1-carboxylate, 30

Prepared according to general procedure C using ^{t}butyl 3-(3-(sulfamoyloxy)propyl)-1*H*-indole-1-carboxylate (28.3 mg, 0.08 mmol). Purification by flash chromatography on silica gel using 2:1 hexanes/EtOAc gave the title compound in 11 % yield (3.1 mg). The ^{1}H NMR data are identical to literature.[8] ^{1}H NMR (400 MHz, $CDCl_3$) δ = 8.12 (br d, H, *J* = 7.4 Hz), 7.74 (d, 1H, *J* = 7.8 Hz), 7.33 (t, 1H, *J* = 7.0 Hz), 7.26 (t, 1H, *J* = 7.6 Hz), 5.20-5.13 (m, 1H), 4.98-4.88 (m, 1H), 4.75-4.66 (m, 1H), 4.36 (d, 1H, *J* = 10.0 Hz), 2.45-2.37 (m, 1H), 2.17 (d, 1H, *J* = 14.0 Hz), 1.66 (s, 9H).

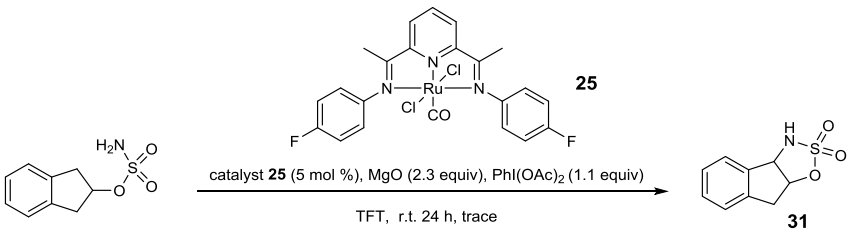

Oxathiazinane, 31

Prepared according to general procedure C using the indanyl sulfamate ester (17.0 mg, 0.08 mmol). Purification by flash chromatography on silica gel using 1:4 hexanes/EtOAc gave the title compound in 3 % (0.5 mg). The ^{1}H NMR data are identical to literature.[8] ^{1}H NMR (400 MHz, $CDCl_3$) 7.42-7.30 (m, 4H), 5.58-5.49 (m, 1H), 5.34-5.28 (m, 1H), 4.62- 4.57 (m, 1H), 3.52-3.40 (m, 2H) ppm.

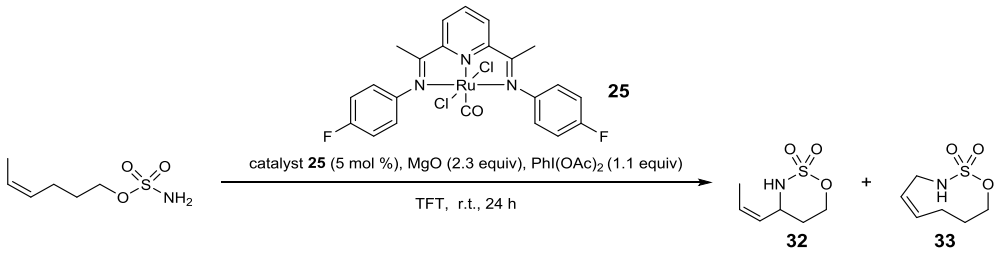

(Z)-hex-4-en-1-yl sulfamate, 32 and (Z)-4,7,8,9-tetrahydro-3*H*-1,2,3-oxathiazonine 2,2-dioxide, 33

Prepared according to general procedure C using (Z)-hex-4-en-1-yl sulfamate (14.3 mg, 0.08 mmol). Purification by flash chromatography on silica gel using 2:1 hexanes/EtOAc gave **32** 6 % (0.9 mg) and **33** in 4 % (0.6 mg). The ^{1}H NMR data are identical to literature.[8] **32:** ^{1}H NMR (400 MHz, $CDCl_3$) δ = 5.79-5.71 (m, 1H), 5.26-5.22 (m, 1H), 4.80-4.75 (m, 1H), 4.63-4.52(m, 2H), 3.98 (d, 1H, *J* = 8.2 Hz), 1.93-1.70 (m, 2H), 1.74 (d, 3H, *J* = 7.8 Hz) ppm. **33:** ^{1}H NMR (400 MHz, $CDCl_3$) δ =5.84-5.72 (m, 2H), 4.59 (s, 1H), 4.20 (t, 2H, *J* = 5.5 Hz), 3.73 (t, 2H, *J* = 6.2 Hz), 2.43 (q, 2H, *J* = 7.8 Hz), 1.83-1.78 (m, 2H) ppm.

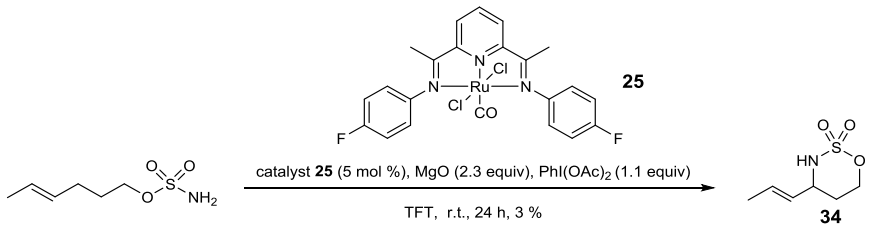

(E)-4-(prop-1-en-1-yl)-1,2,3-oxathiazinane 2,2-dioxide, 34

Prepared according to general procedure C using (E)-hex-4-en-1-yl sulfamate (14.3 mg, 0.08 mmol), purification by flash chromatography on silica gel using 2:1 hexanes/EtOAc gave the title compound in 3 % (0.4 mg). The ^{1}H NMR data are identical to literature.[8]

^{1}H NMR (400 MHz, $CDCl_3$) δ = 5.80-5.73 (m, 1H), 5.45- 5.38 (m, 1H), 4.77-4.70 (m, 1H), 4.59-4.51 (m, 1H), 4.27 (s, 1H), 4.11-4.06 (m, 1H), 1.92-1.79 (m, 3H), 1.73 (d, 3H, *J* = 6.6 Hz) ppm.

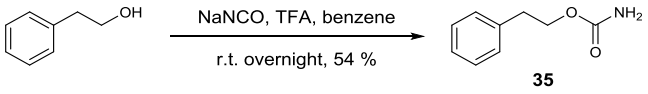

35

Phenethyl Carbamate, 35

Following the literature procedure[15,111] sodium cyanate (533 mg, 8.20 mmol) and 2-phenylethanol (500 mg, 4.10 mmol) were combined in benzene (5 mL). Trifluoroacetic acid was added slowly to the stirring mixture, and the reaction was left at room temperature overnight. H_2O (2 mL) was added, and the layers were separated. The organic layer was dried and concentrated, and the crude material was purified by recrystallization from H_2O to give the title carbamate (365 mg, 54 %). The ^{1}H NMR data are identical to the literature.[111] ^{1}H NMR (400 MHz, $CDCl_3$) δ = 7.31-7.27 (m, 2H), 7.24-7.20 (m, 3H), 4.60 (bs, 2H), 4.27 (t, 2H, *J* = 7.2 Hz), 2.93 (t, 2H, *J* = 7.2 Hz).

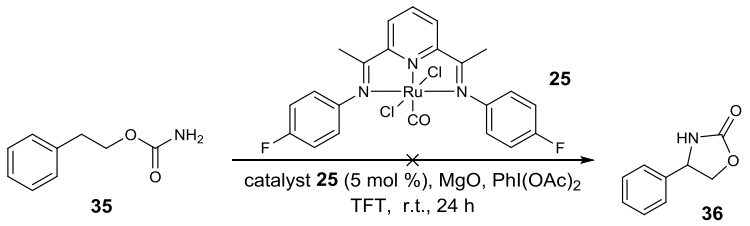

4-Phenyloxazolidin-2-one, 36

A 7mL vial was charged with carbamate **35** (13.2 mg, 0.08 mmol), catalyst **25** (0.004 mmol, 0.05 equiv), MgO (7.4 mg, 0.18 mmol, 2.3 equiv), and $PhI(OAc)_2$ (28.3 mg, 0.088 mmol, 1.1 equiv). The vial was purged with N_2, and 1 mL (0.08 M) of dry trifluorotoluene was added. The suspension was stirred at room temperature for 24 h and then quenched with 1 mL of MeOH. The reaction mixture was filtered through a celite plug. The plug was washed with DCM (3 x 5 ml) and EtOAc (3 x 5 mL). Only starting material was observed by NMR and HRMS; no product was observed.

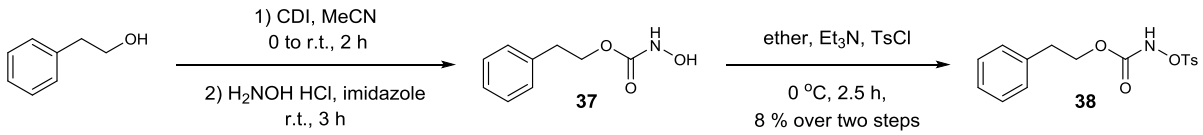

Phenethyl Tosyloxycarbamate, 38

A procedure was adapted from the literature[16,17] as follows: carbonyldiimidazole (850 mg, 5.25 mmol) and acetonitrile (10 mL) were combined and cooled to 0 °C. 2-Phenylethanol (0.60 mL, 5.00 mmol) was added over 30 min, and the reaction mixture was maintained at 0 °C for 2 hours. After warming to room temperature, NH_2OH•HCl (1.045 g, 15.00 mmol) and imidazole (608 mg, 10.00 mmol) were added. The solution became cloudy and was allowed to stir for another 4 hours. The reaction mixture was then concentrated, and the residue was taken up in EtOAc (8 mL) and washed with 1M

HCl (10 mL) and brine (10 mL). The aqueous layer was extracted twice with EtOAc (10 mL) and the combined organic layers were dried over $MgSO_4$ and concentrated under reduced pressure. **37** was taken forward without further purification as the crude oil.

37 was dissolved in Et_2O (10 mL) cooled to 0 °C and tosyl chloride (1.01 g, 5.30 mmol) was added. Et_3N (0.67 mL, 4.84 mmol) was added dropwise over 15 min. The solution became cloudy and was warmed to room temperature over 2.5 h. H_2O was added, and the reaction mixture was washed with brine. The aqueous layer was extracted twice with Et_2O, and the combined organic layers dried over $MgSO_4$. The crude material was purified by flash chromatography on silica gel (10 % EtOAc/DCM) followed by recrystallization from DCM to give the title compound (135 mg, 8% over two steps). Its ^{1}H NMR data were identical to the literature.[16] ^{1}H NMR (400 MHz, $CDCl_3$) δ = 7.84 (d, 2H, *J* = 8.0 Hz), 7.69 (bs, 1H), 7.34-7.23 (m, 5H), 7.12 (d, 2H, *J* = 7.2 Hz), 4.21 (t, 2H, *J* = 7.2 Hz), 2.80 (t, 2H, *J* = 7.2 Hz), 2.44 (s, 3H).

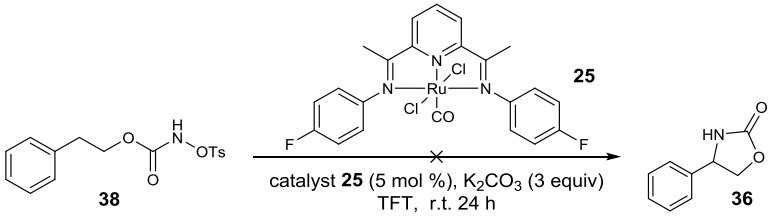

4-Phenyloxazolidin-2-one, 36

A 7 mL vial was charged with tosyl carbamate **38** (26.7 mg, 0.08 mmol), catalyst **25** (0.004 mmol, 0.05 equiv), and K_2CO_3 (30.2 mg, 0.24 mmol, 3 equiv). The vial was purged with N_2, and 1 mL (0.08 M) of dry trifluorotoluene was added. The suspension

was stirred at room temperature for 24 h and then quenched with 1mL of MeOH. The reaction mixture was filtered through a celite plug. The plug was washed with DCM (3 x 5 ml) and EtOAc (3 x 5 mL). Only starting material was observed by ^{1}H NMR and HRMS; no product was observed.

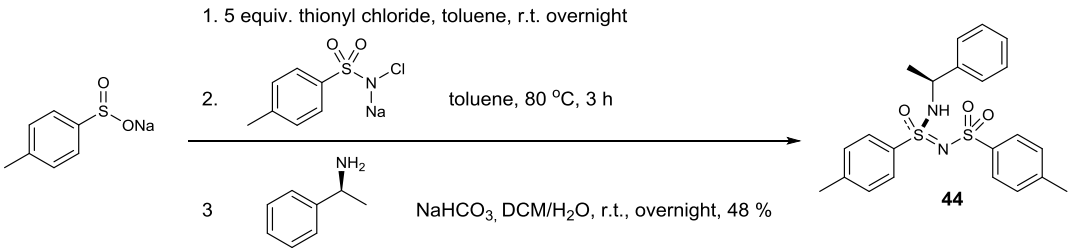

(R)-N-(p-Toluenesulfonyl)-p-toluenesulfonimidamide, 44

Procedure was adapted from the literature[18,112] as follows: a suspension of sodium *p*-toluenesulfinate (3.75 g, 21 mmol) in 40 mL toluene were cooled to 0 °C. Thionyl chloride (12.29 g, 104 mmol) was added, and the reaction mixture was stirred overnight at room temperature. The reaction mixture was concentrated and the resulting oil dissolved in toluene (60mL). Chloramine T (4.78 g, 21 mmol) that had been dried overnight at 40 °C in a drying pistol under vacuum was added to the reaction, and the solution was brought up to 80 °C for 2 hours. The reaction mixture was filtered while still hot and the filtrate concentrated. The resulting yellow oil was dissolved in DCM (80 mL) and cooled to 0 °C. (*S*)-(-)-Methyl benzylamine (3.046 g, 25.2 mmol) and $NaHCO_3$ (2.1 g, 25.2 mmol) in 50 mL H_2O were added to the reaction mixture at which point the solution turned pink and was left stirring overnight at room temperature. The red solution was then washed with 10 % HCl (2 x 25 mL) and H_2O (2 x 30 mL). The

aqueous layers were washed with DCM, and the combined organic layers were dried with $MgSO_4$ and concentrated. The desired sulfonimidamide was recrystallized from EtOH to give the title compound as a single diastereomer in 48 % yield (4.3 g). Its ^{1}H NMR data were a match to the literature.[18,112] ^{1}H NMR (400 MHz, $CDCl_3$) δ = 7.76-7.72 (m, 4H), 7.26-7.16 (m, 9H), 6.05 (d, 1H), 4.47 (q, 1H, *J* = 7.2 Hz), 2.39 (s, 3H), 2.36 (s, 3H), 1.31 (d, 3H, *J* = 7.2 Hz).

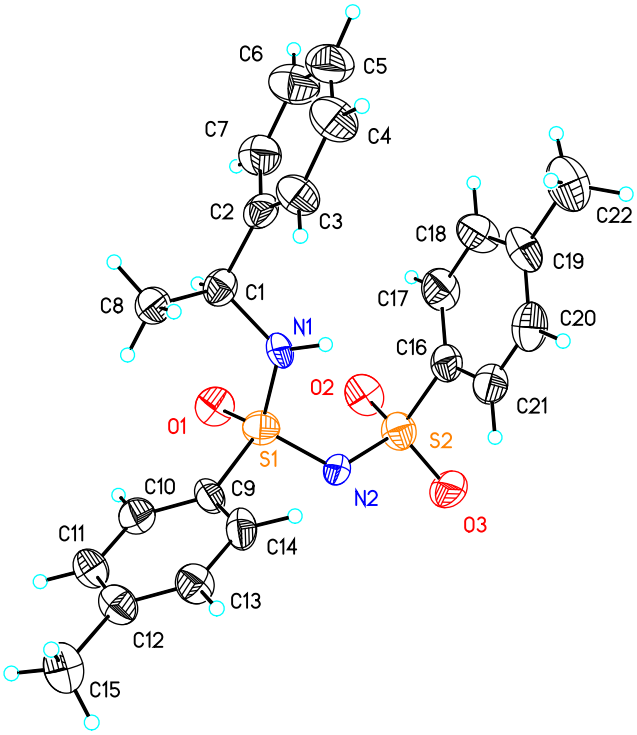

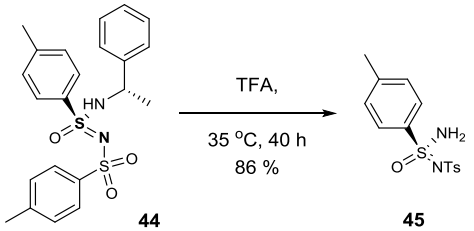

(R)-N-(amino(oxo)(p-tolyl)-l6-sulfanylidene)-4-methylbenzenesulfonamide, 45

Trifluoroacetic acid (1.6 mL) was added to sulfonimidamide **44** (819 mg, 1.91 mmol), and the reaction mixture was brought up to 35 °C for 40 hours. The solution was concentrated and crystallized from EtOAc to give the title compound **45** (378 mg, 61 %). Its ^{1}H NMR data were a match to the literature.[18,112] ^{1}H NMR (400 MHz, $CDCl_3$) δ = 7.86-7.82 (m, 4H), 7.30-7.26 (m, 4H), 5.55 (bs, 2H), 2.42 (s, 3H), 2.39 (s, 3H).

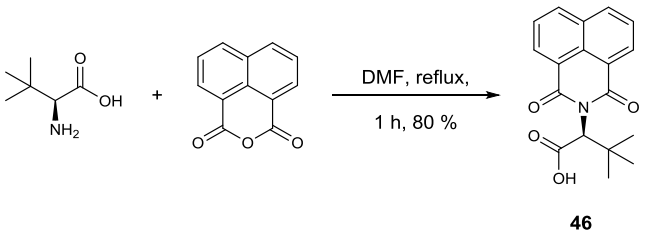

(S)-*N*-1,8-Naphthoyl-*t*leucine, 46

Based on a literature procedure,[18] L-*t*leucine (1.014 g, 7.74 mmol) and 1,8-napthalic acid (1.710 g, 8.63 mmol) were combined in anhydrous DMF (25 mL) and refluxed for 2 h. The oil bath was removed and the mixture was left to cool to room temperature overnight. Purification by flash chromatography on silica gel gave the title compound **46** in 80% yield (1.917 g). Its ^{1}H NMR data were identical to the literature.[18] ^{1}H NMR

(400 MHz, $CDCl_3$) δ = 8.51-8.46 (m, 2H), 8.12 (d, 2H, *J* = 7.6 Hz), 7.66 (t, 2H, *J* = 7.6 Hz), 5.56 (s, 1H), 1.18 (s, 9H).

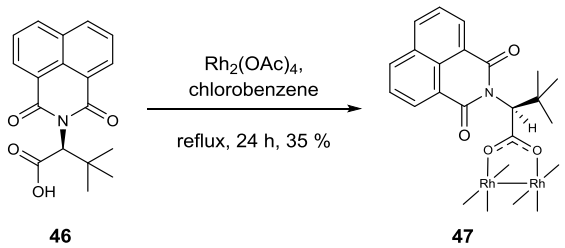

46 **47**

Rh_2[(S)-nttl]$_4$, 47

Based on the literature procedure,[18] chlorobenzene was added to a flask containing (*S*)-*N*-1,8-napthoyl-*t*-leucine (**46)** (371 mg, 1.19 mmol) and $Rh_2(OAc)_4$ (55 mg, 0.124 mmol). The flask was fitted with a Soxhlet extractor that contained a mixture of sand and anhydrous Na_2CO_3, and the mixture was refluxed for 24 hrs. The chlorobenzene was removed and the residue purified by column chromatography on basic alumina using Et_2O and then crystallized from acetonitrile to give the title compound **47** in 35 % yield (123 mg). Its ^{1}H NMR data were identical to the literature.[18] ^{1}H NMR (400 MHz, $CDCl_3$) δ = 8.73 (d, 1H, *J* = 7.2 Hz), 8.36 (d, 1H, *J* = 7.2 Hz), 7.99 (d, 1H, *J* = 8.0 Hz), 7.94 (d, 1H, *J* = 8.0 Hz), 7.78 (t, 1H, *J* = 8.0 Hz), 7.46 (t, 1H, *J* = 7.6 Hz), 5.80 (s, 1H), 1.27 (s, 9H).

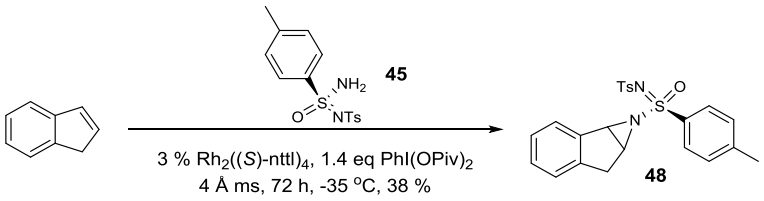

N-tosylsulfonamide aziridine, 48

A procedure from the literature[18] was modified as follows: sulfonimidamide **45** (100 mg, 309 mmol), Rh_2[(S)-nttl]$_4$ **47** (11 mg, 0.0077 mmol) and 110 mg of 4 Å mol sieves were combined in a 7 mL vial and purged with nitrogen. Dichloroethane (1 mL) and methanol (0.5 mL) were added, and the reaction mixture was stirred for 5 min, after which indene (29.8 mg, 0.257 mmol) was added. The vial was cooled to -35 °C and the oxidant, PhI(OPiv)$_2$ (147 mg, 0.360 mmol), was added. The reaction was left to stir at -35 °C for 72 h. The solution was filtered through a plug of silica and washed with DCM (2 x 5 mL) to remove the molecular sieves, the filtrate was concentrated and the resulting oil purified by flash chromatography on silica gel to give the title compound **48** in 38 % yield (36 mg). ^{1}H NMR ($CDCl_3$, 400MHz) δ = 8.05-8.09 (m, 2 H), 7.80 (d, J = 7.6 Hz, 1 H), 7.23-7.39 (m, 9 H), 7.03-7.09 (m, 2 H), 5.36 (d, J = 5.2 Hz, 1 H), 4.62 (t, J = 5.3 Hz, 1 H), 3.12-3.30 (m, 2 H), 2.46 (s, 3 H), 2.32 (s, 3 H).

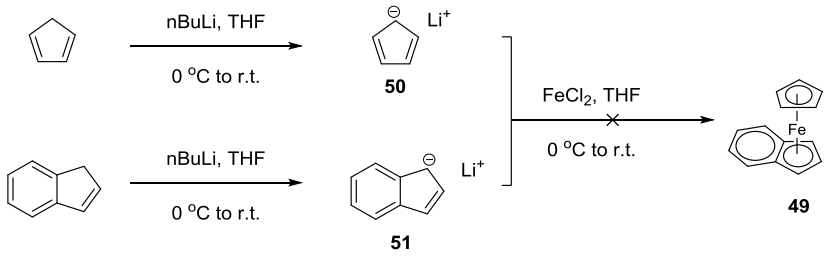

Mixed ferrocene, 49

Freshly cracked cyclopentadiene (103 mg, 1.56 mmol, cracked by the literature procedure[113]) was added to THF (3 mL) at 0 °C. ^{n}BuLi (1.64 mL, 1.56 mmol, 1 equiv) was then added, and the solution was stirred for 5 minutes. While this was stirring, in a separate flask indene (181 mg, 1.56 mmol) was added to THF (3 mL) at 0 °C. ^{n}BuLi (1.64 mL, 1.56 mmol, 1 equiv) was then added and the solution was stirred for 5 minutes. The cyclopentadienide and indeneide solutions were then added to a solution of $FeCl_2$ in THF (5 mL) also at 0 °C. The mixture was stirred at room temperature for 4 hours. The reaction mixture was filtered through a silica plug, and the plug was washed with EtOAc (3 x 10 mL). The filtrate was concentrated under reduced pressure; the crude material was taken up in pentane and purified by flash chromatography on silica gel (20 % EtOAc in hexanes). By ^{1}HNMR analysis only was ferrocene was observed (no mixed ferrocene).

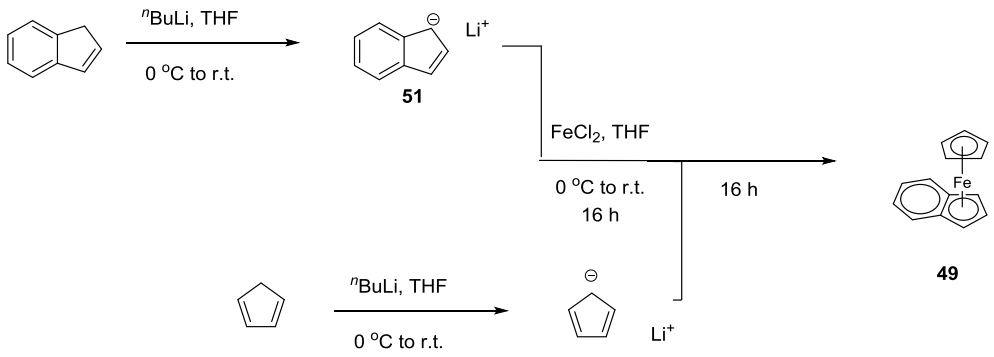

Mixed ferrocene, 49

Indene (181 mg, 1.56 mmol) was added to THF (3 mL) at -78 °C. ^{n}BuLi (1.64 mL, 1.56 mmol, 1 equiv) was then added, and the solution was stirred for 5 minutes. The indene litihiate solution was then added to a solution of $FeCl_2$ in THF (5 mL) at 0 °C, and the solution was left to stir for 16 hours. In a separate flask, freshly cracked cyclopentadiene (103 mg, 1.56 mmol, cracked by the literature procedure[113]) was added to THF (3 mL) at -78 °C. ^{n}BuLi (1.64 mL, 1.56 mmol, 1 equiv) was then added, and the solution was stirred for 5 minutes. The cyclopentadienide solution was then added to the iron/indene solution. The mixture stirred at room temperature overnight. The solvent was evaporated, and the residue was taken up in pentane and purified by flash chromatography on silica gel (20 % EtOAc in hexanes). Crude ^{1}H NMR indicated a small amount of the mixed ferrocene was generated. The material turned green on the column and brown standing in air so none of the title compound was isolated.

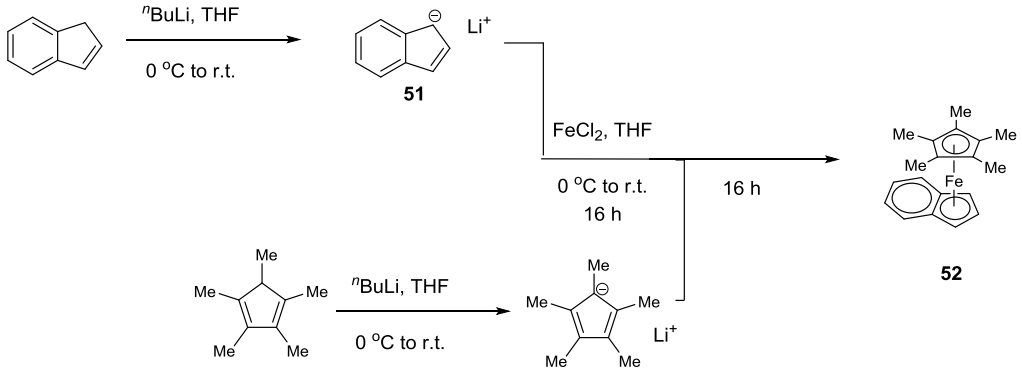

Mixed ferrocene, 52

Indene (181 mg, 1.56 mmol) was added to THF (2 mL) at 0 °C. ^{n}BuLi (1.64 mL, 1.56 mmol, 1 equiv) was then added, and the solution was stirred for 5 minutes. The indene litihiate solution was then added to a solution of $FeCl_2$ in THF (10 mL) at 0 °C and the solution was left to stir overnight. In a separate flask, 1,2,3,4,5-pentamethylcyclopentadiene (212 mg, 1.56 mmol) was added to THF (2 mL) at 0 °C. ^{n}BuLi (1.64 mL, 1.56 mmol, 1 equiv) was then added and the yellow mixture solidified. Additional THF (15 mL) was added to break up the solution. The suspension was then added to the iron/indene mixture at 0 °C and was left to stir for 2 hours. The solvent was evaporated, and the residue was taken up in pentane. Crude ^{1}H NMR indicated a small amount of the mixed ferrocene was generated, however it turned brown on standing in air so none of the title compound could be isolated.

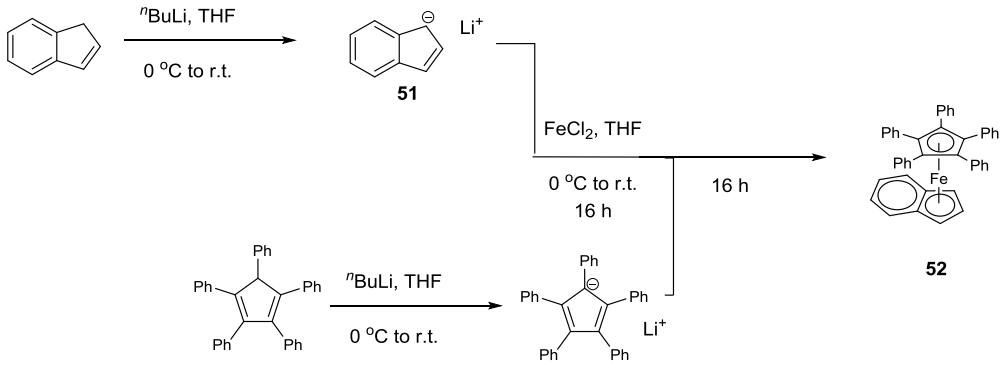

Mixed ferrocene, 53

Adapted from the literature procedure,[21] indene (181 mg, 1.56 mmol) was added to THF (2 mL) at 0 °C. ^{n}BuLi (1.64 mL, 1.56 mmol, 1 equiv) was then added, and the solution was warmed to room temperature. The indene litihiate solution was then added to a solution of $FeCl_2$ in THF (10 mL) at 0 °C, and the solution was left to stir at room temperature overnight. In a separate flask, 1,2,3,4,5-pentaphenylcyclopentadiene (697 mg, 1.56 mmol) was added to toluene (2 mL) at 0 °C. ^{n}BuLi (1.64 mL, 1.56 mmol, 1 equiv) was then added, and the mixture was warmed to 100 °C for 45 minutes. The toluene was removed under vacuum and the solid was suspended in THF (5 mL) and added to the iron mixture at 0 °C. The combined mixture was left to stir for 3 hours after which the solvent was removed under vacuum, and purification was attempted by flash chromatography (5% EtOAc in hexanes). The black crystals decomposed to a brown powder before they could be characterized.

6.3 Chapter 2 Procedures and Characterization

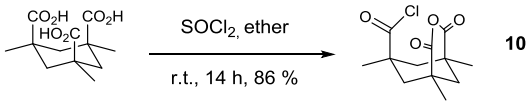

Kemp's anhydride, 10

Following the literature procedure,[114] Kemp's triacid (50 mg, 0.19 mmol) was combined with dry ether (2.5 mL) in a round bottomed flask, and cooled to 0 ^{o}C. Thionyl chloride (0.28 mL, 3.87 mmol) was then added. The ice bath was removed, and the reaction mixture was left to stir for 14 hours at room temperature. The reaction mixture was concentrated under reduced pressure and recrystallized from hot toluene to give the title compound **10** as a bright green solid (44 mg, 90 %). Its ^{1}H NMR data were identical to the literature.[114] ^{1}H NMR (300 MHz, acetone-d_6) δ = 2.67 (d, 2H, *J* = 14.4 Hz), 2.33 (d, 1H, *J* = 13.2 Hz), 1.75 (d, 2H, *J*= 14.7 Hz), 1.64 (d, 1H, *J* = 13.5 Hz), 1.43 (s, 3H), 1.33 (s, 6H).

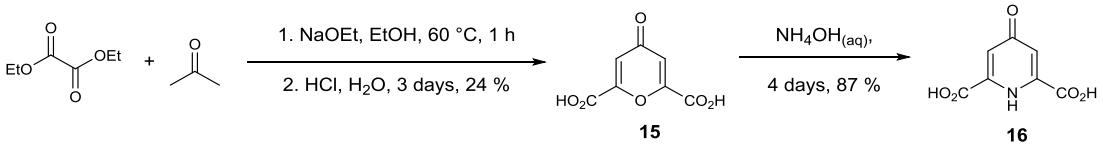

Chelidamic Acid, 16

Following the literature procedure,[28] metallic sodium (23.5 g) was added slowly to freshly distilled ethanol (500 mL) and heated until all of the metal had reacted (1.5 h at reflux). A solution of freshly distilled acetone (38 mL) in diethyloxalate (144 mL) was slowly added. The solution was heated to 60 ^{o}C for 1 h. Concentrated HCl (200 mL) and

water (100 mL) were added, and the mixture was left at 50 ^{o}C overnight. The volume was reduced by half under reduced pressure, and an additional 50 mL concentrated HCl and 300 mL water were added. The reaction mixture was left to stir at room temperature for four days. The brown solution was filtered, washed with water and acetone and recrystallized from 1.5 L of boiling water and decolorizing charcoal to give the title compound **15** in 24 % yield (28.55 g) which was used without further purification. Concentrated aqueous ammonia (100 mL) was added to chelidonic acid **15** (15 g, 81.5 mmol) at 0 ^{o}C. After addition was complete, the ice bath was removed and the mixture was allowed to stir at room temperature for four days. The reaction mixture was concentrated to dryness under reduced pressure and the residue dissolved into water (200 mL). The solution was brought to reflux and decolorizing charcoal was added. After the solution refluxed for 3 minutes it was filtered while still hot. The filtrate was then chilled to 0 ^{o}C and acidified to pH = 1 using concentrated HCl. The precipitate was collected by filtration to give the title compound **16** as a white solid (13 g, 87 %). Its ^{1}H NMR data were in agreement with the literature.[28] ^{1}H NMR (300 MHz, D_6-DMSO) δ = 7.52 (s, 2H)

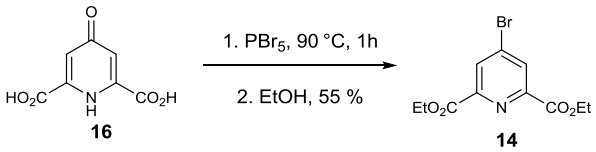

2,6-ethylester-4-bromopyridine, 14

Following the literature procedure,[29] chelidamic acid (2.0 g, 11 mmol) and PBr_5 (19 g, 44 mmol, 4 equiv) were combined in a round bottomed flask fitted with a reflux condenser and a drying tube. The reaction mixture was heated for two hours at 90 ^{o}C. After the reaction was cooled to room temperature, cold ethanol was slowly added. The mixture was concentrated and purified by flash chromatography (2:1 hexanes:EtOAc) to give the title compound **14** in 55 % (1.82 g). Its ^{1}H NMR data were identical to the literature.[29] ^{1}H NMR (300 MHz, $CDCl_3$) δ = 8.41 (s, 2H), 4.47 (q, 4H, J = 5.4 Hz), 1.44 (t, 6H, J = 5.1 Hz)

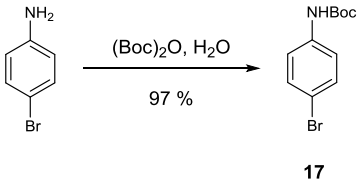

^{t}butyl (4-bromophenyl)carbamate, 17

Based on the literature procedure,[115] bromoaniline (430 mg, 2.5 mmol) was suspended in 5 mL H_2O and di-^{t}butyl dicarbonate (611 mg, 1.1 mmol) was added. Upon addition of the di-^{t}butyl dicarbonate, all of the aniline dissolved into the solution. After 15 minutes the reaction mixture became biphasic. After 45 minutes the white solid was broken up and the water decanted off. The solid was washed with H_2O (2 x 3 mL) and was dried

under vacuum to give the title compound **17** as a white solid (660 mg, 97 %). Its ^{1}H NMR data were in good agreement with the literature.[115] ^{1}H NMR (400 MHz, $CDCl_3$) δ = 7.37 (d, 2H, *J* = 8.8 Hz), 7.23 (d, 2H, *J* = 8.8 Hz), 6.44 (bs, 1H), 1.49 (s, 9H).

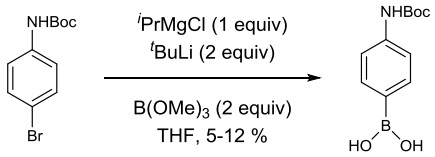

17 **18**

(4-((*t*butoxycarbonyl)amino)phenyl)boronic acid, 18

Bromoaniline **17** (0.50 g, 2.9 mmol) was dissolved in dry THF (25 mL) and cooled to 0 °C. ^{i}PrMgCl (5.8 mmol, 2.9 mL, 2 M in ether) was added slowly and the solution became yellow. The reaction mixture was cooled to -78 °C and ^{t}BuLi (5.8 mmol, 3.8 mL, 1.5 M in pentane) was added over 15 min. The solution was allowed to stand for 30 min. $B(OMe)_3$ (0.48 mL, 5.8 mmol, 2 equiv) was added dropwise, and the solution was allowed to slowly return to room temperature over two hours. The reaction mixture was returned to 0 °C and acidified to pH = 3 with 1 N HCl. The solution was warmed back up to room temperature, extracted with ethyl acetate (20 mL), washed with brine (10 mL) and H_2O (10 mL), dried over $MgSO_4$, and concentrated. Hexane was added to the crude oil, the title compound **18** precipitated out of solution as a white powder and was collected by filtration (12 mg, < 5 %). ^{1}H NMR (400 MHz, DMSO) δ = 7.81 (d, 2H, *J* = 11.2 Hz), 7.64 (d, 2H, *J* = 11.2 Hz), 3.63 (s, 2H), 1.43 (s, 9H).

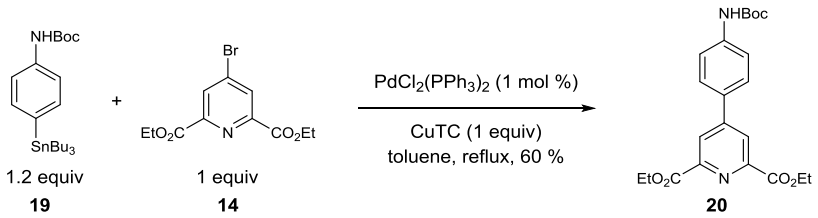

2,6-ethylester-4-(4-(((benzyloxy)carbonyl)amino)phenyl)pyridine, 20

Stannane **19** (600 mg, 1.16 mmol, 1.2 equiv) and bromopyridine **14** (284 mg, 0.97 mmol) were combined in toluene (40 mL). $PdCl_2(PPh_3)_2$ (0.1 mol %) and CuTC (184 mg, 0.97 mmol, 1 equiv) was added and the solution was refluxed (110 °C) for 3 hours. The reaction mixture was cooled to room temperature and concentrated. Purification by flash chromatography on silica gel gave the title compound **20** as an off-white solid (380 mg, 65 %). ^{1}H NMR (400 MHz, $CDCl_3$) δ = 8.48 (s, 2H) 7.73 (d, 2H, *J* = 11.6 Hz), 7.57 (d, 2H, *J* = 11.6 Hz), 7.36- 7.41 (m, 5H), 6.92 (bs, 1H), 5.23 (s, 2H), 4.50 (q, 4H, *J* = 9.2 Hz), 1.48 (t, 6H, *J* = 9.2 Hz). HRMS [+ APCI] calculated for $C_{22}H_{27}N_2O_6$ 449.1714, found 449.1707 [M+H].

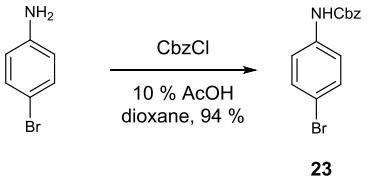

Benzyl (4-bromophenyl)carbamate, 23

Adapted from the literature procedure,[116] bromoaniline (2.0 g, 12 mmol) was added to 90 mL of H_2O and 10 mL of acetic acid. A solution of 1.75 mL CbzCl in 80 mL dioxane was slowly added. The solution turned cloudy and was allowed to stir overnight. H_2O

was added along with ether, and the white solid dissolved in the ether layer. The aqueous layer was brought up to pH = 12 with 1 N NaOH and extracted again with ether. The combined organic layer was dried over Na_2SO_4 and concentrated to give the title compound **23** which was used without further purification (3.3 g, 93 %). Its ^{1}H NMR data were identical to the literature.[117] ^{1}H NMR (400 MHz, $CDCl_3$) δ = 7.26-7.43 (m, 9H), 6.64 (s, 1H), 5.20 (s, 2H).

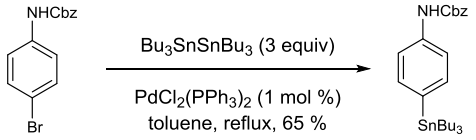

23 **24**

Benzyl (4-(tributylstannyl)phenyl)carbamate, 24

Bromoaniline **23** (1.50 g, 4.90 mmol) was added to toluene (30 mL) and $PdCl_2(PPh_3)_2$ (0.1 mol %). Bistributyl tin (7.4 mL, 14.8 mmol, 3 equiv) was added, and the reaction mixture was refluxed (110 °C) for three hours. The solution was concentrated and purified by flash chromatography on silica gel (0 % to 10 % EtOAc in hexanes) to give the title compound **24** as an off-white solid in 65 % yield (1.64 g). ^{1}H NMR (400 MHz, DMSO) δ = 7.31-7.41 (m, 9H), 6.64 (bs, 1H), 5.19 (s, 2H), 0.85-1.63 (m, 27H).

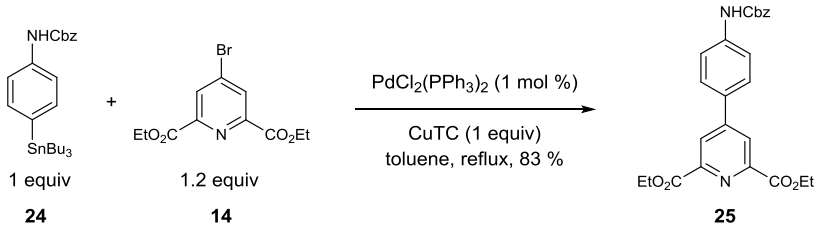

diethyl 4-(4-(((benzyloxy)carbonyl)amino)phenyl)pyridine-2,6-dicarboxylate, 25

Stannane **24** (600 mg, 1.16 mmol, 1.2 equiv) and bromopyridine **14** (284 mg, 0.97 mmol) were combined in toluene (40 mL). $PdCl_2(PPh_3)_2$ (0.1 mol %) and CuTC (184 mg, 0.97 mmol, 1 equiv) was added and the solution was refluxed (110 °C) for 3 hours. The reaction mixture was cooled to room temperature and concentrated. Purification by flash chromatography on silica gel gave the title compound **25** as an off-white solid (431 mg, 83 %). ^{1}H NMR (400 MHz, $CDCl_3$) δ = 8.48 (s, 2H) 7.73 (d, 2H, *J* = 11.6 Hz), 7.57 (d, 2H, *J* = 11.6 Hz), 7.36-7.41 (m, 5H), 6.92 (bs, 1H), 5.23 (s, 2H), 4.50 (q, 4H, *J* = 9.2 Hz), 1.48 (t, 6H, *J* = 9.2 Hz). HRMS [+ APCI] calculated for $C_{25}H_{25}N_2O_6$ 449.1714, found 449.1707 [M+H].

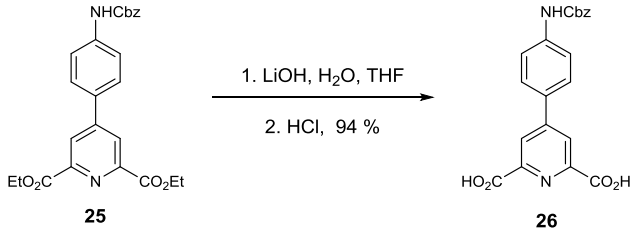

4-(4-(((benzyloxy)carbonyl)amino)phenyl)pyridine-2,6-dicarboxylic acid, 26

Ester **25** (275 mg, 0.63 mmol) was dissolved in THF (3 mL) and H_2O (4 mL) and LiOH (77 mg, 1.89 mmol, 3 equiv) was added. After 4 hours the solution was acidified to pH =

3 with 1 N HCl, the title compound **26** precipitated out of solution as a yellow powder and was collected by filtration (223 mg, 94 %). ^{1}H NMR (400 MHz, DMSO) δ = 10.06 (s, 2H), 8.40 (d, 2H, *J* = 8.4 Hz) 7.86 (s, 2H), 7.62 (d, 2H, *J* = 8.4 Hz), 7.32-7.43 (m, 5H), 5.15 (s, 2H).

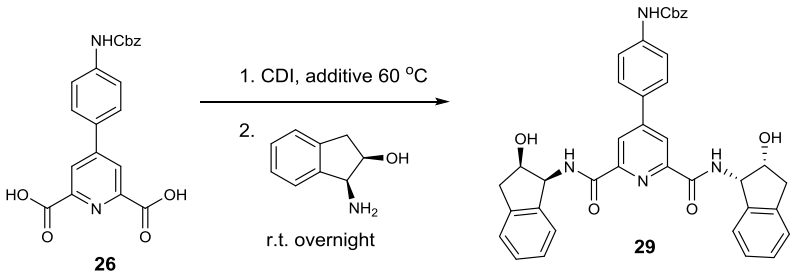

Benzyl (4-(2,6-bis(((1*S*,2*R*)-2-hydroxy-2,3-dihydro-1H-inden-1-yl)carbamoyl)pyridin-4-yl)phenyl)carbamate, 29

The diacid (171 mg, 0.45 mmol) and carbonlydiimidazole (151 mg, 0.93 mmol, 2.1 equiv) were combined in dry THF (3 mL) and left at 60 °C overnight. The amino alcohol (133 mg, 0.89 mmol, 2 equiv) in THF (1 mL) was added, and the solution was allowed to cool to room temperature. The solution was concentrated and purified by flash chromatography on silica gel in 10 % MeOH in DCM to afford the title compound **29** as an off-white solid (113 mg, 39 %). ^{1}H NMR (400 MHz, DMSO) δ = 10.08 (s, 1H), 8.84 (d, *J* = 8.8 Hz, 2H), 8.54 (s, 2H), 7.91 (d, *J* = 8.8 Hz, 2H), 7.67 (d, *J* = 8.8 Hz, 2H), 7.32-7.44 (m, 5H), 7.12-7.21 (m, 8H) 5.40 (dd, *J* = 8.4, 4.8 Hz, 2H), 5.27 (d, *J* = 4.8 Hz, 2H), 5.17 (s, 2H), 4.50 (m, 2H), 3.10 (dd, *J* = 16.4, 3.2 Hz, 2H), 2.82 (d, *J* = 16.4 Hz, 2H); ^{13}C NMR (100 MHz, DMSO) δ = 163.3, 158.3, 153.3, 149.9, 141.9, 141.6, 140.9, 139.9, 135.3, 128.8, 128.5, 128.3, 128.2, 127.9, 127.5, 127.4, 126.5, 125.4, 125.0, 79.6, 60.5,

57.3, 58.2; IR (thin film, cm^{-1}) ν = 3715, 3327, 2342, 2139, 2013, 1751, 1052, 1028, 1008, 951; HRMS [+ APCI] calculated for $C_{39}H_{35}N_4O_6$ 655.2558, found 655.2551 [M+H].

6.4 Chapter 3 Procedures and Characterization

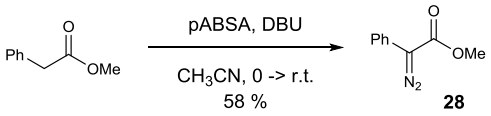

Methyl 2-diazo-2-phenylacetate, 28

Based on the literature procedure,[54] methyl phenylacetate (10.1 g, 10.0 mL, 74 mmol) and *p*ABSA (21.2 g, 88 mmol) were combined in acetonitrile (140 mL) and cooled to 0 °C. DBU (11.2 mL, 112 mmol) in 40 mL acetonitrile was slowly added via addition funnel. The reaction mixture was allowed to warm to room temperature overnight. H_2O (50 mL) and DCM (50 mL) were added and the layers separated. The aqueous layer was washed twice with DCM (2 x 50 mL), the combined organic layers were dried over $MgSO_4$, and the solvent was removed under vacuum. The resulting oil was purified on a silica column using 5% Et_2O in pentane to give the title compound **28** in 53 % yield (6.83 g). The ^1H NMR data were identical to the literature.[118] (6.83g, 53%) ^1H NMR (400MHz, $CDCl_3$) δ = 7.45-7.49 (m, 2H), 7.34-7.40 (m, 2H), 7.14-7.20 (m, 1H), 3.85 (s, 3H).

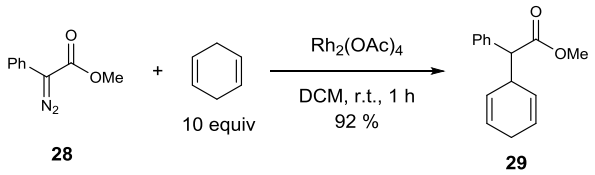

Methyl-2-(cyclohexa-2,5-dien-1-yl)-2-phenylacetate, 29

Based on a procedure adapted from the literature,[43] $Rh_2(OAc)_4$ (9 mg, 0.02 mmol) and 1,4-cyclohexadiene (801 mg, 10 mmol) were dissolved in 10 mL DCM. A solution of diazo **28** (176 mg, 1 mmol) in 10 mL DCM was added over 30 min, and the reaction was stirred for an additional 30 minutes after the addition was complete. The solution was filtered through a plug of silica, and the plug was washed with DCM (3 x 20 mL) and the solvent removed under vacuum. The product was purified on a silica column with 5 % Et_2O in pentane to give the title compound **29** in 92 % yield (210 mg). The ^1H NMR data were identical to the literature.[43] ^1H NMR (400 MHz, $CDCl_3$) δ 7.33-7.23 (m, 5H), 5.82-5.77 (m, 1H), 5.72-5.64 (m, 2H), 5.26-5.21 (m, 1H), 3.66 (s, 3H), 3.50-3.43 (m, 1H), 3.40 (d, 1H, J = 10.2 Hz), 2.62-2.58 (m, 2H).

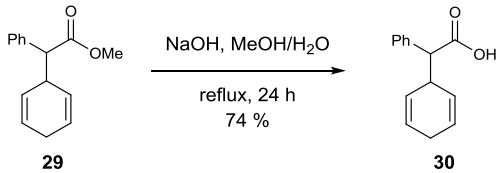

2-(Cyclohexa-2,5-dien-1-yl)-2-phenylacetic acid, 30

Ester **29** (318 mg, 1.3 mmol) and NaOH (210 mg, 5.2 mmol) were combined in 5 mL MeOH and 12 mL H_2O. The solution was heated to reflux for 24 h. The solution was

acidified to approximately pH = 2 using 1N HCl and extracted with EtOAc (5 x 5 mL). The combined organic layers were dried over $MgSO_4$, and the solvent was removed under vacuum to give the title compound **30** in 74 % yield (219 mg). **30** was used without further purification. The ^{1}H NMR data were identical to the literature. ^{1}H NMR (400 MHz, $CDCl_3$): δ = 7.34-7.24 (m, 5H), 5.81-5.75 (m, 1H), 5.68-5.66 (m, 2H), 5.26-5.21 (m, 1H), 3.48-3.38 (m, 2H), 2.61-2.58 (m, 2H).

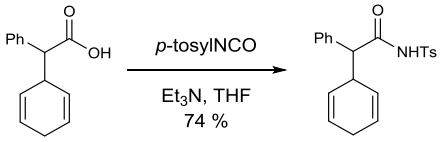

30 **31**

2-(Cyclohexa-2,5-dien-1-yl)-2-phenyl-N-tosylacetamide, 31

Based on a procedure adapted from the literature,[119] acid **30** (219 mg, 0.96 mmol) was added to 5 mL of THF. *p*-Tosyl isocyanate (0.16 mL, 1.06 mmol) was then added, and the reaction mixture was left to stir for 10 min. Et_3N (0.15 mL, 1.06 mmol) was added dropwise, and the reaction was stirred for 1 hour at which point the solution became cloudy. EtOAc (8 mL) was added followed by 1 M HCl (5 mL) and H_2O (5 mL). The aqueous layers were washed with EtOAc (2 x 10 mL), and the combined organic layers were dried over $MgSO_4$. The solvent was removed and the crude tosyl carbamate was purified on a silica column with 30 % EtOAc in hexanes to give the title compound in 74 % yield (270 mg). ^{1}H NMR (400MHz, $CDCl_3$) δ = 8.80 (bs, 1H), 7.73-7.81 (m, 2H), 7.15-7.30 (m, 5H), 7.04-7.13 (m, 2H), 5.68 (ddt, *J* = 8.5, 4.9, 1.7 Hz, 1H), 5.56-5.64 (m, 1H), 5.42-5.50 (m, 1H), 5.15 (ddq, *J* = 10.1, 3.7, 1.9 Hz, 1H), 3.34-3.45 (m, 1H), 3.25 (d,

J = 9.0 Hz, 1H), 2.45-2.56 (m, 2H), 2.43 ppm (s, 3H); ^{13}C NMR (100MHz, $CDCl_3$) δ = 170.1, 145.3, 135.4, 135.2, 129.7, 129.0, 128.9, 128.6, 128.1, 127.1, 126.8, 126.2, 125.6, 59.6, 38.2, 26.4, 21.9; HRMS [- APCI] calculated for $C_{21}H_{20}NO_3S$ 366.11639, found 366.11720 [M-H$^+$].

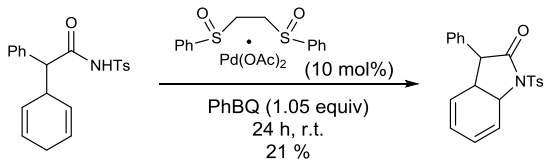

31 **32**

N-tosyl-3-phenyl-3,3a-dihydro-1H-indol-2(7aH)-one, 32

Tosyl amide **31** (36.7 mg, 0.1 mmol), palladium bissulfoxide catalyst (5.0 mg, 0.01 mmol) and phenyl benzoquinone (19.3 mg, 0.105 mmol) were combined, and 0.5 mL of THF was added. The suspension was heated to 45 °C for 20 h. The reaction mixture was filtered through a plug of silica, and the plug was washed twice with DCM (2 mL) and twice with EtOAc (2 mL). The solvent was removed under reduced pressure, and the resulting oil was purified via column chromatography using 20 % EtOAc/hexanes to afford the title compound **32** in 21 % yield (7.5 mg). ^{1}H NMR (600MHz, $CDCl_3$) δ = 7.95-7.99 (m, *J* = 8.6 Hz, 2H), 7.34 (d, *J* = 7.6 Hz, 2 H), 7.21-7.25 (m, 3 H), 7.06-7.11 (m, 2 H), 6.17 (dd, *J* = 9.8, 4.0 Hz, 1 H), 5.92 (dd, *J* = 9.8, 5.5 Hz, 1 H), 5.73 (ddd, *J* = 9.8, 5.5, 1.4 Hz, 1 H), 5.27 (ddd, *J* = 10.0, 3.8, 1.0 Hz, 1 H), 5.15 (ddd, *J* = 10.0, 4.3, 1.4 Hz, 1 H), 3.96 (d, *J* = 9.1 Hz, 1 H), 3.41-3.47 (m, 1 H), 2.44 (s, 3 H).

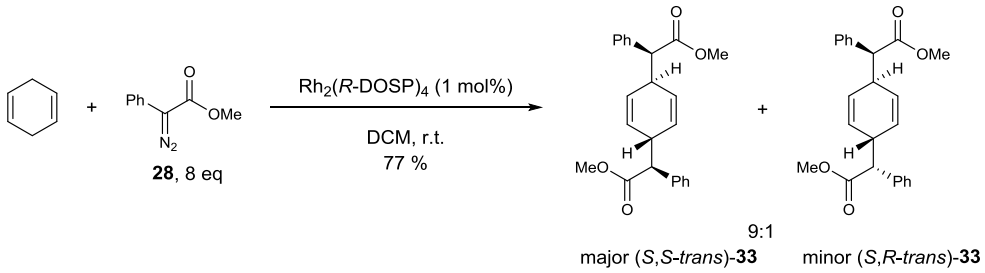

Dimethyl-2,2'-*trans*-cyclohexa-2,5-diene-1,4-diylbis(phenylacetate), 33

DCM (80 mL) added to 1,4-cyclohexadiene (0.23 mL, 2.5 mmol) and Rh_2(*R*-DOSP)$_4$ (47 mg, 0.025 mmol). A solution of diazo **28** (3.52 g, 20 mmol) in 40 mL of DCM was added over 2 hrs via syringe pump. The reaction was left to stir at room temperature overnight. The solution was filtered through a plug of silica and the solvent removed under vacuum. The crude oil was purified on a silica column using 5 % Et_2O in pentane, and the two diastereomers were separated. (724 mg, 77 % combined yield) *S,S-trans* (major diastereomer) white solid, ^{1}H NMR (400MHz, $CDCl_3$) δ = 7.35-7.19 (m, 5 H), 5.79 (d, *J* = 1.2 Hz, 2 H), 5.23 (d, *J* = 0.8 Hz, 2 H), 3.68-3.63 (m, 3 H), 3.42-3.31 (m, 4 H); ^{13}C NMR (100MHz, $CDCl_3$) δ = 173.4, 136.6, 128.8, 128.7, 128.5, 127.7, 127.3, 57.9, 52.2, 39.0; HRMS [+APCI] calculated for $C_{24}H_{25}O_4$ 377.17474, found 377.17456 [$M+H^+$].

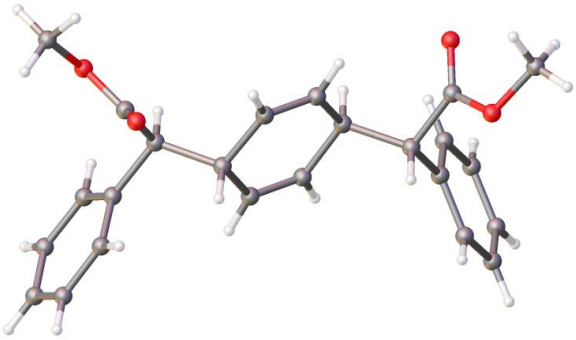

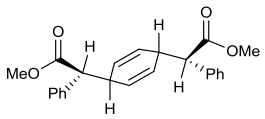

R,S-trans (minor diastereomer) white solid, ^{1}H NMR (400MHz, $CDCl_3$) δ = 7.38-7.21 (m, 5 H), 5.73-5.62 (m, 2 H), 5.41-5.30 (m, 2 H), 3.68-3.61 (m, 3 H), 3.45-3.30 (m, 4 H); ^{13}C NMR (100MHz, $CDCl_3$) δ = 173.4, 136.6, 129.1, 128.9, 128.8, 128.8, 128.6, 128.6, 128.2, 127.7, 127.7, 57.8, 55.1, 52.3, 52.2, 39.0; HRMS [+APCI] calculated for $C_{24}H_{25}O_4$ 377.17474, found 377.17464 [$M+H^+$].

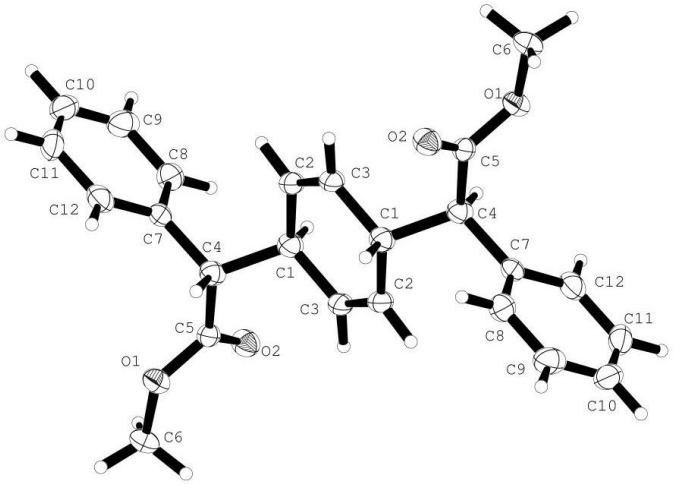

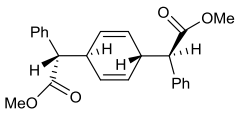

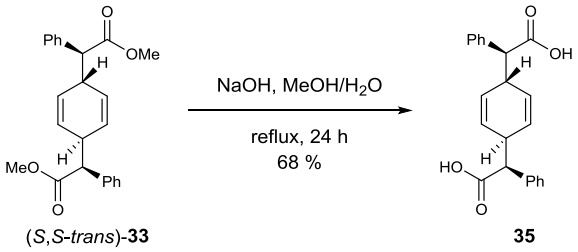

(*S*,*S-trans*)-**33** **35**

(2*S*,2'*S*)-2,2'-((1*S*,4*S*)-cyclohexa-2,5-diene-1,4-diyl)bis(2-phenylacetic acid), 35

Methanol (20 mL) and H_2O (20 mL) were added to diester (*S*,*S-trans*)-**33** (600 mg, 1.59 mmol). NaOH (635 mg, 15.9 mmol) was then added and the reaction mixture was heated to reflux for 24 hours. The solution was acidified to pH = 2 using 1 M HCl,

EtOAc (15 mL) was added, and the layers were separated. The aqueous layer was washed 10 times with EtOAc (10 mL) and 5 times with DCM (10 mL). The combined organic layers were dried over $MgSO_4$ and the solvent removed under reduced pressure to give the title compound **35** as a white solid in 97 % (541 mg) ^{1}H NMR (400MHz, $CDCl_3$) δ = 7.25-7.34 (m, 10 H), 6.06 (s, 2 H), 5.20 (s, 2 H), 3.41-3.50 (m, 2 H), 3.28-3.35 ppm (m, 2 H); ^{13}C NMR (100MHz, $CDCl_3$) δ = 173.9, 137.4, 129.0, 128.9, 128.8, 128.8, 128.7, 128.5, 127.6, 57.3, 38.4; HRMS [-APCI] calculated for $C_{22}H_{19}O_4$ 347.12833, found 347.12875 [M-H$^+$].

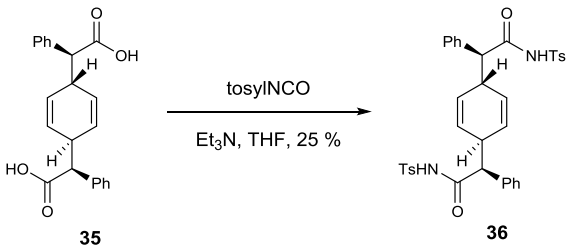

(2*S*,2'*S*)-2,2'-((1*S*,4*S*)-cyclohexa-2,5-diene-1,4-diyl)bis(2-phenyl-N-tosylacetamide), 36

Based on a procedure adapted from the literature,[119] diacid **35** (541 mg, 1.55 mmol) was added to 10 mL of THF. *p*-Tosyl isocyanate (0.52 mL, 3.40 mmol) was then added and the reaction mixture was left to stir for 10 min. Et_3N (0.48 mL, 3.40 mmol) was added dropwise and the reaction stirred for 1 hour at which point the solution became cloudy. Ethyl acetate (8 mL) was added, followed by 1 M HCl (5 mL) and H_2O (5 mL). The aqueous layers were washed with ethyl acetate (2 x 10 mL), and the combined organic layers were dried over $MgSO_4$. The solvent was removed under reduced pressure, and

the crude tosyl carbamate was purified on a silica column with 30 % ethyl acetate in hexanes to give the title compound **36** in 25 % (250 mg). ^{1}H NMR (400MHz, $CDCl_3$) δ = 7.77 (d, *J* = 8.2 Hz, 4 H), 7.36-7.18 (m, 10 H), 6.96 (d, *J* = 7.8 Hz, 4 H), 5.50 (s, 2 H), 5.15 (s, 2 H), 3.23-3.20 (m, 2 H), 3.16-3.12 (m, 2 H), 2.43 (s, 6 H).

6.5 Chapter 4 Procedures and Characterization

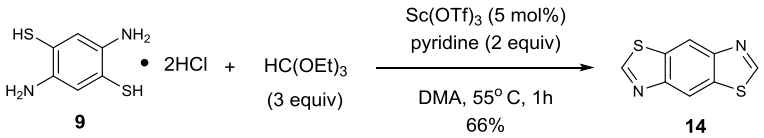

9 14

Benzobisthiazole, 14.

Synthesized according to the literature procedure,[67] 2,5-diamino-1,4-benzenedithiol dihydrochloride (**9**) (1.31 g, 5.37 mmol) and pyridine (0.848 g, 10.74 mmol, 2 equiv) were dissolved into DMA (10 mL). That solution was then added to a mixture of triethyl orthoformate (2.38 g, 16.11 mmol, 3 equiv) and ScOTf (132 mg, 0.0268 mmol, 0.05 equiv). The reaction was heated to 55 °C overnight. After the reaction was cooled to room temperature, H_2O (20 mL) was added to dilute the mixture. The suspension was filtered to give the title compound **14** as an off-white solid in 95 % yield (990 mg). Its NMR data were in good agreement with the literature. ^{1}H NMR (400MHz, D6-DMSO) δ = 9.45 (s, 2H), 8.88 (s, 2H). ^{13}C NMR (100MHz, D6-DMSO) δ = 158.6, 151.9, 133.4, 117.0 ppm.

General procedure for the reaction of benzobisthiazole (14) with bromobenzene for GC assay.

Benzobisthiazole (**14**) (58 mg, 0.3 mmol), bromobenzene (188 mg, 1.2 mmol, 4 equiv), $Cu(OAc)_2$ (10.9 mg, 0.06 mmol, 0.2 equiv), K_2CO_3 (82.8 mg, 0.6 mmol, 2.0 equiv), PPh_3 (39.3 mg, 0.15 mmol, 0.5 equiv), and anthracene (53 mg, 0.3 mmol, 1 equiv) were added

to a 7 mL vial and purged with nitrogen. $Pd(OAc)_2$ (0.67 mg, 0.003 mmol, 1 mol%) was added as a solution in DMF. Dry DMF was then added to bring the total volume of DMF to 1 mL. The reaction was heated to the desired temperature under a balloon of nitrogen. Once the reaction had been up to heat for 30 minutes an aliquot was taken every hour until conversion to product was complete. The aliquots were filtered through celite, washed with DCM and MeOH and analyzed via GC with anthracene as an internal standard.

GC Assay Parameters and Retention Times

JW column (initial 40 ^{o}C 2 min, ramp 15 ^{o}C per min to 300 ^{o}C, hold 10 min)

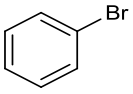

bromobenzene, retention time 3.97 min

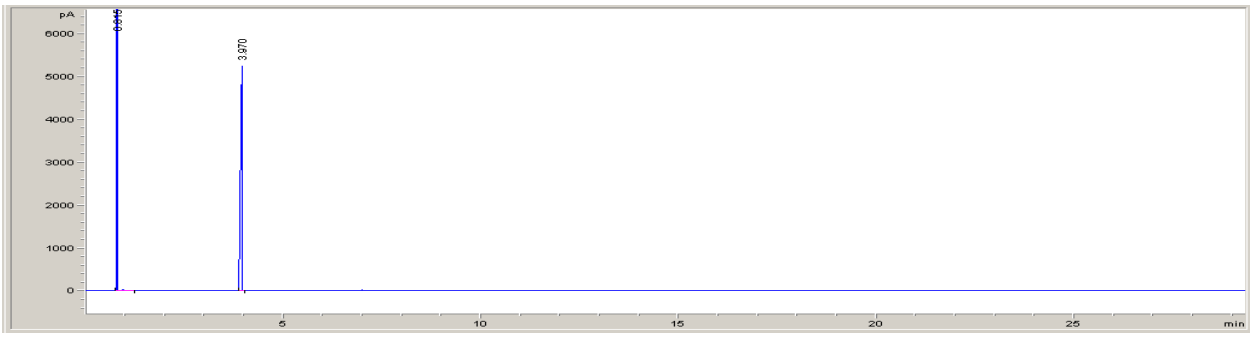

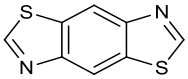

benzobisthiazole (14), retention time 19.3 min

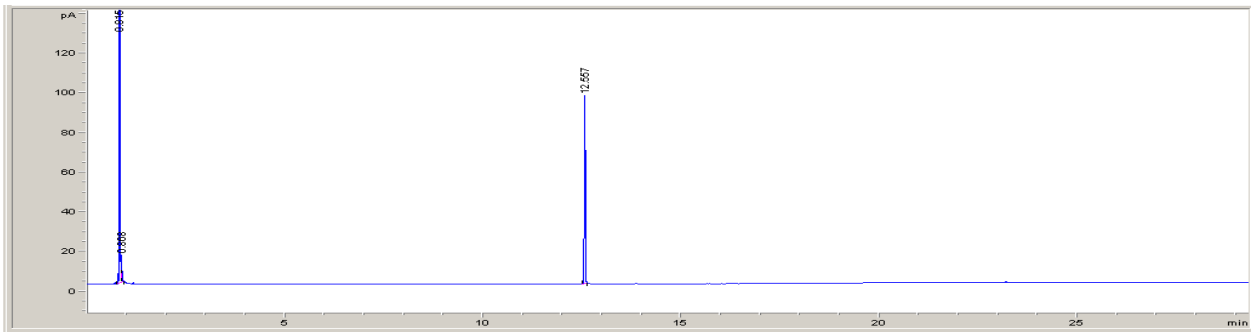

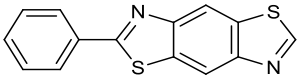

2-phenylbenzobisthiazole (21), retention time 17.7 min

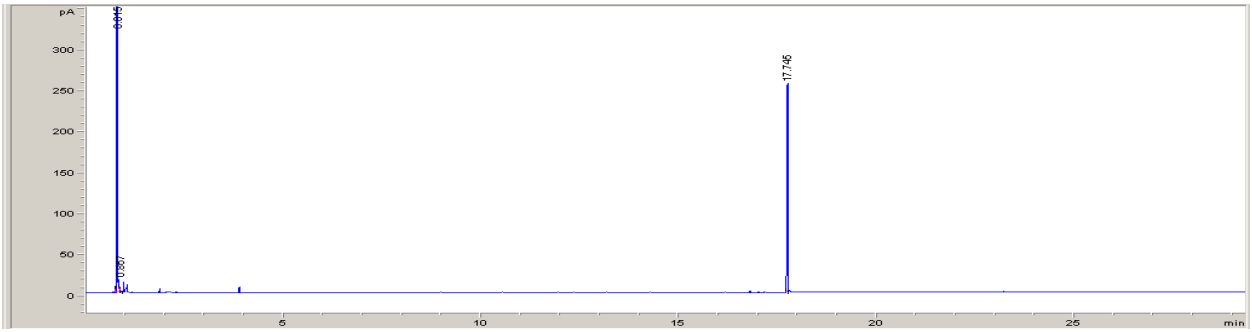

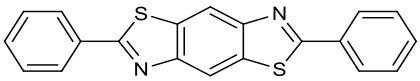

2,6-diphenylbenzobisthiazole (20), retention time 23.2 min (shown doped with anthracene)

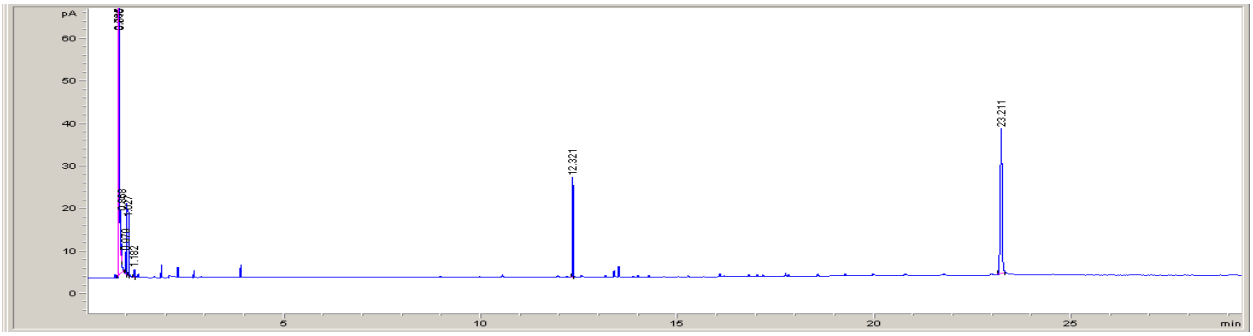

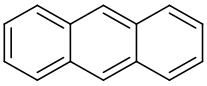

anthracene, retention time 12.36 min

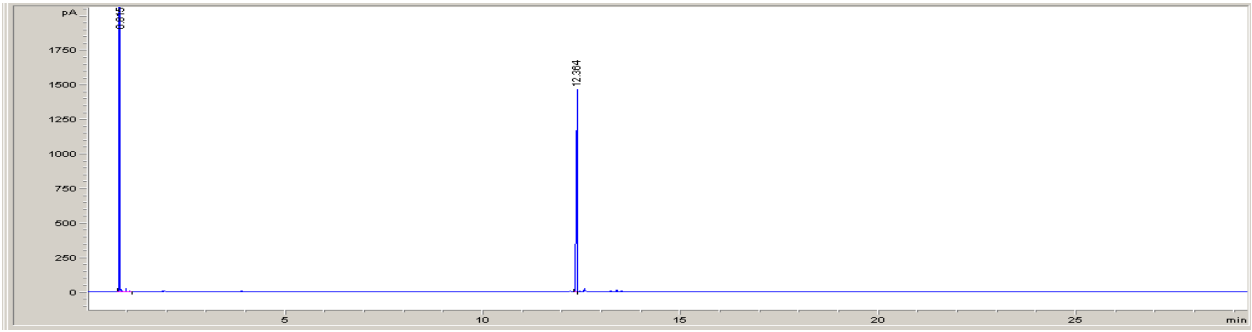

General method A for the synthesis of substituted benzobisthiazoles.

Benzobisthiazole (192 mg, 1.0 mmol), ArBr (4.0 mmol, 4 equiv), $Pd(OAc)_2$ (2.2 mg, 0.01 mmol), $Cu(OAc)_2$ (36 mg, 0.20 mmol, 20 mol%), K_2CO_3 (276 mg, 2.0 mmol, 2.0 equiv), and PPh_3 (131 mg, 0.5 mmol, 0.5 equiv) were combined in an oven dried flask and purged with nitrogen. DMF (3 mL) was added, and the reaction was heated to 135 °C until the starting material was consumed, as indicated by TLC analysis. The reaction

mixture was filtered; the filtrate was washed with water (20 mL) and the aqueous layer extracted with CH_2Cl_2 (10 mL). The organic layers were combined, washed with aqueous copper sulfate and brine, dried over $MgSO_4$ and concentrated under reduced pressure. The title compounds were purified by flash chromatography on silica gel.

General method B for the synthesis of substituted benzobisthiazoles.

Benzobisthiazole (192 mg, 1.0 mmol), ArBr (4.0 mmol, 4 equiv), $Pd(OAc)_2$ (2.2 mg, 0.01 mmol), $Cu(OAc)_2$ (36 mg, 0.20 mmol, 20 mol%), K_2CO_3 (276 mg, 2.0 mmol, 2.0 equiv), and PPh_3 (131 mg, 0.5 mmol, 0.5 equiv) were combined in an oven dried flask and purged with nitrogen. DMF (3 mL) was added, and the reaction was heated to 135 °C until the starting material was consumed, as indicated by TLC analysis. The reaction mixture was filtered and the filter cake washed with water (20 mL). The solid was dried under vacuum to give the title compound.

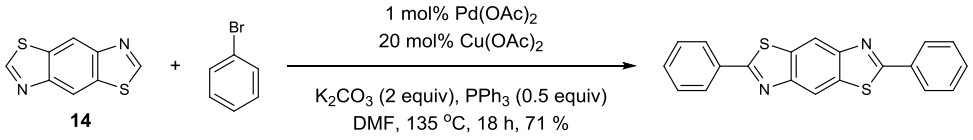

14

2,6-diphenylbenzobisthiazole, 20 (Table 4.1, entry 1)

General method A with bromobenzene (628 mg, 4.0 mmol) provided after chromatography (R_f = 0.2; 15 % hexanes in EtOAc) the title compound as an amorphous yellow powder (244 mg, 71 %). Its spectroscopic data were in good agreement with the literature.[120] ^{1}H NMR (400 MHz, $CDCl_3$) δ = 8.55 (s, 2H), 8.01-8.13 (m, 4H), 7.51-7.52

(m, 6H); ^{13}C NMR (100 MHz, $CDCl_3$) δ = 169.2, 152.4, 134.7, 133.7, 131.5, 129.3, 127.0, 115.7; HRMS [+APCI] calculated 345.0516, found 345.0514 [M+H$^+$].

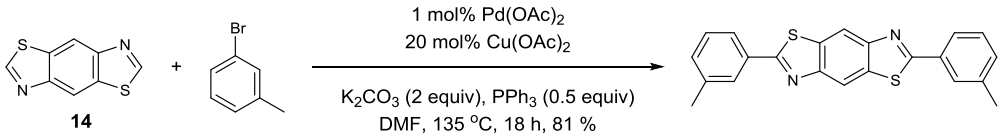

2,6-di-*m*-tolylbenzobisthiazole (Table 4.1, entry 2)

General method B with 1-bromo-3-methylbenzene (684 mg, 4.0 mmol) provided the title compound as an amorphous yellow powder (301 mg, 81 %). Its spectroscopic data were in good agreement with the literature.[121] ^{1}H NMR (400 MHz, $CDCl_3$) δ = 8.54 (s, 2H), 7.95 (s, 2H), 7.89 (d, *J* = 7.8 Hz, 2H), 7.40 (t, *J* = 7.4 Hz, 2H), 7.32 (d, *J* = 7.8 Hz, 2H), 2.46 (s, 6H); HRMS [+APCI] calculated 373.0828, found 373.0825 [M+H$^+$]; IR (thin film, cm^{-1}) ν = 3358, 1624, 1560, 1395, 1308.

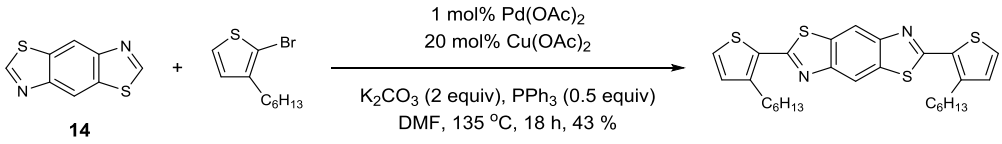

2,6-bis(3-hexylthiophen-2-yl)benzobisthiazole (Table 4.1, entry 3)

General method A with 2-bromo-3-hexylthiophene (988mg, 4.0 mmol) provided after chromatography (R_f = 0.4; 10 % hexanes in EtOAc) the title compound as an amorphous pale green powder (225 mg, 43 %). Its spectroscopic data were in good agreement with the literature.[60] ^{1}H NMR (400 MHz, $CDCl_3$) δ = 8.58 (s, 2H), 7.41 (d, *J* = 5.1, 2H), 7.01

(d, *J* = 5.1, 2H), 3.06 (t, *J* = 7.8, 4H), 1.73 (p, *J* = 7.0, 4H), 1.46 (p, *J* = 7.0, 4H), 1.36-1.29 (m, 8H), 0.89 (t, *J* = 7.0, 6H).

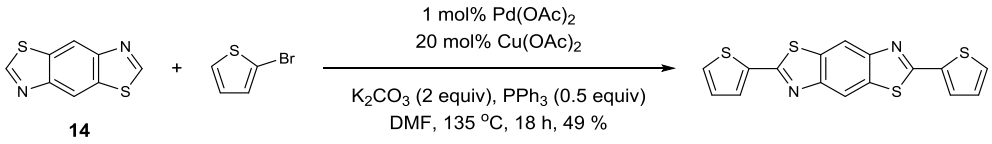

2,6-di(thiophen-2-yl)benzobisthiazole (Table 4.1, entry 4)

General method A with 2-bromothiophene (652 mg, 4.0 mmol) provided after chromatography (R_f = 0.2; 10 % hexanes in EtOAc) the title compound as an amorphous pale green powder (173 mg, 49 %). Its spectroscopic data were in good agreement with the literature.[66] ^{1}H NMR (400 MHz, $CDCl_3$) δ = 8.66 (s, 2H), 8.01 (d, *J* = 3.1, 2H), 7.59 (d, *J* = 3.1, 2H), 7.25 (m, 2H).

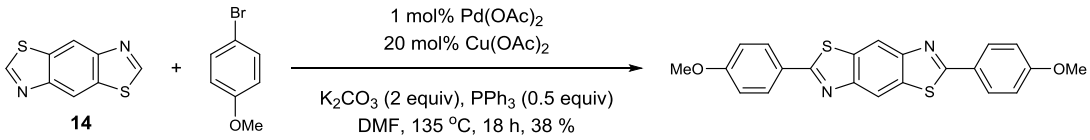

2,6-bis(4-methoxyphenyl)benzobisthiazole (Table 4.1, entry 5)

General method A with 1-bromo-4-methoxybenzene (748 mg, 4.0 mmol) provided after chromatography (R_f = 0.1; 10 % hexanes in EtOAc) the title compound as an amorphous green powder (153 mg, 38 %). Its spectroscopic data were in good agreement with the literature.[122] ^{1}H NMR (400 MHz, $CDCl_3$) δ = 8.57 (s, 2H), 8.06 (d, *J* = 8.6, 4H), 7.02 (d, *J* = 8.6, 4H), 3.89 (s, 3H).

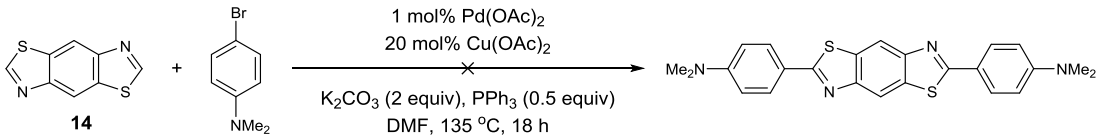

4,4'-(benzobisthiazole-2,6-diyl)bis(*N*,*N*-dimethylaniline) (Table 4.1, entry 6)

General method A was attempted with 1-bromo-4-*N*,*N*-dimethylaniline (800 mg, 4.0 mmol) however none of the title compound was observed by crude ^{1}H NMR or HRMS.

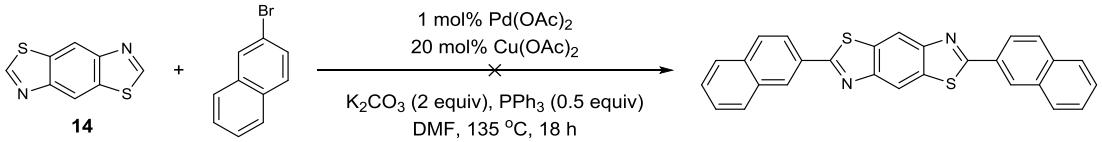

2,6-di(naphthalen-2-yl)benzobisthiazole (Table 4.1, entry 7)

General method A was attempted with 2-bromonaphthalene (820 mg, 4.0 mmol) however none of the title compound was observed by crude ^{1}H NMR or HRMS.

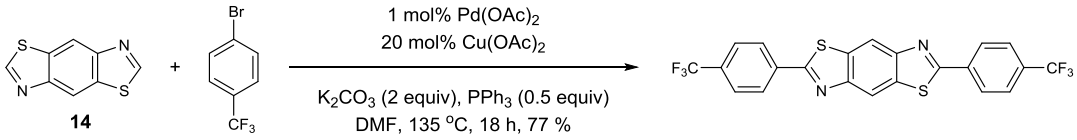

2,6-bis(4-(trifluoromethyl)phenyl)benzobisthiazole (Table 4.1, entry 8)

Method B with 1-bromo-4-(trifluoromethyl)benzene (896 mg, 4.0 mmol) provided the desired compound as an amorphous pale green powder in 77 % yield (370 mg) from the filtrate. ^{1}H NMR (400 MHz, $CDCl_3$) δ = 8.62 (s, 2H), 8.24 (d, *J* = 8.2 Hz, 4 H), 7.78 (d, *J* = 8.2 Hz, 4 H); ^{13}C NMR (600 MHz, solid state) δ = 170.2, 156.3, 155.4, 137.7, 136.7,

129.4, 127.2, 119.0, 118.1; HRMS [+APCI] calculated for $C_{22}H_{11}N_2F_6S_2$ 481.0262, found 481.0273 [M+H$^+$]; IR (thin film, cm^{-1}) ν =1568, 1408, 1323, 1170, 1131.

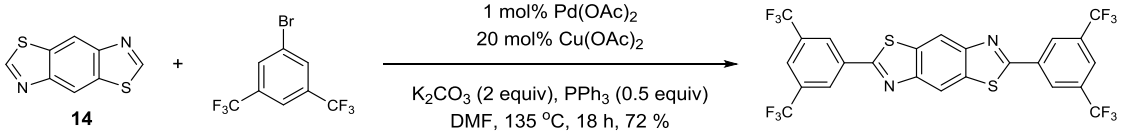

2,6-bis(3,5-bis(trifluoromethyl)phenyl)benzobisthiazole (Table 4.1, entry 9)

Method B with 1-bromo-3,5-bis(trifluoromethyl)benzene (1172 mg, 4.0 mmol) provided the desired compound as an amorphous yellow-green powder in 72 % yield (443 mg) from the filtrate. ^{1}H NMR (400 MHz, $CDCl_3$) δ = 8.67 (s, 2H), 8.56 (s, 4H), 8.02 (s, 2H); ^{13}C NMR (600 MHz, solid state) δ = 162.6, 150.9, 134.1, 132.4, 131.3, 126.8, 122.4, 122.4, 117.1; HRMS [+APCI] calculated for $C_{24}H_9N_2F_6S_2$ 617.0018, found 617.0010 [M+H$^+$]; IR (thin film, cm^{-1}) ν = 3351, 1556, 1621, 1370, 1282, 1124.

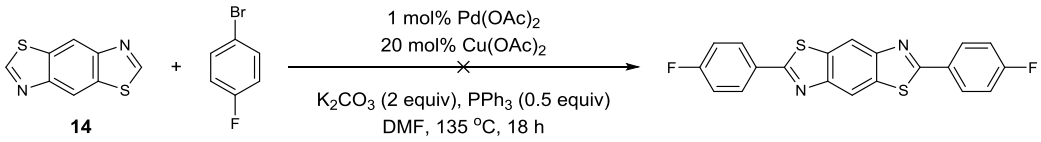

2,6-bis(4-fluorophenyl)benzobisthiazole (Table 4.1, entry 10)

General methods A and B were both attempted with 1-bromo-4-fluorobenzene (690 mg, 4.0 mmol). None of the title compound was observed by crude ^{1}H NMR or HRMS.

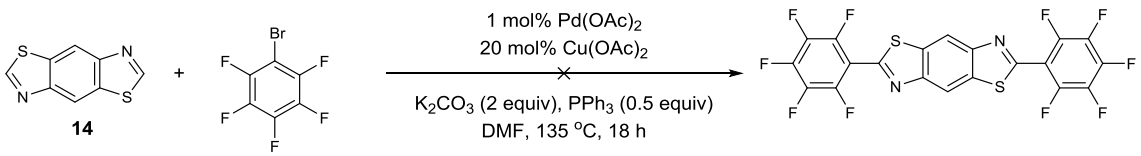

14

2,6-bis(perfluorophenyl)benzobisthiazole (Table 4.1, entry 11)

General methods A and B were both attempted with 1-bromo-2,3,4,5,6-pentafluorobenzene (980 mg, 4.0 mmol). None of the title compound was observed by crude ^{1}H NMR or HRMS.

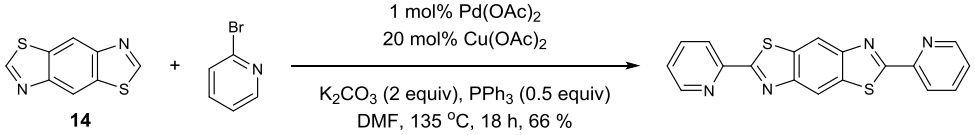

14

2,6-di(pyridin-2-yl)benzobisthiazole (Table 4.1, entry 12)

General method A with 2-bromopyridine (632 mg, 4.0 mmol) provided after chromatography (R_f = 0.2; 1 % DCM in EtOAc) the title compound as an amorphous yellow-green powder (228 mg, 66 %). Its spectroscopic data were in good agreement with the literature.[123] ^{1}H NMR (400 MHz, DMSO-*d6*, 40 °C) δ = 8.88 (s, 2H), 8.74 (d, *J* = 3.9 Hz, 2H), 8.37 (d, *J* = 7.1 Hz, 2H), 8.05 (dd, *J* = 5.9, 2.0 Hz, 2 H), 7.60 (m, 2 H); ^{13}C NMR (600 MHz, solid state) δ = 170.0, 152.4, 151.8, 146.6, 138.1, 135.8, 124.9, 121.8, 116.3; HRMS [+APCI] calculated for $C_{18}H_{13}N_4S_2$ 347.0420, found 347.0417 [M+H$^+$]; IR (thin film, cm^{-1}) ν = 3349, 1559, 1453, 1397, 1315.

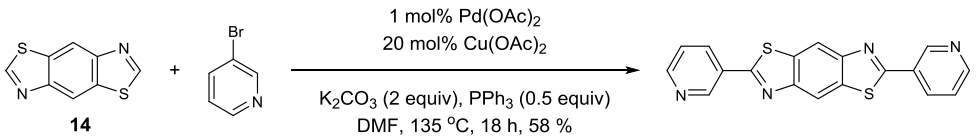

2,6-di(pyridin-3-yl)benzobis(thiazole) (Table 4.1, entry 13)

Method B with 3-bromopyridine (632 mg, 4.0 mmol) provided the desired compound as an amorphous yellow-green powder in 58 % yield (200 mg) from the filtrate. ^{1}H NMR (400 MHz, $CDCl_3$) δ = 9.31 (s, 2H), 8.73 (d, *J* = 4.7 Hz, 2H), 8.64 (s, 2 H), 8.40 (d, *J* = 8.6 Hz, 2H), 7.46 (dd, *J* = 8.2, 5.9 Hz, 2 H); ^{13}C NMR (600 MHz, solid state) δ = 171.2, 162.9, 155.8, 150.2, 139.7, 137.7, 132.5, 124.5, 120.0; HRMS [+APCI] calculated for $C_{18}H_{11}N_4S_2$ 347.0425, found 347.0421 [$M+H^+$]; IR (thin film, cm^{-1}) ν = 3231, 1659, 1573, 1424, 1393, 1307.

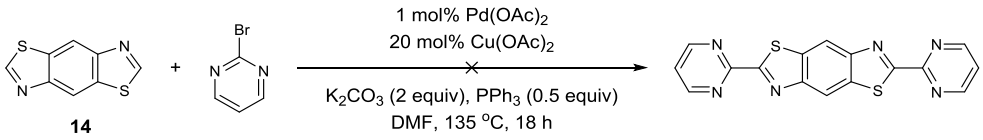

2,6-di(pyrimidin-2-yl)benzobisthiazole (Table 4.1, entry 14)

General methods A and B were both attempted with 2-bromopyrimidine (632 mg, 4.0 mmol). None of the title compound was observed by crude ^{1}H NMR or HRMS.

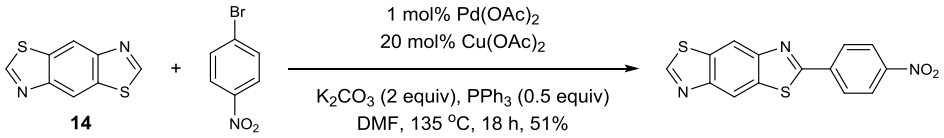

2-(4-nitrophenyl)benzobis(thiazole) (Table 4.1, entry 15)

Method B with 1-bromo-4-nitrobenzene (804 mg, 4.0 mmol) provided the monofunctionalized product as an amorphous yellow-green powder in 51 % yield (159 mg) from the filtrate. ^{1}H NMR (400 MHz, $CDCl_3$) δ = 9.06 (s, 1H), 8.71 (d, *J* = 4.8 Hz, 1H), 8.69 (s, 1H), 8.64 (s, 1H), 8.40 (d, *J* = 7.6 Hz, 1H), 7.88 (dt, *J* = 8.0, 2.0 Hz, 1 H), 7.42 (ddd, *J* = 7.6, 4.8, 1.2 Hz, 1 H); ^{13}C NMR (600 MHz, solid state) δ = 167.29, 152.6, 154.5, 150.0, 140.0, 136.6, 134.2, 128.5, 126.0, 117.8; HRMS [+APCI] calculated for $C_{14}H_8N_3O_2S_2$ 314.0053, found 314.0052 [$M+H^+$]; IR (thin film, cm^{-1}) ν = 3094, 1594, 1514, 1342, 1313.

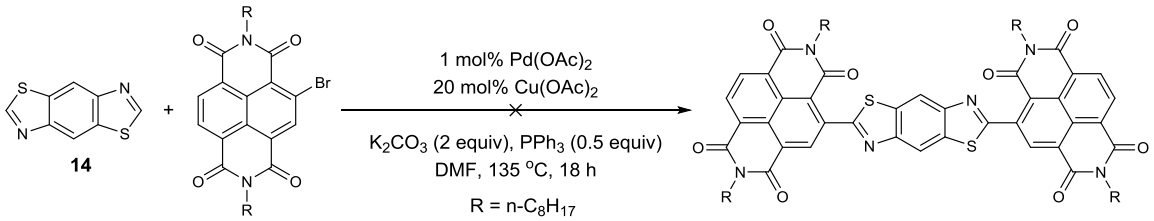

4,4'-(benzobisthiazole-2,6-diyl)bis(2,7-dioctylbenzo[lmn][3,8]phenanthroline-1,3,6,8(2*H*,7*H*)-tetraone) (Table 4.2, entry 1)

General methods A and B were both attempted on 1/8 the normal scale with bromonaphthalenediimide (290 mg, 0.5 mmol). None of the title compound was observed by crude ^{1}H NMR or HRMS.

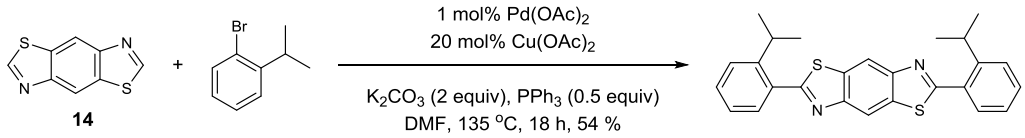

2,6-bis(2-isopropylphenyl)benzobisthiazole (Table 4.2, entry 2)

General method B with 1-bromo-2-isopropylbenzene (796 mg, 4.0 mmol) provided the title compound as an amorphous yellow-green powder (229 mg, 54 %). Its ^{1}H NMR data were in good agreement with the literature.[121] ^{1}H NMR (400 MHz, $CDCl_3$) δ = 8.70 (s, 2 H), 7.68-7.63 (m, 2 H), 7.53-7.44 (m, 6 H), 3.74 (m, 2 H), 1.30-1.23 (m, 12H).

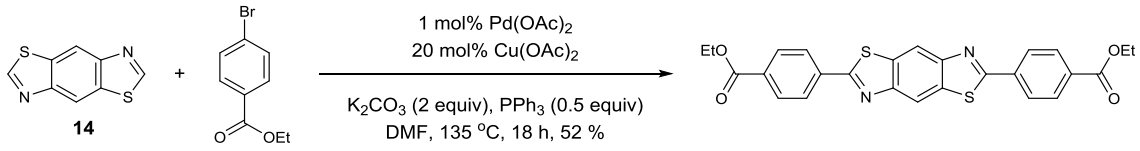

diethyl 4,4'-(benzobisthiazole-2,6-diyl)dibenzoate (Table 4.2, entry 3)

Method B with ethyl 4-bromobenzoate (912 mg, 4.0 mmol) provided the desired compound as an amorphous yellow-green powder in 52 % yield (253 mg) after purification of the organic layer by flash chromatography (2:3 EtOAc/DCM). ^{1}H NMR (400 MHz, $CDCl_3$) δ = 8.60 (s, 1H), 8.18 (bs, 8H), 4.41 (q, *J* = 7.4 Hz, 4 H), 1.42 (t, *J* = 7.4 Hz, 6 H); ^{13}C NMR (600 MHz, solid state) δ = 165.8, 163.6, 155.2, 152.2, 151.0, 135.5, 132.3, 130.6, 128.1, 122.4, 115.1, 62.9, 61.1, 17.0, 15.7, 14.2; HRMS [+APCI] calculated for $C_{26}H_{21}N_2O_4S_2$ 489.0937, found 489.0943 [$M+H^+$]; IR (thin film, cm^{-1}) ν = 1710, 1512, 1406, 1270.

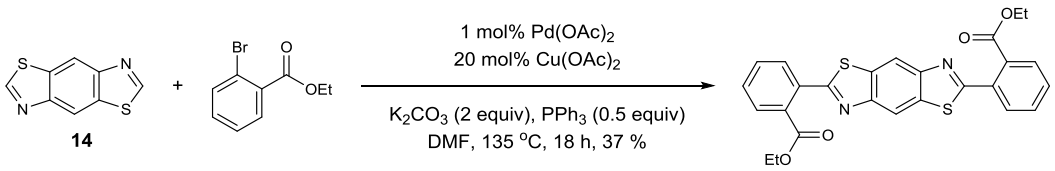

Diethyl 2,2'-(benzobisthiazole-2,6-diyl)dibenzoate (Table 4.2, entry 4)

Method B with ethyl 2-bromobenzoate (912 mg, 4.0 mmol) provided the desired compound as an amorphous yellow powder in 37 % yield (180 mg) after purification of the organic layer by flash chromatography (2:3 EtOAc/DCM). ^{1}H NMR (400 MHz, $CDCl_3$) δ = 8.58 (s, 2H), 7.88 (dd, *J* = 7.0, 1.2 Hz, 2 H), 7.76 (dd, *J* = 7.0, 1.6 Hz, 2 H), 7.65-7.57 (m, 4 H), 4.25 (q, *J* = 7.0 Hz, 4 H), 1.09 (t, *J* = 7.0 Hz, 6 H); ^{13}C NMR (600 MHz, solid state) δ = 170.1, 165.7, 160.3, 155.2, 150.5, 132.3, 128.2, 116.4, 113.5, 61.9, 14.8; HRMS [+APCI] calculated for $C_{26}H_{21}N_2O_4S_2$ 489.0937, found 489.0942 [$M+H^+$]; IR (thin film, cm^{-1}) ν = 3367, 1626, 1594, 1550, 1392.

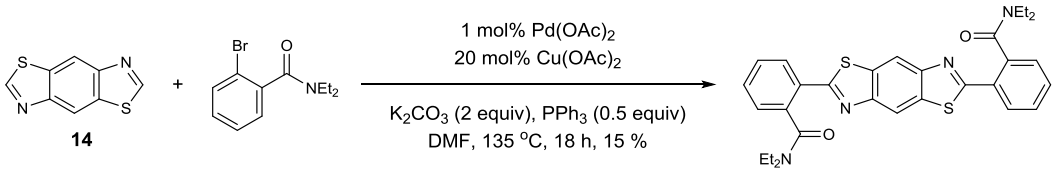

2,2'-(benzobisthiazole-2,6-diyl)bis(N,N-diethylbenzamide) (Table 4.2, entry 5)

Method B with 2-bromo-*N*,*N*-diethylbenzamide (1020 mg, 4.0 mmol) provided the desired compound as an amorphous yellow powder in 15 % yield (80 mg) after purification of the organic layer by flash chromatography (1:1 EtOAc/DCM). ^{1}H NMR (400 MHz, $CDCl_3$) δ = 8.46 (s, 2 H), 7.95 (d, 2 H, *J* = 6.3), 7.53-7.50 (m, 4 H), 7.40-7.38 (m, 2 H), 3.91-3.80 (m, 2H), 3.41-3.30 (m, 2H), 3.21-3.10 (m, 4H), 1.32 (t, *J* = 7.0 Hz, 6 H), 0.97 (t, *J* = 7.0 Hz, 6 H); ^{13}C NMR (600 MHz, solid state) δ = 170.4, 167.7, 165.9, 160.2, 154.4, 153.0, 150.5, 139.0, 137.5, 134.7, 132.8, 130.1, 128.5, 125.8, 114.6, 44.2,

40.3, 14.5, 12.9; HRMS [+APCI] calculated for $C_{30}H_{31}N_4O_2S_2$ 543.1883, found 543.1885 [$M+H^+$]; IR (thin film, cm^{-1}) ν = 1631, 1427, 1310, 1221, 768.

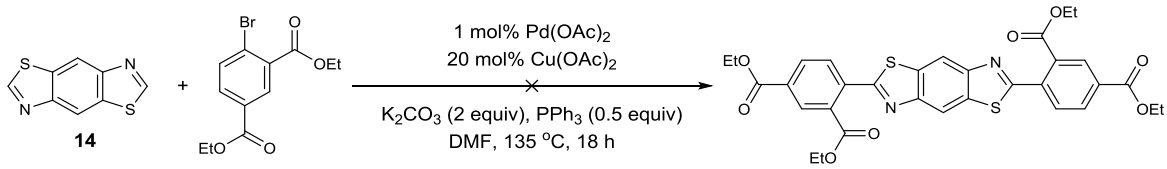

tetraethyl 4,4'-(benzobisthiazole-2,6-diyl)diisophthalate (Table 4.2, entry 6)

General methods A and B were both attempted with diethyl 4-bromoisophthalate (1.20 g, 4.0 mmol). None of the title compound was observed by crude ^{1}H NMR or HRMS.

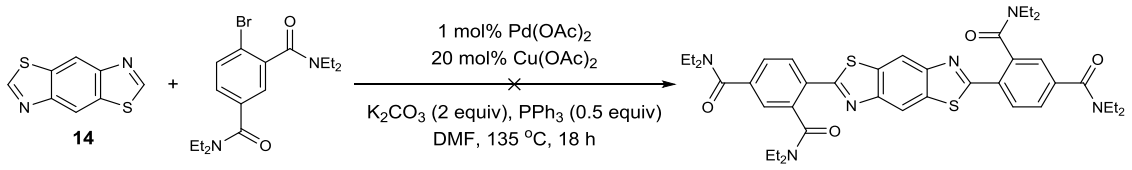

4,4'-(benzobisthiazole-2,6-diyl)bis(*N*^{1},*N*^{1},*N*^{3},*N*^{3}-tetraethylisophthalamide) (Table 4.2, entry 7)

General methods A and B were both attempted with 4-bromo-*N*^{1},*N*^{1},*N*^{3},*N*^{3}-tetraethylisophthalamide (1.42 g, 4.0 mmol). None of the title compound was observed by crude ^{1}H NMR or HRMS.

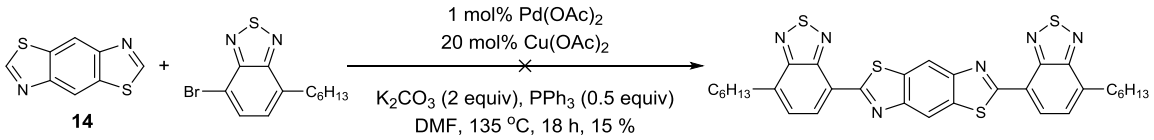

2,6-bis(7-hexylbenzothiadiazol-4-yl)benzobis(thiazole) (Table 4.2, entry 8)

General methods A and B were both attempted at ½ the normal scale with 4-bromo-7-hexylbenzothiadiazole (598 mg, 2.0 mmol). None of the title compound was observed by crude ^{1}H NMR or HRMS.

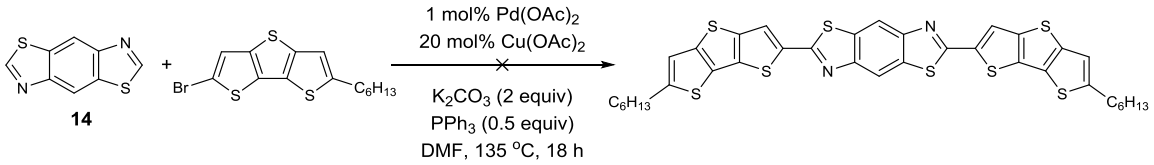

2,6-bis(6-hexyldithienothiophen-2-yl)benzobisthiazole (Table 4.2, entry 9)

General methods A and B were both attempted with 2-bromo-6-hexyldithienothiophene (1.44 g, 4.0 mmol). None of the title compound was observed by crude ^{1}H NMR or HRMS.

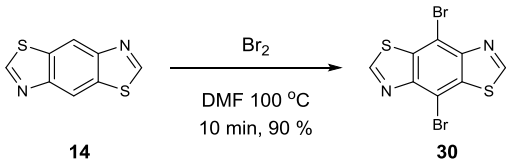

4,8-dibromobenzobisthiazole, **30**

Benzobisthiazole (**14**) (100 mg, 0.53 mmol) and Br_2 (0.4 mL) were combined in anhydrous DMF (2 mL). The reaction vial was put in an oil bath preheated to 100 °C. After 10 minutes, the reaction mixture was cooled to room temperature then poured into a

saturated aqueous solution of $NaHSO_4$. An off-white solid precipitated out and was isolated by filtration to give title compound **30** as an amorphous tan powder (183 mg, 90 %). ^{1}H NMR (400 MHz, DMSO-*d6*) δ = 9.63; ^{13}C NMR (600 MHz, solid state) δ = 159.6, 148.1, 133.1, 113.5; HRMS [+APCI] calculated for $C_8H_3N_2S_2Br_2$ 348.8098, found 348.8099 [$M+H^+$]; IR (thin film, cm^{-1}) ν = 3392, 1649, 1471, 1417, 1389.

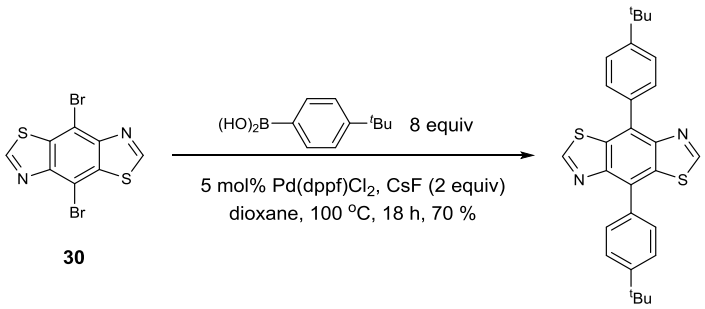

30 **34**

4,8-bis(4-(tert-butyl)phenyl)benzobisthiazole, 34

Dibromobenzobisthiazole **30** (400 mg, 1.14 mmol) was combined with (4-(tert-butyl)phenyl)boronic acid (203 mg, 4.57 mmol, 4 equiv), $Pd(dppf)Cl_2$ (41 mg, 0.057 mmol, 5 mol %), and CsF (347 mg, 2.28 mmol, 2 equiv) in anhydrous dioxane (26 mL). The mixture was heated to reflux and additional 203 mg portions of boronic acid were added every two hours until a total of 1.62 g had been added. The reaction remained at reflux for an additional 12 hours (a total of 18 hours). After the reaction was cooled to room temperature, 10 mL H_2O was added and an off white precipitate formed. The solid was isolated by filtration and purified by column chromatography (5 % EtOAc/hexanes) to afford 365 mg (70 %) of title compound **34** as an amorphous yellow solid. ^{1}H NMR (400MHz, $CDCl_3$) δ = 9.06 (s, 2H), 7.78 (d, *J* = 8.4 Hz, 4H), 7.59 (d, *J* = 8.4 Hz, 4H), 1.40 (s, 18H); ^{13}C NMR (400MHz, $CDCl_3$) δ = 155.8, 151.7, 149.2, 135.3,

134.9, 129.6, 129.3, 126.0, 35.0, 31.6; HRMS [+APCI] calculated for $C_{28}H_{29}N_2S_2$ 269.0202, found 269.0200 [$M+H^+$]; IR (thin film, cm^{-1}) ν = 3026, 2950, 1450, 846.

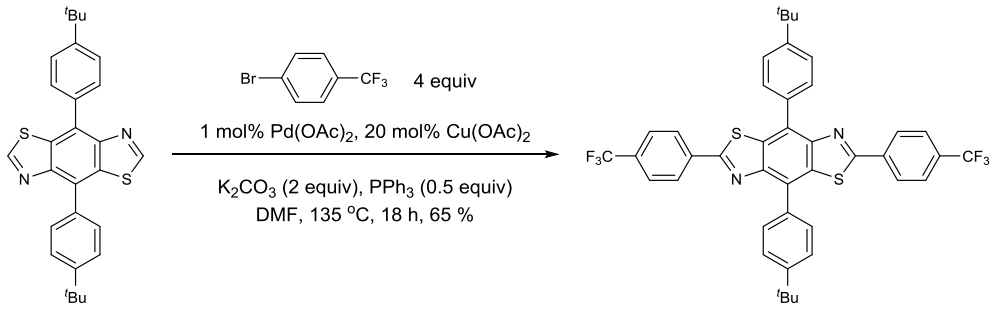

34 **35**

4,8-bis(4-(tert-butyl)phenyl)-2,6-bis(4-(trifluoromethyl)phenyl)benzobisthiazole, **35**

4,8-Bis(4-(tert-butyl)phenyl)benzobis(thiazole) **34** (170 mg, 0.38 mmol), 1-bromo-4-(trifluoromethyl)benzene (375 mg, 0.23 mL, 1.66 mmol, 4 equiv), $Cu(OAc)_2$ (15 mg, 0.08 mmol, 20 mol%), K_2CO_3 (115 mg, 0.83 mmol, 2.0 equiv), and PPh_3 (54.6 mg, 0.21 mmol, 0.5 equiv) were combined in an oven dry flask and purged with nitrogen. $Pd(OAc)_2$ (0.93 mg, 1 mol %) was added as a solution in DMF. Additional DMF was added to bring the total volume of solvent to 2 mL and the reaction was heated to 115 °C until the reaction was complete. After the reaction had cooled to room temperature, H_2O (4 mL) was added and a yellow solid precipitated out. The solid was isolated by filtration and purified by column chromatography (5% EtOAc in hexanes) to give the title compound **35** as an amorphous yellow solid in 65 % yield (180 mg). ^1H NMR (400MHz, $CDCl_3$) δ = 8.18 (d, *J* = 7.6 Hz, 4H), 7.93 (d, *J* = 8.4 Hz, 4H), 7.70 (d, *J* = 7.6 Hz, 4H), 7.62 (d, *J* = 7.6 Hz, 4H), 1.45 (s, 18H); ^{13}C NMR (600 MHz, solid state) δ = 166.3, 152.6, 149.6, 136.8, 134.9, 131.9, 130.4, 129.0, 126.6, 125.2, 35.5, 32.0; HRMS

[+APCI] calculated for $C_{42}H_{35}F_6N_2S_2$ 745.2140, found 745.2150 [$M+H^+$]; IR (thin film, cm^{-1}) ν = 2962, 1320, 1126, 1067.

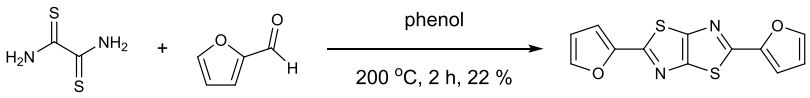

2,5-di(furan-2-yl)thiazolo[5,4-d]thiazole

Dithiooxamide (25 g, 208 mmol) and phenol (75 g, 797 mmol, 3.8 equiv) were added to freshly distilled furfural (250 g, 2.6 mol, 12.5 equiv) and heated to 200 °C in a heating mantle for 2 hours. The reaction was left to stand at room temperature overnight. The reaction was filtered and washed with EtOH (50 mL), Et_2O (50 mL) and hexane (50 mL). The title compound was purified by recrystallization from $CHCl_3$ (1 L) to give a gold powder (12.7 g, 22 %). Its ^{1}H NMR data were identical to the literature.[124] ^{1}H NMR (400MHz, $CDCl_3$) δ = 7.54 (d, *J* = 0.8 Hz, 2H), 7.07 (d, *J* = 2.4 Hz, 2H), 6.57 (dd, *J* = 0.8, 2.0 Hz, 2H).

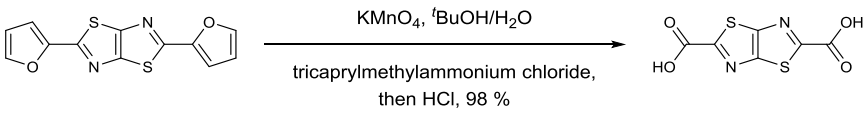

thiazolothiazole-2,5-dicarboxylic acid

The difuran was suspended in 200 mL ^{t}BuOH and brought to reflux (82 °C). The heat was removed, and 50 mL H_2O was added. $KMnO_4$ was added portion-wise to maintain an internal reaction temperature of 70 °C. The reaction became a brown sludge so

100 mL H_2O was added to break up the reaction mixture. Tricaprylmethylammonium chloride (Aliquot 128, 0.88g, 2.3 mL) was added when half the $KMnO_4$ had been added. The reaction was left to stir at room temperature overnight after which it was filtered and the brown solid suspended in aqueous $NaHSO_3$ (400 mL). The suspension was stirred for 30 minutes and during which the solid turned white. The resulting white solid was isolated by filtration and suspended in 150 mL H_2O. After cooling to 0 °C, the suspension was acidified to pH = 0 with concentrated HCl and stirred for another 30 minutes. The title compound was isolated by filtration (4.05 g, 98 %). Its HRMS was in good agreement with the literature.[124] HRMS [-NSI] calculated for $C_6HO_4N_2S_2$ 228.93832, found 228.93830 [$M-H^+$] and 458.88377 [$2M-H^+$].

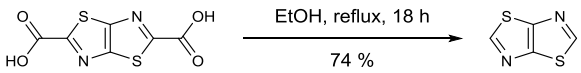

Thiazolothiazole, 43

Thiazolothiazole-2,5-dicarboxylic acid was suspended in EtOH (200 mL) and heated to reflux (80 °C). The reaction was complete after 18 hours by TLC analysis (1:1 DCM/MeOH, R_f = 0.8). The reaction was cooled to room temperature and the solvent removed under reduced pressure. The residue was dissolved into DCM (60 mL), passed through a plug of silica and the DCM removed to give title compound **38** as an off-white solid in 74 % yield (1.58 g). Its ^{1}H NMR data were identical to the literature.[124] ^{1}H NMR (400MHz, $CDCl_3$) δ = 8.92 (s, 2H).

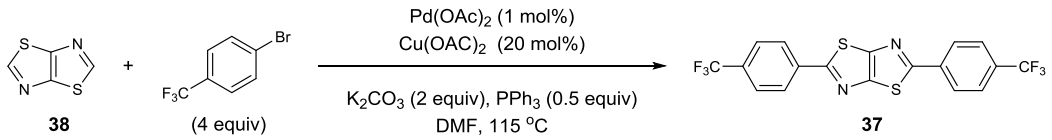

2,5-bis(4-(trifluoromethyl)phenyl)thiazolothiazole, 37

A round bottomed flask was charged with thiazolothiazole **38** (20 mg, 0.14 mmol), 1-bromo-4-(trifluoromethyl)benzene (126 mg, 0.56 mmol, 4 equiv), $Cu(OAc)_2$ (5 mg, 0.028 mmol, 0.2 equiv), K_2CO_3 (38 mg, 0.28 mmol, 2.0 equiv), and PPh_3 (18 mg, 0.07 mmol, 0.5 equiv) and purged with nitrogen. $Pd(OAc)_2$ (0.3 mg, 0.0014 mmol, 0.01 equiv) was added as a solution in anhydrous DMF (0.01 M, 0.14 mL). Additional anhydrous DMF (0.85 mL) was then added, and the reaction was heated to 135 °C under an atmosphere of nitrogen. Once the reaction was complete by TLC (18 h), it was filtered and the solid washed with DCM (2 mL) and water (20 mL) to give 40 mg (65 %) of title compound **37** as an amorphous brown powder. ^{1}H NMR (400 MHz, $CDCl_3$) δ = 8.12 (d, *J* = 8.4 Hz, 4 H), 7.74 (d, *J* = 8.4 Hz, 4 H); ^{13}C NMR (600 MHz, solid state) δ = 168.3, 150.7, 137.1, 131.7, 125.8; HRMS [+APCI] calculated for $C_{18}H_9N_2F_6S_2$ 431.0106, found 431.0106 [$M+H^+$]; IR (thin film, cm^{-1}) ν = 3382, 1615, 1559, 1405, 1323, 1123, 1110.

6.6 Chapter 5 Procedures and Characterization

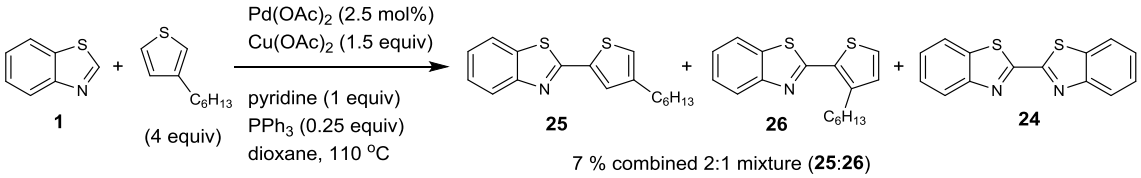

2-(4-hexylthiophen-2-yl)benzothiazole, 25, 2-(3-hexylthiophen-2-yl)benzothiazole, 26

Benzothiazole (**1**) (67.5 mg,, 0.11 mL, 0.5 mmol), 3-hexylthiophene (336 mg, 2.0 mmol, 4 equiv), $Cu(OAc)_2$ (135 mg, 0.75 mmol, 1.5 equiv), pyridine (39 mg, 0.5 mmol, 1.0 equiv), and PPh_3 (0.125 mmol, 0.25 equiv) were added to a 7 mL vial and purged with nitrogen. $Pd(OAc)_2$ (2.8 mg, 0.0125 mmol, 2.5 mol%) was added as a solution in dioxane. Additional dry dioxane was then added to bring the total volume to 1 mL. The reaction was heated to 110 °C under a balloon of nitrogen, and was maintained at reflux for 24 hours. After the reaction had cooled to room temperature, the mixture was filtered through celite, washed with DCM (2 x 3 mL) and MeOH (2 x 3 mL). The solvent was removed under reduced pressure and the crude material purified on silica gel in 4:1 Hexanes/EtOAc to give an inseparable mixture of title compounds **25** and **26** in a 2:1 ratio and 7 % overall yield. Their 1H NMR spectra were identical to the literature.[125,126] **25** and **26**: ^{1}H NMR (400 MHz, $CDCl_3$) δ = 8.03 (t, *J* = 8.4 Hz, 1 H), 7.88-7.82 (m, 1 H), 7.52-7.43 (m, 2 H), 7.36 (q, *J* = 4.8 Hz, 1 H), 7.10 (s, 0.78 H), 6.99 (d, *J* = 5.2 Hz, 0.4 H), 3.05 (dd, *J* = 7.4 Hz, 0.84 H), 2.46 (t, *J* = 7.8 Hz, 1.71 H), 1.75- 1.20 (m, 8 H), 0.91 (t, *J* = 7.0 Hz, 3 H). **24**: ^{1}H NMR (400 MHz, $CDCl_3$) δ = 8.15 (d, *J* = 8.0 Hz, 2 H), 7.97 (d, *J* = 7.6 Hz, 2 H), 7.55 (dt, *J* = 7.2, 1.2 Hz, 2 H), 7.47 (dt, *J* = 8.0, 1.2 Hz, 2 H).

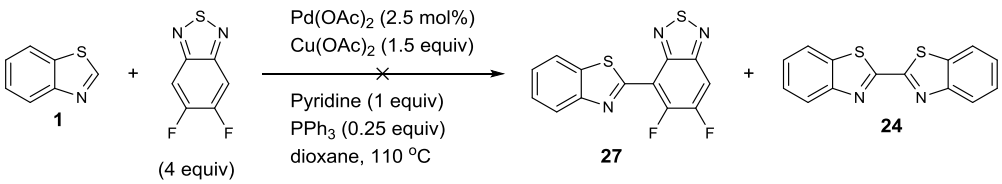

4-(benzothiazol-2-yl)-5,6-difluorobenzothiadiazole, 27

Benzothiazole (**1**) (67.5 mg,, 0.11 mL, 0.5 mmol), 5,6-difluorobenzothiadiazole (344 mg, 2.0 mmol, 4 equiv), $Cu(OAc)_2$ (135 mg, 0.75 mmol, 1.5 equiv), pyridine (39 mg, 0.5 mmol, 1.0 equiv), and PPh_3 (0.125 mmol, 0.25 equiv) were added to a 7 mL vial and purged with nitrogen. $Pd(OAc)_2$ (2.8 mg, 0.0125 mmol, 2.5 mol%) was added as a solution in dioxane. Additional dry dioxane was then added to bring the total volume to 1 mL. The reaction was brought up to 110 °C under a balloon of nitrogen, and was maintained at reflux for 24 hours. After the reaction had cooled to room temperature, the mixture was filtered through celite, and washed with DCM (2 x 3 mL) and MeOH (2 x 3 mL). Title compound **27** was not observed by either crude NMR or HRMS. **24** (3 mg, 10 %) was isolated after purification by column chromatography (9:1 hexanes/EtOAc).

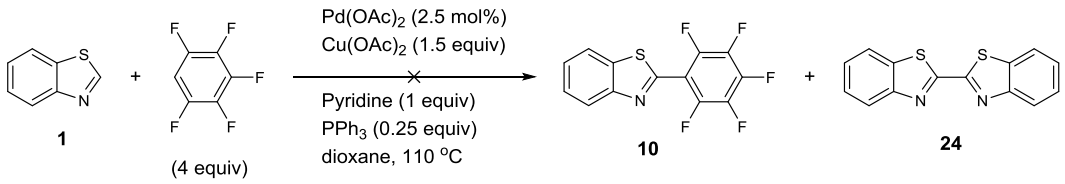

2-(perfluorophenyl)benzothiazole, 10

Benzothiazole (**1**) (67.5 mg,, 0.11 mL, 0.5 mmol), 1,2,3,4,5-pentafluorobenzene (336 mg, 2.0 mmol, 4 equiv), $Cu(OAc)_2$ (135 mg, 0.75 mmol, 1.5 equiv), pyridine (39 mg, 0.5 mmol, 1.0 equiv), and PPh_3 (0.125 mmol, 0.25 equiv) were added to a 7 mL vial and purged with nitrogen. $Pd(OAc)_2$ (2.8 mg, 0.0125 mmol, 2.5 mol%) was added as a solution in dioxane. Additional dry dioxane was then added to bring the total volume to 1 mL. The reaction was brought up to 110 °C under a balloon of nitrogen, and was maintained at reflux for 24 hours. After the reaction had cooled to room temperature, mixture was filtered through celite, washed with DCM (2 x 3 mL) and MeOH (2 x 3 mL). Title compound **10** was not observed by either crude NMR or HRMS. **24** (3.5 mg, 12 %) was isolated after purification by column chromatography using 9:1 hexanes/EtOAc.

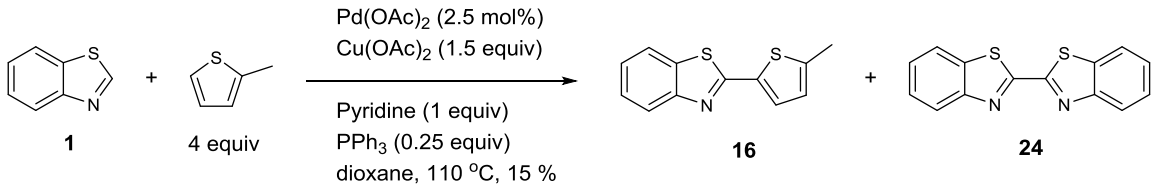

2-(5-methylthiophen-2-yl)benzothiazole, 16

Benzothiazole (**1**) (67.5 mg,, 0.11 mL, 0.5 mmol), 2-methylthiophene (196 mg, 0.36 mL 2.0 mmol, 4 equiv), $Cu(OAc)_2$ (135 mg, 0.75 mmol, 1.5 equiv), pyridine (39 mg, 0.5

mmol, 1.0 equiv), and PPh_3 (0.125 mmol, 0.25 equiv) were added to a 7 mL vial and purged with nitrogen. $Pd(OAc)_2$ (2.8 mg, 0.0125 mmol, 2.5 mol%) was added as a solution in dioxane. Additional dry dioxane was then added to bring the total volume to 1 mL. The reaction was brought up to 110 °C under a balloon of nitrogen, and was maintained at reflux for 24 hours. After the reaction had cooled to room temperature, mixture was filtered through celite, washed with DCM (2 x 3 mL) and MeOH (2 x 3 mL). Purification by column chromatography (9:1 hexanes/EtOAc) gave the title compound **16** as a white solid in 15 % yield (17 mg). The benzothiazole homodimer was also isolated in 9 % yield. Its ^{1}H NMR data were identical to the literature.[100] ^{1}H NMR (400 MHz, $CDCl_3$) δ = 7.98 (d, *J* = 8.0 Hz, 1 H), 7.81 (d, *J* = 8.0 Hz, 1 H), 7.46 (d, *J* = 3.6 Hz, 1 H), 7.44 (t, *J* = 6.0 Hz, 1 H), 7.33 (t, *J* = 8.4 Hz, 1 H), 6.79-6.77 (m, 1 H), 2.54 (s, 3 H).

General procedure for the reaction of benzothiazole (1) with 2-methylthiophene for HPLC assay.

Benzothiazole (**1**) (67.5 mg, 0.11 mL, 0.5 mmol), 2-methylthiophene (196 mg, 0.39 mL 2.0 mmol, 4 equiv), $Cu(OAc)_2$ (9.1 mg, 0.05 mmol, 0.1 equiv), base (0.08 mL, 0.5 mmol, 1.0 equiv), ligand (0.125 mmol, 0.25 equiv), oxidant (1.0 mmol, 2 equiv), and anthracene (22 mg, 0.125 mmol, 0.25 equiv) were added to a 7 mL vial and purged with nitrogen. $Pd(OAc)_2$ (2.8 mg, 0.0125 mmol, 2.5 mol%) was added as a solution in solvent. Additional dry solvent was then added to bring the total volume to 1 mL. The reaction was brought up to the desired temperature under a balloon of nitrogen. Once the reaction had been up to heat for 30 minutes an aliquot was taken every 24 hours for 3 total

aliquots. The aliquots were filtered through celite, washed with DCM (2 x 3 mL) and MeOH (2 x 3 mL) and analyzed *via* HPLC versus anthracene which served as an internal standard.

Column OD-H, method 1_IPA_ODH, 1% IPA in hexanes at 1mL/min.

Retention times:

2-methylthiophene: 4.13 min

Homodimer **24**: 9.17

Benzothiazole: 13.97 min

Heterodimer **16**: 17.41 min

References

(1) Lindsley, C. W. *ACS Chem. Neurosci.* **2010**, *1*, 407.
(2) Collet, F.; Dodd, R. H.; Dauban, P. *Chem. Commun.* **2009**, 5061.
(3) Wolff, M. E. *Chem. Rev.* **1963**, *63*, 55.
(4) Breslow, R.; Gellman, S. H. *J. Am. Chem. Soc.* **1983**, *105*, 6728.
(5) Liang, J.-L.; Yuan, S.-X.; Huang, J.-S.; Yu, W.-Y.; Che, C.-M. *Angew. Chem. Int. Ed.* **2002**, *41*, 3465.
(6) Zalatan, D. N.; Du Bois, J. *J. Am. Chem. Soc.* **2008**, *130*, 9220.
(7) Espino, C. G.; Fiori, K. W.; Kim, M.; Du Bois, J. *J. Am. Chem. Soc.* **2004**, *126*, 15378.
(8) Milczek, E.; Boudet, N.; Blakey, S. *Angew. Chem. Int. Ed.* **2008**, *47*, 6825.
(9) Zohuri, G. H.; Seyedi, S. M.; Sandaroos, R.; Damavandi, S.; Mohammadi, A. *Catal. Lett.* **2010**, *140*, 160.
(10) Dayan, O.; Çetinkaya, B. *J. Mol. Catal. Chem.* **2007**, *271*, 134.
(11) Cetinkaya, B.; Cetinkaya, E.; Brookhart, M.; White, P. S. *J. Mol. Catal. -Chem.* **1999**, *142*, 101.
(12) Bianchini, C.; Lee, H. M. *Organometallics* **2000**, *19*, 1833.
(13) Bon, J. L.; Blakey, S. B. *Heterocycles* **2012**, *84*, 1313.
(14) Hayes, C. J.; Beavis, P. W.; Humphries, L. A. *Chem. Commun.* **2006**, 4501.
(15) Loev, B.; Kormendy, M. F. *J. Org. Chem.* **1963**, *28*, 3421.
(16) Lebel, H.; Huard, K.; Lectard, S. *J. Am. Chem. Soc.* **2005**, *127*, 14198.
(17) Huard, K.; Lebel, H. *Org. Synth.* **2009**, *86*, 59.
(18) Liang, C.; Collet, F.; Robert-Peillard, F.; Müller, P.; Dodd, R. H.; Dauban, P. *J. Am. Chem. Soc.* **2008**, *130*, 343.
(19) King, R. B.; Bisnette, M. B. *Inorg. Chem.* **1964**, *3*, 796.
(20) Ruble, J. C.; Fu, G. C. *J. Org. Chem.* **1996**, *61*, 7230.
(21) Hansen, J. G.; Johannsen, M. *J. Org. Chem.* **2003**, *68*, 1266.
(22) Hull, J. F.; Sauer, E. L. O.; Incarvito, C. D.; Faller, J. W.; Brudvig, G. W.; Crabtree, R. H. *Inorg. Chem.* **2009**, *48*, 488.
(23) Robertson, A. D.; Murphy, K. P. *Chem. Rev.* **1997**, *97*, 1251.
(24) Das, S.; Incarvito, C. D.; Crabtree, R. H.; Brudvig, G. W. *Science* **2006**, *312*, 1941.
(25) Das, S.; Brudvig, G. W.; Crabtree, R. H. *Chem. Commun.* **2008**, 413.
(26) Fackler, P.; Berthold, C.; Voss, F.; Bach, T. *J. Am. Chem. Soc.* **2010**, *132*, 15911.
(27) Menger, F. M.; Bian, J.; Azov, V. A. *Angew. Chem. Int. Ed.* **2002**, *41*, 2581.
(28) Howáth, G.; Rusa, C.; Köntös, Z.; Gerencsér, J.; Huszthy, P. *Synth. Commun.* **1999**, *29*, 3719.
(29) Pryor, K. E.; Shipps Jr., G. W.; Skyler, D. A.; Rebek Jr., J. *Tetrahedron* **1998**, *54*, 4107.
(30) Aguilar-Aguilar, A.; Liebeskind, L. S.; Pena-Cabrera, E. *J. Org. Chem.* **2007**, *72*, 8539.
(31) Nishiyama, H.; Kondo, M.; Nakamura, T.; Itoh, K. *Organometallics* **1991**, *10*, 500.
(32) Phillips, A. J.; Uto, Y.; Wipf, P.; Reno, M. J.; Williams, D. R. *Org. Lett.* **2000**, *2*, 1165.
(33) Cui, W.; Yuen, J.; Wudl, F. *Macromolecules* **2011**, *44*, 7869.

(34) Xiao, P.; Hong, W.; Li, Y.; Dumur, F.; Graff, B.; Fouassier, J. P.; Gigmes, D.; Lalevée, J. *Polymer* **2014**, *55*, 746.
(35) Bronstein, H.; Chen, Z.; Ashraf, R. S.; Zhang, W.; Du, J.; Durrant, J. R.; Shakya Tuladhar, P.; Song, K.; Watkins, S. E.; Geerts, Y.; Wienk, M. M.; Janssen, R. A. J.; Anthopoulos, T.; Sirringhaus, H.; Heeney, M.; McCulloch, I. *J. Am. Chem. Soc.* **2011**, *133*, 3272.
(36) Bijleveld, J. C.; Gevaerts, V. S.; Di Nuzzo, D.; Turbiez, M.; Mathijssen, S. G. J.; de Leeuw, D. M.; Wienk, M. M.; Janssen, R. A. J. *Adv. Mater.* **2010**, *22*, E242.
(37) Pruissen, G. W. P. van; Pidko, E. A.; Wienk, M. M.; Janssen, R. A. J. *J. Mater. Chem. C* **2014**, *2*, 731.
(38) Cui, W.; Wudl, F. *Macromolecules* **2013**, *46*, 7232.
(39) Hong, W.; Guo, C.; Li, Y.; Zheng, Y.; Huang, C.; Lu, S.; Facchetti, A. *J. Mater. Chem.* **2012**, *22*, 22282.
(40) Deng, P.; Liu, L.; Ren, S.; Li, H.; Zhang, Q. *Chem. Commun.* **2012**, *48*, 6960.
(41) Rumer, J. W.; Levick, M.; Dai, S.-Y.; Rossbauer, S.; Huang, Z.; Biniek, L.; Anthopoulos, T. D.; Durrant, J. R.; Procter, D. J.; McCulloch, I. *Chem. Commun.* **2013**, *49*, 4465.
(42) Yue, W.; Huang, X.; Yuan, J.; Ma, W.; Krebs, F. C.; Yu, D. *J. Mater. Chem. A* **2013**, *1*, 10116.
(43) Hansen, J.; Li, B.; Dikarev, E.; Autschbach, J.; Davies, H. M. L. *J. Org. Chem.* **2009**, *74*, 6564.
(44) Davies, H. M. L.; Stafford, D. G.; Hansen, T. *Org. Lett.* **1999**, *1*, 233.
(45) Davies, H. M. L.; Walji, A. M. *Org. Lett.* **2003**, *5*, 479.
(46) Ni, A.; France, J. E.; Davies, H. M. L. *J. Org. Chem.* **2006**, *71*, 5594.
(47) Davies, H. M. L.; Gregg, T. M. *Tetrahedron Lett.* **2002**, *43*, 4951.
(48) Pelphrey, P.; Hansen, J.; Davies, H. M. L. *Chem. Sci.* **2010**, *1*, 254.
(49) Jing, C.; Xing, D.; Qian, Y.; Shi, T.; Zhao, Y.; Hu, W. *Angew. Chem. Int. Ed.* **2013**, *52*, 9289.
(50) Davies, H. M. L.; Walji, A. M.; Townsend, R. J. *Tetrahedron Lett.* **2002**, *43*, 4981.
(51) Rice, G. T.; White, M. C. *J. Am. Chem. Soc.* **2009**, *131*, 11707.
(52) Wu, L.; Qiu, S.; Liu, G. *Org. Lett.* **2009**, *11*, 2707.
(53) Paradine, S. M.; White, M. C. *J. Am. Chem. Soc.* **2012**, *134*, 2036.
(54) Zhou, J.; Xu, X.; Hu, W. *Org. Synth.* **2011**, *88*, 418.
(55) Owens, C. P.; Varela-Álvarez, A.; Boyarskikh, V.; Musaev, D. G.; Davies, H. M. L.; Blakey, S. B. *Chem. Sci.* **2013**, *4*, 2590.
(56) Pang, H.; Vilela, F.; Skabara, P. J.; McDouall, J. J. W.; Crouch, D. J.; Anthopoulos, T. D.; Bradley, D. D. C.; de Leeuw, D. M.; Horton, P. N.; Hursthouse, M. B. *Adv. Mater.* **2007**, *19*, 4438.
(57) Mei, J.; Diao, Y.; Appleton, A. L.; Fang, L.; Bao, Z. *J. Am. Chem. Soc.* **2013**, *135*, 6724.
(58) Osaka, I.; Takimiya, K.; McCullough, R. D. *Adv. Mater.* **2010**, *22*, 4993.
(59) Osaheni, J. A.; Jenekhe, S. A. *Macromolecules* **1993**, *26*, 4726.
(60) Ahmed, E.; Kim, F. S.; Xin, H.; Jenekhe, S. A. *Macromolecules* **2009**, *42*, 8615.
(61) Tan, L.-S.; Srinivasan, K. R.; Bai, S. J. *J. Polym. Sci. Part Polym. Chem.* **1997**, *35*, 1909.
(62) Hu, X.; Polk, M. B.; Kumar, S. *Macromolecules* **2000**, *33*, 3342.

(63) Bradshaw, T.; Westwell, A. *Curr. Med. Chem.* **2004**, *11*, 1009.
(64) Saari, W. S.; Hoffman, J. M.; Wai, J. S.; Fisher, T. E.; Rooney, C. S.; Smith, A. M.; Thomas, C. M.; Goldman, M. E.; O'Brien, J. A. *J. Med. Chem.* **1991**, *34*, 2922.
(65) Bergman, J.; Coleman, P.; Cox, C.; Hartman, G.; Lindsley, C.; Mercer, S. P.; Roecker, A.; Whitman, D. Proline Bis-Amide Orexin Receptor Antagonists. WO2006127550 (A1), November 30, 2006.
(66) Dotrong, M.; Mehta, R.; Balchin, G. A.; Tomlinson, R. C.; Sinsky, M.; Lee, C. Y.-C.; Evers, R. C. *J. Polym. Sci. Part Polym. Chem.* **1993**, *31*, 723.
(67) Mike, J. F.; Inteman, J. J.; Ellern, A.; Jeffries-EL, M. *J. Org. Chem.* **2010**, *75*, 495.
(68) Yoshizumi, T.; Tsurugi, H.; Satoh, T.; Miura, M. *Tetrahedron Lett.* **2008**, *49*, 1598.
(69) Huang, J.; Chan, J.; Chen, Y.; Borths, C. J.; Baucom, K. D.; Larsen, R. D.; Faul, M. M. *J. Am. Chem. Soc.* **2010**, *132*, 3674.
(70) Han, W.; Mayer, P.; Ofial, A. R. *Chem. – Eur. J.* **2011**, *17*, 6904.
(71) Ranjit, S.; Liu, X. *Chem. – Eur. J.* **2011**, *17*, 1105.
(72) Huang, Z.-Z.; Yan, X.-M.; Mao, X.-R. *Heterocycles* **2011**, *83*, 1371.
(73) Alla, S. K.; Sadhu, P.; Punniyamurthy, T. *J. Org. Chem.* **2014**, *79*, 7502.
(74) Wang, R.; Liu, D.; Ren, H.; Zhang, T.; Wang, X.; Li, J. *J. Mater. Chem.* **2011**, *21*, 15494.
(75) Wang, H.; Wang, L.; Shang, J.; Li, X.; Wang, H.; Gui, J.; Lei, A. *Chem. Commun.* **2011**, *48*, 76.
(76) Rey, V.; Soria-Castro, S. M.; Argüello, J. E.; Peñéñory, A. B. *Tetrahedron Lett.* **2009**, *50*, 4720.
(77) Inamoto, K.; Hasegawa, C.; Hiroya, K.; Doi, T. *Org. Lett.* **2008**, *10*, 5147.
(78) Mu, X.-J.; Zou, J.-P.; Zeng, R.-S.; Wu, J.-C. *Tetrahedron Lett.* **2005**, *46*, 4345.
(79) Downer-Riley, N. K.; Jackson, Y. A. *Tetrahedron* **2007**, *63*, 10276.
(80) Bose, D. S.; Idrees, M. *J. Org. Chem.* **2006**, *71*, 8261.
(81) Bose, D. S.; Idrees, M. *Tetrahedron Lett.* **2007**, *48*, 669.
(82) Bon, J. L.; Feng, D.; Marder, S. R.; Blakey, S. B. *J. Org. Chem.* **2014**, *79*, 7766.
(83) Segelstein, B. E.; Butler, T. W.; Chenard, B. L. *J. Org. Chem.* **1995**, *60*, 12.
(84) Tlach, B. C.; Tomlinson, A. L.; Bhuwalka, A.; Jeffries-EL, M. *J. Org. Chem.* **2011**, *76*, 8670.
(85) Lim, J.; Albright, T. A.; Martin, B. R.; Miljanić, O. Š. *J. Org. Chem.* **2011**, *76*, 10207.
(86) Molander, G. A.; Biolatto, B. *J. Org. Chem.* **2003**, *68*, 4302.
(87) Ando, S.; Nishida, J.; Tada, H.; Inoue, Y.; Tokito, S.; Yamashita, Y. *J. Am. Chem. Soc.* **2005**, *127*, 5336.
(88) Ando, S.; Nishida, J.; Inoue, Y.; Tokito, S.; Yamashita, Y. *J. Mater. Chem.* **2004**, *14*, 1787.
(89) Osaka, I.; Sauvé, G.; Zhang, R.; Kowalewski, T.; McCullough, R. D. *Adv. Mater.* **2007**, *19*, 4160.
(90) Iwan, A.; Siwy, M.; Janeczek, H.; Rannou, P. *Phase Transit.* **2012**, *85*, 297.
(91) Han, W.; Mayer, P.; Ofial, A. R. *Angew. Chem. Int. Ed.* **2011**, *50*, 2178.
(92) Qin, X.; Feng, B.; Dong, J.; Li, X.; Xue, Y.; Lan, J.; You, J. *J. Org. Chem.* **2012**, *77*, 7677.

(93) Xi, P.; Yang, F.; Qin, S.; Zhao, D.; Lan, J.; Gao, G.; Hu, C.; You, J. *J. Am. Chem. Soc*. **2010**, *132*, 1822.
(94) Dong, J.; Huang, Y.; Qin, X.; Cheng, Y.; Hao, J.; Wan, D.; Li, W.; Liu, X.; You, J. *Chem. – Eur. J.* **2012**, *18*, 6158.
(95) Liu, B.; Huang, Y.; Lan, J.; Song, F.; You, J. *Chem. Sci.* **2013**, *4*, 2163.
(96) Dong, J.; Long, Z.; Song, F.; Wu, N.; Guo, Q.; Lan, J.; You, J. *Angew. Chem.-Int. Ed.* **2013**, *52*, 580.
(97) Mao, Z.; Wang, Z.; Xu, Z.; Huang, F.; Yu, Z.; Wang, R. *Org. Lett.* **2012**, *14*, 3854.
(98) Fan, S.; Chen, Z.; Zhang, X. *Org. Lett.* **2012**, *14*, 4950.
(99) Wu, G.; Zhou, J.; Zhang, M.; Hu, P.; Su, W. *Chem. Commun.* **2012**, *48*, 8964.
(100) Chen, X.; Huang, X.; He, Q.; Xie, Y.; Yang, C. *Chem. Commun.* **2014**, *50*, 3996.
(101) Stuart, D. R.; Fagnou, K. *Science* **2007**, *316*, 1172.
(102) Stuart, D. R.; Villemure, E.; Fagnou, K. *J. Am. Chem. Soc.* **2007**, *129*, 12072.
(103) Yang, N.; Dong, L.; Su, Z.; Hu, C. *RSC Adv.* **2013**, *3*, 20772.
(104) Fung, B. M.; Khitrin, A. K.; Ermolaev, K. *J. Magn. Reson.* **2000**, *142*, 97.
(105) Fan, R.-Q.; Zhu, D.-S.; Mu, Y.; Li, G.-H.; Yang, Y.-L.; Su, Q.; Feng, S.-H. *Eur. J. Inorg. Chem.* **2004**, *2004*, 4891.
(106) Dayan, O.; Doĝan, F.; Kaya, İ.; Çetinkaya, B. *Synth. React. Inorg. Met.-Org. Nano-Met. Chem.* **2010**, *40*, 337.
(107) Vance, A. L.; Alcock, N. W.; Heppert, J. A.; Busch, D. H. *Inorg. Chem.* **1998**, *37*, 6912.
(108) Wieder, N. L.; Carroll, P. J.; Berry, D. H. *Organometallics* **2011**, *30*, 2125.
(109) Ionkin, A. S.; Marshall, W. J.; Adelman, D. J.; Shoe, A. L.; Spence, R. E.; Xie, T. *J. Polym. Sci. Part Polym. Chem.* **2006**, *44*, 2615.
(110) Leffler, J. E.; Ward, D. C.; Burduroglu, A. *J. Am. Chem. Soc.* **1972**, *94*, 5339.
(111) Dong, G. R.; Li, Q. R.; Woo, S. H.; Kim, I. S.; Jung, Y. H. *Arch. Pharm. Res.* **2008**, *31*, 1393.
(112) Di Chenna, P. H.; Robert-Peillard, F.; Dauban, P.; Dodd, R. H. *Org. Lett.* **2004**, *6*, 4503.
(113) Moffett, R. *Org. Synth.* **1952**, *32*, 41.
(114) Dale, T. J.; Rebek, J. *J. Am. Chem. Soc.* **2006**, *128*, 4500.
(115) Chankeshwara, S. V.; Chakraborti, A. K. *Org. Lett.* **2006**, *8*, 3259.
(116) Perron, V.; Abbott, S.; Moreau, N.; Lee, D.; Penney, C.; Zacharie, B. *Synthesis* **2009**, *2*, 283.
(117) Shrikhande, J. J.; Gawande, M. B.; Jayaram, R. V. *Tetrahedron Lett.* **2008**, *49*, 4799.
(118) Davies, H. M. L.; Hansen, T.; Churchill, M. R. *J. Am. Chem. Soc.* **2000**, *122*, 3063.
(119) Nicolai, S.; Piemontesi, C.; Waser, J. *Angew. Chem. Int. Ed.* **2011**, *50*, 4680.
(120) Hattori, T.; Akita, H.; Kakimoto, M.; Imai, Y. *Macromolecules* **1992**, *25*, 3351.
(121) Trohalaki, S.; Chabinyc, M. L.; Resch, T. J.; Fratini, A. V.; Vance, T. A.; Arnold, F. E.; Dudis, D. S. *Chem. Mater.* **1996**, *8*, 714.
(122) Barche, J.; Janietz, S.; Ahles, M.; Schmechel, R.; von Seggern, H. *Chem. Mater.* **2004**, *16*, 4286.
(123) Haga, M.; Meser Ali; Koseki, S.; Yoshimura, A.; Nozaki, K.; Ohno, T. *Inorganica Chim. Acta* **1994**, *226*, 17.
(124) Johnson, J. R.; Rotenberg, D. H.; Ketcham, R. *J. Am. Chem. Soc.* **1970**, *92*, 4046.

(125) Mori, A.; Tamba, S.; Sugie, A.; Tanaka, S. *Heterocycles* **2012**, *86*, 255.
(126) Yamamoto, T.; Muto, K.; Komiyama, M.; Canivet, J.; Yamaguchi, J.; Itami, K. *Chem. – Eur. J.* **2011**, *17*, 10113.